THESIS

This is to certify that the

dissertation entitled

Application of a Linear Viscoelastic Plate Theory
to Hygroscopic Warping of Laminates

presented by

Hong Xu

has been accepted towards fulfillment
of the requirements for
Ph. D. Forestry
_____ degree in _____

Wo Suddard
Major professor

Date August 5, 1993

O-12771

APPLIC

APPLICATION OF A LINEAR VISCOELASTIC PLATE THEORY TO HYGROSCOPIC WARPING OF LAMINATES

By

Hong Xu

A DISSERTATION

Submitted to
Michigan State University
in partial fulfillment of the requirements
for the degree of

DOCTOR OF PHILOSOPHY

Department of Forestry

1993

APPLI

A linear

Lamination Th

hygroscopic ma

equivalence wa

equation and it

examined when

yellow-poplar (

LVP were com

high humidity e

radial direction

characterized by

model is to acc

viscoelastic defo

was found to be

and the recovera

component. The

coefficients of

represented. Th

ABSTRACT

APPLICATION OF A LINEAR VISCOELASTIC PLATE THEORY
TO HYGROSCOPIC WARPING OF LAMINATES

By

Hong Xu

A linear viscoelastic plate theory (LVP) was formulated based on Classical Lamination Theory (CLT) and the linear viscoelastic constitutive equation for hygroscopic materials such as wood and wood-based materials. Its solvable numerical equivalence was arrived at by linear numerical integration of its integral governing equation and its computation was automated on a desktop computer. Its validity was examined when it was applied to the hygroscopic warping of a two-ply cross laminated yellow-poplar (Liriodendron tulipifera) laminate and the theoretical predictions by the LVP were compared with the measured warps suffered by the laminate subjected to a high humidity environment. The viscoelastic creep properties of yellow-poplar in the radial direction, needed as input in the application of the LVP, were tested and characterized by a four-element Burger body. The non-Newtonian dashpot used in the model is to account for the non-Newtonian behavior of the flow component of the viscoelastic deformation. The general behavior of yellow-poplar in its radial direction was found to be clearly nonlinearly viscoelastic, especially regarding the flow component and the recoverable component, while it is linearly elastic for the instantaneous elastic component. The separate effects of moisture content, stress, and time on the four coefficients of the four-element Burger body were investigated and mathematically represented. The numerical form of the isothermal LVP theory was used to approximate

warping - a r

variations of m

viscoelastic co

improved pred

process satisfa

of the warping

the mechano-s

and relaxation

into the relaxat

effort within th

humidity condi

warping - a nonlinear nonisothermal viscoelastic process - by accounting for the variations of moisture content, stresses, and the four moisture content-stress dependent viscoelastic coefficients in step-wise increments. The LVP theory resulted in much improved predictions over its elastic counterpart. But, it failed to describe the warping process satisfactorily in that it underestimated the drastic relaxation in the early stages of the warping of the yellow-poplar laminate. Much of the error is very possibly due to the mechano-sorptive effect which is known to cause far greater and more rapid creep and relaxation and which is also prominent in warping and which was not incorporated into the relaxation moduli input in the application. It is also demonstrated that any extra effort within the elasticity realm in dealing with the warping problem in high and cyclic humidity conditions will probably result in limited improvement.

Dedicated to my beloved Lan, Hope,
and my dear parents

The au
mentor, Dr.
encouragemer
each member
Specia
for their under
in this journey

ACKNOWLEDGMENTS

The author wishes to express his sincere appreciation to his Ph.D. advisor and mentor, Dr. Otto Suchsland, for his continued guidance, support, patience and encouragement throughout the course of this study. Appreciation is also expressed to each member of the committee for their counsels and recommendations.

Special thanks are extended to my dearest wife, Lan, and lovely daughter, Hope, for their understanding, encouragement and warm companionship every step of the way in this journey.

TABLE OF CONTENTS

LIST OF TABLES

LIST OF FIGURES

LIST OF SYMBOLS

a	coefficient in parabolic mechanical creep model
A	coefficient in the normalized creep compliance of a nonlinear four-element Burger body
A_{ij}	extensional stiffness
$A_{ij}(t-\tau)$	integrand related to extensional stiffness
b	constant in a logarithm mechanical creep model
B	coefficient in the normalized creep compliance of a nonlinear four-element Burger body
B_{ij}	coupling stiffness
$B_{ij}(t-\tau)$	integrand related to coupling stiffness
C	coefficient in the normalized creep compliance of a nonlinear four-element Burger body
D	coefficient in the normalized creep compliance of a nonlinear four-element Burger body
D_{ij}	bending stiffness
$D_{ij}(t-\tau)$	integrand related to bending stiffness
E_{11}, E_{22}, E_k, E_m	respectively, Young's modulus along the grain and across the grain, Kelvin spring coefficient, and Maxwell spring coefficient
G_{12}	plane shear modulus
h	thickness of laminate
i, j	dummy indices on moduli, compliances, etc.

$J(t)$, $J_{\varphi}(t-\tau)$, J

$J_{s}(t)$

$J_{f}(t)$, $J_{f}(t)$

$J_{fs}(t)$, $J_{fs}(t)$

k

$L(\tau)$

m

MC, MC_{G}

M_{x} M_{y} M_{xy}

$M^{M}(t)$, $M^{H}(t)$,

$M^{MC}(t)$

n

N

N_{x} N_{y} N_{xy}

$N^{M}(t)$, $N^{H}(t)$,

$N^{MC}(t)$

P, P_{MC}

Q_{φ} $\overline{Q}_{\varphi}$

s

t

u

$J(t)$, $J_{ij}(t-\tau)$, $J_{ijkl}(t-\tau)$	creep compliances
$J_N(t)$	normalized creep compliance
$J_r(t)$, $J_f(t)$	respectively, recoverable and flow compliance
$J_{rN}(t)$, $J_{fN}(t)$	respectively, normalized recoverable and flow compliance
k	summation index on series
$L(\tau)$	spectrum of retardation times
m	coefficient in parabolic mechanical model
MC, MC_G	respectively, moisture content and moisture content at which mechanical property reaches a minimum
M_x, M_y, M_{xy}	moments
$M^M(t)$, $M^H(t)$, $M^T(t)$	respectively, mechanical, hygroscopic, and thermal moments
$M^{MC}(t)$	hygroscopic moment in reference to moisture content
n	number of layers in a laminate
N	number of Kelvin elements in a Kelvin chain
N_x, N_y, N_{xy}	in-plane forces
$N^M(t)$, $N^H(t)$, $N^T(t)$	respectively, mechanical, hygroscopic, and thermal in-plane forces
$N^{MC}(t)$	hygroscopic in-plane force in reference to moisture content
P, P_{MC}	respectively, creep load and mechanical load at MC moisture content
Q_{ij}, $\overline{Q}_{ij}$	respectively, reduced stiffness and transformed reduced stiffness
s	variable in Laplace domain
t	time
u	displacement in x-direction

u_0

v

v_0

w_0

x, y, z

$Y_i(t),\ Y_{guess}(t-\tau)$

Z_i

Greek Symbols

$\alpha_{ij}(t)$

β

γ^0_{xy}

$\gamma_{xx}\ \gamma_{yz}$

ϵ_0

$\epsilon(t)$

$\epsilon^0_{xx}\ \epsilon^0_{yy}$

ϵ_{zz}

$\epsilon^C,\ \epsilon^M,\ \epsilon^H$

$\epsilon_{ij}(t)$

$\epsilon_{rN}(t)$

ϵ^{MC}

$\epsilon_{ip}\ \epsilon_{id}$

u_0	midplane displacement in x-direction
v	displacement in y-direction
v_0	midplane displacement in y-direction
w_0	midplane displacement in z-direction
x, y, z	cartesian coordinates
$Y_{ij}(t), Y_{ijkl}(t-\tau)$	relaxation moduli
Z_k	coordinate distance from reference surface (top surface of laminate) to bottom of lamina

Greek Symboles

$\alpha_{ij}(t)$	hygroscopic expansion coefficient
β	angular rotation of laminate cross section
γ^0_{xy}	mid-plane plane shear strain referred to x-y axes
γ_{zx}, γ_{yz}	transverse shear strains
ϵ_0	instantaneous elastic strain
$\epsilon(t)$	total strain
$\epsilon^0_{xx}, \epsilon^0_{yy}$	mid-plane normal strains referred to x-y axes
ϵ_{zz}	transverse normal strain
$\epsilon^C, \epsilon^M, \epsilon^H$	respectively, total strain, mechanical strain, and hygroscopic strain
$\epsilon_r(t)$	delayed elastic (recoverable) creep strain
$\epsilon_{rN}(t)$	normalized delayed elastic (recoverable) creep strain
ϵ^{MC}	hygroscopic strain in reference to moisture content
$\epsilon_{ij}, \epsilon_{kl}$	strains

$\epsilon_R(t)$

$\epsilon_\mu(t)$

θ_{ij}, θ_{kl}

θ

κ_x, κ_y, κ_{xy}

$\nu_{ij}(t)$

σ^*

σ_{xx}, σ_{yy}

σ_{zz}

$\sigma_{\phi\phi}$, σ_{RR}

$\Delta\tau$

$\Delta\tau_i$

τ

τ_{xy}

τ_{yz}, τ_{xz}

$\epsilon_R(t)$	relative creep
$\epsilon_v(t)$	viscous creep strain
η_{kd}, η_{md}	respectively, Kelvin and Maxwell dashpot coefficient
θ	angular orientation of a lamina
κ_x, κ_y, κ_{xy}	plate curvatures
$\nu_{ij}(t)$	Poisson's ratio
σ^*	time-wise constant creep stress
σ_{xx}, σ_{yy}	plane normal stresses
σ_{zz}	transverse normal stress
σ_{ij}, σ_{kl}	stresses
$\Delta\tau$	unit time interval
$\Delta\tau_i$	ith time interval
τ	integration variable, retardation time
τ_{xy}	plane shear stress
τ_{yz}, τ_{xz}	transverse shear stresses

1.1 Backgrou

Warpi

initial state.

practical case

1985].

Warp

results in sub

the years hav

one of the m

and research

First,

occurs. Oft

replaced wit

[Suchsland,

Seco

products of

CHAPTER I

INTRODUCTION

1.1 Background

Warping may be defined as the deviation of the geometry of a panel from an initial state. This initial state is almost always desired to be a state of flatness in practical cases. The warped condition would thus be considered a defect [Suchsland, 1985].

Warping, probably one of the most pervasive problem in the wood industry, results in substantial losses to both the manufacturers and users. Even though efforts over the years have been made to solve it, two aspects of this phenomenon make it remain as one of the most puzzling and frustrating problems to both the experienced manufacturing and research professionals.

First, warping is a condition that can rarely be corrected or repaired, once it occurs. Often the entire panel or the entire product of which the panel is a part must be replaced with no real guarantee that the replacement will perform better than the original [Suchsland, 1985].

Secondly, warping usually occurs subsequent to the manufacture of panels or products of which panels are a part as indicated in the definition. This subsequent nature

indicates that e

environments, c

to manifest ther

in the panel its

process of the p

since the proces

are not all unde

processing cond

Warping

changes in panel

in wood and wo

thermal expansio

(Table 1), it can

warping process.

Table 1. Therma
Produc

Species
Walnut
Red Oak
Red Pine
Douglas-fir

indicates that either the panel itself may have experienced some changes under changed environments, or the changing surroundings may have caused certain inherent properties to manifest themselves in the form of warping, or both. In any case, this is an instability in the panel itself, and therefore the control must be directed to the manufacturing process of the panel to avoid it. However, warping potentials are difficult to recognize since the processing variables involved are complex and their contributions to warping are not all understood. It is just difficult to relate the warping of a returned panel to processing conditions at the time of manufacturing [Suchsland, 1985].

Warping is a manifestation of dimensional instability caused by linear dimensional changes in panel elements. The environmental changes that cause dimensional changes in wood and wood-based materials are temperature and humidity changes. Since the thermal expansion coefficient is much smaller than the hygroscopic expansion coefficient (Table 1), it can thus be recognized that the humidity change is the major factor in the warping process.

Table 1. Thermal and hygroscopic expansion coefficients of some wood species [Forest Products Laboratory, 1987].

	Thermal Coefficient (/F°)		Hygroscopic coefficient (/MC(%))		
Species	Longitudinal	Radial - Tangential	Longitudinal	Radial	Tangential
Walnut	0.17×10^{-5} ~ 0.25×10^{-5}	0.85×10^{-5} ~ 2.50×10^{-5}	0.3×10^{-4} ~ 0.6×10^{-4}	0.18×10^{-2}	0.26×10^{-2}
Red Oak				0.15×10^{-2}	0.37×10^{-2}
Red Pine	for dry wood for most species		for most species	0.13×10^{-2}	0.24×10^{-2}
Douglas-fir				0.16×10^{-2}	0.25×10^{-2}

Consider

an eventual sol

elastic approac

success. One ex

Norris [1942], a

results by far ha

However

wood and wood-

these conditions

warping process

approach overest

cross laminated

results at low an

A great

characterization

materials. But, h

has not been esta

It is belie

understanding of

approach that wo

warping panels.

Considerable research work has been directed towards a better understanding and an eventual solution of warping. On the mathematical and theoretical side are many elastic approaches which have been developed and have achieved moderate to good success. One example is the popular beam approach used by Ismar and Paulitsch [1973], Norris [1942], and Suchsland [1985]. The associated simplicity and its fairly reliable results by far have made this approach the most useful analytical tool.

However, it is also recognized that the elastic approach is limited by the fact that wood and wood-based materials behave elastically only under certain conditions. Once these conditions are violated, the elastic approach would not be able to explain the warping process with sufficient accuracy. Suchsland [1985] showed that the elastic beam approach overestimated the warping of three-ply cross laminated red oak and three-ply cross laminated loblolly pine beams at high humidities, while it provided agreeable results at low and moderate humidities.

A great deal so far has been achieved regarding the understanding and characterization of the significant viscoelastic behaviors of wood and wood-based materials. But, how these viscoelastic properties are involved in the warping problems has not been established.

It is believed that there are many avenues that could be taken to improve our understanding of the warping mechanism. One of them is to develop a viscoelastic approach that would account for the viscoelastic properties of constituent materials in warping panels.

1.2 Objective

The fi

derive its sol

significant hy

wood-based

The s

applying it t

high humidit

the measure

In de

for its viscoe

properties w

1.2 Objectives of the Study

The first goal of this research is to formulate a linear viscoelastic plate theory and derive its solvable numerical form for panels of materials that are known to develop significant hygroscopic deformations or strains. Examples of such materials are wood and wood-based materials.

The second objective is to examine the applicability and validity of the theory by applying it to a two-ply cross laminated yellow-poplar laminate and beam, subjected to high humidity. Theoretical predictions of warping by the theory will be compared with the measured values.

In developing the necessary inputs for the application, yellow-poplar will be tested for its viscoelastic properties in radial tension creep, and proper characterization of these properties will be sought.

DEVEL

2.1 Introduction

Laminate

tured composite

orthotropic or is

while homogene

The appr

of two procedur

constitutive equ

viscoelastic con

1967]. Therefo

tions (stress-str

such a viscoela

validity of its e

2.2 Validity of

Exact s

CHAPTER II

DEVELOPMENT OF A LINEAR VISCOELASTIC PLATE THEORY FOR HYGROSCOPIC COMPOSITE LAMINATES

2.1 Introduction

Laminated wood and wood composite panels can be regarded as multi-layer structured composite plates comprised of any number of physical or imaginary layers of orthotropic or isotropic character. Plane homogeneity is usually observed within all layers while homogeneity or heterogeneity exists between layers.

The approach taken here in the development of a viscoelastic plate theory consists of two procedures. First, an appropriate elastic plate theory is chosen. Then, the elastic constitutive equations of the plate theory, namely Hooke's Law, are substituted by linear viscoelastic constitutive equations, namely Boltzmann Superposition Principle [Schapery, 1967]. Therefore, the key that distinguishes the two theories lies in the constitutive equations (stress-strain relations) while all other elements remain the same. The success of such a viscoelastic theory inevitably and inherently depends on, among other things, the validity of its elastic foundation.

2.2 Validity of the Classical Lamination Theory (CLT)

Exact solutions based on three dimensional elasticity are attainable for composite

plates [Pagano.

plate structure.

of this approac

Many pl

theories [Rehfie

the number of l

and of good app

Classical

theory in which

before deformat

displacement fie

dimensional scal

are not accounte

underestimates

composites, thes

modulus ratios

typical isotropic

To impro

high-order theor

examples have b

Sun [1973], Lo &

order variations

plates [Pagano, 1969 and 1970]. However, certain restrictions have to be imposed upon plate structure, boundary conditions, and loading patterns, thereby limiting the extension of this approach to only a number of certain ideal cases.

Many plate theories have been developed as alternatives. While three-dimensional theories [Rehfield and Valesetty, 1983; Pagano and Soni, 1983] tend to be intractable as the number of layers becomes moderately large, two dimensional ones are less rigorous and of good approximation accuracy.

Classical Lamination Theory (CLT) is the most basic and simple two-dimensional theory in which it is [Jones, 1975; Liu, 1987] assumed that normals to the mid-plane before deformation remain straight and normal to the plane after deformation in its displacement field. In this regard it is equivalent to beam theory, but on a two dimensional scale. The implication is that the transverse normal and shear components are not accounted for. The resulting errors are overestimates of natural frequencies, and underestimates of transverse deflections of composite plates. In case of advanced composites, these errors become substantial because of the large elastic modulus to shear modulus ratios of these materials (e.g., of the order of 25 to 40, instead of 2.6 for typical isotropic materials) [Reddy, 1984].

To improve upon CLT, shear deformation theories and further improvement - high-order theories - which include the transverse components have been proposed. Some examples have been offered by Mindlin [1951], Whitney & Pagano [1970], Whitney & Sun [1973], Lo & Christensen & Wu [1977], and Reddy [1984], in which linear or high-order variations of mid-plane displacements through thickness are assumed in their

respective disp

in Figures 1 t

Christensen, a

also noted that

siderably with

This last

by Pagano [196

showed [1972]

specific compos

and high-order

respective CLT

Table 2 - clearly

CLT and exact

aspect ratio of

slower, yet fairl

The effe

in Table 2 displa

increase in num

The desc

CLT with one p

wood composite

panels, whose la

respective displacement fields. They are generally much more accurate, as demonstrated in Figures 1 to 6, where a very precise agreement of the high-order theory by Lo, Christensen, and Wu [1977] with exact solutions is observed as opposed to CLT. It is also noted that the poor agreement between CLT and exact solutions improved considerably with the increase in aspect ratio.

This last observation is not incidental. It became very evident in the investigations by Pagano [1969, 1970, 1971, and 1972] on CLT's relations with exact solutions. He showed [1972] that exact solutions converged to the respective CLT solutions for a specific composite plate as its aspect ratio became very large (Shear deformation theories and high-order theories, converging to exact solutions, subsequently converge to respective CLT solutions under the same condition.). His results - Figures 7 to 10 and Table 2 - clearly illustrate the rapid disappearance of the considerable deviation between CLT and exact solutions in normal stress, shear stress, and in-plane displacement at an aspect ratio of only 10. Convergence in the case of vertical deflection is relatively slower, yet fairly good agreement is already achieved at an aspect ratio of 20.

The effect of number of layers was also examined by Pagano [1972]. His results in Table 2 display a faster convergence for a composite plate of given thickness with the increase in number of layers.

The described convergence property therefore defines the range of validity of CLT with one parameter - aspect ratio. In practical applications, warping of wood and wood composite plates, when identified as a problem, is normally associated with big panels, whose large aspect ratios (larger than 20) thereby place themselves well into the

Table 2a.

Aspect Ratio S	
2	
4	
10	
20	
50	
100	

Table 2b. N

Aspect Ratio S	
2	
4	
10	
20	
50	
100	

Table 2a. Maximum stresses and deflection in 3-ply laminate [Pagano, 1972].

Aspect Ratio S	$\bar{\sigma}_x$ (a/2,a/2,±1/2)	$\bar{\sigma}_y$ (a/2,a/2,±1/4)	$\bar{\tau}_{xz}$ (0,a/2,0)	$\bar{\tau}_{yz}$ (a/2,0,0)	$\bar{\tau}_{xy}$ (0,0,±1/2)	$\bar{w}$ (a/2,a/2,0)
			Elasticity Solution			
2	1.388	0.835	0.153	0.295	-0.0863	11.767
	-0.912	-0.795	0.264	0.298	0.0673	
4	0.720	0.663	0.219	0.292	-0.0467	4.491
	-0.684	-0.666	0.222		0.0458	
10	±0.559	0.401	0.301	0.196	-0.0275	1.709
		-0.403			0.0276	
20	±0.543	0.308	0.328	0.156	∓0.0230	1.189
		-0.309				
50	±0.539	±0.276	0.337	0.141	∓0.0216	1.031
100	±0.539	±0.271	0.339	0.139	∓0.0214	1.008
			CLT Solution			
	±0.539	±0.269	0.339	0.138	∓0.0213	1.000

Table 2b. Maximum stresses and deflection in 5-ply laminate [Pagano, 1972].

Aspect Ratio S	$\bar{\sigma}_x$ (a/2,a/2,±1/2)	$\bar{\sigma}_y$ (a/2,a/2,±1/4)	$\bar{\tau}_{xz}$ (0,a/2,0)	$\bar{\tau}_{yz}$ (a/2,0,0)	$\bar{\tau}_{xy}$ (0,0,±1/2)	$\bar{w}$ (a/2,a/2,0)
			Elasticity Solution			
2	1.332	1.001	0.227	0.186	-0.0836	12.278
	-0.903	-0.848	0.229	0.286	0.0634	
4	0.685	0.633	0.238	0.229	-0.0394	4.291
	-0.651	-0.626	0.238	0.233	0.0384	
10	±0.545	0.430	0.258	0.223	-0.0246	1.570
		-0.432		0.223	0.0247	
20	±0.539	±0.380	0.268	0.212	∓0.0222	1.145
50	±0.539	±0.363	0.271	0.206	∓0.0214	1.023
100	±0.539	±0.360	0.272	0.205	∓0.0213	1.006
			CLT Solution			
	±0.539	±0.359	0.272	0.205	∓0.0213	1.000

Table 2c.

Aspect Ratio S	
2	
4	
10	
20	
50	
100	

Table 2d. M

Aspect Ratio S	
2	
4	
10	
20	
50	
100	

Table 2c. Maximum stresses and deflection in 7-ply laminate [Pagano, 1972].

Aspect Ratio S	$\bar{\sigma}_x$ (a/2,a/2,±1/2)	$\bar{\sigma}_y$ (a/2,a/2,±1/4)	$\bar{\tau}_{xz}$ (0,a/2,0)	$\bar{\tau}_{yz}$ (a/2,0,0)	$\bar{\tau}_{xy}$ (0,0,±1/2)	$\bar{w}$ (a/2,a/2,0)
			Elasticity Solution			
2	1.284	1.039	0.178	0.238	-0.0775	12.342
	-0.880	-0.8.8	0.229	0.239	0.0579	
4	0.679	0.623	0.219	0.236	-0.0356	4.153
	-0.645	-0.610	0.223		0.0347	
10	±0.548	0.457	0.255	0.219	-0.0237	1.529
		-0.458	0.255		0.0238	
20	±0.539	0.419	0.267	0.210	∓0.0219	1.133
		-0.420				
50	±0.539	±0.407	0.271	0.206	∓0.0214	1.021
100	±0.539	±0.405	0.272	0.205	∓0.0213	1.005
			CLT Solution			
	±0.539	±0.404	0.272	0.205	∓0.0213	1.000

Table 2d. Maximum stresses and deflection in 9-ply laminate [Pagano, 1972].

Aspect Ratio S	$\bar{\sigma}_x$ (a/2,a/2,±1/2)	$\bar{\sigma}_y$ (a/2,a/2,±1/4)	$\bar{\tau}_{xz}$ (0,a/2,0)	$\bar{\tau}_{yz}$ (a/2,0,0)	$\bar{\tau}_{xy}$ (0,0,±1/2)	$\bar{w}$ (a/2,a/2,0)
			Elasticity Solution			
2	1.260	1.051	0.204	0.194	-0.0722	12.288
	-0.866	-0.824	0.224	0.211	0.0534	
4	0.684	0.628	0.223	0.223	-0.0337	4.079
	-0.649	-0.612	0.223	0.225	0.0328	
10	±0.551	0.477	0.247	0.226	-0.0233	1.512
				0.226	0.0235	
20	±0.541	±0.444	0.255	0.221	∓0.0218	1.129
50	±0.539	±0.433	0.258	0.219	∓0.0214	1.021
100	±0.539	±0.431	0.259	0.219	∓0.0213	1.005
			CLT Solution			
	±0.539	±0.431	0.259	0.219	∓0.0213	1.000

Figure 1. Fle
L/h

Figure 2. Flex
L/h

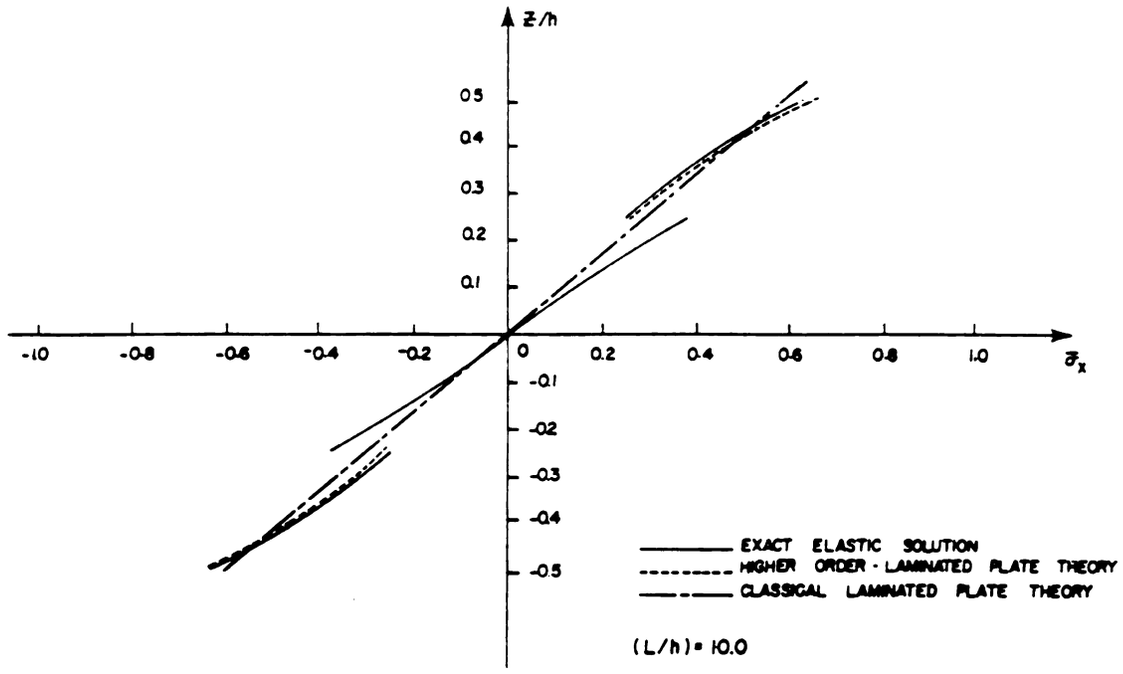

Figure 1. Flexural stress distribution for [+30°, -30°] angle-ply laminate at aspect ratio L/h = 10 [Lo, Christensen, and Wu, 1977].

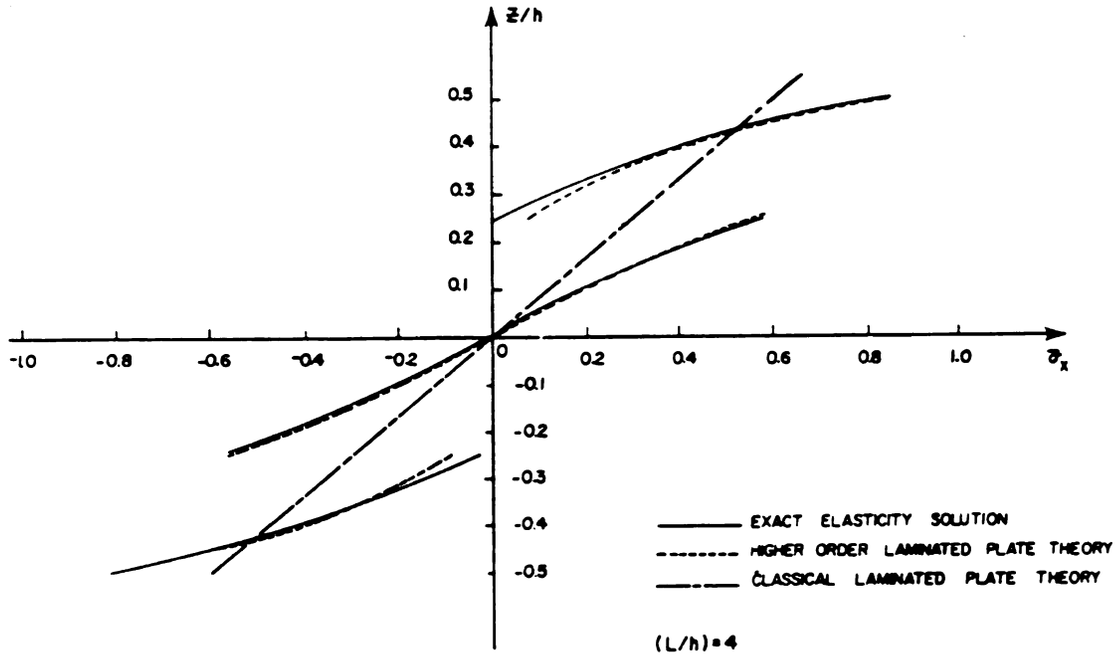

Figure 2. Flexural stress distribution for [+30°, -30°] angle-ply laminate at aspect ratio L/h = 4 [Lo, Christensen, and Wu, 1977].

Figure 3. In-p
= 1

Figure 4. In-pla
= 4

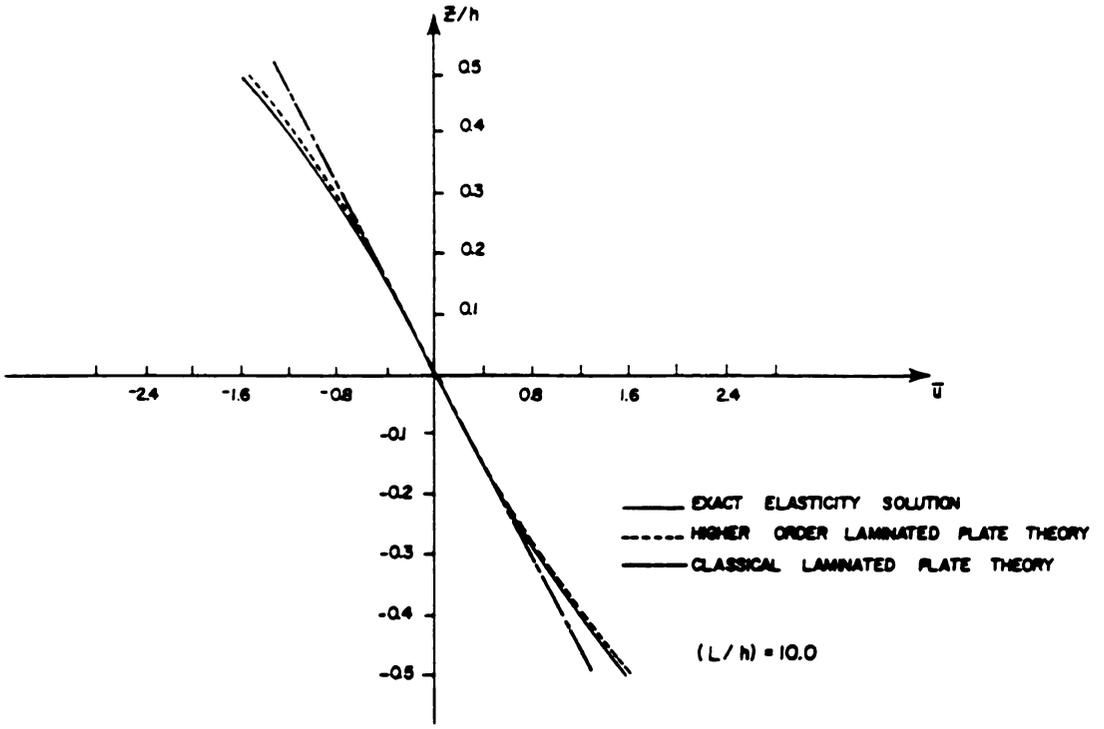

Figure 3. In-plane displacement for [+30°, -30°] angle-ply laminate at aspect ratio L/h = 10 [Lo, Christensen, and Wu, 1977].

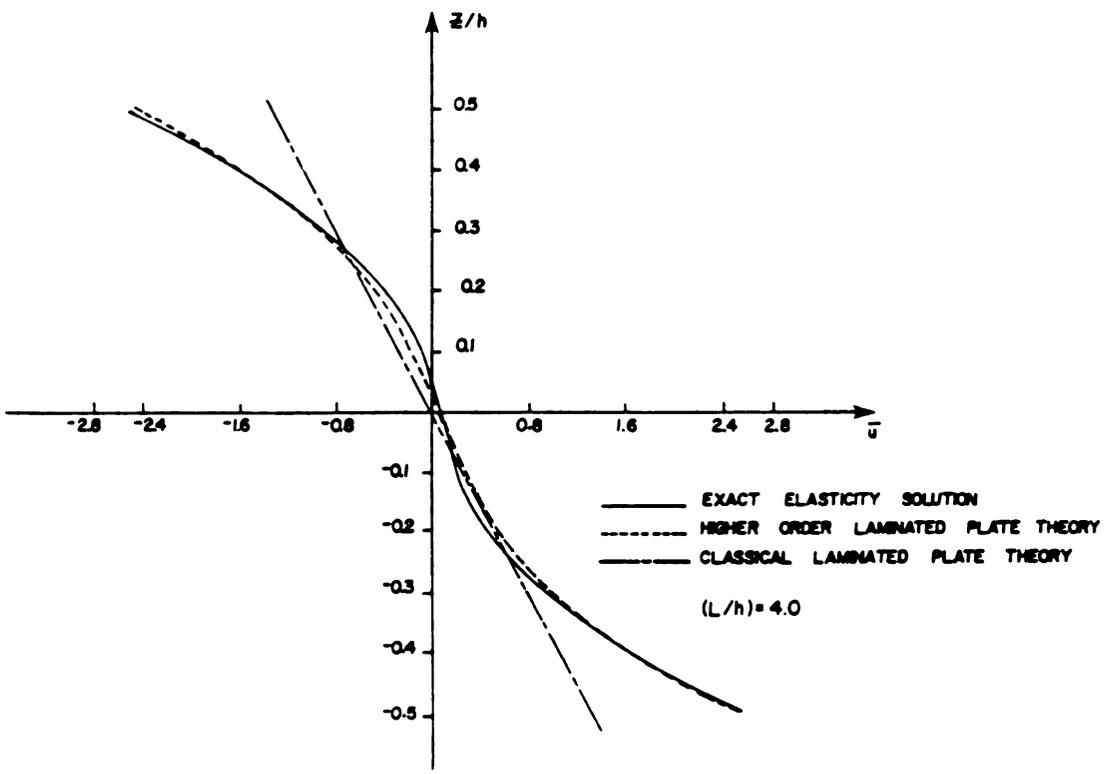

Figure 4. In-plane displacement for [+30°, -30°] angle-ply laminate at aspect ratio L/h = 4 [Lo, Christensen, and Wu, 1977].

Figure 5. Flex
L/h

Figure 6. Flexu
ratio

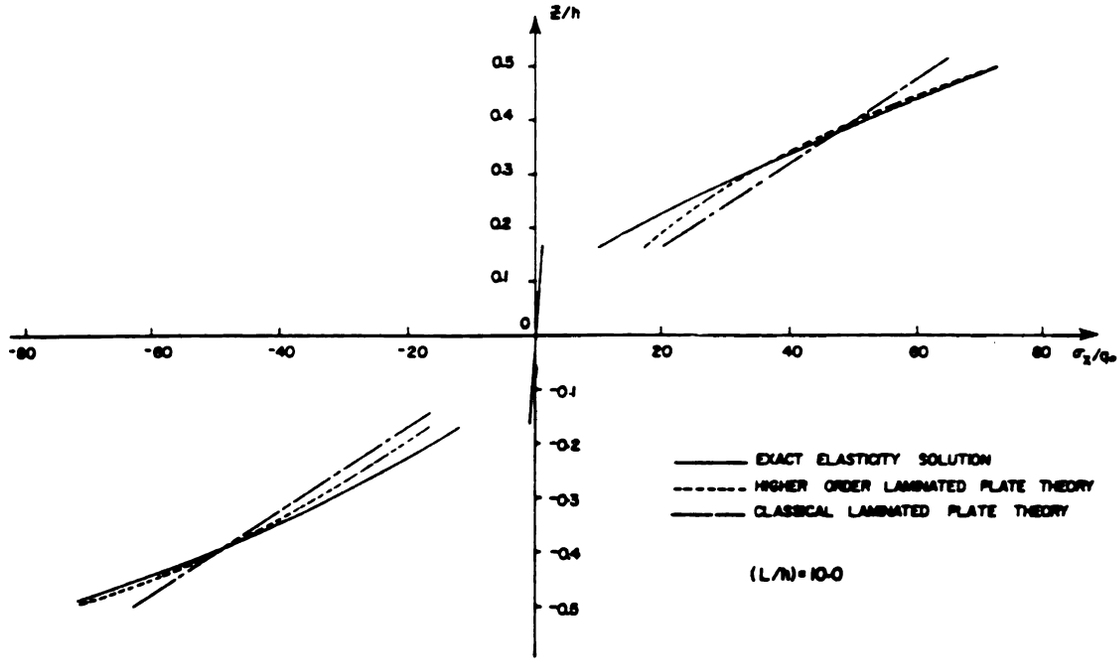

Figure 5. Flexural stress distribution for [0°, 90°, 0°] cross-ply laminate at aspect ratio L/h = 10 [Lo, Christensen, and Wu, 1977].

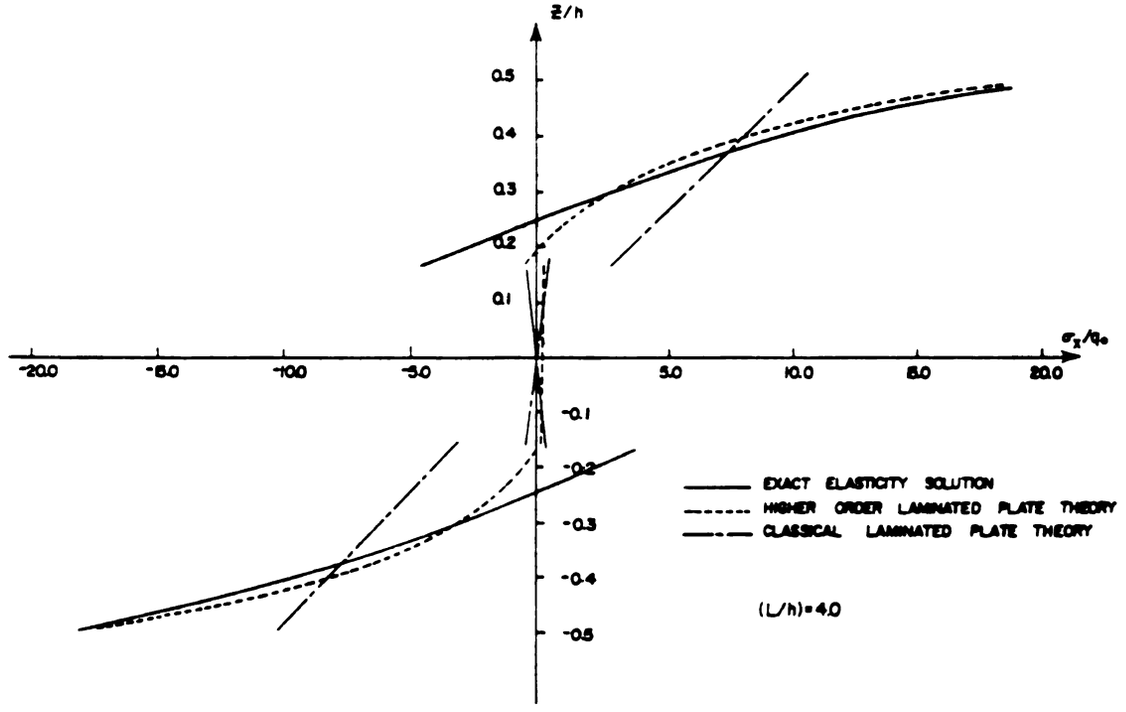

Figure 6. Flexural stress distribution for [0°, 90°, 0°] cross-ply laminate at aspect ratio L/h = 4 [Lo, Christensen, and Wu, 1977].

Figure

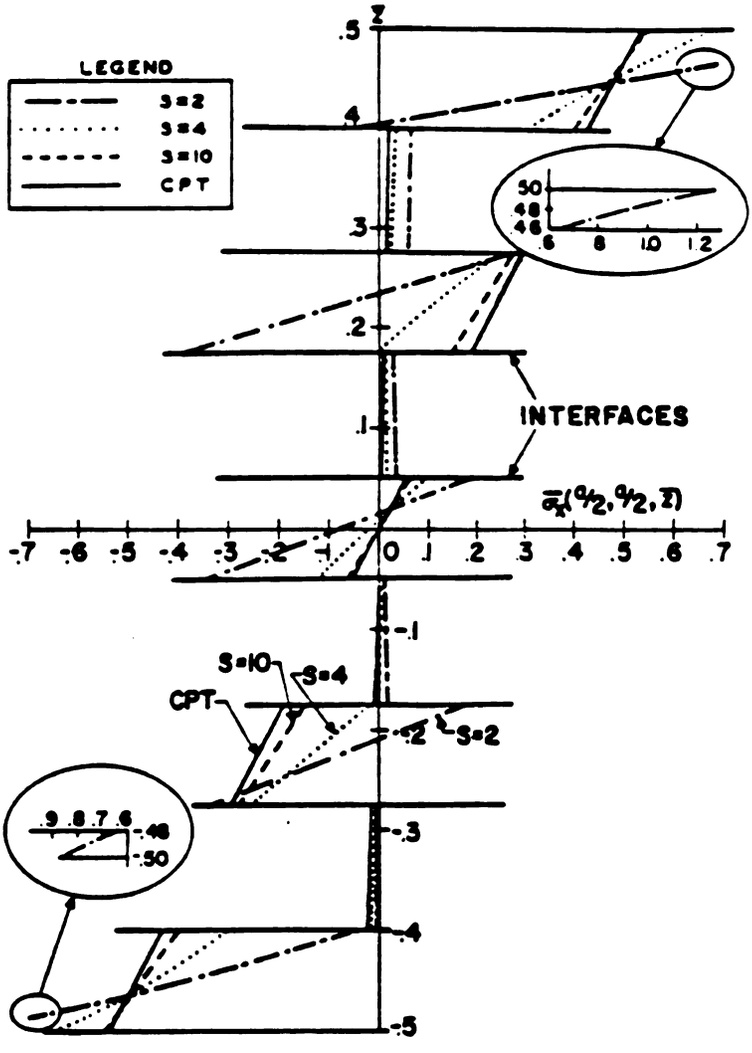

Figure 7. Normal stress distribution in a laminate [Pagano, 1972].

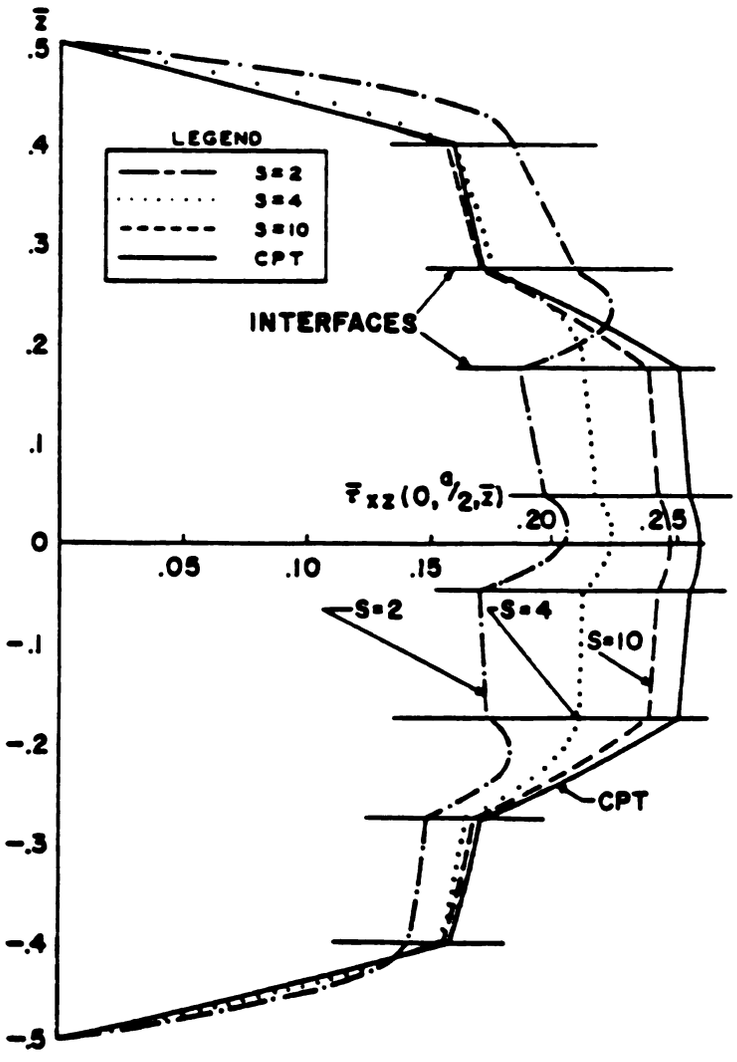

Figure 8. Shear stress distribution in a laminate [Pagano, 1972].

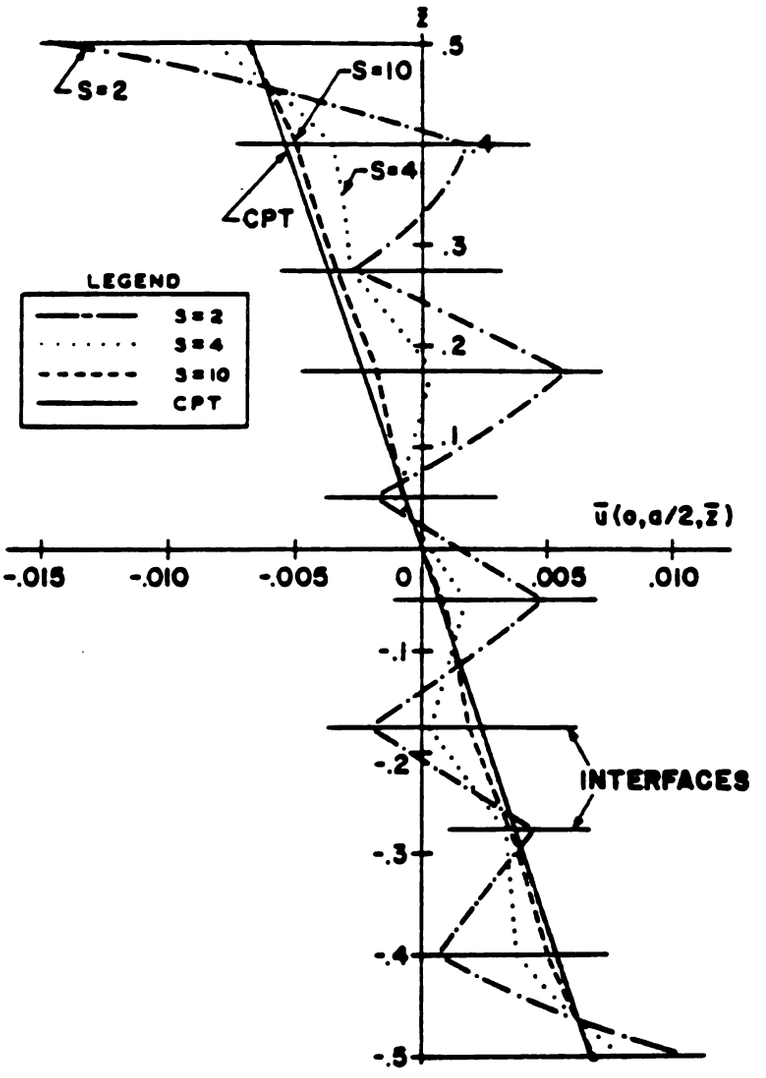

Figure 9. In-plane displacement in a laminate [Pagano, 1972].


16
o o Elasticity Solution
— CLT Solution
1 6
(ksi)

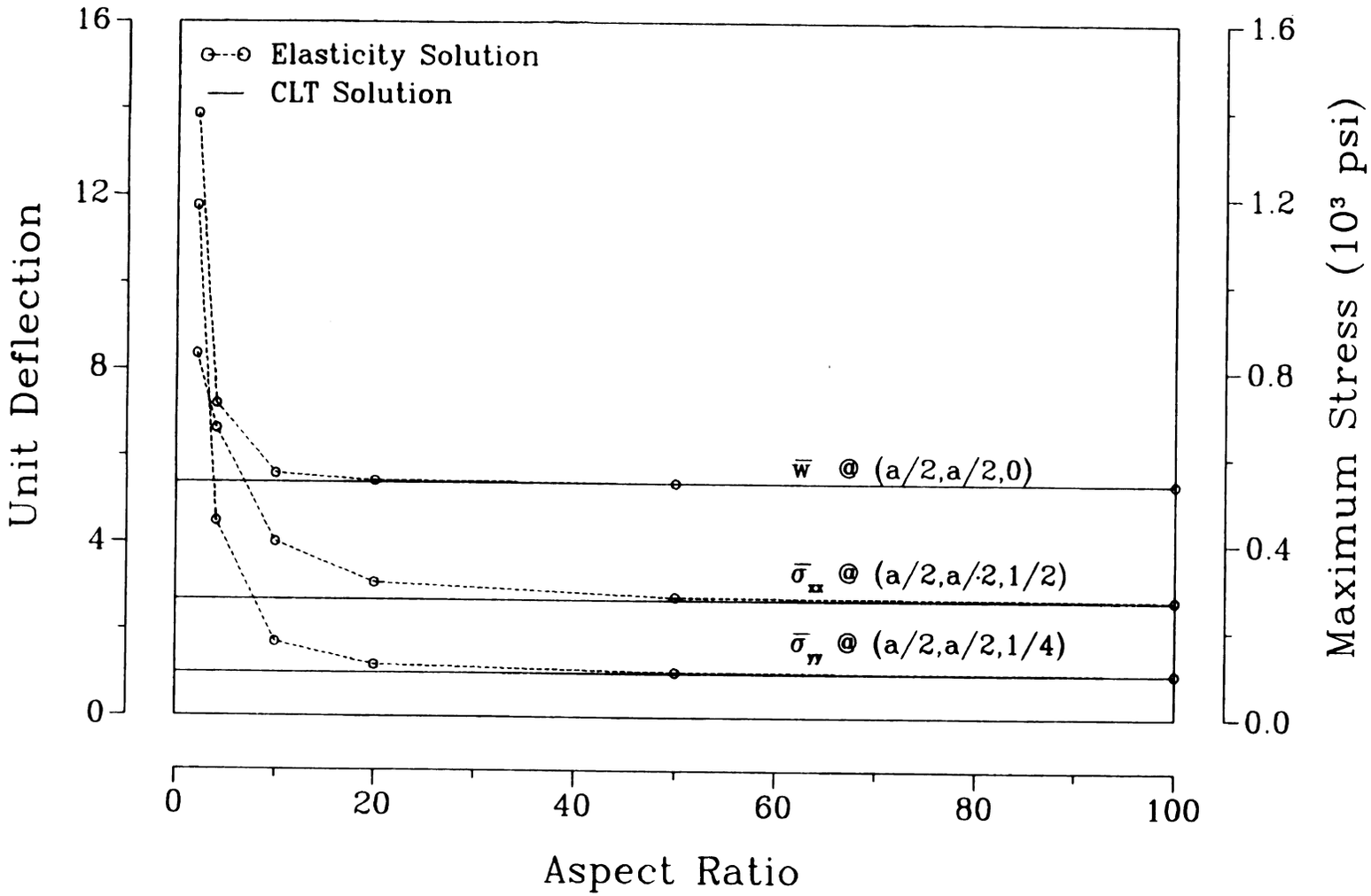

Figure 10. Convergence of exact elasticity solution to respective CLT solution (Data of Pagano [1972]).

validity range

It is se

that the elastic

of advanced c

in accuracy is

ratios. Further

since the analy

development p

Finite E

accuracy and a

FEM to the w

and effort invo

that a sound v

author lacks a

already beyon

speed. Further

(3 Poisson's r

a viscoelastic

dependent beh

nation itself is

of such a visc

approach, in

validity range of CLT, in terms of accuracy.

It is seen in Table 4-1 in the Wood Handbook [Forest Products Laboratory, 1987] that the elastic modulus to shear modulus ratios for wood can be large just as in the case of advanced composites. Improved plate theories seem to be in order. However, the gain in accuracy is very marginal due to the high accuracy of CLT approach at large aspect ratios. Further, CLT has a critical advantage over high-order ones due to its simplicity since the analytical complexity of an elastic foundation will inevitably complicate the development process of a viscoelastic plate theory.

Finite Element Method (FEM) of composite plates is another approach providing accuracy and automation capability. Tong and Suchsland [1992] made an attempt to apply FEM to the warping of wood and wood composite panels. Based on the extensive time and effort involved in the development of their elastic model, it is reasonable to speculate that a sound viscoelastic FEM model may require a level of manpower and time that the author lacks at this time. In addition, the numerical automation of their elastic model is already beyond the capability of today's desktop computers in terms of memory and speed. Further, the elastic FEM model requires 9 independent elastic constants as inputs (3 Poisson's ratios, 3 moduli of elasticity, and 3 shear moduli), and it becomes clear that a viscoelastic counterpart would need as inputs the quantitative descriptions of the time dependent behaviors of these coefficients, which is not yet available and whose determination itself is an extensive and complicated task. Therefore, the practical applicability of such a viscoelastic FEM model may be limited. In contrast a CLT-based viscoelastic approach, in addition to possessing the validity of its elastic foundation at large aspect

ratio, is quite

memory can

of inputs requ

CLT.

field and thus

behavior of

viscoelastic sit

readily availab

applicability -

In summ

number of inp

development of

2.3 Introductio

An intro

CLT-based visc

similar to the

future referenci

2.3.1 Displacer

Displace

of external and

ratio, is quite easy to develop. A personal computer of adequate CPU and moderate memory can carry out the computation automation at a fair speed. The smaller number of inputs required renders it much more powerful.

CLT, by disregarding transverse shear and normal components in its displacement field and thus making it inferior to improved plate theories in terms of defining the behavior of composite plates, offers a blessing property in that the CLT and its viscoelastic sibling are applicable where transverse normal and shear properties are not readily available. Less stringent input requirement by a model characterizes its good applicability - a trait always desired when good accuracy is already at hand.

In summary, the high accuracy at large aspect ratios, ease of analysis, and fewer number of inputs required, justify CLT as being a good elastic foundation for the development of a sound viscoelastic counterpart.

2.3 Introduction to the CLT

An introduction to the elastic CLT will be given prior to the development of the CLT-based viscoelastic plate theory. The representations and derivations, which are quite similar to the work by Liu [1987] and Jones [1975], are intended for convenience in future referencing.

2.3.1 Displacement Field and Strain Field

Displacement field describes how a plate would deform under any combination of external and/or internal forces and moments. Since it establishes a base for a plate

theory, it acc

theory. The c

displacement

theory.

The dis

Hypothesis. It

plane of a lami

is deformed, a

and after lamir

not zero ($\gamma_{xz} \neq$

laminate thickn

normal after l

across the thick

change its leng

condition $\gamma_{xz} =$

across the thic

The bo

thin and few, a

satisfy two ad

straight norma

across the lami

at the bonds.

theory, it accordingly fully governs the development, structure, and accuracy of such a theory. The conditions under which such a description measures well against the actual displacement behavior of plates determine the validity range for the resulting plate theory.

The displacement field assumption for CLT is the familiar and classical Kirchhoff Hypothesis. It assumes that: (1) a line originally straight and perpendicular to the mid-plane of a laminate remains straight and perpendicular to the mid-plane after the laminate is deformed, and (2) such a normal line has a constant length across the thickness before and after laminate deformation, as shown in Figure 11. If transverse shear strains were not zero ($\gamma_{xz} \neq 0$, $\gamma_{yz} \neq 0$), than transverse shear deformation would be present across the laminate thickness, and a straight normal to the mid-plane would not remain straight and normal after laminate deformation, violating assumption (1). If normal strain exists across the thickness ($\epsilon_{zz} \neq 0$), causing plate thickness change, than a straight normal would change its length across laminate thickness, violating assumption (2). Conversely, the condition $\gamma_{xz}=\gamma_{yz}=\epsilon_{zz}=0$ (no transverse shear deformation and no normal deformation across the thickness), must be satisfied in conformation to the Kirchhoff Hypothesis.

The bonds in the laminate can be presumed to be infinitesimally thin if they are thin and few, and may therefore be excluded from consideration. However, they must satisfy two additional requirements in compliance with the Kirchhoff Hypothesis. A straight normal, remaining so under deformation, implies continuous displacements across the laminate thickness, and thus requires that there be no relative interlamina slip at the bonds. Absence of deformation across the thickness requires that the bonds be

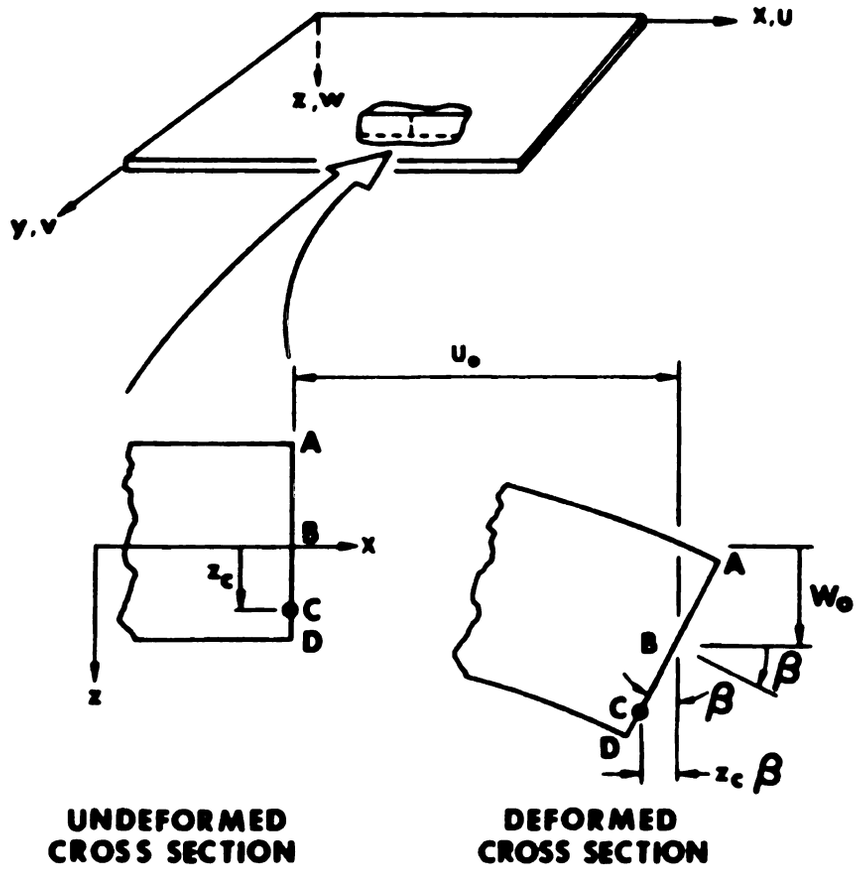

Figure 11. Geometry of deformation in the x-z plane [Jones, 1976].

non-shear-de

The la

representation

direction fro

remains straig

$u_c = u_0 - z_c \sin$

Line *ABCD* al

the slope of th

$$\tan\beta = \frac{\partial w_0}{\partial x}$$

Small displacem

$\sin\beta = \tan\beta$

Therefore, the

$u = u_0 - z \sin$

By similar reas

$$v = v_0 - z \frac{\partial w}{\partial y}$$

non-shear-deformable, as well.

The laminate cross section in the xz plane shown in Figure 11 is a graphic representation of the Kirchhoff Hypothesis. The displacement of point B in the x-direction from the undeformed to the deformed mid-plane is u_o. Since line $ABCD$ remains straight under deformation, the x-direction displacement for point C is,

$$u_c = u_0 - z_c \sin\beta \qquad 2.3.1$$

Line $ABCD$ also remains normal to the mid-plane under deformation, indicating $\tan\beta$ is the slope of the mid-plane in the x-direction, that is,

$$\tan\beta = \frac{\partial w_0}{\partial x} \qquad 2.3.2$$

Small displacement assumption suggests that at very small β, the following relations hold

$$\sin\beta \approx \tan\beta = \frac{\partial w_0}{\partial x} \qquad 2.3.3$$

Therefore, the x-direction displacement, u, at any z across the laminate thickness is

$$u = u_0 - z\sin\beta \approx u_0 - z\frac{\partial w_0}{\partial x} \qquad 2.3.4$$

By similar reasoning, the y-direction displacement, v, is

$$v \approx v_0 - z\frac{\partial w_0}{\partial y} \qquad 2.3.5$$

Therefore, th

$$u = u_0 - z$$

$$v = v_0 - z$$

$$w_0 = w_0(x, y)$$

Since

earlier, the tot

ticity strain-dis

$$\varepsilon_{xx} = \frac{\partial u}{\partial x}$$

$$\varepsilon_{yy} = \frac{\partial v}{\partial y}$$

$$\gamma_{xy} = \frac{\partial u}{\partial y} +$$

three plane stra

$$\varepsilon_{xx} = \frac{\partial u_0}{\partial x} -$$

$$\varepsilon_{yy} = \frac{\partial v_0}{\partial y} -$$

$$\gamma_{xy} = \frac{\partial u_0}{\partial y} +$$

In matrix notati

Therefore, the displacement field is

$$u = u_0 - z\frac{\partial w_0}{\partial x}$$

$$v = v_0 - z\frac{\partial w_0}{\partial y} \qquad 2.3.6$$

$$w_0 = w_0(x, y)$$

Since $\gamma_{xz}=\gamma_{yz}=\epsilon_{zz}=0$ by the virtue of the Kirchhoff Hypothesis as discussed earlier, the total of 6 strains are reduced to 3 plane strains ϵ_{xx}, ϵ_{yy}, and γ_{xy}. By linear elasticity strain-displacement relation

$$\varepsilon_{xx} = \frac{\partial u}{\partial x}$$

$$\varepsilon_{yy} = \frac{\partial v}{\partial y} \qquad 2.3.7$$

$$\gamma_{xy} = \frac{\partial u}{\partial y} + \frac{\partial v}{\partial x} \quad ,$$

three plane strains could subsequently be obtained as

$$\varepsilon_{xx} = \frac{\partial u_0}{\partial x} - z\frac{\partial^2 w_0}{\partial x^2}$$

$$\varepsilon_{yy} = \frac{\partial v_0}{\partial y} - z\frac{\partial^2 w_0}{\partial y^2} \qquad 2.3.8$$

$$\gamma_{xy} = \frac{\partial u_0}{\partial y} + \frac{\partial v_0}{\partial x} - 2z\frac{\partial^2 w_0}{\partial x \partial y}$$

In matrix notation, the strain field is

$$\begin{Bmatrix} \varepsilon_{xx} \\ \varepsilon_{yy} \\ \gamma_{xy} \end{Bmatrix} = \begin{Bmatrix} \frac{\partial u_0}{\partial x} \\ \frac{\partial v_0}{\partial y} \\ \frac{\partial u_0}{\partial y} \end{Bmatrix}$$

or in short

$$\{\varepsilon\} = \{\varepsilon^0\} +$$

where the firs
plane as denc
rotations by
are fully dete
the coordina
translations

2.3.2 Elastic

With
by the elast
Kirchhoff Hy
stress in the
no transverse
three nonzero

$$\begin{Bmatrix} \varepsilon_{xx} \\ \varepsilon_{yy} \\ \gamma_{xy} \end{Bmatrix} = \begin{Bmatrix} \dfrac{\partial u_0}{\partial x} \\ \dfrac{\partial v_0}{\partial y} \\ \dfrac{\partial u_0}{\partial y} + \dfrac{\partial v_0}{\partial x} \end{Bmatrix} + z \begin{Bmatrix} -\dfrac{\partial^2 w_0}{\partial x^2} \\ -\dfrac{\partial^2 w_0}{\partial y^2} \\ -2\dfrac{\partial^2 w_0}{\partial x \partial y} \end{Bmatrix} = \begin{Bmatrix} \varepsilon^0{}_{xx} \\ \varepsilon^0{}_{yy} \\ \gamma^0{}_{xy} \end{Bmatrix} + z \begin{Bmatrix} \kappa_x \\ \kappa_y \\ \kappa_{xy} \end{Bmatrix} \qquad 2.3.9$$

or in short

$$\{\varepsilon\} = \{\varepsilon^0\} + z\{\kappa\} \qquad 2.3.10$$

where the first term on the right hand side is the collection of plane strains of the mid-plane as denoted by the zero superscript, the second term is the collection of curvature rotations by the mid-plane as denoted by κ multiplied by coordinate position z. Strains are fully determined by the mid-plane motions (its stretch, shear, and its rotation) and the coordinate location z as they are the sum of the mid-plane strains and linear translations of the mid-plane curvature rotations at respective z coordinate positions.

2.3.2 Elastic Lamina Constitutive Equations - Stress-Strain Relations

With the strain field determined, the corresponding stress field could be obtained by the elastic constitutive relations (stress-strain relations). A laminate under the Kirchhoff Hypothesis results in $\tau_{xz}=\tau_{yz}=\sigma_{zz}=0$ (no transverse shear stresses and normal stress in the thickness direction) due to $\gamma_{xz}=\gamma_{yz}=\epsilon_{zz}=0$ (no transverse shear strains and no transverse normal strains as implied by the Kirchhoff Hypothesis). The remaining three nonzero stresses, σ_{xx}, σ_{yy}, and τ_{xy}, are confined within a plane geometry, char-

acterizing a p

an orthotropi

$$\begin{Bmatrix} \sigma_{11} \\ \sigma_{22} \\ \tau_{12} \end{Bmatrix} = \begin{bmatrix} Q_{1} \\ Q_{12} \\ 0 \end{bmatrix}$$

or abbreviated

$$\{\sigma\} = [Q]\{\varepsilon$$

where $[Q]$, th

constants, E_{11},

$$[Q] = \begin{bmatrix} \frac{E}{1-\nu} \\ \frac{\nu_{12}E}{1-\nu} \\ 0 \end{bmatrix}$$

The four zero c

principle coord

and cross grain

For mo

schemes, the m

with prescribed

coordinates dev

acterizing a plane stress state. As such, the corresponding stress-strain relations are, for an orthotropic lamina or layer in its material principle coordinates *1-2*,

$$\begin{Bmatrix} \sigma_{11} \\ \sigma_{22} \\ \tau_{12} \end{Bmatrix} = \begin{bmatrix} Q_{11} & Q_{12} & 0 \\ Q_{12} & Q_{22} & 0 \\ 0 & 0 & Q_{66} \end{bmatrix} \begin{Bmatrix} \varepsilon_{11} \\ \varepsilon_{22} \\ \gamma_{12} \end{Bmatrix} \qquad 2.3.11$$

or abbreviated

$$\{\sigma\} = [Q]\{\varepsilon\} \qquad 2.3.12$$

where $[Q]$, the reduced stiffnesses, are defined in terms of four elastic engineering constants, E_{11}, E_{22}, G_{12}, ν_{12}.

$$[Q] = \begin{bmatrix} \dfrac{E_{11}}{1-\nu_{12}\nu_{21}} & \dfrac{\nu_{21}E_{11}}{1-\nu_{12}\nu_{21}} & 0 \\ \dfrac{\nu_{12}E_{22}}{1-\nu_{12}\nu_{21}} & \dfrac{E_{22}}{1-\nu_{12}\nu_{21}} & 0 \\ 0 & 0 & G_{12} \end{bmatrix} \qquad 2.3.13$$

The four zero components resulted from stress-strain relations being described in material principle coordinates *1-2* which in the case of wood is respectively the grain direction and cross grain direction.

For most laminates such as those of cross lamination and angled lamination schemes, the material principle coordinates of constituent laminas do not always coincide with prescribed laminate coordinates. Some constituent laminas have their principle coordinates deviate from the prescribed laminate coordinates by arbitrary angles. Since

the stress-str

defining the

For a

$$\begin{Bmatrix} \sigma_{xx} \\ \sigma_{yy} \\ \tau_{xy} \end{Bmatrix}_k = \begin{bmatrix} \overline{Q} \\ \overline{Q} \\ \overline{Q} \end{bmatrix}$$

or in short

$$\{\sigma\}_k = [\overline{Q}]_k$$

The $[\overline{Q}]$ are tr

the reduced sti

the following

$$\overline{Q_{11}} = Q_{11} \cos$$

$$\overline{Q_{22}} = Q_{11} \sin$$

$$\overline{Q_{12}} = (Q_{11} +$$

$$\overline{Q_{66}} = (Q_{11} +$$

$$\overline{Q_{16}} = (Q_{11} -$$

$$\overline{Q_{26}} = (Q_{11} -$$

where θ is the

coordinates, a

the stress-strain relations of all laminas must be defined in a unified coordinate system, defining the stress-strain relations in arbitrary x-y coordinates is necessary.

For a lamina k, such stress-strain relations in arbitrary coordinates x-y are

$$\begin{Bmatrix} \sigma_{xx} \\ \sigma_{yy} \\ \tau_{xy} \end{Bmatrix}_k = \begin{bmatrix} \overline{Q}_{11} & \overline{Q}_{12} & \overline{Q}_{16} \\ \overline{Q}_{12} & \overline{Q}_{22} & \overline{Q}_{26} \\ \overline{Q}_{16} & \overline{Q}_{26} & \overline{Q}_{66} \end{bmatrix}_k \begin{Bmatrix} \varepsilon_{xx} \\ \varepsilon_{yy} \\ \gamma_{xy} \end{Bmatrix}_k \qquad 2.3.14$$

or in short

$$\{\sigma\}_k = [\overline{Q}]_k \{\varepsilon\}_k \qquad 2.3.15$$

The $[\overline{Q}]$ are transformed reduced stiffnesses for arbitrary x-y coordinates as opposed to the reduced stiffnesses $[Q]$ for 1-2 material principle coordinates. The two are related by the following transformation equations as found in Liu [1987] and Sims [1972],

$$\begin{aligned}
\overline{Q_{11}} &= Q_{11}\cos^4\theta + 2(Q_{12}+2Q_{66})\sin^2\theta\cos^2\theta + Q_{22}\sin^4\theta \\
\overline{Q_{22}} &= Q_{11}\sin^4\theta + 2(Q_{12}+2Q_{66})\sin^2\theta\cos^2\theta + Q_{22}\cos^4\theta \\
\overline{Q_{12}} &= (Q_{11}+Q_{22}-4Q_{66})\sin^2\theta\cos^2\theta + Q_{12}(\sin^4\theta+\cos^4\theta) \\
\overline{Q_{66}} &= (Q_{11}+Q_{22}-2Q_{12}-2Q_{66})\sin^2\theta\cos^2\theta + Q_{66}(\sin^4\theta+\cos^4\theta) \\
\overline{Q_{16}} &= (Q_{11}-Q_{12}-2Q_{66})\sin\theta\cos^3\theta + (Q_{12}-Q_{22}+2Q_{66})\sin^3\theta\cos\theta \\
\overline{Q_{26}} &= (Q_{11}-Q_{12}-2Q_{66})\sin^3\theta\cos\theta + (Q_{12}-Q_{22}+2Q_{66})\sin\theta\cos^3\theta
\end{aligned} \qquad 2.3.16$$

where θ is the angle by which x-y coordinates rotate clock-wise to 1-2 material principle coordinates, as illustrated in Figure 12.

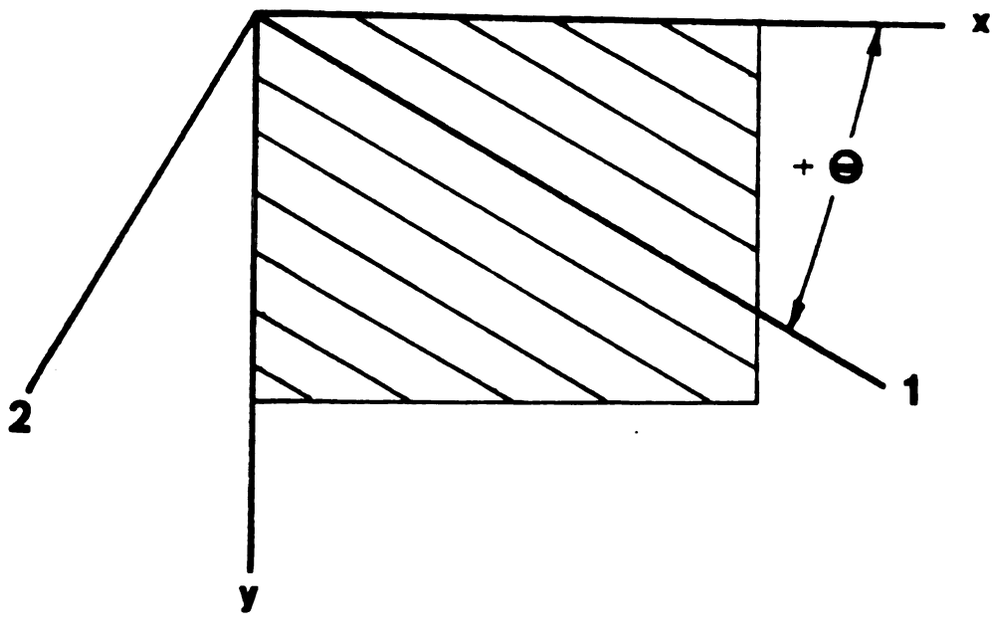

Figure 12. Relation of material principle coordinates *1-2* with *x-y* coordinates.

2.3.3 Strain

The c

variation of s

correspondin

coordinates) i

$$\begin{Bmatrix} \sigma_{xx} \\ \sigma_{yy} \\ \tau_{xy} \end{Bmatrix}_k = \begin{bmatrix} \overline{Q} \\ \overline{Q} \\ \overline{Q} \end{bmatrix}$$

or in short

$$\{\sigma\}_k = [\overline{Q}]$$

which in tu

difference o

does not ne

though the s

are characte

2.3.4 Resul

The

acting on the

1-2 with x-y

2.3.3 Strain and Stress Variations in a Laminate

The derived strain field verifies the Kirchhoff Hypothesis by implying a linear variation of strains through thickness as characterized by Eq's. 2.3.7 and 2.3.9. The corresponding stress field based on Eq. 2.3.14 (linear stress-strain relations in x-y coordinates) is

$$\begin{Bmatrix} \sigma_{xx} \\ \sigma_{yy} \\ \tau_{xy} \end{Bmatrix}_k = \begin{bmatrix} \overline{Q}_{11} & \overline{Q}_{12} & \overline{Q}_{16} \\ \overline{Q}_{12} & \overline{Q}_{22} & \overline{Q}_{26} \\ \overline{Q}_{16} & \overline{Q}_{26} & \overline{Q}_{66} \end{bmatrix}_k \left\{ \begin{Bmatrix} \varepsilon^0{}_{xx} \\ \varepsilon^0{}_{yy} \\ \gamma^0{}_{xy} \end{Bmatrix} + z \begin{Bmatrix} \kappa_x \\ \kappa_y \\ \kappa_{xy} \end{Bmatrix} \right\} \qquad 2.3.17$$

or in short

$$\{\sigma\}_k = [\overline{Q}]_k \{\{\varepsilon^0\} + z\{\kappa\}\} \qquad 2.3.18$$

which in turn follows a linear variation across the k lamina. However, due to the difference of transformed reduced stiffnesses among constituent laminas, the stress field does not necessarily vary linearly across interlamina boundaries in a laminate, even though the strain field behaves so. Such linear variation by strain field and stress field are characteristic of CLT, as shown in Figure 13.

2.3.4 Resultant Laminate Forces and Moments

The stresses in a laminate must be balanced with resultant forces and moments acting on the laminate by integration of stresses across laminate thickness. Resultant force 1-2 with x-y coordinates. N_x and moment M_x are related to stress σ_x by integrating σ_x over

thickness h c

$$N_x = \int_{-h/2}^{h/2} \sigma_{xx}$$

$$M_x = \int_{-h/2}^{h/2} \sigma_{xx}$$

in which the

section, respec

laminate as sh

in terms of str

$$\begin{Bmatrix} N_x \\ N_y \\ N_{xy} \end{Bmatrix} = \int_{-h/2}^{h/2}$$

or

$$\{N\} = \int_{-h/2}^{h/2} \{$$

Similarly, re

$$\begin{Bmatrix} M_x \\ M_y \\ M_{xy} \end{Bmatrix} = \int_{-h/2}^{h/2}$$

or

thickness h of a laminate as follows,

$$N_x = \int_{-h/2}^{h/2} \sigma_{xx}\, dx$$
$$M_x = \int_{-h/2}^{h/2} \sigma_{xx} z\, dx \qquad 2.3.19$$

in which the units for N_x and M_x are force and moment per unit length of the cross section, respectively. By applying 2.3.19 to all three stresses, σ_x, σ_y, and τ_{xy}, in a n-layer laminate as shown in Figure 14 the entire collection of resultant forces can be defined in terms of stresses:

$$\begin{Bmatrix} N_x \\ N_y \\ N_{xy} \end{Bmatrix} = \int_{-h/2}^{h/2} \begin{Bmatrix} \sigma_{xx} \\ \sigma_{yy} \\ \tau_{xy} \end{Bmatrix} dz = \sum_{k=1}^{n} \int_{z_{k-1}}^{z_k} \begin{Bmatrix} \sigma_{xx} \\ \sigma_{yy} \\ \tau_{xy} \end{Bmatrix}_k dz \qquad 2.3.20$$

or

$$\{N\} = \int_{-h/2}^{h/2} \{\sigma\}\, dz = \sum_{k=1}^{n} \int_{z_{k-1}}^{z_k} \{\sigma\}_k\, dz \qquad 2.3.21$$

Similarly, resultant moments are defined as

$$\begin{Bmatrix} M_x \\ M_y \\ M_{xy} \end{Bmatrix} = \int_{-h/2}^{h/2} \begin{Bmatrix} \sigma_{xx} \\ \sigma_{yy} \\ \tau_{xy} \end{Bmatrix} z\, dz = \sum_{k=1}^{n} \int_{z_{k-1}}^{z_k} \begin{Bmatrix} \sigma_{xx} \\ \sigma_{yy} \\ \tau_{xy} \end{Bmatrix}_k z\, dz \qquad 2.3.22$$

or

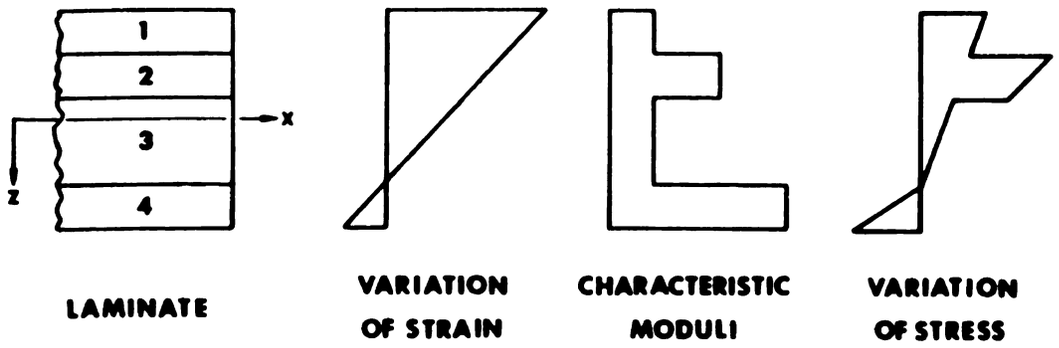

Figure 13. Hypothetical variations of strain and stress across laminate thickness [Jones, 1976].

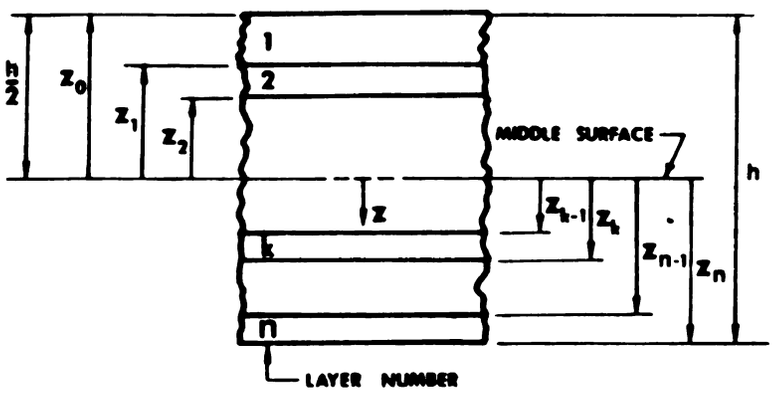

Figure 14. Geometry of a *n*-layer laminate [Jones, 1976].

$$\{M\} = \int_{-h/2}^{h/2}$$

where z_k and

in Figure 14.

after the integ

depicted in F

Substi

Eq's. 2.3.21

$$\{N\} = \sum_{k=1}^{n} \int_{z_{k-}}^{z_k}$$

$$\{M\} = \sum_{k=1}^{n} \int_{z_k}^{z}$$

The reduced

therefore can

$$\{N\} = \sum_{k=1}^{n} [$$

$$\{M\} = \sum_{k=1}^{n} [$$

As we recall,

$$\{M\} = \int_{-h/2}^{h/2} \{\sigma\} z\, dz = \sum_{k=1}^{n} \int_{z_{k-1}}^{z_k} \{\sigma\}_k z\, dz \qquad 2.3.33$$

where z_k and z_{k-1} determine the z position of lamina k in the x-y-z coordinates as defined in Figure 14. The resultant forces and moments become independent of the z coordinate after the integration, but are functions of x and y. Their positions and orientations are depicted in Figures 15 and 16.

Substituting stress-strain relations of Eq. 2.3.15 into resultant-stress relations of Eq's. 2.3.21 and 2.3.23 generates resultant-strain relations

$$\begin{aligned} \{N\} &= \sum_{k=1}^{n} \int_{z_{k-1}}^{z_k} [\bar{Q}]_k \{\varepsilon\}_k \quad dz \\ \{M\} &= \sum_{k=1}^{n} \int_{z_{k-1}}^{z_k} [\bar{Q}]_k \{\varepsilon\}_k \, z dz \end{aligned} \qquad 2.3.24$$

The reduced stiffness matrix is considered constant within each constituent lamina, and therefore can be taken out of the integration to generate

$$\begin{aligned} \{N\} &= \sum_{k=1}^{n} [\bar{Q}]_k \int_{z_{k-1}}^{z_k} \{\{\varepsilon^0\} + z\{\kappa\}\} \quad dz = \sum_{k=1}^{n} [\bar{Q}]_k \left\{ \int_{z_{k-1}}^{z_k} \{\varepsilon^0\} \quad dz + \int_{z_{k-1}}^{z_k} \{\kappa\} \; z dz \right\} \\ \{M\} &= \sum_{k=1}^{n} [\bar{Q}]_k \int_{z_{k-1}}^{z_k} \{\{\varepsilon^0\} + z\{\kappa\}\} z dz = \sum_{k=1}^{n} [\bar{Q}]_k \left\{ \int_{z_{k-1}}^{z_k} \{\varepsilon^0\} z dz + \int_{z_{k-1}}^{z_k} \{\kappa\} z^2 dz \right\} \end{aligned} \qquad 2.3.25$$

As we recall, $\{\varepsilon^0\}$ and $\{\kappa\}$ are mid-plane strains and curvatures and thus are independent

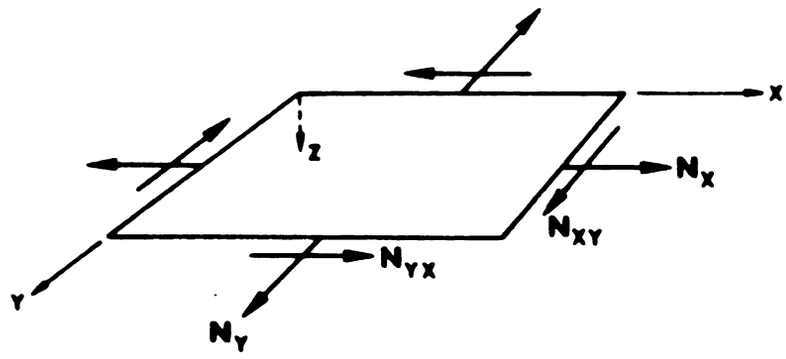

Figure 15. In-plane forces on a flat laminate [Jones, 1976].

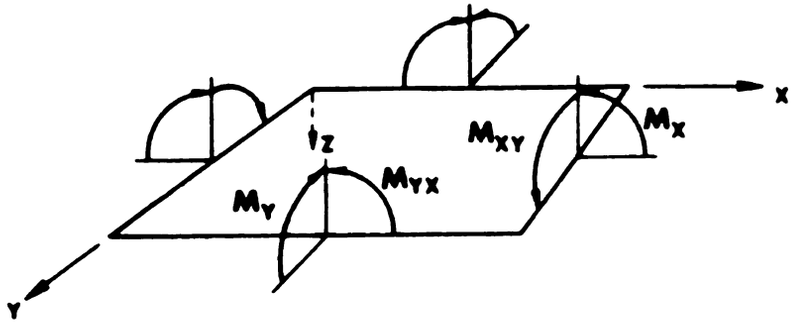

Figure 16. Moments on a flat laminate [Jones, 1976].

of z. They

the above r

$$\{N\} = \sum_{k}$$

$$+ \sum_{k}$$

$$\{M\} = \left[\right.$$

$$+ \left[\right.$$

Further, s

$$\int_{z_{k-1}}^{z_k} dz$$

$$\int_{z_{k-1}}^{z_k} z \, dz$$

$$\int_{z_{k-1}}^{z_k} z^2 \, dz$$

We obtai

of z. They can be positioned outside of the summation and integration over z to simplify the above relations to

$$\{N\} = \left[\sum_{k=1}^{n} [\bar{Q}]_k \int_{z_{k-1}}^{z_k} dz \right] \{\varepsilon^0\} + \left[\sum_{k=1}^{n} [\bar{Q}]_k \int_{z_{k-1}}^{z_k} z\, dz \right] \{\kappa\} \qquad 2.3.26$$

$$\{M\} = \left[\sum_{k=1}^{n} [\bar{Q}]_k \int_{z_{k-1}}^{z_k} z\ dz \right] \{\varepsilon^0\} + \left[\sum_{k=1}^{n} [\bar{Q}]_k \int_{z_{k-1}}^{z_k} z^2 dz \right] \{\kappa\}$$

Further, since

$$\int_{z_{k-1}}^{z_k} dz = (z_k - z_{k-1})$$

$$\int_{z_{k-1}}^{z_k} z\ dz = \frac{1}{2}(z_k^2 - z_{k-1}^2) \qquad 2.3.27$$

$$\int_{z_{k-1}}^{z_k} z^2 dz = \frac{1}{3}(z_k^3 - z_{k-1}^3)$$

we obtain

$$\{N\} = \left[\sum_{k=} \right.$$

$$+ \left[\sum_{k=} \right.$$

$$\{M\} = \left[\right.$$

$$+ \left[\right.$$

or

$$\{N\} = [A$$

$$\{M\} = [B$$

which can

$$\begin{Bmatrix} N \\ \cdots \\ M \end{Bmatrix} = \left[\right.$$

or

$$\{N\} = \left[\sum_{k=1}^{n} [\bar{Q}]_k \quad (z_k - z_{k-1}) \right] \{\varepsilon^0\} + \left[\sum_{k=1}^{n} [\bar{Q}]_k \frac{1}{2}(z_k^2 - z_{k-1}^2) \right] \{\kappa\}$$

$$\{M\} = \left[\sum_{k=1}^{n} [\bar{Q}]_k \frac{1}{2}(z_k^2 - z_{k-1}^2) \right] \{\varepsilon^0\} + \left[\sum_{k=1}^{n} [\bar{Q}]_k \frac{1}{3}(z_k^3 - z_{k-1}^3) \right] \{\kappa\} \qquad 2.3.28$$

or

$$\begin{aligned} \{N\} &= [A]\{\varepsilon^0\} + [B]\{\kappa\} \\ \{M\} &= [B]\{\varepsilon^0\} + [D]\{\kappa\} \end{aligned} \qquad 2.3.29$$

which can be jointly expressed as

$$\begin{Bmatrix} N \\ -- \\ M \end{Bmatrix} = \begin{bmatrix} A & | & B \\ -- & & -- \\ B & | & D \end{bmatrix} \begin{Bmatrix} \varepsilon^0 \\ -- \\ \kappa \end{Bmatrix} \qquad 2.3.30$$

or

$$\begin{Bmatrix} N_x \\ N_y \\ N_{xy} \\ M_x \\ M_y \\ M_{xy} \end{Bmatrix} = \begin{bmatrix} A_{11} & A_{12} & A_{16} & B_{11} & B_{12} & B_{16} \\ A_{12} & A_{22} & A_{26} & B_{12} & B_{22} & A_{26} \\ A_{16} & A_{26} & A_{66} & B_{16} & B_{26} & B_{66} \\ B_{11} & B_{12} & B_{16} & D_{11} & D_{12} & D_{16} \\ B_{12} & B_{22} & B_{26} & D_{12} & D_{22} & D_{26} \\ B_{16} & B_{26} & B_{66} & D_{16} & D_{26} & D_{66} \end{bmatrix} \begin{Bmatrix} \varepsilon^0_{xx} \\ \varepsilon^0_{yy} \\ \varepsilon^0_{xy} \\ \kappa_x \\ \kappa_y \\ \kappa_{xy} \end{Bmatrix} \qquad 2.3.31$$

where

$$A_{ij} = \sum_{k=1}^{n} (\overline{Q_{ij}})_k (z_k - z_{k-1})$$

$$B_{ij} = \frac{1}{2} \sum_{k=1}^{n} (\overline{Q_{ij}})_k (z_k^2 - z_{k-1}^2) \qquad 2.3.32$$

$$D_{ij} = \frac{1}{3} \sum_{k=1}^{n} (\overline{Q_{ij}})_k (z_k^3 - z_{k-1}^3)$$

The derived equations (Eq's. 3.3.30 - 2.3.32) establish how the resultant forces and moments acting on a laminate are related to the strains and curvatures at the mid-plane surface of the laminate deformed under such forces and moments. Usually called the governing equations of CLT, they fully dictate the mechanical behavior of a laminate under the Kirchhoff Hypothesis.

The relating matrix is called the general stiffness matrix because of its reflection on the stiffnesses of a laminate. Its components as seen in Eq. 3.3.31 are summations over all laminas of the product of each lamina's transformed reduced stiffnesses and the

lamina's z p

lamina are f

its orientatio

determined b

their geomet

The *[*

distinct impli

the extensiona

only, and are

with curvatur

suggests that

would necessa

twist under ju

ted to bending

plane, that is

stiffnesses.

2.3.5 Hygro

Previ

from mecha

This mere m

prominent.

lamina's z position characteristics. Due to that the transformed reduced stiffnesses of a lamina are functions of the lamina's four engineering constants, E_{11}, E_{22}, G_{12}, ν_{12}, plus its orientation θ with regard to the laminate coordinates. The stiffness matrix is fully determined by the engineering properties (E_{11}, E_{22}, G_{12}, ν_{12}) of all constituent laminas and their geometric positions (coordinate orientation θ and z coordinate position).

The ***[A]***, ***[B]***, and ***[D]*** in the combined stiffness matrix shown in Eq. 3.3.30 have distinct implications. Relating only plane forces $\{N\}$ to plane strains $\{\epsilon^0\}$, ***[A]*** are called the extensional stiffnesses. ***[D]*** relates bending moments $\{M\}$ to bending curvatures $\{\kappa\}$ only, and are thus called the bending stiffnesses. ***[B]*** by bridging both plane forces $\{N\}$ with curvatures $\{\kappa\}$, and plane strains $\{\epsilon^0\}$ with bending moments $\{M\}$, however, suggests that extensional plane forces $\{N\}$ applied to a laminate with a nonzero ***[B]*** term would necessarily generate a curvature $\{\kappa\}$ term, that is, the laminate would bend and/or twist under just extensional plane forces. In addition, such a laminate can not be subjected to bending moments $\{M\}$ without at the same time experiencing extension at the mid-plane, that is, plane strains $\{\epsilon^0\}$ would not be zero. ***[B]*** are therefore named the coupling stiffnesses.

2.3.5 Hygroscopic Strains and Stress Analysis

Previous analysis of CLT considers mechanical strains, that are strains resulting from mechanical forces and moments, while strains from other sources are disregarded. This mere mechanical analysis does not suffice in cases where non-mechanical strains are prominent. As is the case with laminates made of hygroscopic materials such as wood

and wood-b

changes in

analysis in c

Tota

expressed as

$$\{\varepsilon^C\} = \{\varepsilon^M$$

where super

superscript ^{H}

gives the mec

$$\{\varepsilon^M\} = \{\varepsilon^C\}$$

For laminates

the plane strai

Eq. 2.3.10.

$$\{\varepsilon^M\} = \{\varepsilon^0\}$$

The correspon

$$\{\sigma\}_k = [\bar{Q}]_k$$

where hygrosco

mechanical resu

and wood-based materials, which could deform due to hygroscopic strains from humidity changes in their environments. CLT must account for the hygroscopic strains in its analysis in order for it to be applicable to hygroscopic composites.

Total strains, including mechanical strains and hygroscopic strains, would be expressed as the sum of both

$$\{\varepsilon^C\} = \{\varepsilon^M\} + \{\varepsilon^H\} \qquad 2.3.33$$

where superscript ^{C} indicates total strains, superscript ^{M} mechanical strains and superscript ^{H} hygroscopic strains. Subtraction of humidity strains from the total strains gives the mechanical strains

$$\{\varepsilon^M\} = \{\varepsilon^C\} - \{\varepsilon^H\} \qquad 2.3.34$$

For laminates under the Kirchhoff Hypothesis, total strains are expressed as the sum of the plane strains and the linear translations of curvatures at the mid-plane as defined in Eq. 2.3.10. Hence, the mechanical strains are

$$\{\varepsilon^M\} = \{\varepsilon^0\} + z\{\kappa\} - \{\varepsilon^H\} \qquad 2.3.35$$

The corresponding mechanical stresses for lamina k, by Eq. 2.3.15, would be

$$\{\sigma\}_k = [\overline{Q}]_k \left\{\{\varepsilon^0\} + z\{\kappa\} - \{\varepsilon^H\}_k\right\} \qquad 2.3.36$$

where hygroscopic strains $\{\epsilon^H\}$ are assumed constant within each lamina. The associated mechanical resultant forces and moments as denoted by superscript ^{M} would be, by Eq.

2.3.25

$$\{N^M\} = \sum_{k=1}^{n} [\bar{Q}]_k \int_{z_{k-1}}^{z_k} \{\{\varepsilon^0\} + z\{\kappa\} - \{\varepsilon^H\}_k\}\, dz$$

$$= \sum_{k=1}^{n} [\bar{Q}]_k \left\{ \int_{z_{k-1}}^{z_k} \{\varepsilon^0\}\ dz + \int_{z_{k-1}}^{z_k} \{\kappa\}\ z dz - \int_{z_{k-1}}^{z_k} \{\varepsilon^0\}_k\ dz \right\} \qquad 2.3.37$$

$$\{M^M\} = \sum_{k=1}^{n} [\bar{Q}]_k \int_{z_{k-1}}^{z_k} \{\{\varepsilon^0\} + z\{\kappa\} - \{\varepsilon^H\}_k\} z dz$$

$$= \sum_{k=1}^{n} [\bar{Q}]_k \left\{ \int_{z_{k-1}}^{z_k} \{\varepsilon^0\} z dz + \int_{z_{k-1}}^{z_k} \{\kappa\} z^2 dz - \int_{z_{k-1}}^{z_k} \{\varepsilon^0\}_k z dz \right\}$$

which, in analogy to the derivation of Eq. 2.3.28 from Eq. 2.3.25, could be reduced to

$$\{N^M\} = \left[\sum_{k=1}^{n} [\bar{Q}]_k \quad (z_k - z_{k-1}) \right] \{\varepsilon^0\}$$

$$+ \left[\sum_{k=1}^{n} [\bar{Q}]_k \frac{1}{2} (z_k^2 - z_{k-1}^2) \right] \{\kappa\}$$

$$- \left\{ \sum_{k=1}^{n} [\bar{Q}]_k \{\varepsilon^H\}_k (z_k - z_{k-1}) \right\} \qquad 2.3.38$$

$$\{M^M\} = \left[\sum_{k=1}^{n} [\bar{Q}]_k \frac{1}{2} (z_k^2 - z_{k-1}^2) \right] \{\varepsilon^0\}$$

$$+ \left[\sum_{k=1}^{n} [\bar{Q}]_k \frac{1}{3} (z_k^3 - z_{k-1}^3) \right] \{\kappa\}$$

$$- \left\{ \sum_{k=1}^{n} [\bar{Q}]_k \{\varepsilon^H\}_k \frac{1}{2} (z_k^2 - z_{k-1}^2) \right\}$$

or

$\{N^M\} = [$

$\{M^M\} = -$

where $\{N^H\}$

$\{N^H\} = \left\{ \right.$

$\{M^H\} = \left\{ \right.$

are called hu

and moments

$\{N^M\} + \{M$

$\{M^M\} + \{N$

or

$$\left\{ \begin{array}{c} N^M + N^H \\ \hline M^M + M^H \end{array} \right\}$$

which is the g

and M^H.

The str

hygroscopic eff

or

$$\begin{aligned} \{N^M\} &= [A]\{\varepsilon^0\} + [B]\{\kappa\} - \{N^H\} \\ \{M^M\} &= [B]\{\varepsilon^0\} + [D]\{\kappa\} - \{M^H\} \end{aligned} \tag{2.3.39}$$

where $\{N^H\}$ and $\{M^H\}$, defined as

$$\begin{aligned} \{N^H\} &= \left\{ \sum_{k-1}^{n} [\bar{Q}]_k \{\varepsilon^H\}_k (z_k - z_{k-1}) \right\} \\ \{M^H\} &= \left\{ \sum_{k-1}^{n} [\bar{Q}]_k \{\varepsilon^H\}_k \frac{1}{2}(z_k^2 - z_{k-1}^2) \right\} \end{aligned} \tag{2.3.40}$$

are called humidity forces and moments. They are therefore not real mechanical forces and moments. Eq. 2.3.40 may be regrouped to

$$\begin{aligned} \{N^M\} + \{M^H\} &= [A]\{\varepsilon^0\} + [B]\{\kappa\} \\ \{M^M\} + \{N^H\} &= [B]\{\varepsilon^0\} + [D]\{\kappa\} \end{aligned} \tag{2.3.41}$$

or

$$\begin{Bmatrix} N^M + N^H \\ \hline M^M + M^H \end{Bmatrix} = \left[\begin{array}{c|c} A & B \\ \hline B & D \end{array}\right] \begin{Bmatrix} \varepsilon^0 \\ \hline \kappa \end{Bmatrix} \tag{2.3.42}$$

which is the governing equation that includes hygroscopic effects with the terms of N^H and M^H.

The strains and curvatures of a laminate under given mechanical actions and hygroscopic effects can be obtained by inversion of the governing equation

$$\left\{\begin{matrix}\varepsilon^0\\---\\\kappa\end{matrix}\right\} = \left[\begin{matrix}A\\---\\B\end{matrix}\right.$$

In cases wh

laminate are

$$\left\{\begin{matrix}N^H\\---\\M^H\end{matrix}\right\} = \left[\begin{matrix}A\\---\\B\end{matrix}\right.$$

and vice versa

$$\left\{\begin{matrix}\varepsilon^0\\---\\\kappa\end{matrix}\right\} = \left[\begin{matrix}A\\---\\B\end{matrix}\right.$$

It can

the mid-plane

properties and

that is such lam

$[B]$ and $\{M^H\}$

($\{\kappa\}$) result, s

effects.

Wood a

changes in thei

$$\begin{Bmatrix} \varepsilon^0 \\ -- \\ \kappa \end{Bmatrix} = \begin{bmatrix} A & | & B \\ -- & & -- \\ B & | & D \end{bmatrix}^{-1} \begin{Bmatrix} N^M + N^H \\ ------ \\ M^M + M^H \end{Bmatrix} \qquad 2.3.43$$

In cases where the mechanical action is absent, hygroscopic effects imposed upon a laminate are related to the strains and curvatures by

$$\begin{Bmatrix} N^H \\ --- \\ M^H \end{Bmatrix} = \begin{bmatrix} A & | & B \\ -- & & -- \\ B & | & D \end{bmatrix} \begin{Bmatrix} \varepsilon^0 \\ -- \\ \kappa \end{Bmatrix} \qquad 2.3.44$$

and vice versa by

$$\begin{Bmatrix} \varepsilon^0 \\ -- \\ \kappa \end{Bmatrix} = \begin{bmatrix} A & | & B \\ -- & & -- \\ B & | & D \end{bmatrix}^{-1} \begin{Bmatrix} N^H \\ --- \\ M^H \end{Bmatrix} \qquad 2.3.45$$

It can be shown that $[B]$ and $\{M^H\}$ are zero for laminates that are symmetric to the mid-plane of the laminate in both geometry and material properties (both elastic properties and hygroscopic properties). As such, curvatures must be zero by Eq. 2.3.45, that is such laminates would not bend and/or twist under hygroscopic effects. However, $[B]$ and $\{M^H\}$ are not necessarily zero with nonsymmetric laminates where curvatures ($\{\kappa\}$) result, suggesting bending and/or twisting by the laminate under hygroscopic effects.

Wood and wood-based materials respond to humidity changes with proportionate changes in their moisture contents. It is, therefore, equivalent to express hygroscopic

effects or s

MC become

Ther

procedure.

$$\begin{cases} N^M + N^H \\ \hline M^M + M^H \end{cases}$$

where

$$\{N^T\} = \left\{ \right.$$

$$\{M^T\} = \left\{ \right.$$

and superscr

2.4 Develop

Visc

(constitutive

time-wise co

relation, hov

theory attemp

relation, the

relation in C

effects or strains with reference to either humidity or moisture content. Superscript ^{H} and ^{MC} become interchangeable in all expressions.

Thermal effects can also be included into the CLT analysis following the same procedure. It can be shown that the resulting governing equation would then be

$$\begin{Bmatrix} N^M + N^H + N^T \\ \text{----------} \\ M^M + M^H + M^T \end{Bmatrix} = \begin{bmatrix} A & | & B \\ -- & & -- \\ B & | & D \end{bmatrix} \begin{Bmatrix} \varepsilon^0 \\ -- \\ \kappa \end{Bmatrix} \qquad 2.3.46$$

where

$$\{N^T\} = \left\{ \sum_{k=1}^{n} [\bar{Q}]_k \{\varepsilon^T\}_k (z_k - z_{k-1}) \right\}$$
$$\{M^T\} = \left\{ \sum_{k=1}^{n} [\bar{Q}]_k \{\varepsilon^T\}_k \frac{1}{2}(z_k^2 - z_{k-1}^2) \right\} \qquad 2.3.47$$

and superscript ^{T} refers to thermal effects with other terms defined as before.

2.4 Development of the Linear Viscoelastic Plate Theory (LVP)

Viscoelastic behavior differs from elastic behavior in terms of stress-strain relation (constitutive equation). The elastic relation, being time independent, is described by a time-wise constant algebraic tensor equation, namely Hooke's Law. The viscoelastic relation, however, is not such a simple case due to the time dependence. Since any theory attempting to represent material behavior must account for appropriate stress-strain relation, the viscoelastic stress-strain relation must be substituted in place of the elastic relation in CLT in the evolution of the viscoelastic CLT.

2.4.1 Linea

The

while exist

strain varia

at the very

stress is als

material, as

stress states

history as w

it has been

Boltzman fir

means of re

Principle of S

The a

a three-dimen

tion [Christen

$$e_{ij} = \int_{0^-}^{t} J_{ijkl}(t-$$

$$\sigma_{ij} = \int_{0^-}^{t} Y_{ijkl}(t-$$

where $J_{ijkl}(t-\tau)$

respectively. T

2.4.1 Linear Viscoelastic Stress-Strain Relations for Plane Stress

The definite one-to-one correspondence between stresses and associated strains, while existing for elastic behavior, however, is not observed in viscoelastic behavior. The strain variation with time under stress implies that strains depend not only on the stress at the very current moment, but also on the time under stress. The past history under stress is also contributing to the material response (strains), which suggests that the material, aside from responding to the current stresses, remembers the past history of stress states. This memory effect, observed of stresses in relation to strains and strain history as well, is characteristic of the stress-strain relation in viscoelastic behavior, and it has been quantitatively represented by the Boltzman principle since 1874 when Boltzman first proposed it. This principle is still considered one of the most important means of representing material behavior. It is also known in the literatures as the Principle of Superposition [Gross, 1953] and as the Hereditary Integral [Flugge, 1967].

The above principle, if expressed for a linear viscoelastic anisotropic material in a three-dimensional stress state, gives the following stress-strain relations in tensor notation [Christensen, 1982; Schapery, 1967; Sims, 1972]]

$$\varepsilon_{ij} = \int_{0^-}^{t} J_{ijkl}(t-\tau)\,\frac{\partial \sigma_{kl}}{\partial \tau}\,d\tau$$

$$\sigma_{ij} = \int_{0^-}^{t} Y_{ijkl}(t-\tau)\,\frac{\partial \varepsilon_{kl}}{\partial \tau}\,d\tau \qquad i, j, k, l = 1, 2, 3 \qquad 2.4.1$$

where $J_{ijkl}(t-\tau)$ and $Y_{ijkl}(t-\tau)$ are defined to be the creep compliances and relaxation moduli respectively. The 0^- in the lower integration limit suggests inclusion of a step discontinu-

ity of stres

change the

$$\varepsilon_{ij} - J_{ijkl}(t)$$

$$\sigma_{ij} - Y_{ijkl}(t)$$

However, th

The

presumes the

τ_{xy}, are consi

$$\begin{Bmatrix} \varepsilon_{11}(t) \\ \varepsilon_{22}(t) \\ \gamma_{12}(t) \end{Bmatrix}_k -$$

$$\begin{Bmatrix} \sigma_{11}(t) \\ \sigma_{22}(t) \\ \tau_{12}(t) \end{Bmatrix}_k -$$

or

$$\{\varepsilon(t)\}_k - \int_{0^-}^{t}$$

$$\{\sigma(t)\}_k - \int_{0^-}^{t}$$

ity of stresses or strains at $t = 0$, which upon separation from the integration would change the relations to:

$$\varepsilon_{ij} - J_{ijkl}(t)\,\sigma_{kl}(0) + \int_0^t J_{jikl}(t-\tau)\,\frac{\partial \sigma_{kl}}{\partial \tau}\,d\tau$$

$$\sigma_{ij} - Y_{ijkl}(t)\,\varepsilon_{kl}(0) + \int_0^t Y_{jikl}(t-\tau)\,\frac{\partial \varepsilon_{kl}}{\partial \tau}\,d\tau \qquad i, j, k, l = 1, 2, 3 \qquad 2.4.2$$

However, the notation in Eq. 2.4.1 is more compact and will be used here.

The viscoelastic plate theory which is to be developed on the frame of CLT presumes the CLT plane stress state in which only the three plane stresses, σ_x, σ_y, and τ_{xy}, are considered. The resulting reduced stress-strain relations for lamina k are

$$\begin{Bmatrix} \varepsilon_{11}(t) \\ \varepsilon_{22}(t) \\ \gamma_{12}(t) \end{Bmatrix}_k - \int_{0^-}^t \begin{bmatrix} J_{11}(t-\tau) & J_{12}(t-\tau) & 0 \\ J_{12}(t-\tau) & J_{22}(t-\tau) & 0 \\ 0 & 0 & J_{66}(t-\tau) \end{bmatrix}_k \begin{Bmatrix} \sigma_{11}(\tau) \\ \sigma_{22}(\tau) \\ \tau_{12}(\tau) \end{Bmatrix}_k' d\tau$$

$$\begin{Bmatrix} \sigma_{11}(t) \\ \sigma_{22}(t) \\ \tau_{12}(t) \end{Bmatrix}_k - \int_{0^-}^t \begin{bmatrix} Y_{11}(t-\tau) & Y_{12}(t-\tau) & 0 \\ Y_{12}(t-\tau) & Y_{22}(t-\tau) & 0 \\ 0 & 0 & Y_{66}(t-\tau) \end{bmatrix}_k \begin{Bmatrix} \varepsilon_{11}(\tau) \\ \varepsilon_{22}(\tau) \\ \gamma_{12}(\tau) \end{Bmatrix}_k' d\tau \qquad 2.4.3$$

or

$$\{\varepsilon(t)\}_k - \int_{0^-}^t [J(t-\tau)]_k \{\sigma(\tau)\}_k' d\tau$$

$$\{\sigma(t)\}_k - \int_{0^-}^t [Y(t-\tau)]_k \{\varepsilon(\tau)\}_k' d\tau \qquad 2.4.4$$

where the

Wh

principle c

stress and s

$\bar{Y}_i(t-\tau)$ in p

obtained sim

$$\begin{Bmatrix} \varepsilon_{xx}(t) \\ \varepsilon_{yy}(t) \\ \gamma_{xy}(t) \end{Bmatrix}_k -$$

$$\begin{Bmatrix} \sigma_{xx}(t) \\ \sigma_{yy}(t) \\ \tau_{xy}(t) \end{Bmatrix}_k -$$

or

$$\{\varepsilon(t)\}_k -$$

$$\{\sigma(t)\}_k -$$

where $[\bar{Y}(t-$

creep compl

The

of elastic C

where the prime (') represents differentiation $\partial/\partial\tau$.

While the above viscoelastic stress-strain relations are with respect to material principle coordinates *1-2*, their expression in arbitrary coordinates *x-y* is desired. By stress and strain transformation defined in Eq. 2.3.16 (with $J_{ij}(t-\tau)$, $\overline{J}_{ij}(t-\tau)$ or $Y_{ij}(t-\tau)$, $\overline{Y}_{ij}(t-\tau)$ in place of Q_{ij}, $\overline{Q}_{ij}$), the viscoelastic stress-strain relations in *x-y* coordinates are obtained similarly to the elastic CLT analysis:

$$\begin{Bmatrix} \varepsilon_{xx}(t) \\ \varepsilon_{yy}(t) \\ \gamma_{xy}(t) \end{Bmatrix}_k = \int_{0^-}^{t} \begin{bmatrix} \overline{J_{11}}(t-\tau) & \overline{J_{12}}(t-\tau) & \overline{J_{16}}(t-\tau) \\ \overline{J_{12}}(t-\tau) & \overline{J_{22}}(t-\tau) & \overline{J_{26}}(t-\tau) \\ \overline{j_{16}}(t-\tau) & \overline{J_{26}}(t-\tau) & \overline{J_{66}}(t-\tau) \end{bmatrix}_k \begin{Bmatrix} \sigma_{xx}(\tau) \\ \sigma_{yy}(\tau) \\ \tau_{xy}(\tau) \end{Bmatrix}_k' d\tau$$

$$\begin{Bmatrix} \sigma_{xx}(t) \\ \sigma_{yy}(t) \\ \tau_{xy}(t) \end{Bmatrix}_k = \int_{0^-}^{t} \begin{bmatrix} \overline{Y_{11}}(t-\tau) & \overline{Y_{12}}(t-\tau) & \overline{Y_{16}}(t-\tau) \\ \overline{Y_{12}}(t-\tau) & \overline{Y_{22}}(t-\tau) & \overline{Y_{26}}(t-\tau) \\ \overline{Y_{16}}(t-\tau) & \overline{Y_{26}}(t-\tau) & \overline{Y_{66}}(t-\tau) \end{bmatrix}_k \begin{Bmatrix} \varepsilon_{xx}(\tau) \\ \varepsilon_{yy}(\tau) \\ \gamma_{xy}(\tau) \end{Bmatrix}_k' d\tau \qquad 2.4.5$$

or

$$\{\varepsilon(t)\}_k = \int_{0^-}^{t} [\overline{J}(t-\tau)]_k \{\sigma(\tau)\}_k' d\tau$$

$$\{\sigma(t)\}_k = \int_{0^-}^{t} [\overline{Y}(t-\tau)]_k \{\varepsilon(\tau)\}_k' d\tau \qquad 2.4.6$$

where $[\overline{Y}(t-\tau)]_k$ and $[\overline{J}(t-\tau)]_k$ indicate that they are transformed relaxation moduli and creep compliances in the arbitrary *x-y* coordinates.

The sharp contrast between Eq. 2.4.6 of linear viscoelastic CLT and Eq. 2.3.15 of elastic CLT is due to the time involvement and resulting complexity. The algebraic

time-wise constant tensor ***[Q]*** in elastic CLT states the definite match between current stresses and strains, while the functional integration in time space in linear viscoelastic CLT analysis accounts for not only the effect of current stresses or strains, but also the characteristic memory effect (effect of strain history or stress history).

2.4.2 Linear Viscoelastic Governing Equation

When a hygroscopic effect is present, the mechanical strain rates, by differentiation of Eq. 2.3.35, are

$$\{\varepsilon^{M}(\tau)\}' = \{\varepsilon^{0}(\tau)\}' + z\{\kappa(\tau)\}' - \{\varepsilon^{MC}(\tau)\}' \qquad 2.4.7$$

where the hygroscopic strain rates are expressed in reference to moisture content (superscript ^{MC}). If the hygroscopic strain rates are constant within each constituent lamina, but different across the laminas in a laminate, the mechanical strain rates for a particular lamina k are

$$\{\varepsilon^{M}(\tau)\}'_{k} = \{\varepsilon^{0}(\tau)\}' + z\{\kappa(\tau)\}' - \{\varepsilon^{MC}(\tau)\}'_{k} \qquad 2.4.8$$

The corresponding mechanical stresses in this particular lamina k which are related to strains by linear viscoelastic stress-strains relations defined in Eq. 2.4.6, are

$$\begin{aligned}\{\sigma(t)\}_{k} &= \int_{0^-}^{t} [\bar{Y}(t-\tau)]_{k} \{\varepsilon^{M}(\tau)\}'_{k} d\tau \\ &= \int_{0^-}^{t} [\bar{Y}(t-\tau)]_{k} \left\{\{\varepsilon^{0}(\tau)\}' + z\{\kappa(\tau)\}' - \{\varepsilon^{MC}(\tau)\}'_{k}\right\} d\tau\end{aligned} \qquad 2.4.9$$

CLT a

results

$$\begin{cases} N_x(t) \\ N_y(t) \\ N_{xy}(t) \end{cases}$$

or

$$\{N(t)\}$$

and mo

$$\begin{cases} M_x(t) \\ M_y(t) \\ M_{xy}(t) \end{cases}$$

or

$$\{M(t)\}$$

B

$\{N_w(t)\}$

The balance between the resultant forces-moments and the stresses in the elastic CLT analysis defined in Eq's. 2.3.19 - 2.3.21 must be maintained at any instant t, which results in the following forces-stresses relation

$$\begin{Bmatrix} N_x(t) \\ N_y(t) \\ N_{xy}(t) \end{Bmatrix} = \int_{-h/2}^{h/2} \begin{Bmatrix} \sigma_{xx}(t) \\ \sigma_{yy}(t) \\ \tau_{xy}(t) \end{Bmatrix} dz = \sum_{k=1}^{n} \int_{z_{k-1}}^{z_k} \begin{Bmatrix} \sigma_{xx}(t) \\ \sigma_{yy}(t) \\ \tau_{xy}(t) \end{Bmatrix}_k dz \qquad 2.4.10$$

or

$$\{N(t)\} = \int_{-h/2}^{h/2} \{\sigma(t)\}\, dz = \sum_{k=1}^{n} \int_{z_{k-1}}^{z_k} \{\sigma(t)\}_k\, dz \qquad 2.4.11$$

and moments-stresses relation

$$\begin{Bmatrix} M_x(t) \\ M_y(t) \\ M_{xy}(t) \end{Bmatrix} = \int_{-h/2}^{h/2} \begin{Bmatrix} \sigma_{xx}(t) \\ \sigma_{yy}(t) \\ \tau_{xy}(t) \end{Bmatrix} z\, dz = \sum_{k=1}^{n} \int_{z_{k-1}}^{z_k} \begin{Bmatrix} \sigma_{xx}(t) \\ \sigma_{yy}(t) \\ \tau_{xy}(t) \end{Bmatrix}_k z\, dz \qquad 2.4.12$$

or

$$\{M(t)\} = \int_{-h/2}^{h/2} \{\sigma(t)\}\, z\, dz = \sum_{k=1}^{n} \int_{z_{k-1}}^{z_k} \{\sigma(t)\}_k\, z\, dz \qquad 2.4.13$$

By viscoelastic stress-strain relations of Eq. 2.4.9, mechanical resultant forces $\{N^M(t)\}$ for a n-layer laminate are expressed in terms of strains as

$$\{N^M(t)\} - \sum_{k-1}^{n} \int_{z_{k-1}}^{z_k} \{\sigma(t)\}_k dz$$

$$- \sum_{k-1}^{n} \int_{z_{k-1}}^{z_k} \left\{ \int_{0^-}^{t} [\bar{Y}(t-\tau)]_k \left\{ \{\varepsilon^0(\tau)\}' + z\{\kappa(\tau)\}' - \{\varepsilon^{MC}(\tau)\}'_k \right\} d\tau \right\} dz \qquad 2.4.14$$

Switching t-integration with z-integration and moving them outside of summation results in

$$\{N^M(t)\} - \int_{0^-}^{t} \left\{ \sum_{k-1}^{n} \int_{z_{k-1}}^{z_k} [\bar{Y}(t-\tau)]_k \left\{ \{\varepsilon^0(\tau)\}' + z\{\kappa(\tau)\}' - \{\varepsilon^{MC}(\tau)\}'_k \right\} dz \right\} d\tau$$

$$- \int_{0^-}^{t} \left\{ \sum_{k-1}^{n} \int_{z_{k-1}}^{z_k} [\bar{Y}(t-\tau)]_k \{\varepsilon^0(\tau)\}' \, dz \right\} d\tau +$$

$$\int_{0^-}^{t} \left\{ \sum_{k-1}^{n} \int_{z_{k-1}}^{z_k} [\bar{Y}(t-\tau)]_k \{\kappa(\tau)\}' \, z \, dz \right\} d\tau - \qquad 2.4.15$$

$$\int_{0^-}^{t} \left\{ \sum_{k-1}^{n} \int_{z_{k-1}}^{z_k} [\bar{Y}(t-\tau)]_k \{\varepsilon^{MC}(\tau)\}'_k dz \right\} d\tau$$

$\{\epsilon^0(\tau)\}'$, $\{\kappa(\tau)\}'$ are strain and curvature rates at the mid-plane, respectively. Constant with respect to z, they are moved outside of z-integration and summation. $[\bar{Y}(t-\tau)]_k$ and hygroscopic strain rates $\{\epsilon^{MC}(\tau)\}'_k$ are only constant within the k lamina with respect to z, and hence are only moved outside of z-integration. These manipulations, which are similar to those in elastic analysis, reduce the above to

$$\{N^M(t)\} = \int_{0^-}^{t} \left(\sum_{k=1}^{n} [\bar{Y}(t-\tau)]_k \int_{z_{k-1}}^{z_k} dz \right) \{e^0(\tau)\}' \, d\tau +$$

$$\int_{0^-}^{t} \left(\sum_{k=1}^{n} [\bar{Y}(t-\tau)]_k \int_{z_{k-1}}^{z_k} z \, dz \right) \{\kappa(\tau)\}' \, d\tau - \qquad 2.4.16$$

$$\int_{0^-}^{t} \left\{ \sum_{k=1}^{n} \left([\bar{Y}(t-\tau)]_k \int_{z_{k-1}}^{z_k} dz \right) \{e^{MC}(\tau)\}'_k \right\} d\tau$$

which, due to Eq. 2.3.27, are further simplified to be

$$\{N^M(t)\} = \int_{0^-}^{t} \left(\sum_{k=1}^{n} [\bar{Y}(t-\tau)]_k \quad (z_k - z_{k-1}) \right) \{e^0(\tau)\}' \, d\tau +$$

$$\int_{0^-}^{t} \left(\sum_{k=1}^{n} [\bar{Y}(t-\tau)]_k \frac{1}{2}(z_k^2 - z_{k-1}^2) \right) \{\kappa(\tau)\}' \, d\tau - \qquad 2.4.17$$

$$\int_{0^-}^{t} \left\{ \sum_{k=1}^{n} [\bar{Y}(t-\tau)]_k (z_k - z_{k-1}) \{e^{MC}(\tau)\}'_k \right\} d\tau$$

or

$$\{N^M(t)\} = \int_{0^-}^{t} [A(t-\tau)] \{e^0(\tau)\}' \, d\tau +$$

$$\int_{0^-}^{t} [B(t-\tau)] \{\kappa(\tau)\}' \, d\tau - \{N^{MC}(t)\} \qquad 2.4.18$$

where

$$
\begin{aligned}
[A(t-\tau)] \quad &- \sum_{k-1}^{n} [\bar{Y}(t-\tau)]_k \quad (z_k - z_{k-1}) \\
[B(t-\tau)] \quad &- \sum_{k-1}^{n} [\bar{Y}(t-\tau)]_k \frac{1}{2}(z_k^2 - z_{k-1}^2) \\
\{N^{MC}(t)\} \quad &- \int_{0^-}^{t} \{\bar{N}^{MC}(t-\tau, \varepsilon^{MC}(\tau)')\}\, d\tau \\
\{\bar{N}^{MC}(t-\tau, \varepsilon^{MC}(\tau)')\} &- \sum_{k-1}^{n} [\bar{Y}(t-\tau)]_k (z_k - z_{k-1}) \{\varepsilon^{MC}(\tau)\}'_k
\end{aligned}
\qquad 2.4.19
$$

$\{N^{MC}(t)\}$ denotes hygroscopic forces in reference to moisture content change. Similarly, mechanical resultant moments $\{M^{MC}(t)\}$ are expressed in terms of strains as

$$
\begin{aligned}
\{M^{M}(t)\} - &\int_{0^-}^{t} [B(t-\tau)]\{\varepsilon^{0}(\tau)\}'\, d\tau + \\
&\int_{0^-}^{t} [D(t-\tau)]\{\kappa(\tau)\}'\, d\tau - \{M^{MC}(t)\}
\end{aligned}
\qquad 2.4.20
$$

where

$$
\begin{aligned}
[B(t-\tau)] \quad &- \sum_{k-1}^{n} [\bar{Y}(t-\tau)]_k \frac{1}{2}(z_k^2 - z_{k-1}^2) \\
[D(t-\tau)] \quad &- \sum_{k-1}^{n} [\bar{Y}(t-\tau)]_k \frac{1}{3}(z_k^3 - z_{k-1}^3) \\
\{M^{MC}(t)\} \quad &- \int_{0^-}^{t} \{\bar{M}^{MC}(t-\tau, \varepsilon^{MC}(\tau)')\}\, d\tau \\
\{\bar{M}^{MC}(t-\tau, \varepsilon^{MC}(\tau)')\} &- \sum_{k-1}^{n} [\bar{Y}(t-\tau)]_k \frac{1}{2}(z_k^2 - z_{k-1}^2) \{\varepsilon^{MC}(\tau)\}'_k
\end{aligned}
\qquad 2.4.21
$$

$\{M^{MC}(t)\}$ are the hygroscopic moments.

Eq's. 2.4.18 and 2.4.20 are jointly expressed as

$$\begin{Bmatrix} N^{M}(t) \\ \hline M^{M}(t) \end{Bmatrix} = \int_{0^-}^{t} \left[\begin{array}{c|c} A(t-\tau) & B(t-\tau) \\ \hline B(t-\tau) & D(t-\tau) \end{array}\right] \begin{Bmatrix} \varepsilon^{0}(\tau) \\ \hline \kappa(\tau) \end{Bmatrix}' d\tau - \begin{Bmatrix} N^{MC}(t) \\ \hline M^{MC}(t) \end{Bmatrix} \qquad 2.4.22$$

and abbreviated to

$$\{NM^{M}(t)\} + \{NM^{MC}(t)\} = \int_{0^-}^{t} [ABD(t-\tau)] \{\varepsilon^{0}\kappa(\tau)\}' d\tau \qquad 2.4.23$$

where

$$\{NM^{M}(t)\} = \begin{Bmatrix} N^{M}(t) \\ \hline M^{M}(t) \end{Bmatrix}$$

$$\{NM^{MC}(t)\} = \begin{Bmatrix} N^{MC}(t) \\ \hline M^{MC}(t) \end{Bmatrix} = \int_{0^-}^{t} \begin{Bmatrix} \overline{N}^{MC}(t-\tau, \varepsilon(\tau)') \\ \hline \overline{M}^{MC}(t-\tau, \varepsilon(\tau)') \end{Bmatrix} d\tau$$

$$= \int_{0^-}^{t} \{\overline{NM}^{MC}(t-\tau, \varepsilon(\tau)')\} d\tau \qquad 2.4.24$$

$$[ABD(t-\tau)] = \left[\begin{array}{c|c} A(t-\tau) & B(t-\tau) \\ \hline B(t-\tau) & D(t-\tau) \end{array}\right]$$

$$\{\varepsilon^{0}\kappa(\tau)\}' = \begin{Bmatrix} \varepsilon^{0}(\tau) \\ \hline \kappa(\tau) \end{Bmatrix}'$$

Eq's. 2.4.22 - 2.4.24 express mechanical and hygroscopic forces-moments in terms of the strain and curvature at the mid-plane, and are called the governing equations in linear hygroscopic viscoelastic analysis. They are convolution-type integrals and are similar to that developed by Sims [1972].

The difference between the elastic stress-strain relation and governing equation (Eq's. 2.3.14 - 2.3.15) and the linear viscoelastic counterparts (Eq's. 2.4.5 - 2.4.6) lies, as expected, in the time domain - reflecting the distinction between elastic behavior and viscoelastic behavior. The parallelness becomes more conspicuous in the Laplace domain where the linear viscoelastic stress-strain and governing equation are transformed to be, respectively

$$\begin{aligned} \{\bar{\sigma}(s)\} &= s\,[\bar{Y}(s)]\,\{\bar{\varepsilon}(s)\} \\ \{\bar{\varepsilon}(s)\} &= s\,[\bar{J}(s)]\,\{\bar{\sigma}(s)\} \end{aligned} \qquad \text{2.4.24.A}$$

and

$$\left\{\begin{array}{c} \overline{N^{M}}(s) + \overline{N^{MC}}(s) \\ \hline \overline{M^{M}}(s) + \overline{M^{MC}}(s) \end{array}\right\} = s \left[\begin{array}{c|c} \bar{A}(s) & \bar{B}(s) \\ \hline \bar{B}(s) & \bar{D}(s) \end{array}\right] \left\{\begin{array}{c} \overline{\varepsilon^{0}}(s) \\ \hline \bar{\kappa}(s) \end{array}\right\} \qquad \text{2.4.24.B}$$

With time involvement hidden, they resemble their respective elastic counterparts (Eq's. 2.3.14 - 2.3.15 and Eq's. 2.4.5 - 2.4.6) in the algebraic form. Such resemblance, which is always observed between corresponding elastic and linear viscoelastic equations, is the basis of the poplar and useful Correspondence Principle.

Theoretically, history of strain and curvature rates at mid-plane $\{\epsilon\kappa(\tau)\}'$ can be

obtained by Eq. 2.4.23 given mechanical actions and hygroscopic effect, namely $\{N^M(t)\}$, $\{M^M(t)\}$, $\{N^{MC}(t)\}$, and $\{M^{MC}(t)\}$. Yet, an exact analytical solution is probably only possible in certain simple and ideal situations, presenting little practical usage for the analytical governing equation. A numerical alternative has to be attempted.

2.4.3 Numericalization of Linear Viscoelastic Governing Equation and Successive Computation of Strains and Stresses

A convolution-type integral like the following can be subdivided into a series of integrals,

$$\int_{0^-}^{t} f(t-\tau)g(\tau)'d\tau$$

$$= f(t)g(0) + \int_{0}^{t} f(t-\tau)g(\tau)'d\tau$$

$$= f(t)g(0) + \int_{\tau_0=0}^{\tau_1} f(t-\tau)g(\tau)'d\tau + \int_{\tau_1}^{\tau_2} + \int_{\tau_2}^{\tau_3} + \cdots\cdots + \int_{\tau_{m-2}}^{\tau_{m-1}} + \int_{\tau_{m-1}}^{\tau_m=t} f(t-\tau)g(\tau)'d\tau \qquad 2.4.25$$

$$= f(t)g(0) + \sum_{i=1}^{m} \int_{\tau_{i-1}}^{\tau_i} f(\tau_m-\tau)g(\tau)'d\tau$$

where integration limits $\tau_0=0$ through $\tau_m=t$ are $m+1$ t-points along the time domain and

$$(\tau_0=0) < \tau_1 < \tau_2 < \tau_3 < \cdots\cdots < \tau_{m-2} < \tau_{m-1} < (\tau_m=t) \qquad 2.4.26$$

As shown in Figure 17, if the time interval is very small, that is

$$\Delta\tau_i = (\tau_i - \tau_{i-1}) = R_i\Delta\tau < 1 \qquad 2.4.27$$

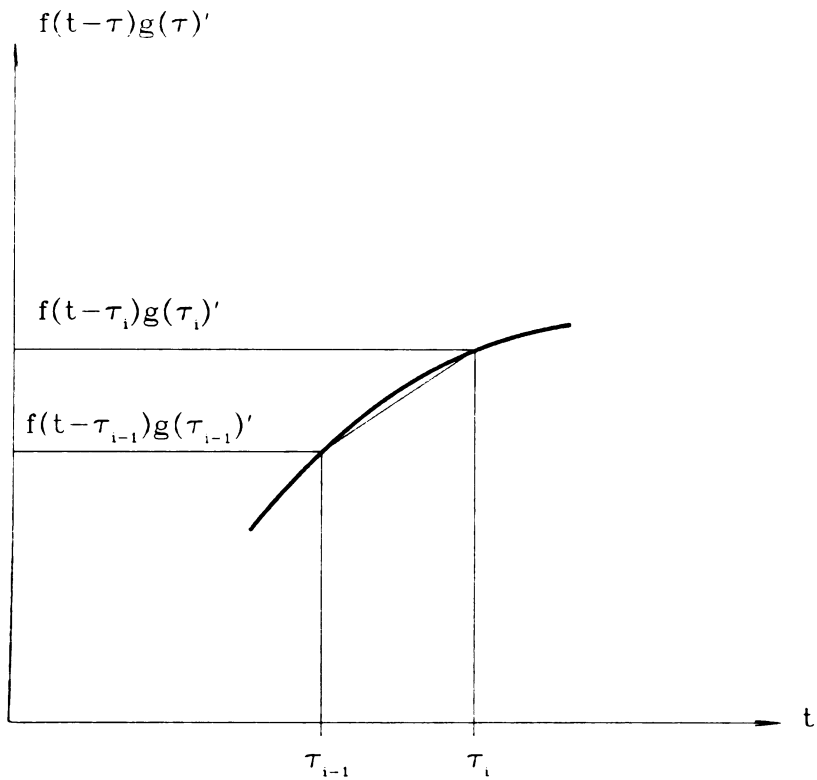

Figure 17. Illustration of linear finite difference approximation.

the area under the curve could be approximated by the shaded area of a trapezoid,

$$\int_{\tau_{i-1}}^{\tau_i} f(t-\tau)g(\tau)'d\tau = \frac{1}{2}(\tau_i - \tau_{i-1})[f(t-\tau_{i-1})g(\tau_{i-1})' + f(t-\tau_i)g(\tau_i)'] - \frac{1}{2}R_i\Delta\tau[f(t-\tau_{i-1})g(\tau_{i-1})' + f(t-\tau_i)g(\tau_i)'] \quad 2.4.28$$

As such, integral of Eq. 2.4.25 becomes

$$\int_{0^-}^{t} f(t-\tau)g(\tau)'d\tau - f(t)g(0) + \frac{1}{2}\Delta\tau\sum_{i-1}^{m} R_i[f(\tau_m-\tau_{i-1})g(\tau_{i-1})' + f(\tau_m-\tau_i)g(\tau_i)'] \quad 2.4.29$$

The integral has been degenerated into a summation of algebraic expressions. Note that all individual time intervals $\Delta\tau_i$ are measured against and expressed in terms of a unit time interval $\Delta\tau$.

By Eq. 2.4.29, the hygroscopic forces-moments in governing equation Eq. 2.4.23 can be degenerated to

$$\{NM^{MC}(t)\} = \int_{0^-}^{t-\tau_m} \{\overline{NM}^{MC}(t-\tau,\varepsilon^{MC}(\tau)')\}_k\, d\tau - \{\overline{NM}^{MC}(\tau_m-0,\varepsilon^{MC}(0))\}_k + \frac{1}{2}\Delta\tau\sum_{i-1}^{m} R_i\left(\{\overline{NM}^{MC}(\tau_m-\tau_{i-1},\varepsilon^{MC}(\tau_{i-1})')\} + \{\overline{NM}^{MC}(\tau_m-\tau_i,\varepsilon^{MC}(\tau_i)')\}\right) \quad 2.4.30$$

and the right side of the governing equation Eq. 2.4.23 to

$$\int_{0^-}^{t-\tau_m} [ABD(t-\tau)]\{\varepsilon^0\kappa(\tau)\}' \, d\tau$$

$$- [ABD(\tau_m)]\{\varepsilon^0\kappa(0)\} + \qquad 2.3.31$$

$$\frac{1}{2}\Delta\tau\sum_{i=1}^{m} R_i\left([ABD(\tau_m-\tau_{i-1})]\{\varepsilon^0\kappa(\tau_{i-1})\} + [ABD(\tau_m-\tau_i)]\{\varepsilon^0\kappa(\tau_i)\}\right)$$

The governing equation could then be written in algebraic form as

$$\{NM^M(t)\} + \{\overline{NM}^{MC}(\tau_m-0,\varepsilon^{MC}(0))\} +$$

$$\frac{1}{2}\Delta\tau\sum_{i=1}^{m} R_i\left(\{\overline{NM}^{MC}(\tau_m-\tau_{i-1},\varepsilon^{MC}(\tau_{i-1})')\} + \{\overline{NM}^{MC}(\tau_m-\tau_i,\varepsilon^{MC}(\tau_i)')\}\right) - \qquad 2.4.32$$

$$[ABD(\tau_m)]\{\varepsilon^0\kappa(0)\} +$$

$$\frac{1}{2}\Delta\tau\sum_{i=1}^{m} R_i\left([ABD(\tau_m-\tau_{i-1})]\{\varepsilon^0\kappa(\tau_{i-1})\}' + [ABD(\tau_m-\tau_i)]\{\varepsilon^0\kappa(\tau_i)\}'\right)$$

where

$$(\tau_0-0) < \tau_1 < \tau_2 < \tau_3 < \cdots < \tau_{m-2} < \tau_{m-1} < (\tau_m-t) \qquad 2.4.33$$

Next, successive computation is employed to obtain the history of strain-curvature and their rates at the $t+1$ discrete time points, τ_0, through τ_m.

At $m=1$, which is $t=\tau_m=\tau_1$, there is

$\{N$

$\frac{1}{2}\Delta$

AB

$\frac{1}{2}\Delta$

As r

$\{N$

$\lim_{(r_j - r$

AB

$\lim_{(r_j - r_i}$

Sinc

seco

$= \{($

$\lim_{(r_j - r_0}$

$\lim_{(r_j - r_0}$

and s

$$\left\{NM^{M}(\tau_1)\right\} + \left\{\overline{NM}^{MC}(\tau_1-0,\varepsilon^{MC}(0))\right\} +$$

$$\frac{1}{2}\Delta\tau R_1\left(\left\{\overline{NM}^{MC}(\tau_1-\tau_0,\varepsilon^{MC}(\tau_0)')\right\} + \left\{\overline{NM}^{MC}(\tau_1-\tau_1,\varepsilon^{MC}(\tau_1)')\right\}\right) -$$

2.4.34

$$\left[ABD(\tau_1)\right]\left\{\varepsilon^0\kappa(0)\right\} +$$

$$\frac{1}{2}\Delta\tau R_i\left(\left[ABD(\tau_1-\tau_0)\right]\left\{\varepsilon^0\kappa(\tau_0)\right\}' + \left[ABD(\tau_1-\tau_1)\right]\left\{\varepsilon^0\kappa(\tau_1)\right\}'\right)$$

As τ_1 approaches $\tau_0=0$, it is obtained that

$$\left\{NM^{M}(0)\right\} + \left\{\overline{NM}^{MC}(0,\varepsilon^{MC}(0))\right\} +$$

$$\lim_{(\tau_1-\tau_0)\to 0}\frac{1}{2}\Delta\tau R_1\left(\left\{\overline{NM}^{MC}(\tau_1-\tau_0,\varepsilon^{MC}(\tau_0)')\right\} + \left\{\overline{NM}^{MC}(\tau_1-\tau_1,\varepsilon^{MC}(\tau_1)')\right\}\right) -$$

2.4.35

$$\left[ABD(0)\right]\left\{\varepsilon^0\kappa(0)\right\} +$$

$$\lim_{(\tau_1-\tau_0)\to 0}\frac{1}{2}\Delta\tau R_i\left(\left[ABD(\tau_1-\tau_0)\right]\left\{\varepsilon^0\kappa(\tau_0)\right\}' + \left[ABD(\tau_1-\tau_1)\right]\left\{\varepsilon^0\kappa(\tau_1)\right\}'\right)$$

Since no sudden hygroscopic strain input at $t=0$ is possible ($\{\epsilon^{MC}(0)\}_k = \{0\}$), the second term on the left hand side is zero. Assuming no mechanical action ($\{NM^{M}(0)\} = \{0\}$) and no initial strains at $t=0$ ($\{\epsilon^0\kappa(0)\} = \{0\}$), we then have

$$\lim_{(\tau_1-\tau_0)\to 0}\frac{1}{2}\Delta\tau R_1\left(\left\{\overline{NM}^{MC}(\tau_1-\tau_0,\varepsilon^{MC}(\tau_0)')\right\} + \left\{\overline{NM}^{MC}(\tau_1-\tau_1,\varepsilon^{MC}(\tau_1)')\right\}\right) -$$

2.4.36

$$\lim_{(\tau_1-\tau_0)\to 0}\frac{1}{2}\Delta\tau R_i\left(\left[ABD(\tau_1-\tau_0)\right]\left\{\varepsilon^0\kappa(\tau_0)\right\}' + \left[ABD(\tau_1-\tau_1)\right]\left\{\varepsilon^0\kappa(\tau_1)\right\}'\right)$$

and subsequently arrive at

$\overline{NM}$

The s

$\{\varepsilon^0$

The s

$\{\varepsilon^0$

where

curva

$t=\tau_0$

expan

$\{\varepsilon^0$

$\left(\frac{2}{\Delta\tau}\right.$

The st

$\{\varepsilon^0$

Eq. 2.

rates a

$$\left\{\overline{NM}^{MC}(0,\varepsilon^{MC}(0)')\right\} - [ABD(0)]\left\{\varepsilon^0\kappa(\tau_0)\right\}' \qquad 2.4.37$$

The strain and curvature rates at $t=\tau_0=0$ are then determined to be

$$\left\{\varepsilon^0\kappa(0)\right\}' - [ABD(0)]^{-1}\left\{\overline{NM}^{MC}(0,\varepsilon^{MC}(0)')\right\} \qquad 2.4.38$$

The strains and curvatures at $t=\tau_1$ can subsequently be approximated by

$$\left\{\varepsilon^0\kappa(\tau_i)\right\} \approx \left\{\varepsilon^0\kappa(\tau_{i-1})\right\}' R_i\,\Delta\tau + \left\{\varepsilon^0\kappa(\tau_{i-1})\right\} \qquad at\ i\text{-}1 \qquad 2.4.39$$

where small interval condition of Eq. 2.4.27 is to be maintained, and initial strains and curvatures at $t=\tau_0=0$ ($\{\epsilon^0\kappa(\tau_0)\}$) are assumed given. With strain and curvature rates at $t=\tau_0=0$ ($\{\epsilon^0\kappa(\tau_0)\}'$) known, the rates at $t=\tau_1$ ($\{\epsilon^0\kappa(\tau_1)\}'$) can then be determined by expanding Eq. 2.4.32 to be

$$\begin{aligned}\left\{\varepsilon^0\kappa(\tau_1)\right\}' = {} & \left[ABD(\tau_1-\tau_1)\right]^{-1} \\ & \left(\frac{2}{\Delta\tau}\left(\left\{NM^M(\tau_1)\right\} + \left\{\overline{NM}^{MC}(\tau_1,\varepsilon^{MC}(\tau_0))\right\} - \left[ABD(\tau_1)\right]\left\{\varepsilon^0\kappa(\tau_0)\right\}\right) + \right. \\ & R_1\left\{\overline{NM}^{MC}(\tau_1-\tau_0,\varepsilon^{MC}(\tau_0)')\right\} + R_1\left\{\overline{NM}^{MC}(\tau_1-\tau_1,\varepsilon^{MC}(\tau_1)')\right\} - \\ & \left. R_1\left[ABD(\tau_1-\tau_0)\right]\left\{\varepsilon^0\kappa(\tau_0)\right\}'\right)\end{aligned} \qquad 2.4.40$$

The strains and curvatures at $t=\tau_2$ are then

$$\left\{\varepsilon^0\kappa(\tau_i)\right\} \approx \left\{\varepsilon^0\kappa(\tau_{i-1})\right\}' R_i\,\Delta\tau + \left\{\varepsilon^0\kappa(\tau_{i-1})\right\} \qquad at\ i\text{-}2 \qquad 2.4.41$$

Eq. 2.4.32 could be further expanded to obtain the rates at $t=\tau_2$, subsequently. Similarly, rates at $t=\tau_3$, τ_4, and till τ_m, could be successively determined, as well as the strains and

curvatures in analogy to Eq. 2.4.39. The general form for this successive computation at discrete time point, $t=\tau_m$, is derived to be

$$\left\{\varepsilon^0\kappa(\tau_m)\right\}' = \left[ABD(\tau_m-\tau_m)\right]^{-1}$$
$$\left(\frac{2}{\Delta\tau}\left(\left\{NM^M(\tau_m)\right\} + \left\{\overline{NM}^{MC}(\tau_m,\varepsilon^{MC}(\tau_0))\right\} - \left[ABD(\tau_m)\right]\left\{\varepsilon^0\kappa(\tau_0)\right\}\right) + \right. \qquad 2.4.42$$
$$\sum_{i=1}^{m}(R_{i-1}+R_i)\left(\left\{\overline{NM}^{MC}(\sum_{j=i}^{m}R_i\Delta\tau,\varepsilon^{MC}(\tau_{i-1})')\right\} - \left[ABD(\sum_{j=i}^{m}R_j\Delta\tau)\right]\left\{\varepsilon^0\kappa(\tau_{i-1})\right\}'\right)$$
$$\left. + R_m\left\{\overline{NM}^{MC}(\tau_m-\tau_m,\varepsilon^{MC}(\tau_m)')\right\}\right)$$

where

$$R_0=0$$
$$m=1,2,3,\cdots \qquad 2.4.43$$
$$\sum_{j=i}^{m}R_j\Delta\tau = \sum_{j=1}^{m}R_j\Delta\tau - \sum_{j=1}^{i-1}R_j\Delta\tau$$

The second term within the enclosing parenthesis on the right hand side of Eq. 2.4.42 which results from step-wise elevation of hygroscopic strains at $t=\tau_e=0$ ($\{\epsilon^{MC}(\tau_0)\}_k$) must be zero since $\{\epsilon^{MC}(\tau_0)\}_k = \{0\}$ (It is not possible to elevate hygroscopic strains instantaneously as discussed in the derivation of Eq. 2.4.36). As such, Eq. 2.4.42 becomes

$\{\varepsilon$

$\left\{-\right.$

$\sum_{i=1}^{n}$

mus

acti

2.4.

$\{\varepsilon^0$

$\left\{\sum_{i=1}^{n}\right.$

the li

curva

theref

degen

points

stress

$$\left\{\varepsilon^0\kappa(\tau_m)\right\}' = \left[ABD(\tau_m-\tau_m)\right]^{-1}$$
$$\left(\frac{2}{\Delta\tau}\left(\left\{NM^M(\tau_m)\right\} - \left[ABD(\tau_m)\right]\left\{\varepsilon^0\kappa(\tau_0)\right\}\right) + \right.$$
$$\sum_{i=1}^{m}(R_{i-1}+R_i)\left(\left\{\overline{NM}^{MC}(\sum_{j=i}^{m}R_i\,\Delta\tau,\varepsilon^{MC}(\tau_{i-1})')\right\} - \left[ABD(\sum_{j=i}^{m}R_j\,\Delta\tau)\right]\left\{\varepsilon^0\kappa(\tau_{i-1})\right\}'\right) \qquad 2.4.44$$
$$\left. + R_m\left\{\overline{NM}^{MC}(\tau_m-\tau_m,\varepsilon^{MC}(\tau_m)')\right\}\right)$$

$\{\epsilon^o\kappa(\tau_0)\}$, the sudden step-wise elevation of strains and curvatures at $t=\tau_0=0$, must also be zero ($\{\epsilon^o\kappa(\tau_0)\}=\{0\}$) if there is no provocation by initial mechanical actions. In addition, if mechanical actions are never introduced ($\{NM^M(\tau_m)\}=\{0\}$), Eq. 2.4.44 is reduced to

$$\left\{\varepsilon^0\kappa(\tau_m)\right\}' = \left[ABD(\tau_m-\tau_m)\right]^{-1}$$
$$\left(\sum_{i=1}^{m}(R_{i-1}+R_i)\left(\left\{\overline{NM}^{MC}(\sum_{j=i}^{m}R_i\,\Delta\tau,\varepsilon^{MC}(\tau_{i-1})')\right\} - \left[ABD(\sum_{j=i}^{m}R_j\,\Delta\tau)\right]\left\{\varepsilon^0\kappa(\tau_{i-1})\right\}'\right) \qquad 2.4.45$$
$$\left. + R_m\left\{\overline{NM}^{MC}(\tau_m-\tau_m,\varepsilon^{MC}(\tau_m)')\right\}\right)$$

The associated stresses could be computed from the strain and curvature rates by the linear viscoelastic stress-strain relations defined in Eq. 2.4.6. However, the strain and curvature rates are known only at discrete time points rather than continuously, and therefore the integral linear viscoelastic stress-strain relations of Eq. 2.4.6 needs to be degenerated to express stresses in terms of strain and curvature rates at those discrete points. By the same numericalization technique as specified in Eq's. 2.4.25 - 2.4.29, the stress for lamina k is degenerated to

$\{\sigma($

$\cdot \dot{\Sigma}$

$\sum_{i=1}$

whic

strai

$\{\sigma($

$\frac{1}{2}\Delta$

where

$\{\varepsilon^M($

as in

be det

$w_j(x, y$

if the l

point, a

$$\{\sigma(t)\}_k = \int_{0^-}^{t-\tau_m} [\bar{Y}(t-\tau)]_k \{\varepsilon^M(\tau)\}'_k d\tau$$

$$\approx [\bar{Y}(t)]_k \{\varepsilon^M(0)\}_k + \qquad 2.4.46$$

$$\sum_{i-1}^{m} \frac{1}{2} R_i \Delta\tau \left(\left[\bar{Y}\left(\sum_{j-i+1}^{m} R_j \Delta\tau \right) \right]_k \{\varepsilon^M(\tau_i)\}'_k - \left[\bar{Y}\left(\sum_{j-i}^{m} R_j \Delta\tau \right) \right]_k \{\varepsilon^M(\tau_{i-1})\}'_k \right)$$

which, by further expansion and regrouping and by assuming zero sudden step input of strains and curvatures at $t=\tau_0=0$ ($\{\epsilon^M(0)\}_k=\{0\}$), becomes

$$\{\sigma(\tau_m)^M\}_k \approx$$

$$\frac{1}{2} \Delta\tau \left(\sum_{i-1}^{m} (R_{i-1}+R_i) \left[\bar{Y}\left(\sum_{j-i+1}^{m} R_j \Delta\tau \right) \right]_k \{\varepsilon^M(\tau_{i-1})\}'_k + R_m [\bar{Y}(0)]_k \{\varepsilon^M(\tau_m)\}'_k \right) \qquad 2.4.47$$

where

$$\{\varepsilon^M(\tau_i)\}'_k = \{\varepsilon^0(\tau_i)\}' + z\{\kappa(\tau_i)\}' - \{\varepsilon^{MC}(\tau_i)\}'_k \qquad 2.4.48$$

as in Eq. 2.4.8.

For a laminate as depicted in Figure 18, its vertical deflection at an instant t could be determined by

$$w_0(x,y,t) = -\frac{1}{2}\left(\kappa_x(t)x^2 + \kappa_y(t)y^2 + \kappa_{xy}(t)xy\right) \qquad 2.4.49$$

if the laminate's geometrical center $(x/2, y/2, z, t)$ is fixed to the coordinate reference point, and the mid-plane of the flat laminate coincides with the $z=0$ x-y *plane*. This is

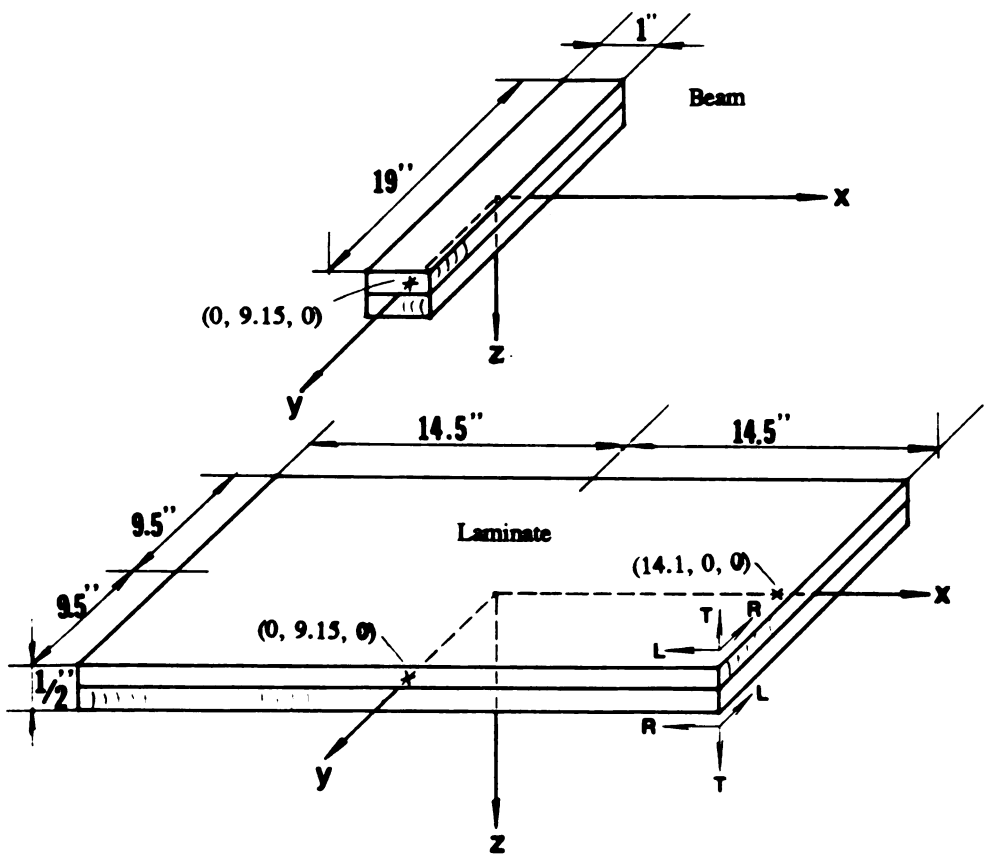

Figure 18. Coordinate positions of the yellow-poplar laminate and beam.

readily verified by use of the curvature-vertical deflection relation defined in the strain field of Eq. 2.3.9.

In summary, Eq's. 2.4.45, 2.4.41, 2.4.47, and 2.4.49 form the set of formulas of the developed linear viscoelastic plate theory for solving numerically for the history of strain and curvature rates, strains, stresses, and vertical deformations of a laminate described in Figure 18 subjected to hygroscopic effects. Upon the added presence of mechanical actions and sudden elevation of mechanical strains and curvatures at $t=0$, Eq's. 2.4.44 and 2.4.46 replace Eq's. 2.4.45 and 2.4.47 respectively in the formula set.

2.4.4 Linearity and Isothermal Requirements

The linear isothermal viscoelastic constitutive equations of Eq. 2.4.3 or 2.4.4, the basis upon which the LVP theory is developed, determined that the analytical governing equation of Eq. 2.4.23 is only applicable to linear isothermal viscoelastic problems which are defined by the stress independence of the relaxation moduli or creep compliances (linear), and the steady and uniform temperature distribution (isothermal). Such application restrictions on the integral governing equation (Eq. 2.4.23), once carried over to its numerical equivalence (Eq's. 2.4.43 - 2.4.45), however are much lessened. The first step (Eq. 2.4.25) in the numericalization process which establishes the conditional numerical-integral equivalence, clearly determines that the linearity and isothermal requirements only need to be imposed within each time segments $\tau_i - \tau_{i-1} = R_i \Delta\tau$, while nonlinearity and nonisothermal conditions would be allowed across time segments in the numerical equivalence (Eq's. 2.4.43 - 2.4.45). Further, since time

seg

reas

isot

app

the

ther

mois

whic

mate

2.4.

relax

hygr

expa

prop

theor

this c

last c

lamir

segments are sufficiently small due to the small interval assumption (Eq. 2.4.27), it is reasonable to approximate nonlinearity and nonisothermal conditions with linear and isothermal behavior within each segment. Therefore, the linearity and isothermal application restrictions are no longer imposed on the numerical equivalence outlined in the formula set, and the LVP theory is therefore applicable to nonlinear and nonisothermal viscoelastic problems such as hygroscopic warping.

If parallelness can be drawn regarding the effects of temperature and that of moisture content, the aforementioned isothermal requirement extends to moisture content, which would require a uniform and steady moisture content distribution for hygroscopic materials.

2.4.5 Hygroscopic Strain Rates and Relaxation Moduli

It is evident in the set of formulas that the hygroscopic strain rates and linear relaxation moduli denoted as $\{\epsilon^{MC}(t)\}'_k$ and $[Y(t)]_k$ are two of the essential inputs. While hygroscopic strain rates $\{\epsilon^{MC}(t)\}'_k$ are the results of changing moisture contents and expansion coefficients, linear relaxation moduli $[Y(t)]_k$ are determined by the viscoelastic properties of constituent laminas which are the subject of the next chapter. As the theoretical development of the CLT-based linear viscoelastic plate theory is the focus of this chapter, the discussion and formulation of all required inputs will be furnished in the last chapter when the numerical form of the LVP theory is applied to an actual physical laminate.

3.1

ma

the

des

to

our

requ

of b

time

cons

and

Dav

mole

due

struc

CHAPTER III

CHARACTERIZATION OF VISCOELASTIC BEHAVIOR

3.1 Introduction

The proper characterization of the viscoelastic behavior of the constituent materials in a laminate in the form of relaxation moduli is the key to the application of the theory to practical problems. A perfect and complete description, though ideally desired, may not be obtained since it is, in many cases, not only painstakingly difficult to achieve, but also unnecessary as the associated efforts and complexity may far outweigh any benefits and the limited gains may prove to be overkill under given requirements. Therefore, an adequate description which must be contemplated in light of balancing factors should give a sufficiently accurate characterization, but at the same time should be as simple an expression as possible, and achievable with moderate effort.

It is known that wood and wood-based materials behave viscoelastically as a consequence of their amorphous and crystalline components, cellulose, hemicellulose, and lignin, and the structures revolving among them [Alexopoulos, 1989; Pentoney and Davidson, 1962]. Characterization of the viscoelastic behavior based on a complete molecular theory, though theoretically feasible, is rather difficult to develop however, due to the complexity and lack of understanding of the wood components and the structures of both wood and wood-based materials. As a result, the most dominant

appr

is th

the v

woo

some

relat

of st

assu

of a

and

linea

anal

3.2

othe

all p

of t

approach has been from the phenomenological point of view, that is the macro behavior is the subject of investigation while transcending the micro-mechanism responsible for the viscoelastic behaviors. It is not surprising that the same approach is adopted here.

It is widely proven in the enormous literature and very evident in applications that wood and wood-based materials generally behave nonlinearly viscoelastically. The sometimes so-called linear regions are no more than regions where nonlinearity is relatively insignificant as a result of minimum influence from low and/or moderate levels of stress, moisture content and temperature, and can be approximated to be linear. This assumption is usually necessary for achieving a successful analysis, yet at the sacrifice of accuracy that may be large when nonlinearity becomes relatively pronounced.

An attempt is made in the following to quantitatively characterize the nonlinear and nonisothermal viscoelastic behavior of wood and wood-based materials, but with linear concepts and linear mechanical viscoelastic models for simplicity and ease of analysis.

3.2 Literature Reviews

New ideas and additional work are always conceived and build upon the work by others of today and yesterday. This thesis is no exception. A review and discussion of all pertinent information is the foundation for the development of a quantitative depiction of the nonlinear viscoelastic behavior.

3.2.

com

whi

$J(t)$

whe

appl

ratio

$\varepsilon_R($

It o

to c

wit

visc

loa

star

3.2.1 The Nonlinearity - Relation Between Viscoelastic Properties and Stress Levels

Viscoelastic behavior is defined as being linear if stress independence of creep compliance $J(t)$ is observed in a creep test (or relaxation modulus in a relaxation test), which is defined as

$$J(t) = \frac{\varepsilon(t)}{\sigma^*} \qquad 3.2.1$$

where $J(t)$ and $\epsilon(t)$ are creep compliance and strain history, respectively and σ^*_0 the applied time-wise constant creep stress in the test. The relative creep is defined as the ratio of creep strain over the initial instantaneous strain,

$$\begin{aligned} \varepsilon_R(t) &= \frac{\varepsilon(t) - \varepsilon(0)}{\varepsilon(0)} \\ &= \frac{J(t)\sigma^* - J(0)\sigma^*}{J(0)\sigma^*} \\ &= \frac{J(t) - J(0)}{J(0)} \end{aligned} \qquad 3.2.2$$

It obviously observes the same stress independence, and is therefore a criteria often used to check for linearity. The stress independence is the equivalent to strain being linear with stress, as indicated in Eq. 3.2.1.

Reported limits of stress levels within which wood may be assumed to be linearly viscoelastic vary widely due to differences in testing environments, designs, species, and loading with respect to grain direction. Nielsen [1972] reported 30 percent of the ultimate static strength to be the limit of linearity, yet according to a review by Schniewind [1968]

many authors in their experiments arrived at values from 38 percent to as high as 75 percent. It was shown that once above those limits wood and wood-based materials clearly exhibited nonlinear viscoelastic behavior. It is a well documented and established fact that a region where wood and wood-based materials can be treated as being linearly viscoelastic definitely exists. Due to the simplicity of linear viscoelastic analysis, it is of great practical significance if wood and wood-based materials in use would usually fall into such linear regions and therefore can be treated so. Since actual load levels in application are rarely greater than 50 percent of the static strength which is about the limit of linearity found by many authors [Schniewind, 1968], linear treatment may seem to be a rather promising approach as suggested by Schniewind [1968].

In further examining the test conditions under which those limits of linearity were arrived at, one may raise some doubts as to the validity of the linear treatment. The relative humidity and temperature in those tests were low and moderate, and maintained at constant levels. In contrast, they vary continuously in actual applications and could rise to very high levels. Bach and Pentoney [1968] found that the deformation-stress relation of maple subjected to longitudinal tension was definitely nonlinear at high humidity and temperature values.

Bach and Pentoney [1968] succeeded in expressing total compliance as well as its components as quadratic functions of stress, moisture content, and temperature in longitudinal tension tests on maple in which the separate effects of the three variables were included. They showed that wood responds to longitudinal tension stress as an elastic body at low temperatures and moisture contents (total compliance being constant).

At

cor

rel

of

cor

[19

be

dir

mo

the

con

of

var

con

cha

con

mu

pri

and

cre

At very low stress, wood approximates the response of a linear viscoelastic body (total compliance stress independent) even if the temperatures and moisture contents are relatively high, and changing. However, stress dependence of the compliance (character of nonlinear viscoelasticity) at moderate and higher stress levels when varying moisture content and temperature is evident in the compliance expressions by Bach and Pentoney [1968] who pointed out that wood must be treated as a nonlinear viscoelastic material to be realistic.

Compliance results by Bach and Pentoney [1968] were obtained for the grain direction which is the most crystalline and elastic since the orientation of microfibrils are mostly in the grain direction. Nonlinearity is expected to be much more prominent across the grain of wood.

Though functions of moisture content, temperature, and stress levels, the compliance results by Bach and Pentoney [1968] do not represent the combined actions of the involved variables on actual compliances since Bach and Pentoney did not really vary moisture content and temperature under stress during their tests, but kept them constant in each creep test and varied their levels between tests. The actual effects of changing moisture content and temperature under stress are much more severe and complex. Numerous references have indicated that creep rates and the total creep were much larger when moisture content and temperature were changed under load rather than prior to loading and kept constant under load. The interaction between mechanical stress and moisture content-temperature changes obviously contributes a great deal more to creep than if they acted alone separately. Consequently, a creep compliance which would

otherwise have been stress independent (linear viscoelasticity) will be stress dependent (nonlinear viscoelastic behavior) in addition to being dependent on moisture content. To reflect the coupling effects of stress and moisture content changes, the interaction is often referred to as the mechano-sorptive effect. The prevalent view regarding the mechanism [Gibson, 1965] suggests structural changes at the micro level. Since structural changes occur under temperature changes [Davidson, 1962] as well, temperature changes under load are speculated to exert similar thermal-mechanical coupling effects.

In short, the region in which wood and wood-based materials may be assumed to be linearly viscoelastic, though it exits, unfortunately has not as much practical significance as expected, largely due to the pervasive humidity and temperature changes (mechano-sorptive and thermal-mechanical coupling effects) in application environments which violate the conditions under which the linear assumption is valid. In reality wood and wood-based materials inevitably exhibit nonlinearity in their viscoelastic behavior.

3.2.2 Relation Between Viscoelastic Properties and Moisture Contents, and Mechano-Sorptive Effects

Moisture acts as a plasticizer, and increases in moisture content will usually lead to increases in creep compliance and decreases in relaxation modulus [Schniewind, 1968]. Bach and Pentoney [1968] found in longitudinal tension on maple that total compliance, as well as its components, were proportional to quadratic terms of moisture content. Increase in creep at increasing moisture content was also observed in bending [Nemeth, 1964; Ota and Tsubota, 1966], in tension and compression parallel and

perp

in to

repo

note

tests.

direc

of th

unfo

stres

beha

loade

whic

beam

creep

while

test.

1960

creep

and

[195

perpendicular to the grain of beech [Schniewind, 1968] and red oak [Youngs, 1957], and in torsion of Hinoki [Norimoto, Hiyano and Yamada, 1965]. Sharp stress relaxation was reported with increases in moisture content [Ugolev, 1964; Kunesh, 1961]. It is to be noted that moisture content changes were not introduced during creep and relaxation tests, but prior to the tests. For this reason, this phenomenon is sometimes called the direct effect of moisture content as in a review by Schniewind [1968].

The moisture content changes in wood and/or wood-based materials as a result of the frequent and sometimes drastic humidity changes in their application environment unfortunately coincide with the materials being in one or another state of loading or stress. As briefly mentioned earlier, the resulting coupling effect on the viscoelastic behavior is much greater than if moisture content changes had acted alone.

Armstrong and Kingston [1960] noted that small beams made of three species loaded green and kept so during creep test showed about the same relative creep as those which were loaded and kept dry, but the relative creep doubled when initially green beams were allowed to dry under load during the creep test. They also indicated that creep increased markedly in wood subjected to increasing moisture content during test while under load as compared to the case where moisture content was raised before the test. Similar trends were observed in relaxation test of beams [Armstrong and Kingston, 1960]. Cyclic changes under load amplify the above effect and lead to much larger total creep as observed by Armstrong and Christensen [1961] and Hearmon and Paton [1964], and to greater stress relaxation rate and residual deformation, as reported by Lawniczak [1958], Takemura and Ikeda [1963], and Takemura [1966 & 1967]. For example,

extensive cycling of moisture content at a given load caused a beam to deflect over 20 times more than keeping the beam conditioned at the extreme moisture content at the same load throughout the test [Hearmon and Paton, 1964].

Some manifestations of this mechano-sorptive effect are actually very common phenomena which have been used to advantage in practice. During either kiln or air drying, timber tends to distort because of spiral grain, growth stresses, reaction wood, and even its own gravity weight. However, good stacking and application of loads to the stack while drying takes place, can prevent most of such distortions [Koch, 1971]. In contrast, stacking and application of load even for an extended period of time after the timber is dried eliminates little of such drying distortions. In restrained swelling, the final pressure required to keep a wood body within its original dimensions as the body absorbs or desorbs moisture in the restraining process is much lower than that required at the end of the restraining process if the body's moisture content is raised or lowered preceding the restraint [Perkitny and Kingston, 1972]. Therefore, the resistance force exerted to a structure by a restrained wood member due to its hygroscopic expansion or shrinkage is greatly minimized.

Hearmon and Paton [1964] noticed that the known moisture content-MOE relation was not changed by cycling moisture content under load, suggesting that the elastic component is only affected by moisture content, regardless of whether and how moisture content is changed. Grossman [1976] indicated that upon removal of a load maintained during moisture content changes as much immediate and delayed recovery of shape occurred as would occur had the moisture content changes preceded the application of

load, indicating that both the elastic and the recoverable components of the deformation do not suffer from the mechano-sorptive effect. Only the flow portion of deformation are susceptible to the mechano-sorptive coupling.

One of the explanations regarding the mechanism is that the coupling effect results from interaction between the applied stress and stresses arising from the swelling or shrinkage differential caused by moisture content gradient. Armstrong and Christensen [1961] in testing both 1mm thick beams so as to eliminate the influence of moisture content gradient and 2cm thick beams for comparison observed similar effects on beams of both sizes, which suggested that stresses arising from nonuniform expansion or shrinkage were not likely involved. The most attractive hypothesis which is capable of explaining most aspects of this effect is that during the breaking and remaking of hydrogen bonds that must occur during moisture content changes in either direction, stress bias will favor slippage, resulting in new positions and shape [Schniewind, 1968; Gibson, 1965; Grossman, 1976].

There are many other aspects and characters to this mechano-sorptive effect as thoroughly discussed by Grossman [1976]. It is a phenomenon of considerable interest and practical significance, but nevertheless remains very perplexing with a great lack of understanding regarding its description and interpretation. A number of postulates were proposed over the years, yet fail to explain all the features of this effect cohesively. Finding a characterization that is compatible with all the observations remains a big challenge to wood scientists, and may take years of extensive research effort cooperatively put forward by all interested researchers.

Significant as this effect is, its lack of understanding also presents an impasse at the moment. For this reason, it was not included in the creep experiments and characterization of nonlinear viscoelastic behavior in this study. However, the direct effect of moisture content and stress level changes will be accounted for as they, even in the absence of mechano-sorptive effects, still exert great effects on the behaviors of wood and wood-based materials (hygroscopic materials).

An interesting characteristic displayed by wood and wood-based materials stands alone among materials in that the permanent deformation resulting from direct and mechano-sorptive effects of varying moisture contents under load are not really totally permanent, but at least a large portion can be recovered when the unloaded material is taken through another moisture content cycle. This is revealed by permanent deformation due to mechano-sorptive effect by Armstrong and Christensen [1961] and Christensen [1962]. It is demonstrated that the strain energy is not dissipated in the loading process and that some component within the structure "remembers" its original length and shape [Grossman, 1976]. This perplexing phenomenon, while a very significant and live component in the viscoelastic behavior of wood and wood-based materials because of the constant irregular humidity variation (cycling) in actual applications, can not be characterized yet due to the little information and understanding of it.

3.2.3 Relation Between Viscoelastic Properties and Temperature, and Thermal-Mechanical Coupling

As in the case of moisture content, we can distinguish between direct effect of

temperatures and interaction effect of temperature changes while under stress [Schniewind, 1968].

In general, increase in temperature leads to increase in creep compliance and decrease in relaxation modulus. In hard maple subjected to tensile creep parallel to grain in the temperature range from 30 ... 70° C, the total creep compliance as well as its components were reported to be proportional to quadratic terms of temperature [Bach and Pentoney, 1968]. In bending creep test on green specimens, the deflection increased exponentially with increasing temperature in the range of 5 to 70° C [Kitahara and Okabe, 1959]. Similar relation is observed in compression creep on oven-dry Hinoki in the temperature range from 100 to 180° C [Arima, 1967]. In torsional creep of Hinoki, the temperature effect seemed somewhat inconsistent, but in general caused an increase in creep compliance with increasing temperature [Norimoto, Hiyano and Yamada, 1965]. The results of Norimota and Yamada [1965] showed a decrease in relaxation modulus as temperature rose from 15 to 62.5° C, though the relaxation rate was affected little within this range. Other authors also found increased relaxation at elevated temperatures [Youngs, 1957; Ugolev and Pimenowa, 1963]. The results in many other references show the same general trend, but are rather diverse and inconclusive in terms of a quantitative description of the temperature effect.

More profound than the direct effect of temperature is the interaction arising from temperature changes occurring under load during test (thermal-mechanical coupling). It is noted in creep bending [Kitahara and Yukawa, 1964] that when the temperature was raised from 20 to 50° C during a creep test, the creep response was greater than that

occurring under constant temperature at the highest level throughout the test, though cooling during the test resulted in a sharp reduction of creep.

Temperature changes when coupled with moisture content changes while under load result in even more complex viscoelastic behavior [Schniewind, 1968]. This, unfortunately, occurs commonly in the applications of wood and wood-based materials. Very limited information regarding this phenomenon is available and much lack of understanding remains.

To isolate the direct effect of moisture content changes on the viscoelastic behavior, both the direct and interactive effects by temperatures variations are not included in this work. The results of the direct effect of increasing moisture content may be extended to the direct effect of increasing temperature to some degree of approximation according to Bach and Pentoney [1968], who noted an equivalence between one percent moisture content increase and 6° C temperature increase regarding their direct effects on the viscoelastic properties of hard maple tensioned parallel to the grain.

3.2.4 Functional Forms and Linear Viscoelastic Models

One of the basic aims of the study of viscoelastic behavior is the determination of mathematical representation of material response in relation to material parameters and time. Numerous models have been proposed in the literature which simulate the real materials with varying degree of success. In essence, they fall into two categories: empirical curve fitting, and mechanical models (springs and dashpots).

3.2.4.1 Empirical Models

Clouser [1959] in his bending creep work found that over relatively long time spans, the power law (parabolic) model was rather useful. Other researcher have had good success in using this model under mild and high humidity conditions. The model takes the form

$$\varepsilon(t) = \varepsilon_0 + at^m \qquad 3.2.3$$

where

$$\begin{aligned} \varepsilon(t) &= \textit{total strain} \\ \varepsilon_0 &= \textit{instantaneous elastic strain} \\ t &= \textit{elapsed time} \\ a, m &= \textit{constants} \end{aligned} \qquad 3.2.4$$

A variant is

$$\varepsilon(t) = at^m \qquad 3.2.5$$

which was also employed by some others. These two models prove to be the most popular representations.

King, Jr. used another form for very short term experiments in tension parallel to grain [King, Jr., 1961]:

$$\varepsilon(t) = \varepsilon_0 + b\log(t+1) \qquad 3.2.6$$

The sum of Eq's. 3.2.5 and 3.2.6 was also used to fit experimental results [Yamada,

Takemura and Kadita, 1961]. Bodig and Jane [1982] compiled a list of commonly used empirical equations in their publication on wood and wood mechanics.

3.2.4.2 Linear Mechanical Models

The empirical representations attempt to achieve the best mathematical fit to existing experimental data. They are simple and successful, but, only valid within the test conditions under which they are obtained. Different models may have to be employed once test conditions are changed to produce good fit. It is obvious that this test condition dependence does not allow comparison across tests in different environments, thus reducing the empirical models' application significance. And moreover the empirical method does not help in providing insights into the underlying processes controlling the viscoelastic behavior.

Rheological models or mechanical models, however, do not have those limitations. They are comprised of springs and dashpots interconnected in various fashions and model linear viscoelastic behavior if the springs and dashpots are linear elements. To be specific, linear springs (Hookean springs) which feature linear proportionality between stress and strain are used to simulate elastic components. Linear dashpots (Newtonian dashpots) possessing linear proportionality between stress and strain rates represent the flow components.

The most significant classical linear models are the Kelvin element, the Maxwell element, and the various combinations of the two, shown in Figure 19. A Kelvin element consists of a linear spring and a linear dashpot in parallel, while a Maxwell element

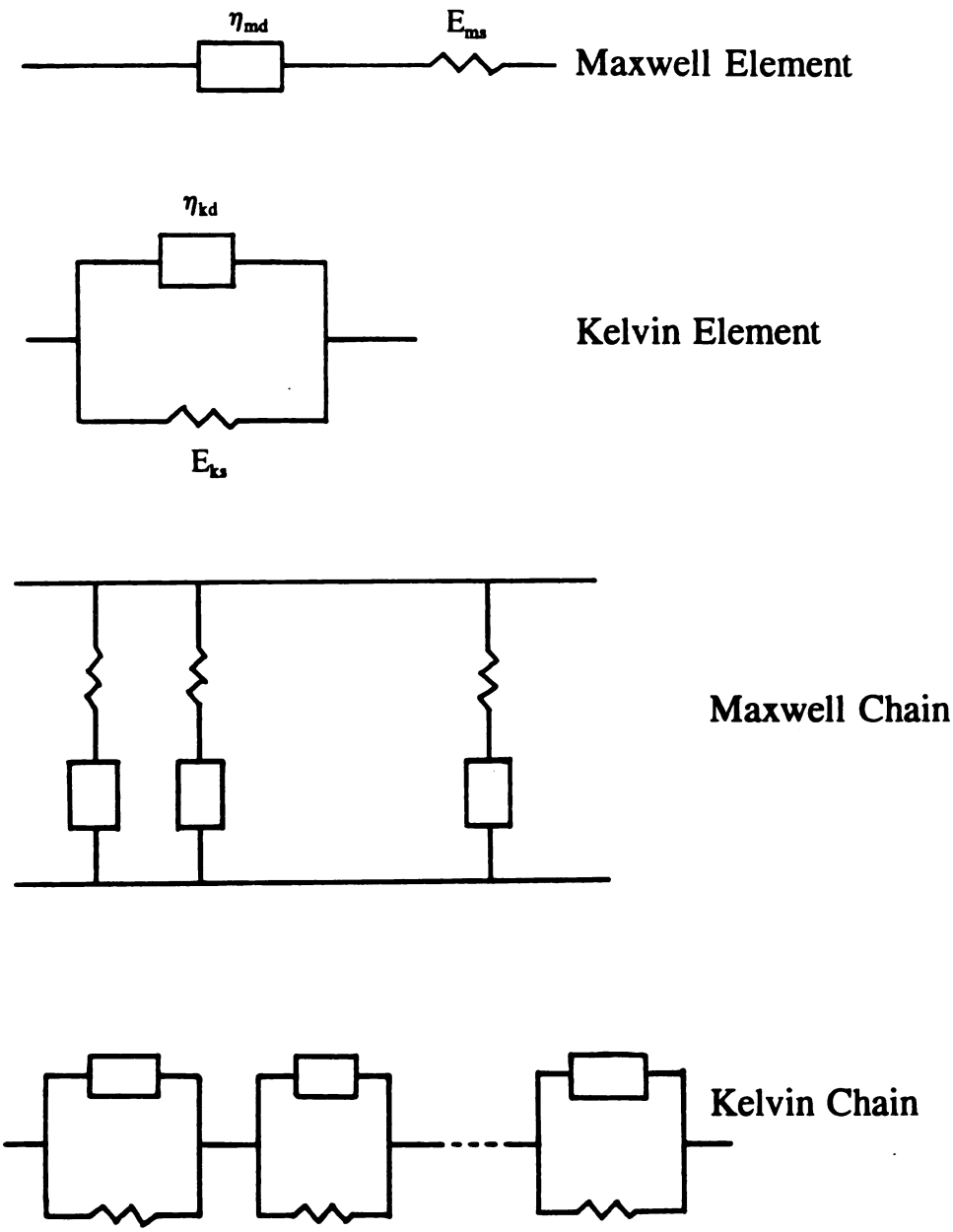

Figure 19. Classical linear viscoelastic models.

consists of a linear spring and a linear dashpot in series. A Kelvin chain is any number of Kelvin elements connected in series, whereas a Maxwell chain is any number of Maxwell elements linked in parallel.

The most convenient and simple linear model which has been used successfully to describe wood and wood-based materials is the four-element Burger body found in the book by Bodig and Jane [1982]. It is a Kelvin and a Maxwell element chained in series, as seen in Figure 20. By and large, it is accepted as capable of sufficiently and qualitatively explaining some of the fundamental aspects of the viscoelastic behavior of wood and wood-based materials. The Kelvin element accounts for the recoverable component of the behavior, while the spring and dashpot in the Maxwell element represent instantaneous elastic and flow behavior, respectively.

A good illustration of the creep deformation process by this Burger body is given in Figure 21. As seen, when a load is suddenly applied at t_0, only the spring responds by an instantaneous deformation equal to the product of the spring constant (E) and applied load (P) while the others remain in their original positions. With passage of time under the action of the load (P), both the Kelvin element and the Maxwell dashpot begin to extend gradually. Upon the removal of the applied load (P) at (t_1), the Maxwell spring instantaneously returns to its original position. The Kelvin element will return to its undeformed position too (elastic), however over a period of time, showing delayed character. The lone Maxwell dashpot will remain in its extended and irrecoverable position. For a more detailed discussion refer to Bodig and Jane [1982].

The mathematical form of the model, expressed in terms of creep compliance, is

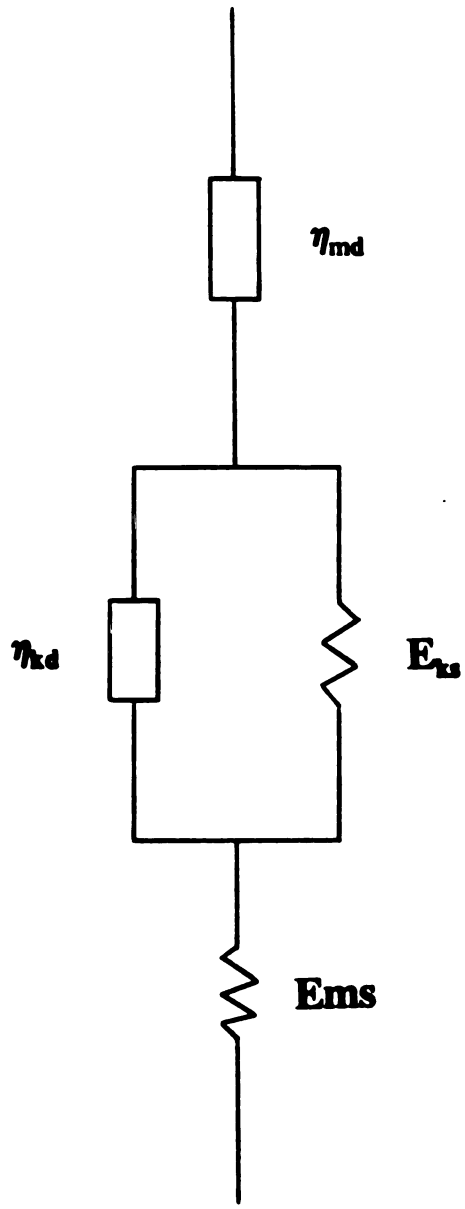

Figure 20. Four-element Burger body.

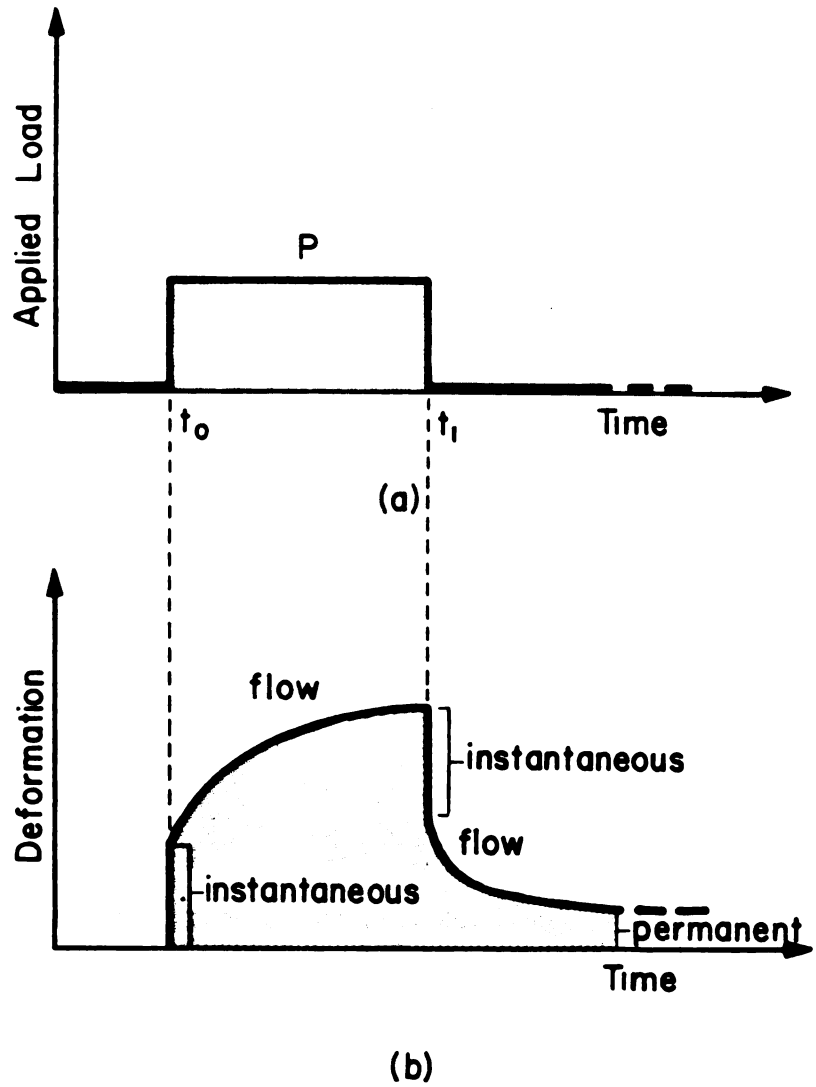

Figure 21. A typical creep curve [Bodig and Jane, 1982].

(a) load-time function.
(b) deformation-time function.

$$J(t) = \frac{\epsilon(t)}{\sigma^*} = \frac{1}{E_{ms}} + \frac{(1 - e^{-t/\tau})}{E_{ks}} + \frac{t}{\eta_{md}} \qquad 3.2.7$$
$$= J(0) + J_r(t) + J_f(t)$$

where $J(t)$, $J_r(t)$, and $J_f(t)$ are the total compliance, the recoverable compliance, and the flow compliance, respectively. $\epsilon(t)$ and σ^* are the total strain and time-wise constant creep stress. E_{ks}, E_{ms}, η_{kd}, and η_{md} are respectively the Kelvin and Maxwell spring constants, the Kelvin and Maxwell dashpot coefficients. The first term represents the Maxwell spring (elastic compliance), the second term represents the Kelvin element (recoverable compliance), and the last the Maxwell dashpot (flow compliance). Clearly, the total compliance is the sum of the contributions of the three elements.

The retardation time for the Kelvin element, τ, defined as

$$\tau = \frac{\eta_{kd}}{E_{ks}} \qquad 3.2.8$$

is determined by the relative ratio of the Kelvin spring constant over the Kelvin dashpot coefficient. With $t=\tau$ time elapsed, a Kelvin element has extended about 1/3 (almost one e^{th}) of or recovered about 2/3 of the total possible extension depending on whether a load is applied at zero extension or released at full extension. It is therefore a convenient measure of the retardation of the element's response.

The Burger body may be extended by inserting any number of Kelvin elements into the serial linking. Each element may have a different retardation time (defined in Eq. 3.2.8) which characterizes the time response of the element. Such models with

discrete retardation times have been applied by several authors [Ugolev, 1963; Rose, 1965; Ethington and Youngs, 1965]. Higher degree of approximation is expected of the extended Burger body in describing the recoverable component.

Since each Kelvin element's contribution to creep compliance is

$$J_r(t) = \frac{(1 - e^{-t/\tau})}{E_{ks}} \qquad 3.2.9$$

the creep compliance of a Burger body with N Kelvin elements, in analogy to Eq. 3.2.7, is

$$J(t) = \frac{\varepsilon(t)}{\sigma^*} = \frac{1}{E_{ms}} + \sum_{i}^{N} \frac{(1 - e^{-t/\tau_i})}{E_{ks_i}} + \frac{t}{\eta_{md}} \qquad 3.2.10$$
$$= J(0) + J_r(t) + J_f(t)$$

The extreme is reached when the number of Kelvin elements approaches infinity, at which time retardation times are continuously distributed. The summation in Eq. 3.2.10 becomes an integral and the total compliance is

$$J(t) = \frac{\varepsilon(t)}{\sigma^*} = \frac{1}{E_{ms}} + \int_{-\infty}^{\infty} L(\tau)(1 - e^{-\frac{t}{\tau}}) d\ln\tau + \frac{t}{\eta_{md}} \qquad 3.2.11$$
$$= J(0) + J_r(t) + J_r(t)$$

where $L(\tau)$ is the spectrum of retardation times.

It is possible to approximate both the retardation spectrum and its counterpart the relaxation spectrum from experimental data if they do exist. Both Alfrey [1948] and Leaderman [1958] developed a first approximation method. The result is quite good , but

only when the distribution is constant or changing slowly. Schwarzl and Staverman [1953] have extended this method to yield a better approximation. Pentoney and Davidson [1962] found in their study that the spectrum was quite flat, while Noritomo did find spikes in the spectra. The experimental work in obtaining the spectra is no easy task. As the moisture content and the temperature change, the spectra will both shift and change as a result of their sensitivity to moisture content [Norimoto, Hiyano and Yamada, 1965] and temperature [Davidson, 1962]. Obtaining spectra functions in terms of moisture content and temperature should be more challenging.

It should be emphasized that nonlinearity in a recoverable component would void all the effort on spectrum analysis which is based on linear mechanical models. The recoverable component may possibly be characterized as being linearly viscoelastic only at low stress levels and at temperature below 50° C [Davidson, 1962], and at low and moderate moisture content [Bach, 1968]. As significant as the contribution of the infinite Kelvin chain is in the extended Burger body, the extensive effort involved results in no more than a better depiction of the recoverable component, while a much larger part of the viscoelastic deformation is due to the flow element.

3.2.4.3 Nonlinear Models

It has been clearly indicated that at least the flow component in wood is non-Newtonian (nonlinear) [Davidson, 1962; Ethington and Youngs, 1965; Bach, 1965; Youngs and Hilbrand, 1963]. Among the attempts to model nonlinearity, Kühne [1961] proposed a hinged frame containing linear springs and dashpots where nonlinearity arises

out of frame geometry. Kingston and Clarke [1961] had moderate success with reaction rate theory and a model following the hyperbolic sine law. Ylinen [1965] devised a model consisting of a Maxwell element paralleled with a nonlinear spring to be applied to compressive loading parallel to the grain and to the long term load effects on columns [Ylinen, 1966]. The most complete treatment of nonlinearity is an empirical one by Bach [1965] in which total creep compliance, as well as its three components (instantaneous compliance, recoverable compliance, and flow compliance) were expressed as a function of linear and quadratic terms of logarithmic time, stress, moisture content, temperature, and their products.

3.3 Creep Experimentation

As stated in the literature review section, only direct effects of moisture content and stress levels will be tested.

Yellow-poplar (Liriodendron tulipifera) is the species chosen for the creep experiments. However, only viscoelastic properties in the radial direction will be tested and characterized. This will satisfy the input requirements for the application of the LVP theory, as detailed in the last chapter.

3.3.1 Experimental Design

Tension creep tests were carried out in the radial direction at three stress levels, approximately 25%, 50%, and 90% of the static strength, and at three moisture contents, 11.5%, 15.7%, and 21.5%, respectively. Temperature was maintained constant. With

two replications, there were a total of $3 \times 3 \times 3 = 18$ creep tests.

Edge grained boards were cut from large flat sawn yellow-poplar lumber free of juvenile wood. After being jointed and planed to appropriate thickness, they were edge glued with epoxy to form larger edge grained panels which after conditioning at 70° F and 65% R.H. were jointed and planed again to achieve flatness and a final thickness of 1/4 inch.

Long and slender radial tension specimens of 1/4 inch by 1/4 inch cross section and about 12 inch in length were cross cut from the prepared flat edge grained panel. The specimen ends were inserted into tension grips, leaving a usable specimen length of about 9 inches. The sample dimension and configuration are illustrated in Figure 22.

Holes were drilled through the tension grips at the ends of the tension specimen to fit loading pins. One of them anchored the creep sample to a frame, while the other transferred the static creep load (consisting of dead weights) to the creep specimen. Figure 23 shows the loading and extensometer assembly.

The three stress levels were achieved by combinations of different weights. The three moisture content levels were achieved by a light and simple apparatus affixed to the loading assembly. As shown in Figure 24a and Figure 24b, the apparatus consists of a rectangular plexi glass plate and two layers of thick plastic bags. The plate is supported by the top pin by means of four wires attached to the plate's four corners, and the hole in the plate center allows the weight hanger rod to pass through so that the plate does not interfere with the loading mechanism. The two-ply plastic bag with a hole in its closed end for the hanger rod to go through encloses the plexi glass plate and the entire

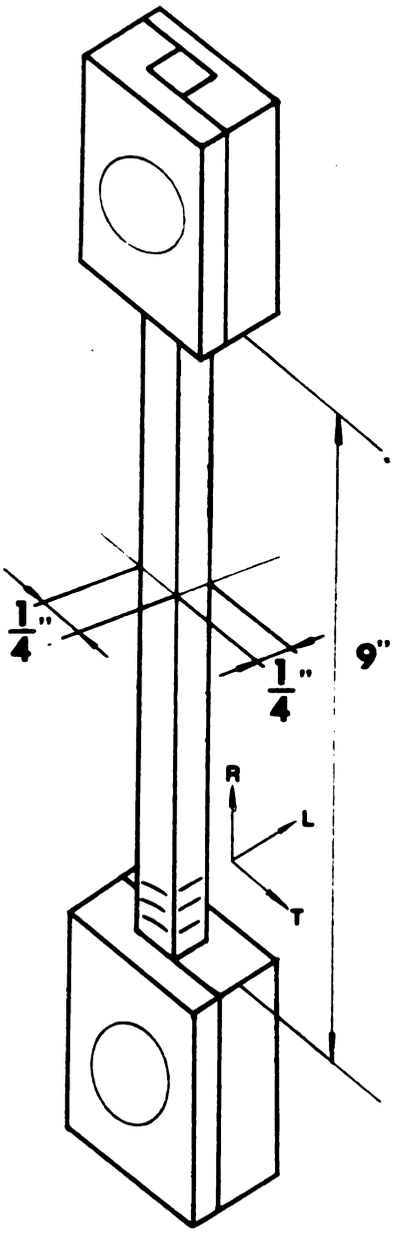

Figure 22. Radial tension creep specimen of yellow-poplar.

Figure 23. Loading frame and extensometer assembly.

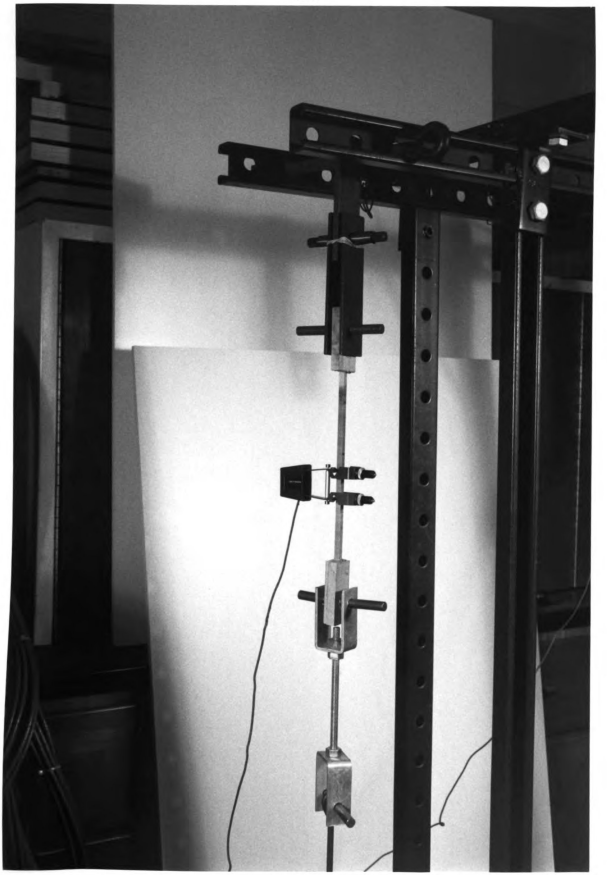

Figure 24a. Complete test setup with flexible humidity chamber open.

Figure 24b. Complete test setup with charged flexible humidity chamber enclosing tension creep specimen.

specimen. Tying up the open end of the plastic bag tight above the top pin creates an insulated humidity chamber in which the tension specimen could be placed and loaded. The flexible chamber is very small and is sealed at the top and at the bottom. By placing two dishes of saturated salt solutions on the plexi glass plate inside the flexible chamber, appropriate relative humidities could be created and maintained. (Figure 25a and Figure 25b are closeups of the flexible humidity chamber.) The three nominal relative humidities for achieving the three moisture content levels are 66% RH, 86% RH, and 93% RH which were created over saturated salt solutions listed in Table 3.

Table 3. Relative humidity over saturated salt solutions.

	Relative Humidity (%)
Chemical	@ 20° C
Sodium Nitrite	66
Potassium Chloride	86
Ammonium Phosphate	93

The specimen was placed into the loading mechanism and the flexible humidity chamber charged with appropriate salt solution with no load applied. As shown in Figure 24a, an calibrated Instron extensometer of 1 inch gauge length was affixed to the center portion of the specimen. Any extension within the gauge length was detected and recorded by the connected strain indicator.

To reduce possible slippage between the contact edges of the Instron extensometer and the specimen surface, the specimen was first sanded and then coated with a very narrow thin smooth layer of super glue where the extensometer edges contacted the

Figure 25a. Closeup of open flexible humidity chamber.

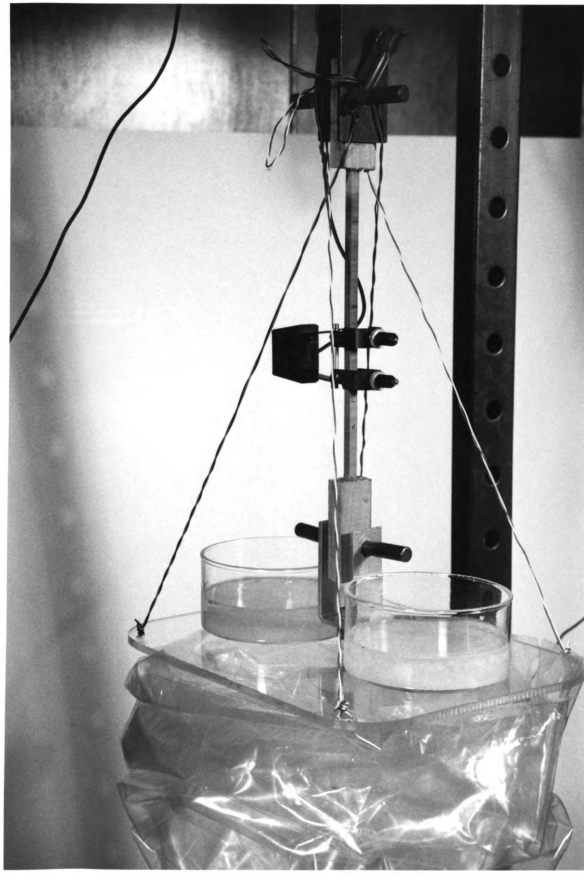

Figure 25b. Closeup of closed charged flexible humidity chamber.

specimen. To further eliminate any possible slack in the assembly, a 20 psi load was applied to the whole setup for 2 seconds, which increased reproducability.

While the stress-free specimen was being conditioned in the flexible humidity chamber to the equilibrium moisture content, the strain indicator indicated the hygroscopic expansion of the specimens. The extensometer-indicator system was calibrated to a sensitivity of 1/50000 extension per inch per scale unit indicator reading, that equals to an expansion strain of ((1/50000)/1)100 = 1/500% = 0.002%. (The extensometer-indicator system can be calibrated to higher sensitivity, but readings become unstable at sensitivities finer than 0.001% expansion strain.) When the indicator reading did not change more than 2 units (a 0.004% extension strain) over 12 hours, equilibrium moisture content was assumed to have been reached. At that point, the indicator was reset to zero and predetermined load was applied to the creep specimen by lowering a laboratory jack. The instantaneous elastic response was recorded immediately. Subsequent creep extension readings were recorded at selected time intervals.

Creep was allowed to continue in the charged flexible humidity chamber for about 600 hours, after which time the load was released by raising the laboratory jack. The instantaneous recovery was immediately recorded. The delayed recovery was recorded intermittently till the indicator reading became stable. The whole assembly was then taken down and preparations were made for the next creep test.

The modulus of elasticity (MOE) of a sample can be tested nondestructively with the extensometer-indicator mechanism. By subjecting the specimen to increments of load and recording corresponding strains on the indicator, a linear stress-strain relation was

obtained. The tangent of the linear line is the MOE. However, this test procedure by this must be completed within a couple minutes to avoid the onset of time dependent behavior.

All specimens, after having been conditioned and equalized at room conditions of 70° F and 65% RH, had their MOE so tested. Those with very similar MOE values were selected for the 18 creep tests to assure uniformity among test samples. The statistical basis for this selection was the normal distribution of the MOEs. Samples whose MOEs were around the average of the sample population were retained with others eliminated.

A small piece of control sample of yellow-poplar was placed into the charged flexible humidity chamber at the time a test sample was fitted into the loading set up. It was weighed both at the end of the test and after subsequent overnight oven-drying at 103° C, after which the equilibrium moisture content were computed.

The test setup is very simple and worked well, yet it is also very delicate and sensitive. Even the slightest disturbances to any part of it, like, repositioning of the extensometer wire, caused at least small changes of the indicator reading, and therefore had to be avoided. It is far from fool-proof, but care and practice reduce failures and mistakes.

3.3.2 Experimental Results and Observations

The recorded indicator readings were converted to extension strains based on the calibrated extensometer-indicator sensitivity. Dividing the extension strains by the applied

constant creep stress yields creep compliance

$$J(t) = \frac{\varepsilon(t)}{\sigma^*} \qquad 3.3.1$$

The initial creep compliance $J_o=J(0)$ is the elastic instantaneous strain divided by creep stress, which is the elastic compliance. Creep compliance can be normalized by dividing it by the corresponding initial creep compliance, that is

$$J_N(t) = \frac{J(t)}{J(0)} = \frac{J(t)}{J_0} \qquad 3.3.2$$

$J_N(t)$, the normalized creep compliance which is a compliance ratio, is related to relative creep $\epsilon_R(t)$ by

$$J_N(t) = \varepsilon_R(t) + 1 \qquad 3.3.3$$

according to Eq's. 3.3.2 and 3.2.2.

For comparability, data of all tension creep tests compiled in Table 4 were expressed in terms of normalized creep compliance. They are the average of two replications of tests for each of the nine test conditions outlined in Table 5. Nine sets of normalized creep compliances are presented in Figure 26.

It is shown in Figure 26 that the three normalized creep compliances for 11.5% moisture content almost coincide with each other. The stress level has no effect on the creep compliances (the criteria for linear viscoelasticity). At the two higher moisture content levels, however, the normalized creep compliances increase substantially with

Table 4. Normalized creep compliance of yellow-poplar in the radial direction at nine creep test conditions.

Test Condition Number					
11		12		13	
t (hour)	J(t)/J(0)	t (hour)	J(t)/J(0)	t (hour)	J(t)/J(0)
0	1	0	1	0	1
0.42	1.043	0.5	1.1	0.17	1.062
1.25	1.1	1	1.17	0.33	1.085
2.92	1.143	2	1.157	0.5	1.101
9.25	1.193	9.67	1.22	1	1.127
19.42	1.25	41.51	1.318	1.33	1.144
32.92	1.293	118.81	1.425	1.67	1.149
42.92	1.314	184.22	1.473	2	1.158
67.5	1.357	253.1	1.51	3.33	1.175
104.17	1.4	335.14	1.54	5.08	1.189
152.08	1.443	440.21	1.57	6.75	1.203
209.1	1.478	541.31	1.586	9.67	1.22
207.17	1.521	600	1.598	19.83	1.26
423.58	1.55	600	0.618	31.5	1.294
544	1.578	600.54	0.592	41.5	1.319
600	1.585	602	0.58	66.08	1.364
600	0.6	619.5	0.552	118.8	1.427
600.17	0.586	654	0.536	184.08	1.474
600.5	0.578	745.19	0.528	253.83	1.511
602	0.564			335.08	1.54
619	0.535			440.93	1.571
643.6	0.521			541.5	1.588
725	0.514			600	1.599
				600	0.619
				600.19	0.607
				611.54	0.593
				602.5	0.579
				618.7	0.554
				654.2	0.537
				765	0.528

Test Condition Number					
21		22		23	
t (hour)	J(t)/J(0)	t (hour)	J(t)/J(0)	t (hour)	J(t)/J(0)
0	1	0	1	0	1
0.5	1.08	0.08	1.1	0.07	1.15
5.5	1.292	0.17	1.128	0.15	1.205

Table 4 (cont'd)

25	1.604	0.25	1.15	0.23	1.26
49.67	1.792	0.42	1.182	0.4	1.291
76	1.979	0.67	1.215	1.07	1.474
101	2.104	2	1.332	1.73	1.574
148	2.25	2.67	1.364	2.73	1.685
189.5	2.354	3.67	1.407	3.73	1.771
241.67	2.458	4.67	1.439	4.73	1.84
292.5	2.5	5.67	1.472	5.73	1.904
351.67	2.604	6.67	1.504	6.82	1.949
404	2.625	7.75	1.536	9.07	2.018
471.25	2.667	10	1.579	10.73	2.073
509.42	2.708	11.67	1.611	11.73	2.109
559.13	2.729	12.67	1.632	22.4	2.42
600	2.75	23.33	1.804	48.57	2.767
600	1.771	46.5	2.041	69.4	3
600.17	1.75	71.33	2.233	135.42	3.465
600.5	1.708	94.33	2.393	207.9	3.77
602	1.688	154.67	2.67	265.37	3.965
619	1.625	203.33	2.8	312.5	4.048
643.67	1.604	257	2.93	353.83	4.131
667	1.583	304	3.004	447.5	4.27
766.48	1.563	353.5	3.079	516.27	4.325
		418.67	3.154	569.47	4.375
		474.27	3.209	620	4.408
		521.07	3.241	620	3.424
		610	3.284	620.5	3.41
		610	2.265	620.8	3.408
		610.53	2.19	621.75	3.362
		610.78	2.146	627.85	3.296
		611.78	2.093	638.75	3.258
		617.78	2.041	675.1	3.195
		628.78	1.976	709.2	3.17
		653.45	1.921	755.1	3.16
		676.78	1.889	830.8	3.15
		708.28	1.869		
		798	1.846		

Test Condition Number					
31		32		33	
t (hour)	J(t)/J(0)	t (hour)	J(t)/J(0)	t (hour)	J(t)/J(0)
0	1	0	1	0	1
0.08	1.059	0.07	1.121	0.05	1.151

Table 4 (cont'd)

0.33	1.078	0.23	1.204	0.13	1.263
0.67	1.137	0.57	1.287	0.3	1.368
1	1.157	0.73	1.316	0.63	1.528
1.33	1.196	1.23	1.371	0.97	1.644
2.12	1.235	3.23	1.566	1.3	1.735
2.75	1.274	5.23	1.678	1.72	1.844
3.5	1.314	6.23	1.704	2.08	1.918
4.5	1.373	10.23	1.891	2.72	2.05
5	1.412	22.9	2.242	3.47	2.177
6.67	1.471	46.23	2.613	4.47	2.352
9.17	1.627	74.23	2.946	4.97	2.422
10	1.647	84.23	3.021	6.63	2.623
12.97	1.784	103.73	3.197	9.13	2.918
22.5	2.039	118.73	3.271	9.97	2.97
24.75	2.078	142.73	3.392	10.13	2.988
28	2.137	166.73	3.502	12.88	3.191
30.75	2.157	176.4	3.55	22.47	3.613
34	2.216	180.18	3.567	24.72	3.669
47.5	2.412	189.68	3.596	25.97	3.75
54	2.431	214.68	3.66	30.75	3.815
82.75	2.627	237.93	3.725	33.97	3.887
97.5	2.745	252.68	3.8	47.47	4.093
119.83	2.784	274.35	3.826	53.97	4.131
143.67	2.882	298.18	3.892	82.72	4.333
166.25	2.941	357.42	4.03	97.47	4.444
190.75	3.019	442.02	4.179	119.8	4.5
237.27	3.137	509.2	4.272	143.63	4.585
287.5	3.255	562.02	4.327	237.17	4.844
347.9	3.333	610	4.392	297.05	4.968
407.5	3.451	610	3.392	333.33	5.055
467.9	3.529	610.05	3.335	385.1	5.131
528.5	3.568	610.18	3.289	437.5	5.2
600	3.647	610.93	3.216	516.77	5.313
600	2.686	611.93	3.16	620	5.387
600.07	2.314	615.43	3.076	620	4.433
600.22	2.294	633.1	2.975	620.02	4.431
600.97	2.255	659.43	2.891	620.05	4.4
601.47	2.235	730.18	2.742	620.3	4.354
603.97	2.196	871.93	2.65	620.88	4.313
649.47	2.118	991.93	2.613	624.22	4.229
692.93	2.078	1052.67	2.604	631.3	4.179

Table 4 (cont'd)

795.4	2.039	641.72	4.132
861.87	2.02	650.22	4.1
911.37	2	672.22	4.055
		696.22	4.011
		742.72	3.988
		809.22	3.946
		937.22	3.917
		1179.75	3.901

stress levels, evidencing the nonlinear viscoelastic behavior of yellow-poplar in the radialdirection at moderate and high moisture content levels.

The two MOEs were obtained from each creep test based on the instantaneous elastic strain from load application and from load removal, respectively. The former is called the initial MOE and the latter the recovery MOE. It is seen in Table 5 that there are slight increases in the range of 0 to 5 percent in the recovery MOE over the corresponding initial MOE. The elastic component showed time dependent creep at constant moisture content. Such time dependence is larger at high stress and moisture content levels. To substantiate the above finding, further investigation on larger numbers of observations is necessary. Nevertheless, the observed time dependence is very marginal and can probably be disregarded. Actually, both Herman and Paton [1964], and Grossman [1976] indicated that the elastic component quantified by MOE only, increases or decreases directly according to moisture content (temperature not considered here) under moisture content changes and/or moisture content cycling during stress, suggesting no such time dependent variation is experienced by MOE under either the direct effect of moisture content or mechano-sorptive coupling effect.

Table 5. Instantaneous MOEs of yellow-poplar in the radial direction at nine creep test conditions.

Test Condition Number	Moisture Content (%)	Creep Stress (psi)	Instantaneous MOE (10^3 psi)		MOE Change (%)
			Initial MOE	Recovery MOE @ 600 hrs	
11	11.5	100	145.96	146.92	0.66
12	11.5	310	148.72	149.96	0.83
13	11.5	650	145.54	148.59	2.10
Average:			146.74	148.49	
Predicted[1]:			145.25	148.12	
Difference (%)[2]:			-1.02	-0.25	
21	15.7	133	135.89	138.57	1.97
22	15.7	314	136.93	140.57	2.65
23	15.7	785	135.56	142.22	4.91
Average:			136.13	140.45	
Predicted:			136.94	140.66	
Difference (%):			0.59	0.15	
31	21.5	130	124.80	129.89	4.08
32	21.5	321	124.58	130.65	4.88
33	21.5	600	124.02	131.00	5.62
Average:			124.47	130.51	
Predicted:			122.72	130.06	
Difference (%):			-1.4	-0.35	

1: MOE computed according to Eq. 3.3.5 on the basis of the MOEs at two other moisture content levels.
2: Difference between the computed MOE and the measured MOE.

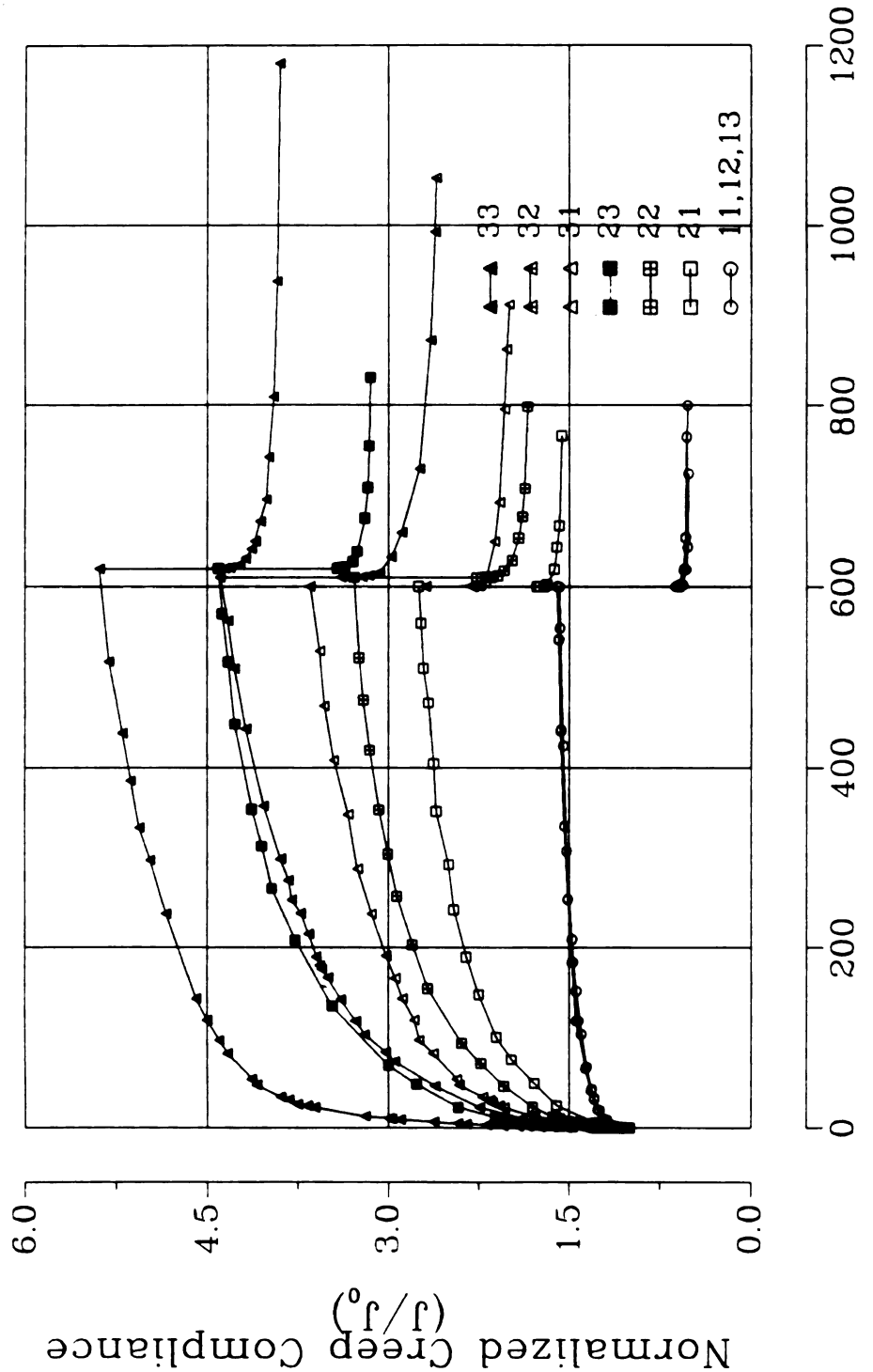

Figure 26. Normalized creep compliance of yellow-poplar in the radial direction at nine creep test conditions.

As expected, both MOEs decrease with increase in moisture content, as shown in Figure 27. The experimental data were checked for their agreement with the known moisture content-MOE relationship given in the Wood Handbook [Forest Products Laboratory, 1987]. A mechanical property at moisture content MC is found to be

$$P_{MC} = P_{12}\left(\frac{P_{12}}{P_G}\right)^{\left(\frac{MC-12}{12-MC_G}\right)} \qquad 3.3.4$$

where

P_{MC} - mechanical property at moisture content of MC percent

P_{12} - mechanical property at moisture content of 12 percent

P_G - mechanical property at green condition

MC_G is the moisture content at which the mechanical property ceases to decrease with moisture content. A variant form of the same relation is

$$P_{MCx} = P_{MC_1}\left(\frac{P_{MC_1}}{P_{MC_2}}\right)^{\left(\frac{MCx-MC_1}{MC_1-MC_2}\right)} \qquad 3.3.5$$

where

P_{MCx} - mechanical property at moisture content of Mcx percent

P_{MC1} - mechanical property at moisture content of MC_1 percent

P_{MC2} - mechanical property at moisture content of MC_2 percent

This version allows for the calculation of the mechanical property at any moisture content (Mcx) given the property at moisture content MC_1 and MC_2. The MOE at the third

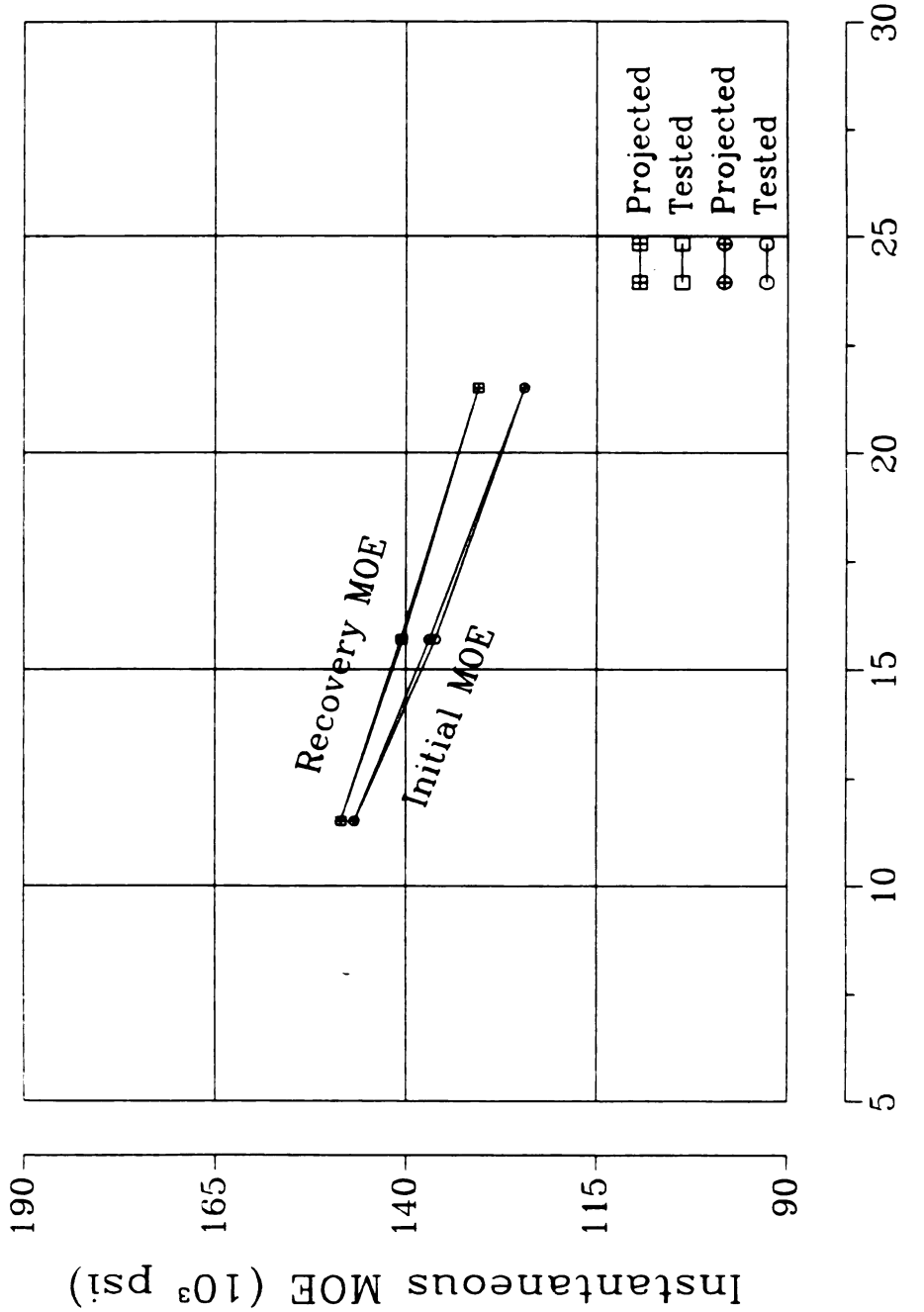

Figure 27. Instantaneous MOEs of yellow-poplar in the radial direction.

moisture content calculated based on the MOEs at two other moisture content levels was found to be within 2% of the actual MOE value. Table 5 and Figure 27 illustrate such close agreement.

The recoverable component is the part of creep deformation that can recover over time following the instantaneous recovery upon the load release. For comparability, it was expressed as normalized recoverable strain, defined as

$$\varepsilon_{r_N}(t) = \frac{\varepsilon_r(t)}{\varepsilon(0)} = \frac{\varepsilon_r(t)}{\varepsilon_0} \qquad 3.3.6$$

where

$\epsilon_{rN}(t)$ = normalized recoverable strain in percent

$\epsilon_r(t)$ = recoverable strain

ϵ_o = instantaneous elastic strain at the time of load application

The normalized recoverable strain is equivalent to the normalized recoverable compliance as demonstrated in

$$\varepsilon_{r_N}(t) = \frac{\varepsilon_r(t)}{\varepsilon(0)} = \frac{\varepsilon_r(t)/\sigma^*}{\varepsilon(0)/\sigma^*} = \frac{J_r(t)}{J_0} = J_{r_N}(t) \qquad 3.3.7$$

In Figure 28 which shows recovery strain at nine test conditions, it may be noted that increases in both stress level and moisture content result in an increase of the normalized recoverable compliance (or normalized recoverable strain) and in longer recovery time, which is more profound at higher stress levels and moisture contents. The observed moisture content dependence, and the stress dependence of the normalized

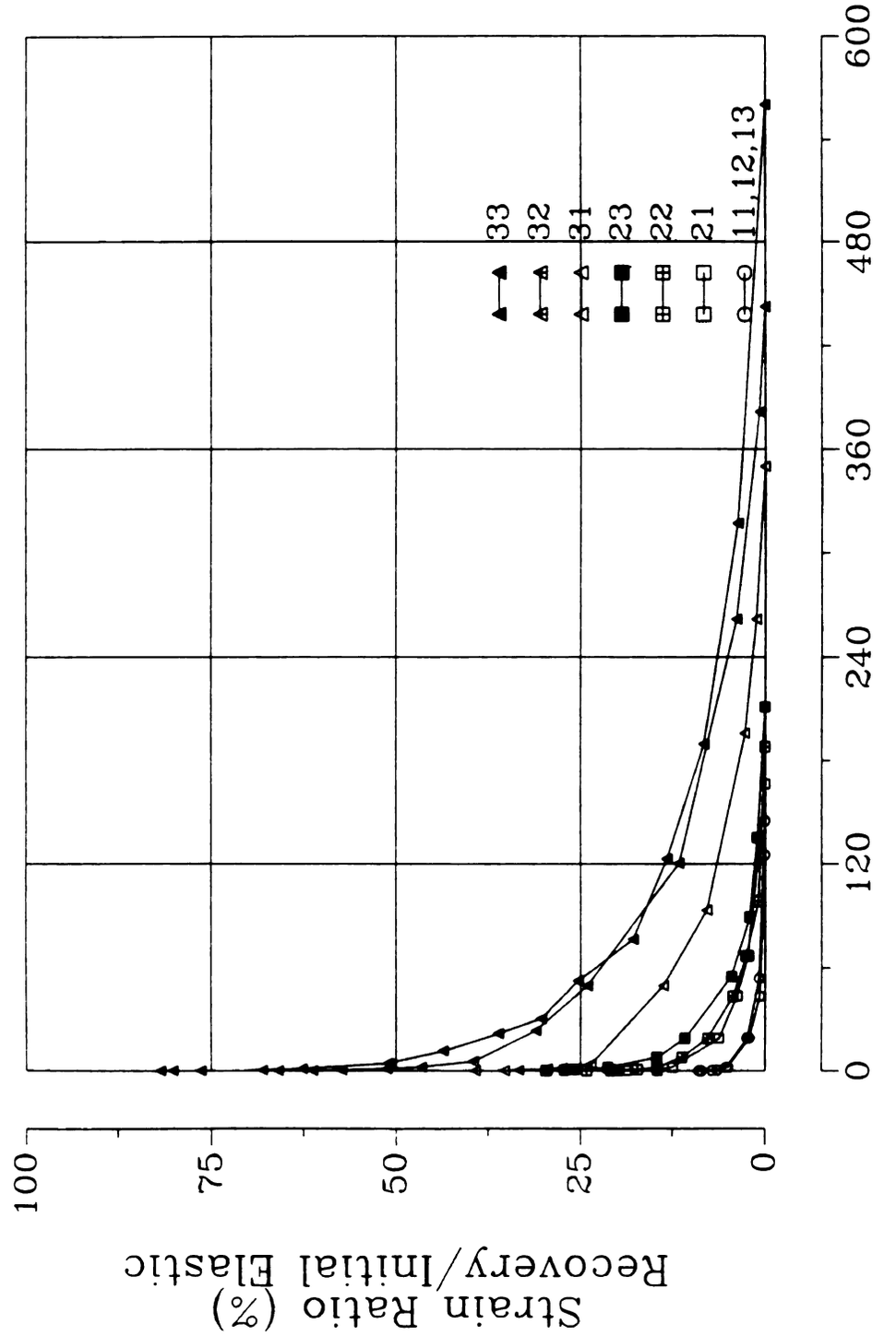

Figure 28. Recovery creep strain of yellow-poplar in the radial direction at nine creep test conditions.

recoverable compliance - indicating nonlinear behavior of the recoverable component - agree with the findings of Bach [1968] that recoverable compliance is a nonlinear function of stress levels and moisture content.

The effect of mechano-sorptive coupling on the recoverable component was not investigated in this work. The indication by Grossman [1976] is that the coupling should impose no further influence on the recoverable component.

Measurement at the end of the creep test (about 600 hours) does not reveal whether the recoverable component is time dependent during the creep test maintained at constant moisture content. Investigation of this time dependence would require the release of the creep load at different times during the creep tests on a number of matching specimens.

The recoverable component is, therefore, assumed to be time independent in this study. Consequently, any such time dependence is being factored into the flow component. Characterization is made much simpler this way as there is only one time dependent component - the flow component - to deal with. The rationale rests in the relative insignificant contribution by the recoverable component as outlined in Table 6 which shows that the recoverable component accounts for only about 20 percent of the total creep, while 80% is due to the flow component.

The flow component results in permanent deformation that does not recover after the release of load. It is apparent in Figure 29 that the normalized flow strain increases with an increase in both stress and moisture content, as found by Bach and Pentoney [1968] that the flow component is clearly nonlinearly viscoelastic.

3.4 Modelling Creep Behavior by Mechanical Model

As opposed to empirical models, the mechanical ones provide a unified approach to the analysis of viscoelastic behavior in that the behavior of a material can be described

Table 6. Composition of tension creep strain of yellow-poplar in the radial direction.

Test Condition Number	Normalized Creep Strain			(%)	
	Total	Recoverable	Permanent	Recoverable	Permanent
11	0.5857	0.0747	0.511	12.75	87.25
12	0.598	0.084	0.514	14.05	85.95
13	0.5989	0.0709	0.528	11.84	88.16
21	1.75	0.188	1.563	10.71	89.29
22	2.28	0.211	2.069	9.25	90.75
23	3.41	0.258	3.15	7.57	92.43
31	2.65	0.65	2	24.53	75.47
32	3.39	0.61	2.78	17.99	82.01
33	4.39	0.77	3.62	17.54	82.46

by a finite number of parameters that can be compared to those of other materials as well as of the same material subject to different environmental conditions [Bodig and Jane, 1982]. Therefore, a unified mechanical model must be used for the nine test conditions in this study.

The model proposed is based on the ever popular 4-element Burger body defined in Eq. 3.2.7. Since the initial creep compliance is the elastic compliance - the reciprocal of modulus of elasticity -

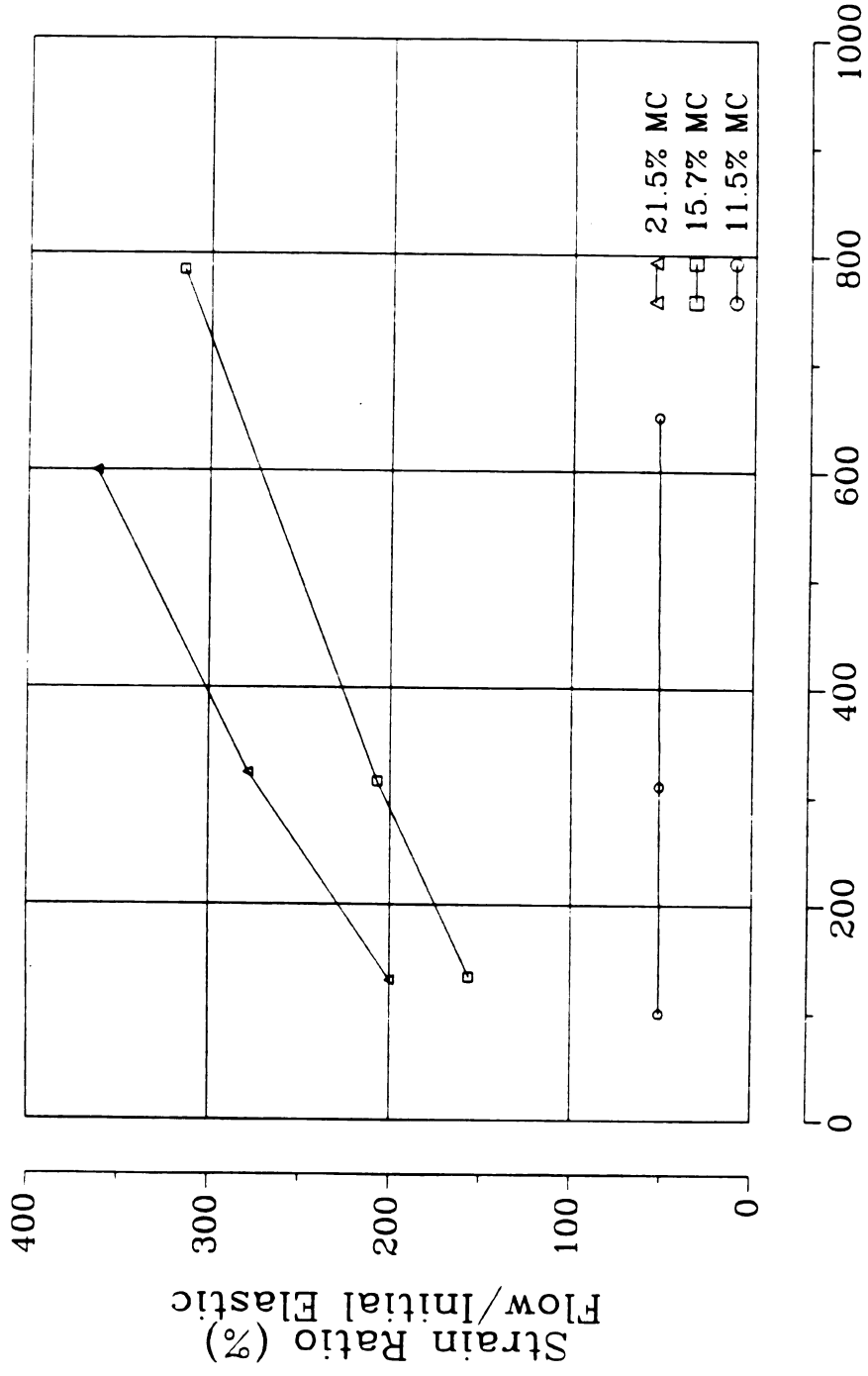

Figure 29. Flow creep strain of yellow-poplar in the radial direction.

$$J(0) = J_0 = \frac{1}{E_{ms}} \quad , \tag{3.3.8}$$

the normalized total creep compliance is

$$\begin{aligned} J_N(t) &= \frac{J(t)}{J(0)} = \frac{J(t)}{J_0} \\ &= \frac{1}{E_{ms}} E_{ms} + \frac{(1 - e^{-\frac{E_{ks}}{\eta_{ks}} t})}{E_{ks}} E_{ms} + \frac{t}{\eta_{md}} E_{ms} \\ &= 1 + J_r(t) E_{ms} + J_f(t) E_{ms} \\ &= 1 + J_{r_N}(t) + J_{f_N}(t) \end{aligned} \tag{3.3.9}$$

where

$J_N(t)$ = normalized total creep compliance

$J_{rN}(t)$ = normalized recoverable compliance

$J_{fN}(t)$ = normalized flow compliance

with others defined in the same manner as specified in Eq. 3.2.7. The total creep compliance can then be easily obtained by dividing a given normalized creep compliance by the initial MOE or the reciprocal of the initial creep compliance.

The normalized total creep compliance and its components described in Eq. 3.3.9 are shown in Figure 30 to demonstrate relations among them. The instantaneous component is normalized to unity. The recoverable component rises and levels off relatively quickly, and recovers completely after load release at t, evidencing the behavior of the Kelvin element. The flow component increases linearly with time and

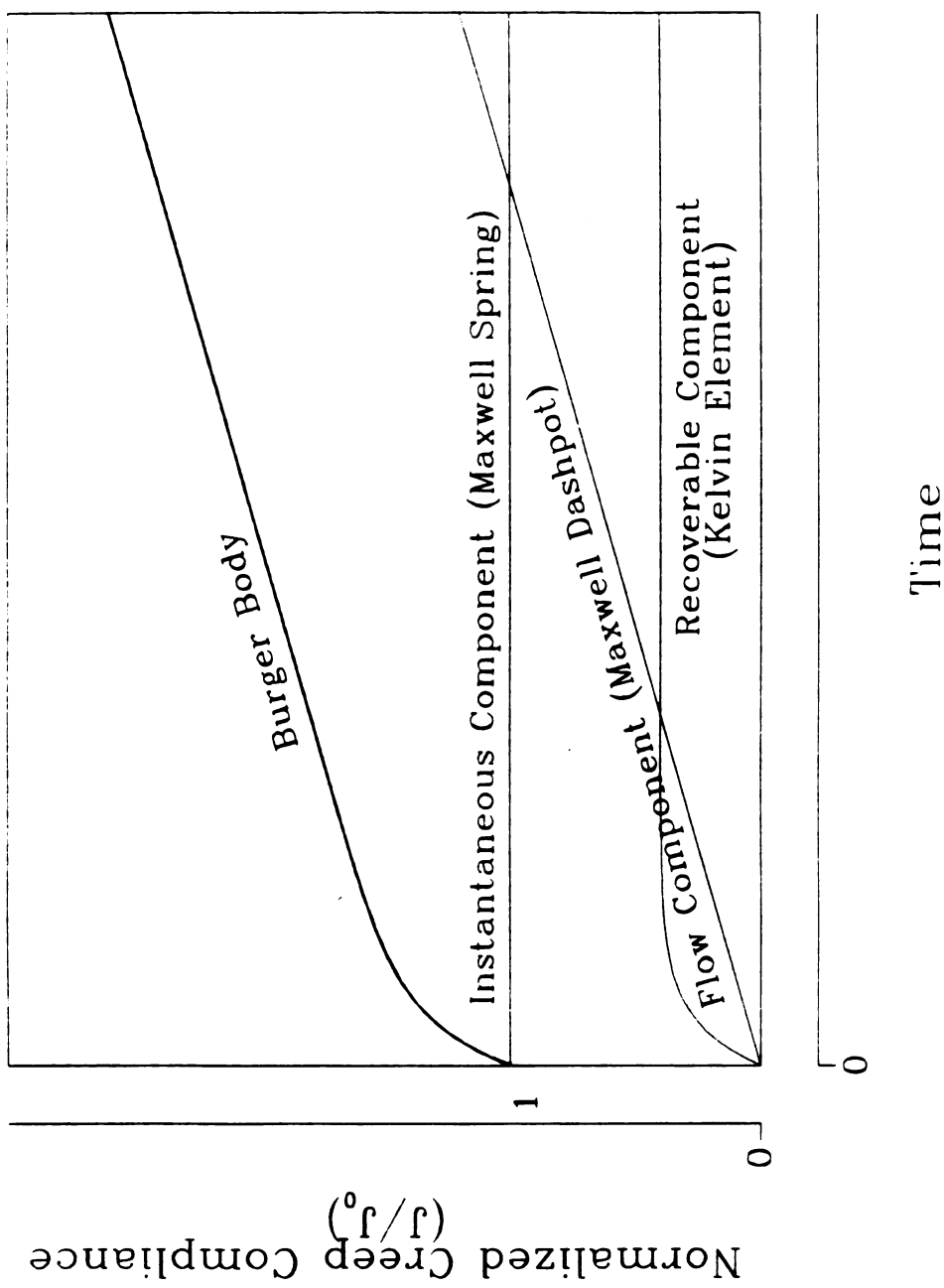

Figure 30. Components of normalized creep compliance of the 4-element Burger body.

remains permanent after load release, indicating Newtonian behavior (linear dashpot). (The Newtonian dashpot, by definition, maintains linear proportionality of its strain rate with stress

$$\sigma^* = \eta_{ms}\, \varepsilon_f(t)' = \eta_{ms} \frac{d\varepsilon_f(t)}{dt} \qquad 3.3.10$$

Integration of the above results in

$$\varepsilon_f(t) = \frac{1}{\eta_{ms}} t\, \sigma^* \qquad 3.3.11$$

The creep compliance is then

$$J_f(t) = \frac{\varepsilon_f(t)}{\sigma^*} = \frac{1}{\eta_{ms}} t \qquad 3.3.12$$

and its normalization over the initial creep compliance J_o is

$$J_{f_N}(t) = \frac{J_f(t)}{J_0} = \frac{\frac{1}{\eta_{ms}} t}{\frac{1}{E_{ms}}} = \frac{E_{ms}}{\eta_{ms}} t \qquad 3.3.13$$

This shows that the normalized creep compliance of the Newtonian dashpot is represented by a straight line.). In the superimposition of the three elements, the instantaneous part establishes a starting base at unity, the recoverable component raises it to another level, and the flow segment rides atop. The only transient phase is before the recoverable component reaches its equilibrium level. This phase whose length depends on the Kelvin

element's retardation time is however generally short in comparison to the total creep span. Therefore, the slope behavior of normalized total compliance is dominated by that of the Newtonian flow component. The tangent of the slope for the normalized total creep compliance could be approximated by that of its flow component as

$$\frac{dJ_N(t)}{dt} = \frac{d(1 + J_{r_N}(t) + J_{f_N}(t))}{dt} \approx \frac{dJ_{f_N}(t)}{dt} = \frac{E_{ms}}{\eta_{md}} \qquad 3.3.14$$

In absolute creep compliance, the slope tangent of a Newtonian dashpot is then just the reciprocal of the dashpot's coefficient

$$\frac{dJ(t)}{dt} = \frac{d(J_N(t)J_0)}{dt} = \frac{d(J_N(t)/E_{ms})}{dt} = \frac{1}{\eta_{ms}} \qquad 3.3.15$$

However, it is shown in Figure 26 that the actual normalized total compliances never reach straight slopes. In another words, the flow component is not linear and can not be represented by a Newtonian dashpot. This is neither new nor surprising as many others have arrived at the same finding [Davidson, 1962; Ethington and Youngs, 1965; Bach, 1965; Youngs and Hilbrand, 1963]. Realistic characterization must employ a non-Newtonian dashpot.

Before addressing the mathematical form of an appropriate non-Newtonian flow component, we first explore possible relations between Newtonian and non-Newtonian dashpots. If one agrees that a curve (nonlinear) can be divided into an infinitely large number of infinitely short straight lines and that each line segment is the slope or derivative of the nonlinear curve within the respective segment, one could in the same

way divide a non-Newtonian compliance curve into an infinite number of infinitely short straight compliance lines. Since each individual straight compliance segment corresponds to a Newtonian dashpot whose coefficient is the reciprocal of the tangent of the straight segment within the respective infinitesimal time interval, a non-Newtonian dashpot can be viewed as a Newtonian one with its coefficient varying in accordance with the tangent or the differentiation of the non-Newtonian compliance curve.

By trial, the parabolic function (at^m) which has been a successful empirical model for wood and wood-based materials defined in Eq. 3.2.5 is found to be an appropriate non-Newtonian dashpot that best fits the experimental data of the normalized creep compliance in this study. The reciprocal of the coefficient of its Newtonian equivalence is therefore

$$\frac{1}{\eta_{md}} = amt^{m-1} \qquad 3.3.16$$

which is the differentiation of the parabolic function. The coefficient

$$\eta_{md} = \frac{1}{amt^{m-1}} \qquad 3.3.17$$

is no longer a constant as it is in a Newtonian dashpot, but time dependent.

The recoverable component which makes only a small contribution to the total creep (Table 6) is approximated with a single Kelvin element which contributes a compliance of

$$\frac{(1 - e^{-\frac{E_{ks}}{\eta_{kd}}t})}{E_{ks}}$$

The proposed four element linear Burger body model is then modified to

$$J_N(t) = 1 + E_{ms}\frac{(1 - e^{-\frac{E_{ks}}{\eta_{kd}}t})}{E_{ks}} + E_{ms}at^m$$

$$= 1 + E_{ms}\frac{(1 - e^{-\frac{E_{ks}}{\eta_{kd}}t})}{E_{ks}} + E_{ms}\int_0^t amt^{(m-1)}dt \qquad 3.3.18$$

$$= 1 + E_{ms}\frac{(1 - e^{-\frac{E_{ks}}{\eta_{kd}}t})}{E_{ks}} + E_{ms}\int_0^t \frac{1}{\eta_{md}}dt$$

in terms of the normalized compliance. It differs from the proposed linear Burger body (Eq. 3.3.9) in the flow term. Equation 3.3.18 will be used to characterize the experimental normalized creep compliance data in Figure 26 in order to determine the coefficients, namely E_{ms}, E_{ks}, η_{kd}, and η_{md}.

E_{ms} is easily determined from the instantaneous elastic strain at the start of the creep test - load application.

The Kelvin element with which E_{ks} and η_{kd} are associated is governed by the differential equation

$$E_{ks}e_r(t) = \eta_{kd}\frac{de_r(t)}{dt} \quad (= \sigma^*) \qquad 3.3.19$$

as a result of its parallel arrangement of spring and dashpot. At the initial condition of zero extension, the solution of the differential equation results in the normalized compliance

$$J_{r_N}(t) = \frac{J_r(t)}{J_0} = \frac{\frac{\varepsilon_r(t)}{\sigma^*}}{\frac{\varepsilon(0)}{\sigma^*}} = \frac{\varepsilon_r(t)}{\varepsilon(0)} = E_{ms}\frac{(1 - e^{-\frac{E_{ks}}{\eta_{kd}}t})}{E_{ks}} \qquad 3.3.20$$

At the initial condition of full extension, the normalized compliance would be

$$J_{r_N}(t) = \frac{J_r(t)}{J_0} = \frac{\frac{\varepsilon_r(t)}{\sigma^*}}{\frac{\varepsilon(0)}{\sigma^*}} = \frac{\varepsilon_r(t)}{\varepsilon(0)} = E_{ms}\frac{e^{-\frac{E_{ks}}{\eta_{kd}}t}}{E_{ks}} \qquad 3.3.21$$

It also follows from Eq. 3.3.20 that when t goes to infinity, which is when the Kelvin model is fully extended,

$$J_{r_N}(\infty) = \frac{E_{ms}}{E_{ks}} \qquad 3.3.22$$

or

$$J_r(\infty) = \frac{1}{E_{ks}} \qquad 3.3.23$$

Therefore, the Kelvin spring constant, E_{ks}, and the Kelvin dashpot coefficient, η_{kd}, can be obtained from experimental recovery strain data. First, E_{ks} was found by dividing

the creep stress by the total recoverable strain according to Eq. 3.3.23. Next, Eq. 3.3.21 was forced on the recovery portion of the normalized creep compliance curve (Figure 31) to arrive at E_{ks}/η_{kd} (the reciprocal of the retardation time $1/\tau$) to obtain η_{kd}. It is apparent in Figure 31 that one Kelvin element does not suffice for good approximation of the behavior, but can account for the most important two aspects of the recoverable component -the total recovery and the total recovery time.

The a, and m coefficients in the flow term were obtained by nonlinear regression fitting of Eq. 3.3.18 to the nine sets of normalized total creep compliances in Figure 26. An example is given in Figure 32 for the normalized creep compliance at test condition 21.

To express the normalized creep compliance as function of moisture content, stress, and time, Eq. 3.3.18 may be rewritten as

$$J_N(MC,\sigma,t) = 1 + E_{ms}(MC)\frac{(1 - e^{-\frac{E_{ks}(MC,\sigma)}{\eta_{kd}(MC,\sigma)}t})}{E_{ks(MC,\sigma)}} + E_{ms}(MC)\,a(MC,\sigma)\,t^{m(MC,\sigma)} \qquad 3.3.24$$

where

MC - moisture content

σ - stress

Alternatively, it could be alternatively written as

$$J_N(MC,\sigma,t) = 1 + A(MC,\sigma^n)(1 - e^{-Bt}) + C(MC,\sigma)\,t^{D(MC,\sigma)} \qquad 3.3.25$$

where

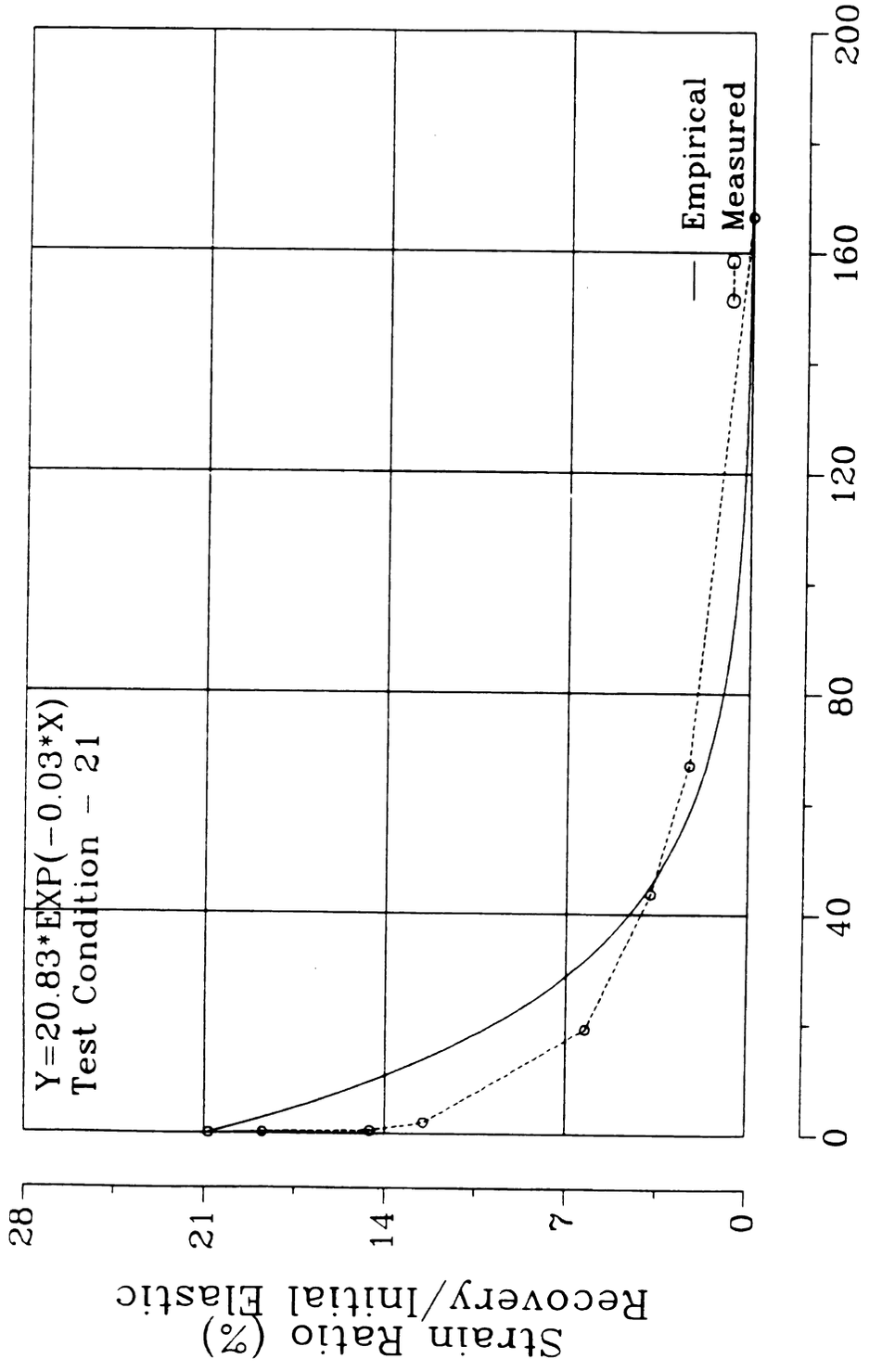

Figure 31. Obtaining retardation time by fitting single Kelvin element to recovery creep strain.

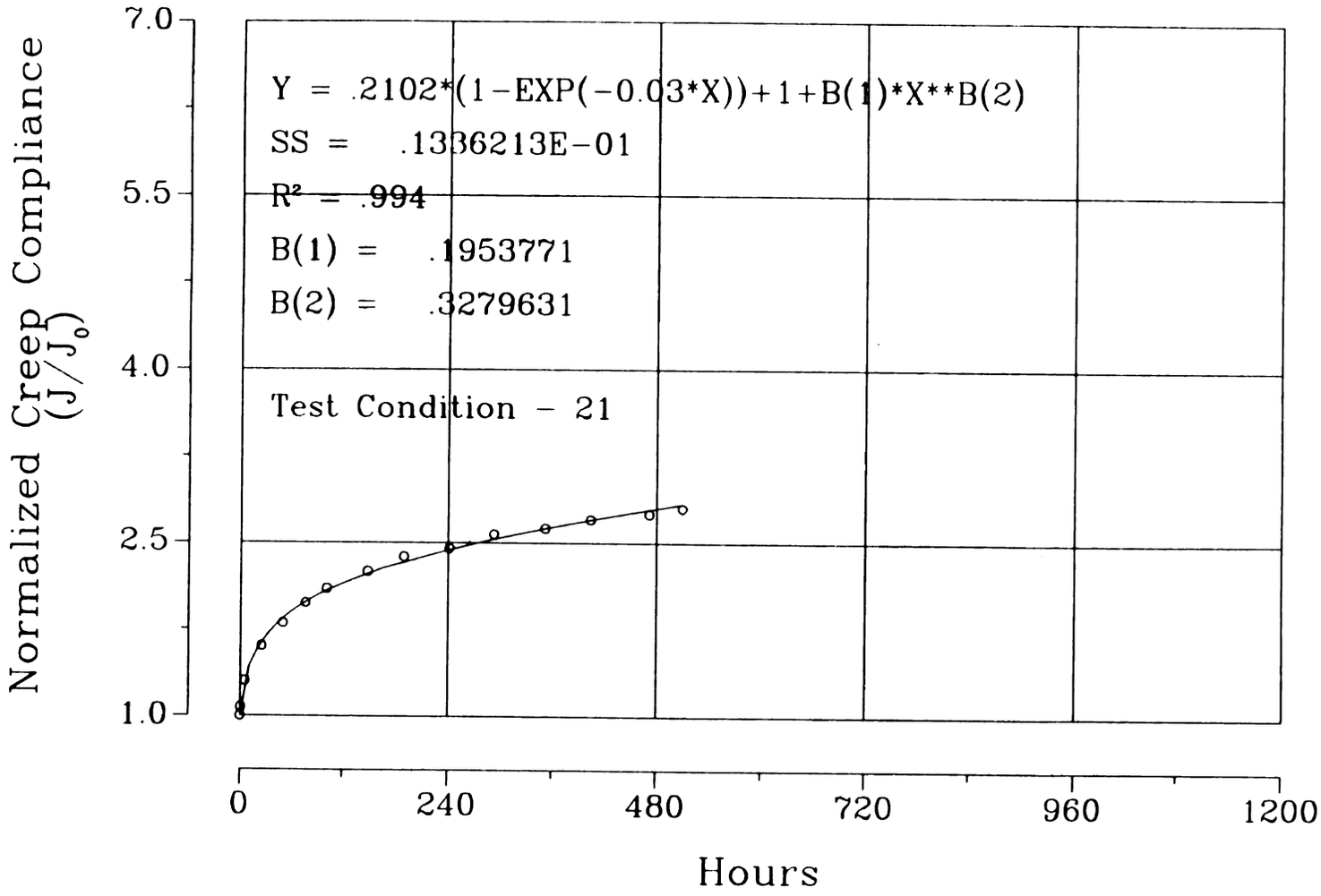

Figure 32. Nonlinear regression on normalized creep compliance of yellow-poplar in the radial direction at test condition 21.

$$A(MC,\sigma) = \frac{E_{ms}(MC)}{E_{ks}(MC,\sigma)}$$

$$B(MC,\sigma) = \frac{E_{ks}(MC,\sigma)}{\eta_{kd}(MC,\sigma)}$$

$$\frac{1}{\eta(MC,\sigma,t)} = \frac{C(MC,\sigma)D(MC,\sigma)t^{(D(MC,\sigma)-1)}}{E_{ms}} \qquad 3.3.26$$

$$C(MC,\sigma) = E_{ms}(MC)\,a(MC,\sigma)$$

$$D(MC,\sigma) = m(MC,\sigma)$$

Given A, B, C, D, and E_{ms}, E_{ks}, η_{kd}, and η_{md} can be readily computed. The A, B, C, and D values for the 9 conditions were obtained and are listed in Table 7. Though multi-variable regression analysis is the best choice for the procurement of the empirical A, B, C, and D functions of stress and moisture content, the author opted for two steps of single variable empirical curve fitting. Because there is no coupling between stress and moisture content changes, their effects on A, B, C, and D may be dealt with independently. The A, B, C, and D functions of stress at each of the three moisture content levels were obtained in the first empirical fitting. The variations of the coefficients in the acquired A, B, C, and D functions of stress with the three levels of moisture content were then captured in the second empirical fitting, which yields A, B, C, and D functions of both stress and moisture content as presented in Table 8.

The normalized creep compliances based on the empirical functions of A, B, C, and D at the three stress levels and three moisture contents were drawn against the experimental normalized creep compliances in Figure 33 to show the fairly good agreement between them.

Table 7. Coefficients of normalized creep compliance of yellow-poplar in the radial direction at nine creep test conditions.

Test Condition Number	Moisture Content (%)	Creep Stress (psi)	Coefficient A	B	C	D
11	11.5	100	0.08566	0.035	0.10927	0.2366
12	11.5	310	0.08566	0.035	0.11526	0.2367
13	11.5	650	0.08927	0.035	0.11526	0.2318
21	15.7	133	0.2102	0.030	0.19538	0.3280
22	15.7	314	0.2503	0.030	0.38578	0.2582
23	15.7	785	0.3038	0.030	0.51460	0.2866
31	21.5	130	0.4302	0.015	0.28780	0.3267
32	21.5	321	0.7420	0.011	0.54078	0.2472
33	21.5	600	0.9210	0.010	0.70318	0.2622

In summary, the creep behavior of yellow-poplar in its radial tension as influenced by stress levels and moisture contents has been mathematically characterized by a four element Burger body containing a non-Newtonian Maxwell dashpot. The coefficients of the Burger body are successfully expressed as functions of their dependent variables, namely, stress, moisture content, and time. Though there are many available choices for the function forms, the chosen one presumably is the simplest and did produce good conformity with the actual experimental data. It is to be kept in mind that the current mathematical characterization only includes the direct effects of stress and moisture content changes during moisture content gain. Its validity is not certain beyond the tested stress and moisture content ranges.

Table 8. Empirical functions of coefficients of normalized creep compliance of yellow-poplar in the radial direction.

$$J_N(t) = \frac{J(t)}{J_0} = 1 + A(1 - e^{-Bt}) + Ct^D$$

$$A = \frac{1}{A_1 e^{-A_2\sigma} + A_3}$$

$$B = -0.0014e^{0.142MC} + 0.0424$$

$$C = C_1(1 - e^{-C_2\sigma})$$

$$D = 0.154756e^{-0.000445MC} + 0.25$$

$$A_1 = -2.85 + 0.467931MC - 0.00799MC^2$$

$$A_2 = -0.00085912 + 0.00004962MC + 0.00001658MC^2$$

$$A_3 = 247.08e^{-0.2718MC}$$

$$C_1 = 1.01(1 - e^{-0.151(MC - 10.5)})$$

$$C_2 = 0.00019(1 - e^{0.35(MC - 20.4)}) - 0.0031$$

MC - Moisture Content

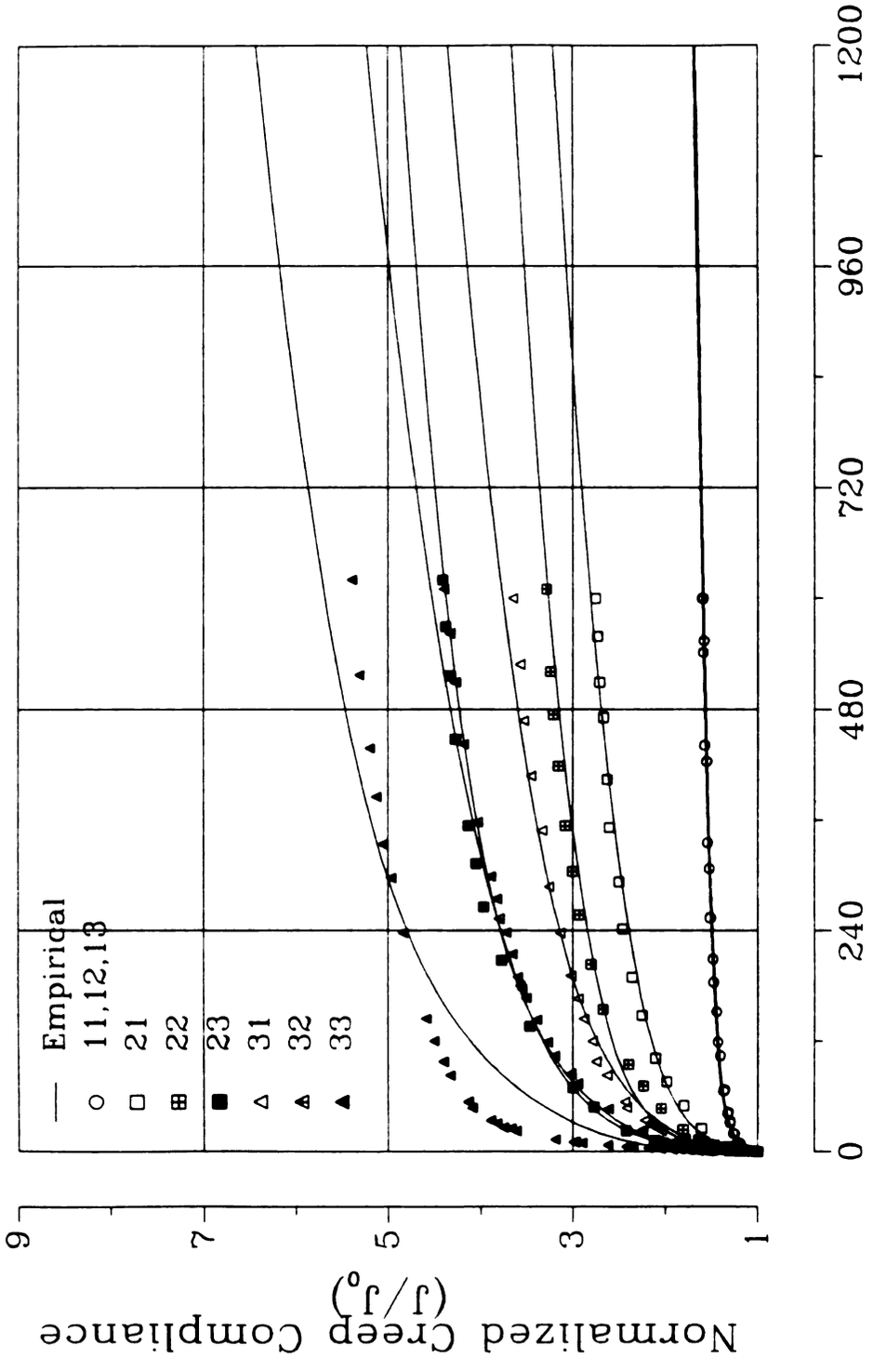

Figure 33. Empirical function vs. experimental data of normalized creep compliance of yellow-poplar in the radial direction.

CHAPTER IV

APPLICATION OF THE LVP THEORYTO HYGROSCOPIC WARPING

In this chapter, the hygroscopic warping is viewed as being a highly viscoelastic, as well as a dynamic process. With the viscoelastic properties characterized in Chapter 3 as one of the necessary inputs, the LVP theory developed in Chapter 2 is to be applied to a cross laminated yellow-poplar wood plate and beam. Theoretical predictions of the warping development of the plate and beam are to be compared with the measured values along the experimentally determined moisture content path.

4.1 The Process of Hygroscopic Warping of Wood and Wood-based Material Panels

Hygroscopic warping of a panel occurs when the hygroscopic expansions or shrinkages resulting from moisture content changes at any pair of planes that are symmetrical with respect to the mid-plane of the panel differ and generate bending moments. Such differentiation can come from either the structural unsymmetry such as difference in species - difference in hygroscopic expansion or shrinkage coefficient - or unsymmetry in moisture content gradient across the thickness of the panel. It is theoretically possible for a panel of structural unsymmetry to become flat at some point if subjected to opposing and equal moisture content gradient unsymmetry. In reality, this temporary stability however can not be maintained. A panel of perfect structural

symmetry can still warp when the moisture content gradient is unbalanced, but the problem is not inherent in the structure. Therefore, such panel is considered hygroscopically stable. Perfect structural symmetry is ideal, but difficult to achieve in manufacturing practice. The best effort can only result in the reduction of any unsymmetry to a minimum, according to potential application requirements. However, it often has to be compromised due to cost, availability of species, etc..

The viscoelastic nature of warping in wood and wood-based panels is soundly evidenced in the following manifestation. When the moisture content of an unsymmetrical panel is elevated to moderate and high levels, the resulting warp is much less than the elastic estimate. Reversing the moisture content to its original level which would have reversed the warp backward to its initial value were the panel elastic, however, leaves a significant part of the original warp unrecovered or permanent. This is nevertheless expected as the panel behavior must reflect the viscoelastic properties of constituent wood and wood-based materials.

In the following thought process which attempts to analyze a viscoelastic warping process, a wood panel cross laminated of two very thin plies of the same thickness and species is selected. The layers are so thin that the moisture content is assumed to change uniformly across the panel thickness so that there is no differential expansion or shrinkage within each of the layer of the panel. The plate is presumed to be at some initial moisture content where the panel is flat, and therefore stress free (due to its structural instability). The hygroscopic expansion or shrinkage differential between the two cross laminated layers in each of the two coordinate directions is the cause of

potential mutual restraint between them. This restraint is triggered by any deviation of the moisture content from its initial value and will result in a saddle shaped warp of the panel.

Suppose the panel's moisture content is going to be increased along a path to $MC+\Delta MC$ over a time period of Δt. As soon as the moisture content strays away from its initial point, both layers start to expand. The much larger hygroscopic expansion across the grain relative to that along the grain results in mutual restraint, leading to tension along the grain and compression across the grain in the panel. The resulting bending moment would then cause the panel to warp away from its original flat position. Immediately at the onset of tension and compression stresses, the viscoelastic property of the constituent would emerge in the process (viscoelastic properties are dormant in the stress free state). It asserts itself in that the tension layer would tend to creep-stretch, and the compression layer tend to compression-creep under their respective stresses. This creep, here called deformation creep, would lessen the mutual restraint between the two layers, resulting in lower stresses (stresses relaxed), and consequently smaller bending moment and warp than would be the case if the constituents were completely elastic. Here, the onset of stresses and deformation creep (plus stress relaxation) are related in a sequential manner. These two are actually simultaneous, intertwined, and inseparable in time space. No sooner than with the onset of the tension and compression stresses will deformation creep begin and stresses start to relax, resulting in a reduced potential for bending moment and warp.

As moisture content further increases, the expansion differential becomes larger,

causing greater mutual restraint and restraining stresses. In the meantime, it is known that the hygroscopic constituent layers will creep and relax more at higher moisture contents and under higher stresses. Therefore, the deformation creep and stress relaxation in the two layers are expected to occur to a greater extent and at a faster rate with each increment of moisture content and stress increase, thereby lessening the relative restraint and slowing down the otherwise much larger and faster elastic warp development. The concurrent development of the two phases (restraint and restraining stresses versus deformation creep and stress relaxation) represents a balancing mechanism which minimizes the restraint and resulting warp. Due to larger and faster creep at higher stress of wood and wood-based materials, the more severe and the faster the condition of restraint develops, the more significant and the faster the deformation creep and stress relaxation occur. Conversely, the less severe the restraint is, the less significant the deformation creep will be and the slower the stress relaxation will take place. It should be emphasized that these events take place along a continuous moisture content path as it is impossible to elevate moisture content instantaneously.

As moisture content stabilizes, no further hygroscopic expansion is introduced. Yet the mutual restraint and restraining stresses, and the warp resulting from the previous moisture content path are still present. Therefore the deformation creep and stress relaxation will continue. As the restraint is further lessened, less deformation creep and stress relaxation occur due to less creep by wood under lower stresses. This downward trend would continue until a balance between the lessening of the restraint and the development of the deformation creep has been reached. It needs to be emphasized that

the laminate is not necessarily free of stress or restraint free at this point. It is merely in a temporary stable state. The permanent portion of the deformation creep (the Maxwell dashpot) would be embedded in such a stable warp by manifesting itself as the irrecoverable portion of the warp if the panel is subjected to the reverse of the moisture content path back to its initial moisture content level.

In real panels there exist moisture content gradients since moisture content can not be raised uniformly across a thickness, just like temperature. It is by the gradient that the moisture gets diffused and uniform moisture content is reached over a period of time. The presence of a moisture content gradient poses a more complicated scenario in that aside from the mutual restraint as caused by the directional expansion differential between the two layers, there is mutual restraint everywhere within each layer, caused by moisture content differentials. Every imaginary layer as thin as necessary is restrained by its adjacent ones, and therefore two phases of the warping process must be taking place concurrently in the involved layers.

Another source of mutual restraint for this two-layer panel could come from the warp itself. It is known that when the panel warps, a stress distribution develops in such a way that the stresses in the outer layers are the largest, and that they gradually diminish towards the mid-plane. The stress differential between adjacent imaginary layers imposes constraint between them.

In short, the hygroscopically induced mutual restraint due to either imbalance in structure and/or moisture content gradient and the simultaneously resulting deformation creep and stress relaxation due to the viscoelastic nature of the constituent wood and

wood-based materials are the two inherently cohesive phases in the warping process. Though conceptually conceived and separated here for the analysis of the warping process, they actually are inseparable, interdependent, counter balancing and canceling each other. Consideration of just one of them in a fixed time frame in any analysis is not feasible.

The complexity of this warping process is further increased by the fact that moisture content and stresses not only vary across the thickness of each physical layer in a panel due to moisture content gradients and stress distributions, but also that such gradients and distributions do not remain constant, but vary with time. These two variations have to be captured somehow in any realistic approach.

The LVP theory is not capable of capturing them in a continuous manner since it must treat a panel as composed of a finite number of layers, however thin they may be, and consider the process within a finite number of discrete time intervals. The moisture content within a layer must be uniform as required by the CLT structure and constant within a time interval as required by the isothermal requirement of the LVP theory (We can extend the isothermal concept to moisture content if moisture content and temperature are considered to have equivalent effects. Warping where moisture content gradient changes with time actually falls in the realm of thermal viscoelasticity. However, the isothermal LVP theory is a lot simpler, and the isothermal restriction is only to be enforced within each of, but not across the discretized time intervals in the numerical form of the LVP theory achieved by linear finite difference approximation. Therefore, the isothermal LVP theory in its numerical form can be and is used in this

study to approximate the thermal viscoelastic problem.). If we treat moisture content increase as a step-wise process, that is moisture content within a layer is uniform and remains constant during time interval Δt_1 before advancing to a new level at the next time interval Δt_2 as shown in Figure 34, the LVP theory is able to numerically capture moisture content variations in the thickness direction along a time scale. This treatment is feasible provided that the layers are specified to be very thin and time intervals are sufficiently small so that the moisture content gradient within a layer is small enough to be viewed as uniform, and its variation with time in a single time interval so little as to be considered constant.

Secondly, the viscoelastic properties of wood and wood-based material such as yellow-poplar for each imaginary thin layer in the panel are stress and moisture content dependent, and therefore would change accordingly with the changes in moisture content and stresses in the warping process. Such changes should be accounted for, if not precisely, then at least numerically to a good approximation. The moisture content dependent changes in viscoelastic coefficients can be numerically captured since moisture content variation across the thickness along the time scale can be numerically captured as just discussed and the viscoelastic coefficients-moisture content relations have already been characterized mathematically for yellow-poplar in Chapter 3. To account for the stress dependent changes in viscoelastic coefficients, a similar numerical approach is applied where the stress distribution within each thin layer would be assumed to be uniform and to change in the same step wise manner as the moisture content. Stress distributions exist inside each layer, however thin the layer may be. But, they are

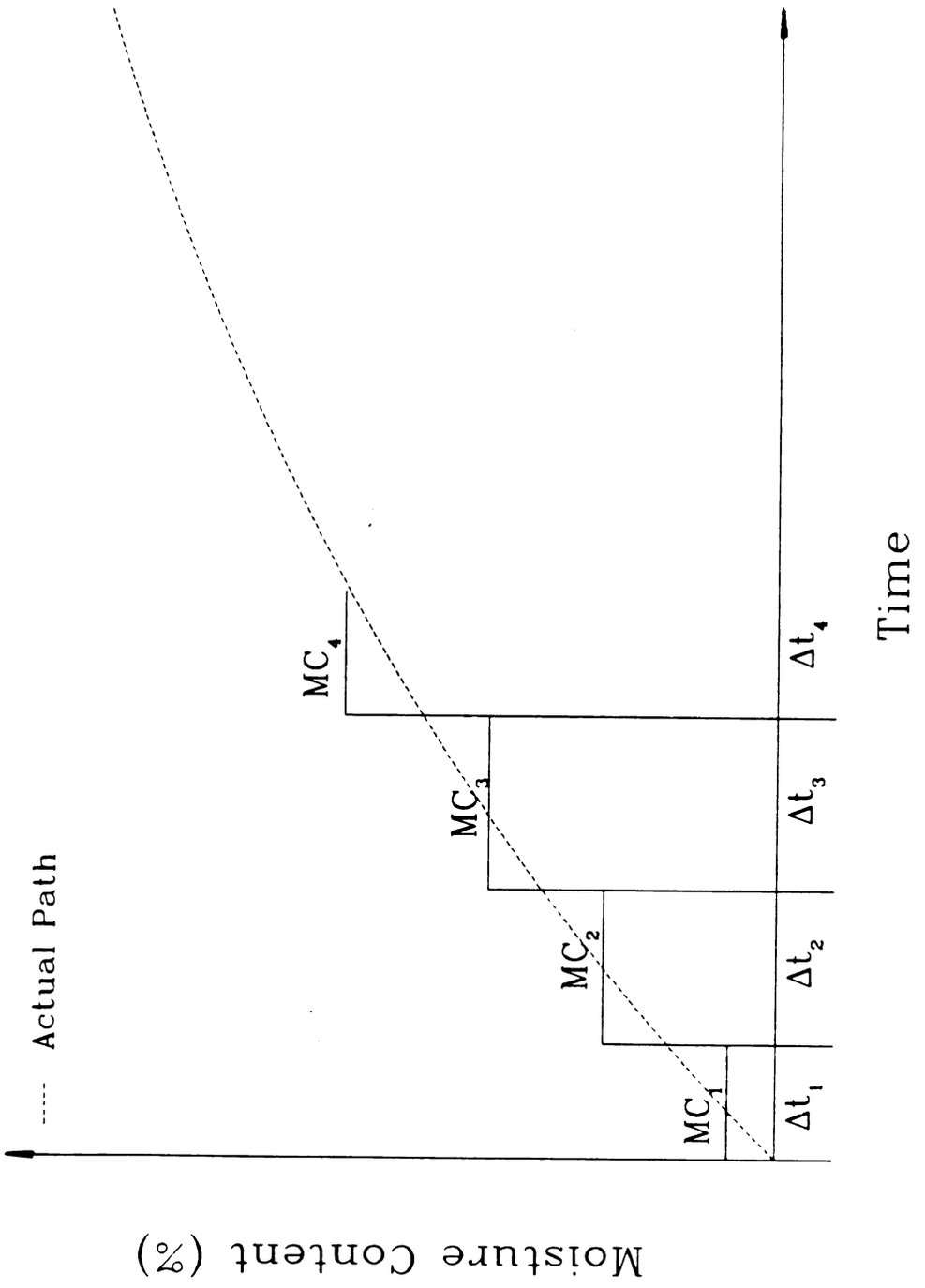

Figure 34. Step-wise moisture content increase.

averaged within a layer for the purpose of determining the stress effect on the viscoelastic coefficients of the layer during a time interval according to the viscoelastic coefficients-stress relationships defined in Chapter 3. (The CLT structure of this LVP theory determined that the viscoelastic coefficients must be uniform within a layer. Therefore the stress dependence of the coefficients must be computed based on one stress within a layer.). This account of stress dependence would be a close approximation if the layer was thin enough.

It is seen that dividing a panel into thin imaginary plane layers is the basis of the LVP theory. The thinner and the larger the number of layers, the closer the theoretical predictions should be to actual results, if the LVP theory proves itself valid. An exact account of the actual behavior would necessarily resort to analytical solutions which consider the continuous nature of the warping process, but this is not achievable. A discrete method has to be the alternative, just as in so many other science and engineering problems where numerical methods such as the finite element method are widely used. Actually in a sense, the thin imaginary layer strategy resembles the finite element method in a sense as the panel is divided into a finite number of parallel adjacent layers.

4.2 Warping Experimentation

A yellow-poplar panel was constructed in the laboratory of 65 % RH and subjected to 91 % relative humidity. Its subsequent warp development was measured and compared with the theoretical predictions by the LVP theory to examine validity of this theory.

4.2.1 Panel Design and Manufacturing

A two-ply cross laminate of yellow-poplar layers of identical thickness was selected for it is of the simplest unsymmetrical structure, and requires the least effort in lamination and manufacturing. The most important reason however is that the structural unsymmetry would not allow any stresses in it without manifesting the stresses in the form of warping of the panel. Every effort was made to minimize any possible residual stresses arising from the laminating process.

As shown in Figure 35, edge grained strips of yellow-poplar of 3/4 by 1/2 by 50 in were cut from flat sawn yellow-poplar lumber and edge-glued with conventional white glue to form two large edge grain panels with dimension 50 by 23 by 1/2. The panels were then conditioned at a room condition of 70° F and 65% RH for three weeks before they were planed to a final thickness of 0.25 inches. These panels were monitored to remain flat at further conditioning at the prior room conditions, indicating dimensional stability. Three 1 in wide strips were cross cut from each of the two panels for use as radial linear expansion samples. One of the panels was then cut in half and the two halves were turned around for 90 degrees before being cross laminated to the other panel with Epoxy AW-106/HV-953 made by Ciba-Geigy. To avoid any potential moisture content change, the glue spreading and laminating operation were conducted in the same room condition. The Epoxy which is 100% chemical reactive in its curing process does not contain water or other solvents thus eliminating any hygroscopic expansions during the lamination and curing. The AW-106/HV-953 Epoxy was recommended by the manufacturer based on our requirements that the glue line must be able to cure under

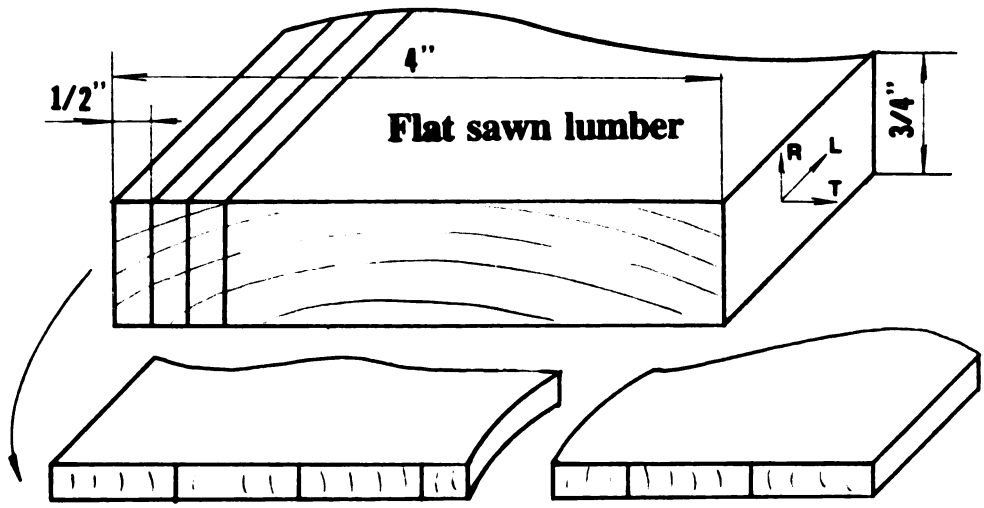

Figure 35. Manufacturing of edge grain yellow-poplar panel.

room temperatures as hot press curing would introduce thermal stresses, must be relatively rigid with as little creep and slippage as possible so that glue line could be considered as being of zero thickness and in compliance with the Kirchhoff deformation field, and must be highly moisture or humidity resistant as it is to be subjected to high humidity for extended periods of time, and must have moderate viscosity for ease of handling during the lamination process. The laminate assembly was then transferred to a plywood press to cure under pressure. As suggested by the manufacturer, a relatively low press pressure (15 psi) was used to minimize the development of residual stresses, while maintaining sufficiently good contact. The laminate was allowed to remain under such pressure to cure for over 18 hours before it was taken out and placed in the prior room condition. As the press is situated in a room of lower humidity, some moisture along the four edges of the laminate may have escaped during the 18 hour pressing time, and some stresses may have been introduced along the edge areas. For that reason, the laminate was trimmed to a final size of 42 by 19 by 0.5 inches. The samples prepared from this piece are a 1 by 19 in beam, and a 19 by 29 in plate for the warping test, and eight 4 by 4 in square blocks for the determination of moisture content gradients, as shown in Figure 36.

The laminate should have remained flat when returned to the prior room condition since its constituent panels had been equalized under such conditions. However, the laminate when placed in the same room conditions warped as though the constituent panels were conditioned at a higher relative humidity condition, though it came out of the press flat. It was later confirmed that on the day of the lamination the valve system

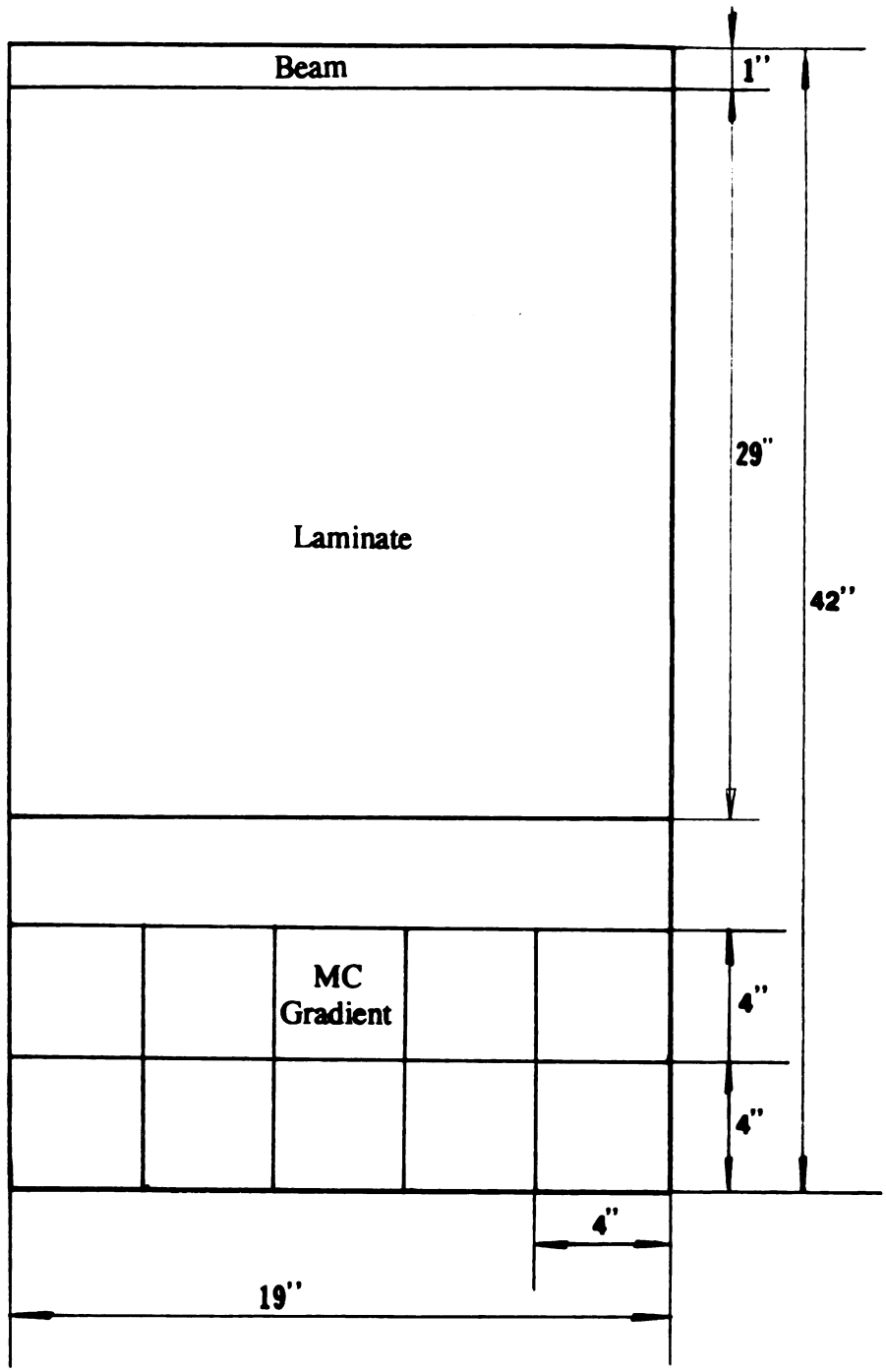

Figure 36. Specimen arrangement on the yellow-poplar laminate.

controlling the conditioning room malfunctioned for a short time without the author's knowledge. As a result, the actual room humidity did go up somewhat above 65% RH. When the laminate was placed in a conditioning chamber maintained at 70% RH, it straightened out eventually and remained flat. Therefore, 70° F and 70% RH are considered the initial condition at which the laminate was both stress free and free of warp.

Longitudinal tension samples for testing static MOEs of the laminating material and longitudinal linear expansion samples were prepared from some of the randomly selected strips cut from the flat sawn lumber. Radial tension samples for radial MOEs and radial linear expansion samples were cross cut from the edge glued radial panels shown in Figure 35 prior to laminating. A total of 11 longitudinal and 10 radial tension samples were made. Their shape and dimensions are shown in Figure 37. A total of 10 longitudinal and 4 radial linear expansion samples were prepared. Figure 38 shows the their dimensions and shape.

4.2.2 Warp, Moisture Content Gradient, and Expansion Coefficients

To avoid horizontal moisture content gradients due to faster moisture penetration through the four edge surfaces, the edge surfaces of the prepared samples - the laminate of 42 by 20 by 0.5 in, the beam of 1 by 19 in, and 10 4 by 4 in control squares - were sealed with wax before transfer into the humidity chamber. After the laminate and the beam had straightened out at 70% RH in the humidity chamber, the relative humidity in the chamber was raised to 91% RH within only 5 minutes. As a consequence, moisture

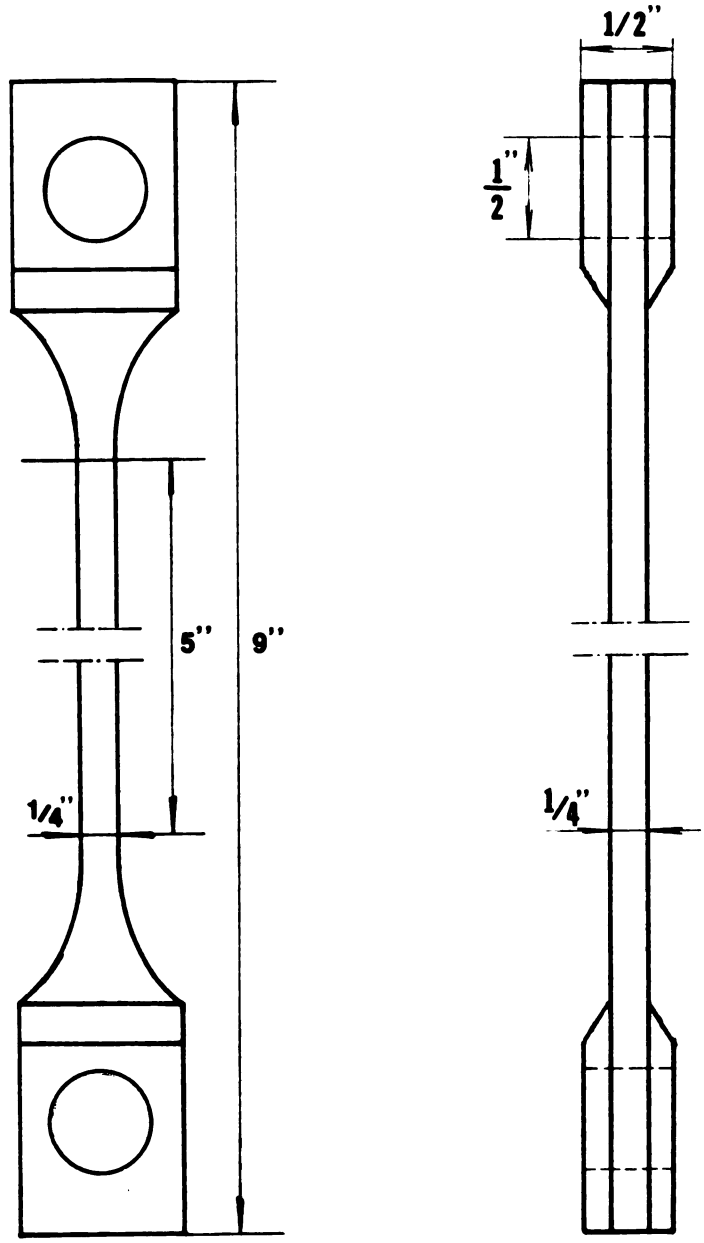

Figure 37. Static tension specimen of yellow-poplar.

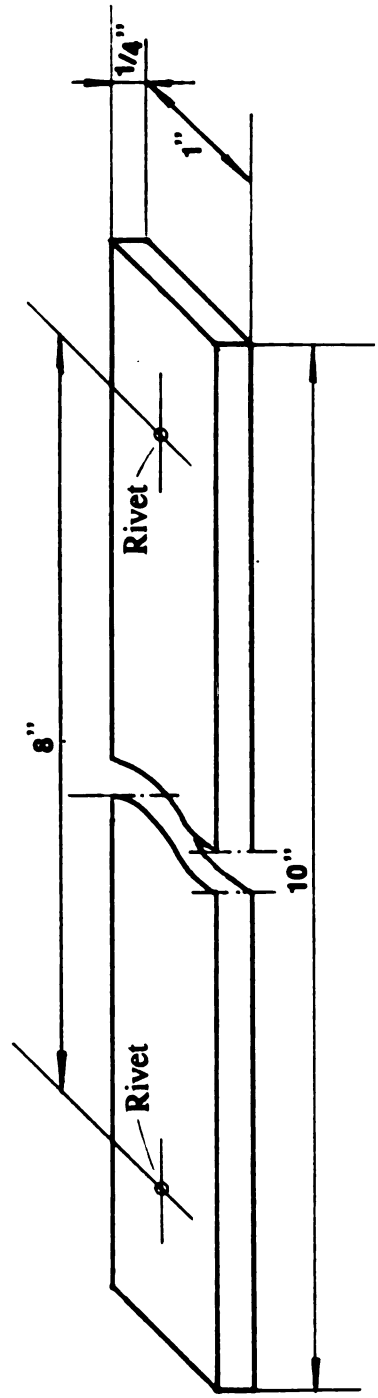

Figure 38. Linear expansion specimen of yellow-poplar.

content gradients developed and increased. Laminate and beam started to warp.

In this study warp was recorded as the vertical deflection of a laminate in reference to the original flat position of the panel. In Figure 18 which shows the positioning of the laminate in x-y-z coordinate system, the geometrical center of the laminate is fixed to the coordinate origin, and the mid-plane of the original flat laminate coincides with the $z=0$ x-y plane, as implied in Eq. 2.4.49. The vertical deflection of the laminate at coordinate position $(x, y, 0)$ therefore is in reference to the $z=0$ x-y plane. Positive vertical deflection indicates a downward deflection, while a negative one identifies a upward deflection. Due to cross lamination of two identical yellow-poplar plies, the vertical deflection is symmetrical to x-z and y-z planes, that is the vertical deflections at $(0, y, 0)$ and $(0, -y, 0)$, or at $(x, 0, 0)$ and $(-x, 0, 0)$ are identical.

At certain time intervals, vertical deflections relative to the geometrical center were measured at $(14.1, 0, 0)$ and $(0, 9.15, 0)$, respectively on the laminate, and at $(0, 9.15, 0)$ on the ***19 in*** beam shown in Figure 18. The measuring device is an aluminum beam with contact points at each end and with a conventional dial gauge affixed to its center as shown in Figure 39a. By placing the two end pins at $(\pm 14.1, 0, 0)$ or at $(0, \pm 9.15, 0)$ where the vertical deflections are identical, the dial gauge which touches the geometrical center of the laminate or the beam thereby indicates the vertical deflections at the two end pin locations, as shown in Figure 39b. The device was first leveled by adjusting the heights of the two end pins.

The focus of this study is on only the hygroscopic warp, and therefore any other sources affecting the warp including the effect of the laminate own gravity force on

Figure 39a. Deflection measuring apparatus.

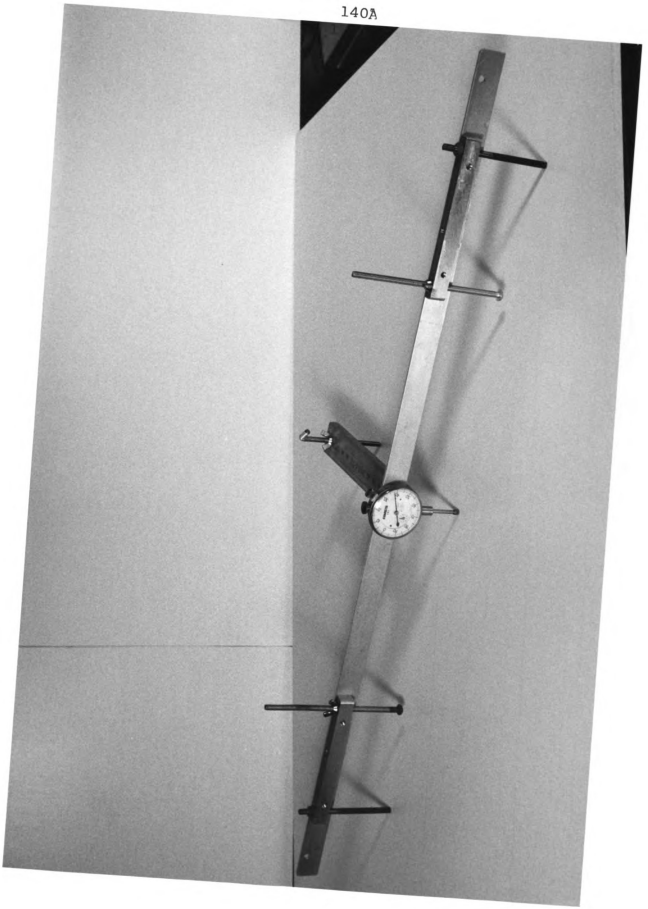

Figure 39b. Measuring apparatus on the warped yellow-poplar laminate.

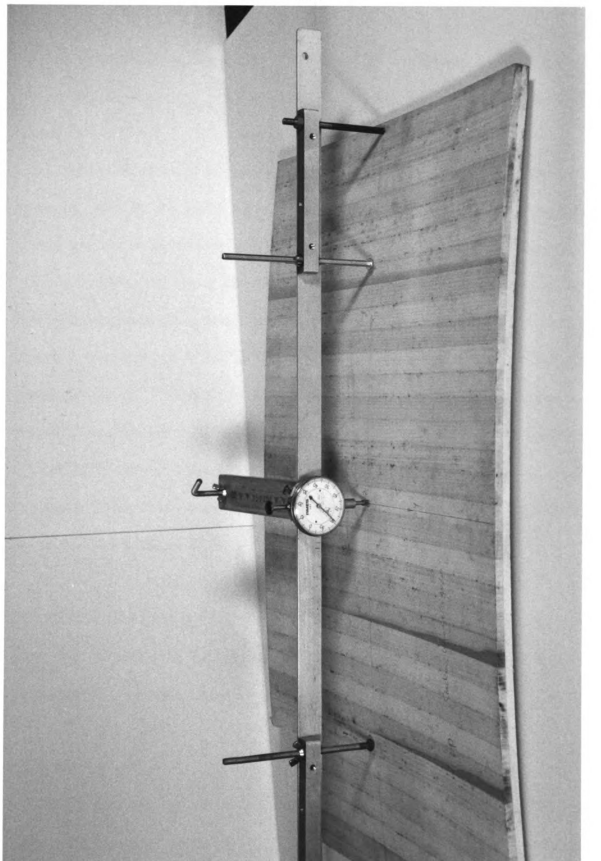

vertical deflection had to be avoided. For this reason, the laminate and the beam were placed on their edges both inside the humidity chamber (Figure 40) and when being measured.

The development of the moisture content gradient in the thickness direction is the necessary input for the application of the LVP theory. The measurement of moisture content gradient in the laminate was conducted on 4 by 4 in square blocks cut from the original laminate. The blocks were place in the humidity chamber simultaneously with the laminate. Each block was taken out at certain time interval after the chamber humidity was raised to 91% RH and tested by the method developed by Feng and Suchsland [1993]. The depth increment used is 0.1 inches and only three layers of sampling were taken as the moisture content gradient in this laminate can be considered symmetrical to the mid-plane of the laminate. The new method using Forstner drill bit was demonstrated to be superior in accuracy to the conventional layer sawing technique [Feng and Suchsland, 1993].

The linear expansion samples were first conditioned at 65% RH and then subjected to a humidity cycle of from 65% to 86% to 93% RH. Measurements were taken when the specimens had equalized at 86% and 93% RH, respectively on an optical comparator developed by Suchsland [1970].

4.2.3 Test Results

The developments of vertical deflections at locations $(\pm 14.1, 0, 0)$ and $(0, \pm 9.15, 0)$ on the laminate and $(0, \pm 9.15, 0)$ on the beam as indicated in Figure 18, are

Figure 40. Yellow-poplar laminate and beam in humidity chamber.

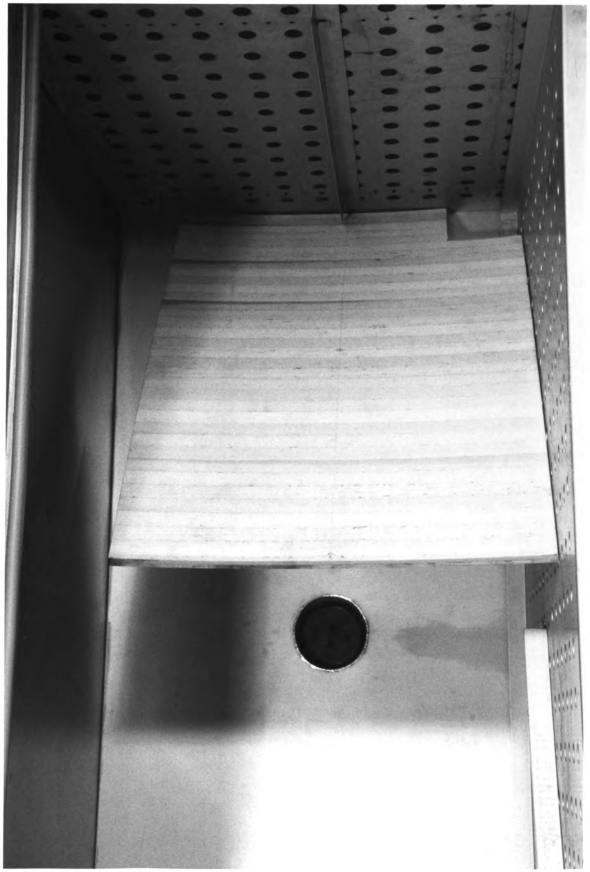

presented in Figure 41. The vertical deflections for these particular locations may be interpreted as the center deflections over a span of $14.1 \times 2 = 28.2$ in one direction and $9.15 \times 2 = 18.3$ in the other direction for the laminate, and a span of $9.15 \times 2 = 18.3$ for the beam. Time zero is when the humidity in the chamber was at 91% RH. The jump from 70% to 91% RH took only 5 minutes during which time no noticeable warp occurred in either the laminate or the beam.

The vertical deflections are seen in Figure 41 to rise quickly, slow down about 50 hours into the exposure, and eventually level off at 200 hours. The beam shows larger vertical deflection than the laminate over the same span, which is probably due to the absence of two dimensional restraint on the beam.

In Table 9 and Figure 42 which both indicate moisture content gradient progress, it is seen that the moisture content gradient is uniform at the beginning and end of the exposure test. As expected, the moisture contents in the outer layers rise first and rather quickly, while they lag behind for the inner layers. Describing the empirical gradients with quadratic equation resulted in a good fit (see regression coefficients in Table 9).

The expansion coefficients for both longitudinal and radial directions were obtained by the method introduced by Xu and Suchsland [1992] as a function of moisture content in the considered moisture content range which in this case is from 11.5% to 21.5%. As shown in Figure 43, expansion coefficients in both directions experience a reduction with increase in moisture content. Figure 44 is the sorption isotherm obtained based on measurements performed on expansion specimens.

The tension test for MOE was performed on the prepared longitudinal and radial

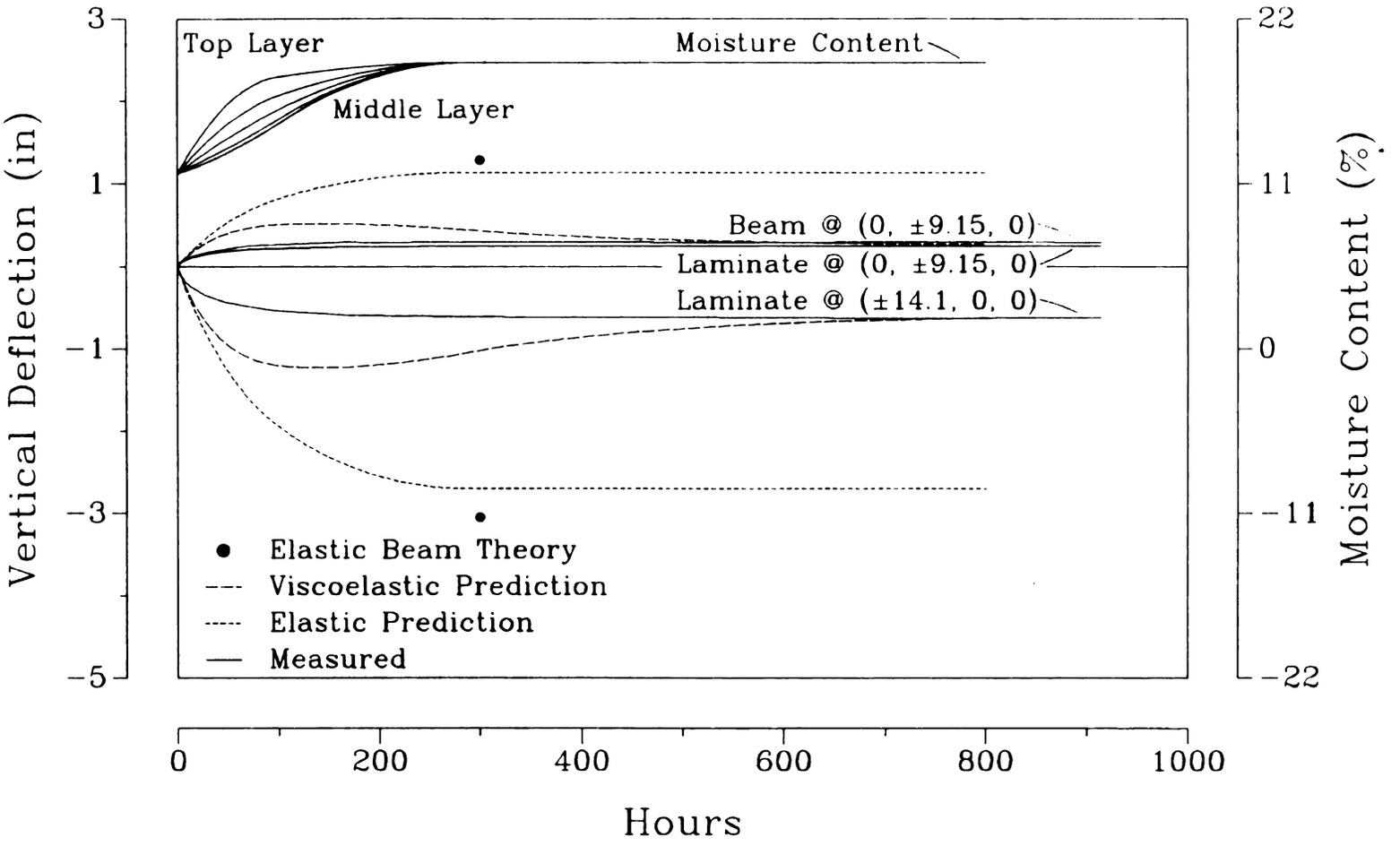

Figure 41. Theoretical predictions vs. measured vertical deflections of the yellow-poplar laminate and beam.
Beam: deflection measured over 18.3 in span
Laminate: deflection measured over 18.3 in span in one direction
28.2 in span in other direction

Table 9. Measured moisture content gradients in the yellow-poplar laminate.

	Distance From Surface (in)				
	0.05	0.15	0.25	0.35	0.45
Exposure Time (X)	Moisture Content (%) (Y)				
0.00 hours	11.72	11.68	11.66	11.68	11.72
1.33 hours	13.63	12.27	11.67	12.27	13.63
7.00 hours	14.81	12.93	12.05	12.93	14.81
12.50 hours	15.71	13.36	12.38	13.36	15.71
27.50 hours	16.30	13.97	13.06	13.97	16.30
47.50 hours	16.60	14.64	13.33	14.64	16.60
97.00 hours	17.37	15.59	14.68	15.59	17.37
6.00 days	17.64	16.29	15.44	16.29	17.64
12.00 days	19.09	19.09	19.09	19.09	19.09

	Regression Curve Fitting of Moisture Content Gradients			
	Quadratic Function: $Y = B(0) + B(1)X + B(2)X^2$			
	B(0)	B(1)	B(2)	Coefficient r^2
0.00 hours	11.737	-0.503	0.893	0.999
1.33 hours	14.713	-23.714	47.428	0.998
7.00 hours	16.312	-33.000	66.000	0.994
12.50 hours	17.545	-40.500	81.000	0.997
27.50 hours	18.097	-39.785	79.572	0.999
47.50 hours	18.338	-37.343	74.685	0.973
97.00 hours	18.824	-31.823	63.686	0.992
6.00 days	18.810	-25.357	50.714	0.978
12.00 days	19.090	0.000	0.000	1.000

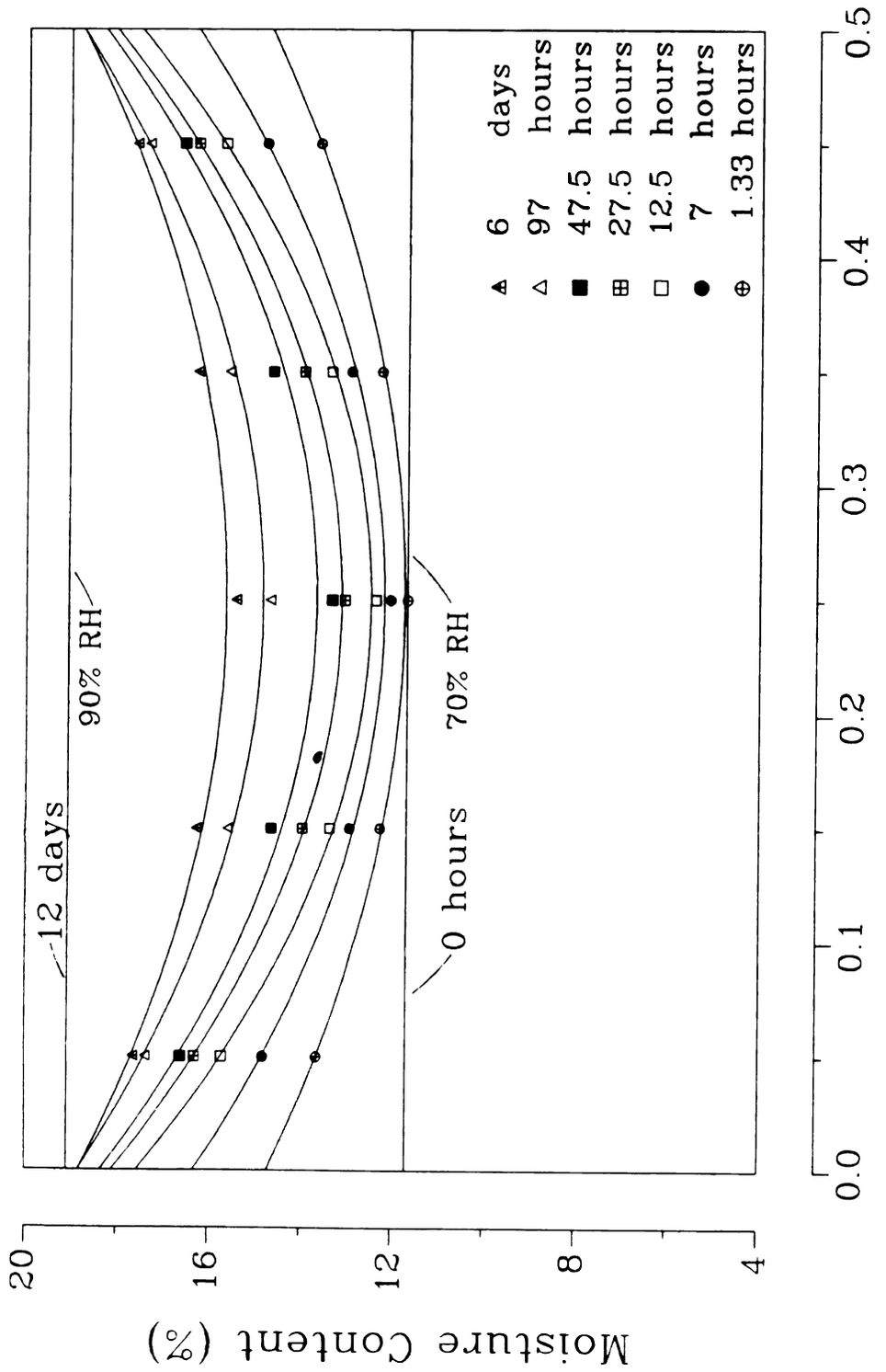

Figure 42. Moisture content gradient development in the yellow-poplar laminate.

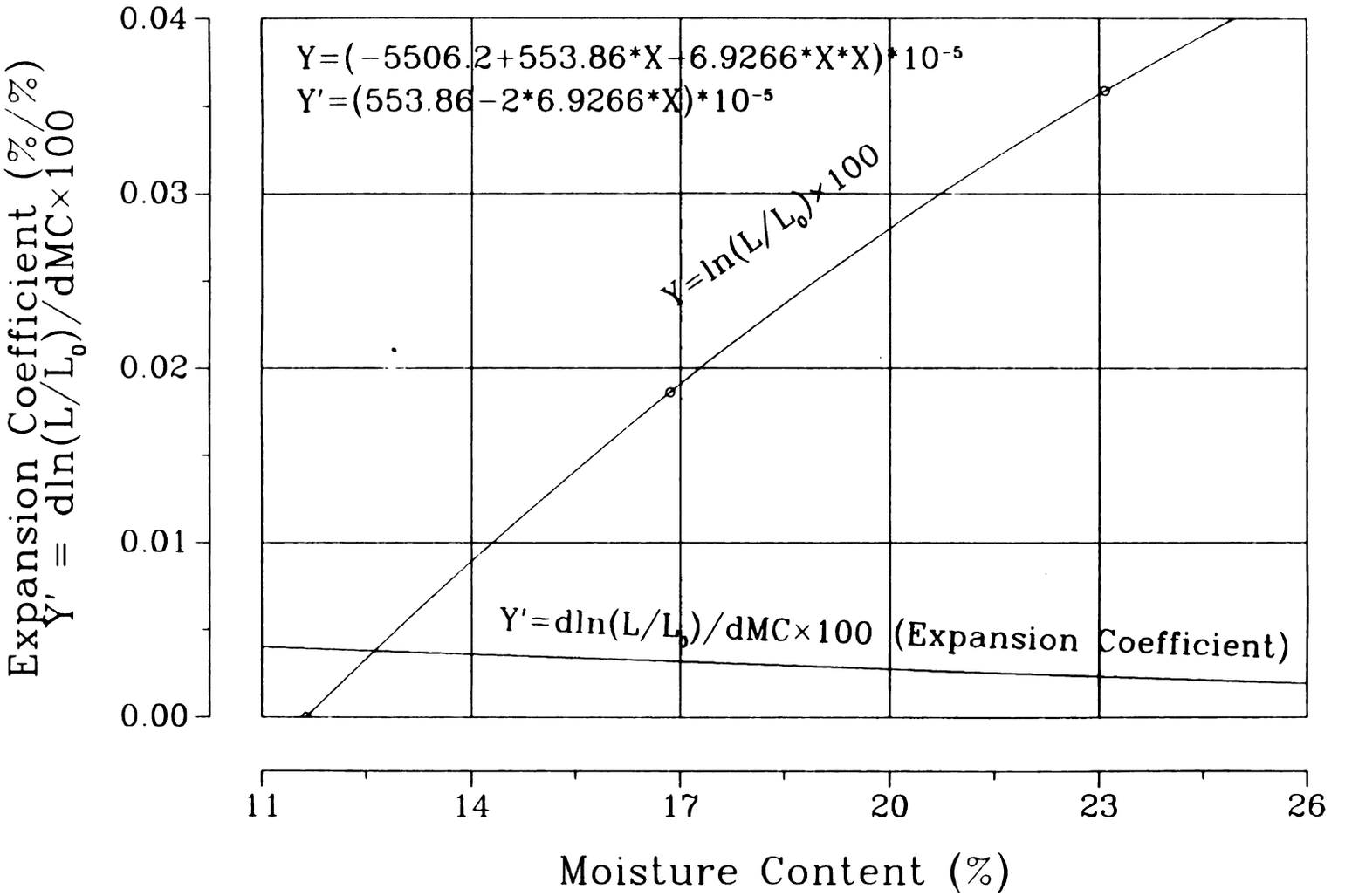

Figure 43a. Hygroscopic expansion coefficient of yellow-poplar in the longitudinal direction.

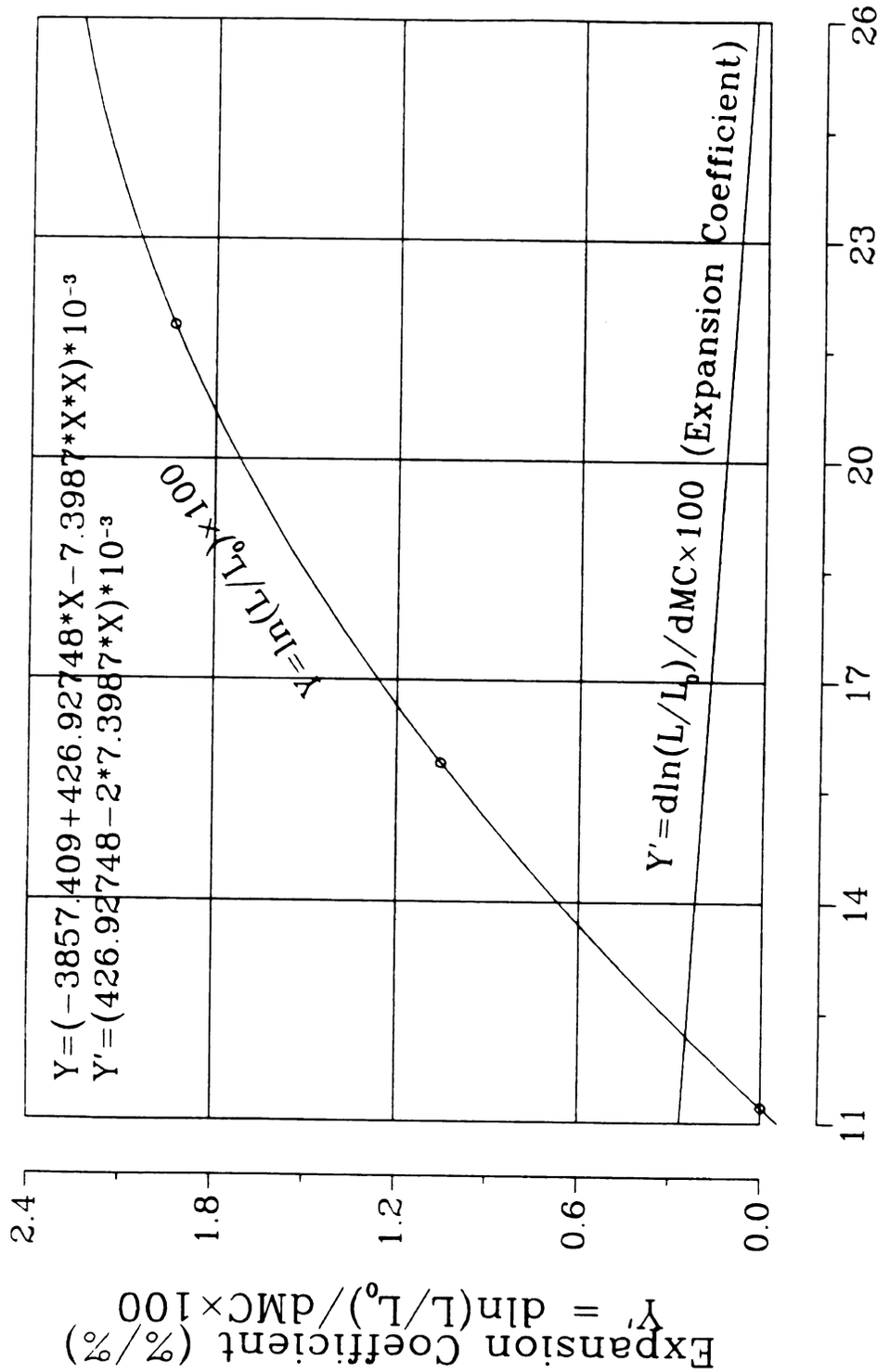

Figure 43b. Hygroscopic expansion coefficient of yellow-poplar in the radial direction.

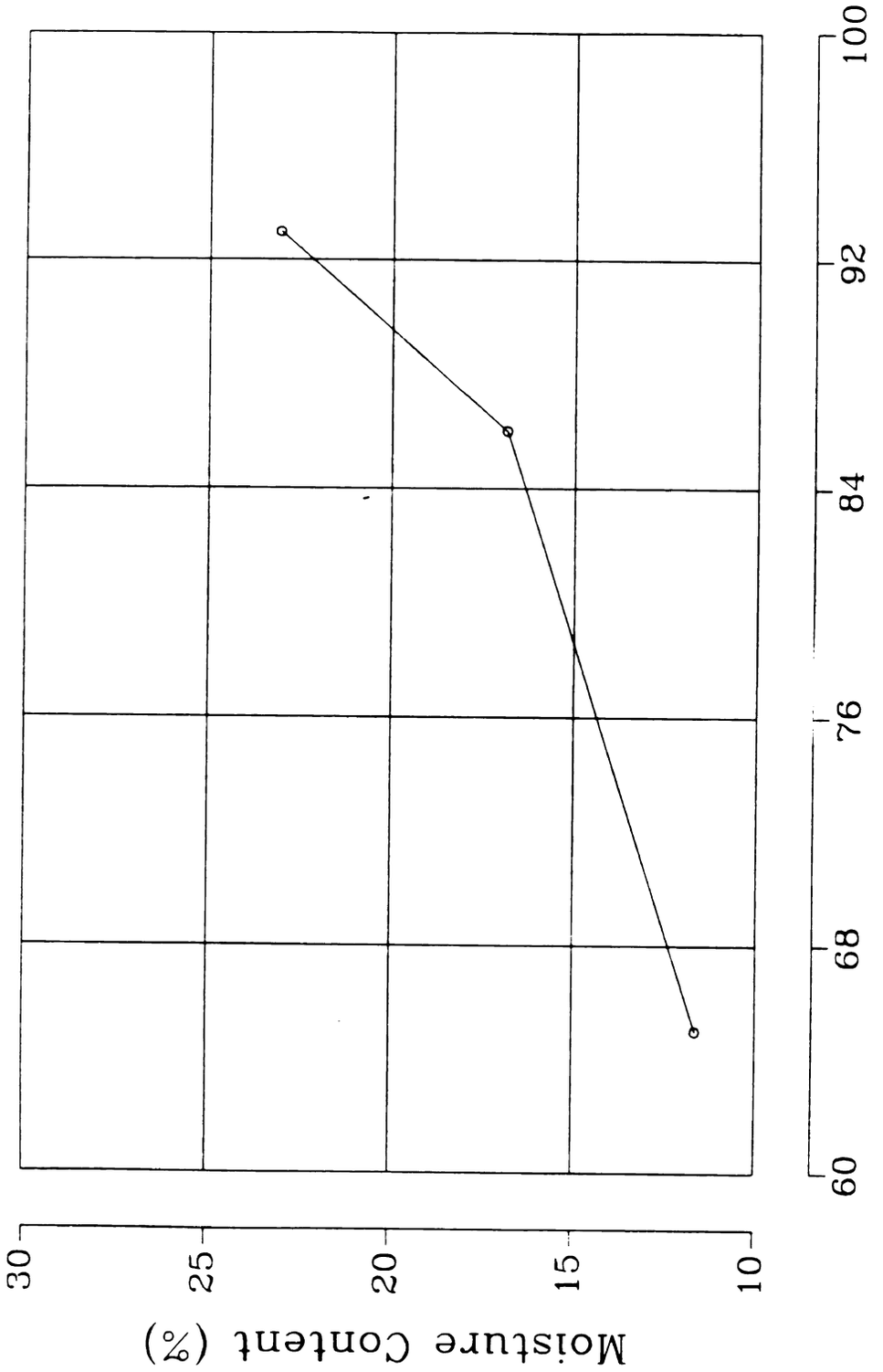

Figure 44. Sorption isotherm of yellow-poplar based on linear expansion data.

tension samples using the previously described extensometer-strain indicator loading setup. The results at three moisture content levels are listed in Table 10 and plotted in Figure 45. The projected indicates the MOE-moisture content relation according to the Wood Handbook [Forest Products Laboratory, 1987].

4.3 Application of the LVP Theory

4.3.1 Creep Compliances and Relaxation Moduli

One of the primary inputs for the LVP theory are the relaxation moduli described in a two dimensional plane stress state - namely ***[Y]***.

When Onsager's principal is applicable, one can draw upon results directly from elasticity theory for each type of geometric symmetry of interest [Schapery, 1967]. Therefore, for an orthotropic material, there are 9 independent relaxation moduli. Upon reducing the stress state down to plane stress, that number is reduced to 4, that is

$$\begin{Bmatrix} \sigma_{11}(t) \\ \sigma_{22}(t) \\ \sigma_{12}(t) \end{Bmatrix} = \begin{bmatrix} Y_{11}(t) & Y_{12}(t) & 0 \\ Y_{12}(t) & Y_{22}(t) & 0 \\ 0 & 0 & Y_{66}(t) \end{bmatrix} \begin{Bmatrix} \varepsilon^*_{11} \\ \varepsilon^*_{22} \\ \varepsilon^*_{12} \end{Bmatrix} \qquad 4.3.1$$

or

$$\{\sigma(t)\} = [Y(t)]\{\varepsilon^*\} \qquad 4.3.2$$

Superscript * indicates time-wise constant strains in a two dimensional relaxation test. The counterpart of the relaxation moduli ***[Y]***, the creep compliances ***[J]*** in a two

Table 10. Static tension MOEs of yellow-poplar.

	Moisture Content (%)		
	11.63	16.85	23.08
Specimen #	Longitudinal Tension MOE (10^3 psi)		
1R	2081.04	1712.90	1587.63
2	1529.95	1324.50	1125.91
5	2075.81	1794.06	1488.51
8R	1917.83	1689.10	1424.80
12	1330.26	1202.30	1079.40
14R	1780.15	1544.26	1287.23
15	1748.54	1536.81	1308.21
17	1616.92	1452.02	1288.86
18	1467.14	1237.54	1109.24
20	1586.09	1436.22	1260.47
23	1709.05	1502.36	1212.30
Average:	1712.98	1493.82	1297.60
STD Coeff.[1] (%):	13.42	12.20	11.65
Projected[2]:	1680.91	1509.27	1268.66
Difference[3] (%):	-1.87	1.03	-2.23
	Radial Tension MOE (10^3 psi)		
R1	155.96	126.54	111.60
R2	127.48	115.21	104.19
R3	127.10	113.40	105.40
R4R	111.22	105.28	98.49
R5	150.21	132.28	114.67
R6	153.03	124.13	110.5
R7	126.97	114.90	106.81
R8R	156.23	138.14	121.33
R9	169.02	149.63	128.88
R10	188.09	169.55	146.77
Average:	146.53	128.93	114.86
STD Coeff. (%):	15.02	14.28	11.75
Projected:	142.03	131.14	110.66
Difference (%):	-3. 07	1.71	-3.66

1: Deviation coefficient.
2: MOE computed according to Eq. 3.3.5 on the basis of the MOEs at two other moisture content levels.
3: Difference between the computed MOE and the measured MOE.

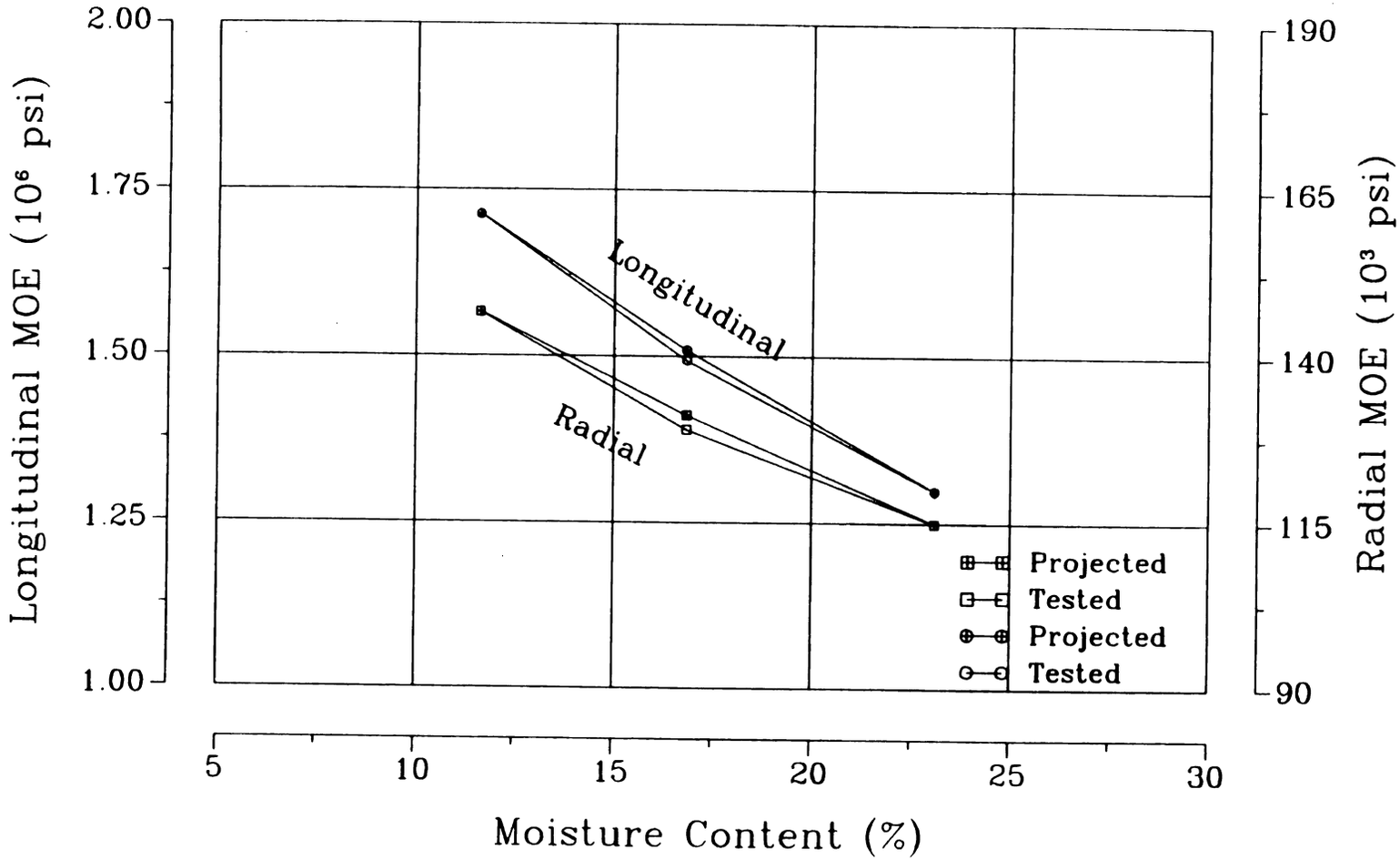

Figure 45. Static tension MOEs of yellow-poplar.

dimensional creep test is expressed as

$$\begin{Bmatrix} \varepsilon_{11}(t) \\ \varepsilon_{22}(t) \\ \varepsilon_{12}(t) \end{Bmatrix} = \begin{bmatrix} J_{11}(t) & J_{12}(t) & 0 \\ J_{12}(t) & J_{22}(t) & 0 \\ 0 & 0 & J_{66}(t) \end{bmatrix} \begin{Bmatrix} \sigma_{11}^{*} \\ \sigma_{22}^{*} \\ \sigma_{12}^{*} \end{Bmatrix} \qquad 4.3.3$$

where superscript * refers to time-wise constant creep stresses. If Poisson's ratio is introduced as in elasticity theory, then ***[J]*** can be expressed as

$$\begin{bmatrix} J_{11}(t) & -\nu_{21}(t)J_{22}(t) & 0 \\ -\nu_{12}(t)J_{11}(t) & J_{22}(t) & 0 \\ 0 & 0 & J_{66}(t) \end{bmatrix} \qquad 4.3.4$$

If the two viscoelastic quantities are linear, they may be related through Laplace transformation

$$[\bar{Y}(s)] = \frac{[\bar{J}(s)]^{-1}}{s^2} \qquad 4.3.5$$

Where s is the variable in the Laplace domain. Thus the relaxation moduli may be obtained if all components of the creep compliances are known, namely $J_{11}(t)$, the creep compliance in the grain direction, $J_{22}(t)$, the creep compliance across the grain, $J_{12}(t)$, a compliance of the nature of Poisson's ratio, and $J_{66}(t)$, the plane shear creep compliance. However, only the creep compliance across the grain (radial) of yellow-poplar $J_{22}(t)$ was tested and known. This is sufficient for the purpose of this study as shown in the following.

Wood is viscoelastic radially as well as longitudinally as has been shown in the literature. It is also known that wood is relatively very rigid in the grain direction compared to the radial direction with a MOE ratio of 10:1 for yellow-poplar (Wood Handbook) [Forest Products Laboratory, 1987]. The mutual restraint due to cross lamination must result in much larger viscoelastic activity in the radial direction. It is therefore reasonable to disregard the relatively small viscoelastic activity in the longitudinal direction and assume complete elasticity in the grain direction in a cross laminated structure. $J_{11}(t)$ is thus known to be $J_{11}(0)$ - longitudinal elastic compliance, easily obtainable by a static test. If a simple radial tension creep test is performed on a radial sample which creates a stress state of

$$\begin{Bmatrix} 0 \\ \sigma^* \\ 0 \end{Bmatrix}, \tag{4.3.6}$$

the strain in the longitudinal direction by Eq's. 4.3.3 and 4.3.4 would be

$$\varepsilon_{11}(t) = -\nu_{21} J_{22}(t)\, \sigma^* \tag{4.3.7}$$

Due to creep associated with longitudinal strain, $\epsilon_{11}(t)$ should not change with time. Therefore,

$$\varepsilon_{11}(t) = \varepsilon_{11}(0) = -\nu_{21}(t) J_{22}(t) = -\nu_{21}(0) J_{22}(0) \tag{4.3.8}$$

and

$$v_{21}(t) = -\frac{J_{22}(0)}{J_{22}(t)} v_{21}(0) \qquad 4.3.9$$

$J_{22}(0)$ is the initial radial creep compliance which happens to be the radial elastic compliance. $v_{21}(0)$, the initial creep Poisson's ratio at $t=0$ happens to be the elastic Poisson's ratio. Since both of them plus the radial compliance $J_{22}(t)$ are all known, $v_{21}(t)$ is easily found by Eq. 4.3.9. By compliance symmetry

$$-v_{21}(t)J_{22}(t) = -v_{12}(t)J_{11}(t) \quad , \qquad 4.3.10$$

Poisson's ratio $v_{12}(t)$ can be easily found to be

$$v_{12}(t) = v_{21}(t)\frac{J_{22}(t)}{J_{11}(0)} \qquad 4.3.11$$

$J(t)_{12}$ defined in 4.3.3 and 4.3.4 can subsequently be obtained.

In a cross lamination structure, the plane shear stress and strain are absent. The shear compliance term $J_{66}(t)$ therefore is irrelevant and could take any nonzero value. This may be an important for the wood industry where cross lamination is the most widely practiced lamination scheme for wood and wood-based composite panels.

Obtaining the relaxation moduli *[Y]* from the creep compliances *[J]* by Laplace transformation is only valid if both quantities are linear and isothermal. But, they are not, since warping is a nonlinear nonisothermal viscoelastic phenomenon. However, we have become familiar with the technique of discretization of the time domain in the numerical form of the LVP theory, the viscoelastic behavior and thus these two quantities may be

considered as linear and isothermal within a small enough time interval, where stresses, moisture content, and Poisson's ratio all vary so little that it is both practical and realistic for them to be assumed constant.

The expressions for creep compliance terms depend on the chosen mechanical model which in this study is the four element Burger body with an non-Newtonian Maxwell dashpot, as discussed in Chapter 3. Such a nonlinear model may be linearized if considered in a sufficiently small time interval where the non-Newtonian (nonlinear) dashpot would have such a minor variation in its coefficient that it can be regarded as a Newtonian (linear) dashpot with constant coefficient.

For a linear four element model, the creep compliance in terms of the coefficients of its four elements is

$$J_{ii}(t) = \frac{1}{E_{ks_{ii}}}\left(1 - e^{-\frac{E_{ks_{ii}}}{\eta_{md_{ii}}}t}\right) + \frac{1}{E_{ms_{ii}}} + \frac{t}{\eta_{md_{ii}}} \qquad ii = 11, 22, 66 \tag{4.3.12}$$

If Poisson's ratio is assumed constant, the corresponding relaxation moduli by Laplace transformation is found to be

$$[Y(t)] = \begin{bmatrix} \dfrac{E_{ms_{11}}R_{11}(t)}{(1 - \nu_{12}\nu_{21})} & \dfrac{-\nu_{21}E_{ms_{11}}R_{11}}{(1 - \nu_{12}\nu_{21})} & 0 \\ \dfrac{-\nu_{12}E_{ms_{22}}R_{22}(t)}{(1 - \nu_{12}\nu_{21})} & \dfrac{E_{ms_{22}}R_{22}(t)}{(1 - \nu_{12}\nu_{21})} & 0 \\ 0 & 0 & E_{ms_{66}}R_{66}(t) \end{bmatrix} \tag{4.3.13}$$

where

$$R_{ii}(t) = A_{ii}e^{-p_{ii_1}t} + B_{ii}e^{-p_{ii_2}t}$$

$$A_{ii} = \frac{p_{ii_1} - \frac{E_{ks_{ii}}}{\eta_{kd_{ii}}}}{p_{ii_1} - p_{ii_2}}$$

$$B_{ii} = \frac{\frac{E_{ks_{ii}}}{\eta_{kd_{ii}}} - p_{ii_2}}{p_{ii_1} - p_{ii_2}} \qquad 4.3.14$$

$$p_{ii_{1,2}} = \frac{1}{2}(b_{ii} \pm \sqrt{b_{ii}^2 - 4c_{ii}})$$

$$b_{ii} = (\frac{E_{ks_{ii}}}{\eta_{kd_{ii}}} + \frac{E_{ms_{ii}}}{\eta_{ks_{ii}}} + \frac{E_{ms_{ii}}}{\eta_{md_{ii}}})$$

$$c_{ii} = \frac{E_{ks_{ii}}E_{ms_{ii}}}{\eta_{kd_{ii}}\eta_{md_{ii}}}$$

$$ii = 11,22,66$$

It is to be remembered that this conversion is made under the condition that the Poisson's ratio is constant and is therefore only valid during a small time interval where Poisson's ratio can be regarded as constant. It is seen that both creep compliances and relaxation moduli are functions of the coefficients of the four elements of the proposed mechanical model. In other words, the study of creep compliances and relaxation moduli is reduced to that of the coefficients of the elements comprising the model.

Due to the continuous variations of moisture contents and stresses during hygroscopic warping, the four coefficients in the relaxation moduli would vary accordingly. The numerical form of the LVP theory due to its discrete nature allows only

discretized descriptions of those variations. Within each thin layer, moisture content and stresses are assumed to be the averages of their distributions in the layer, and remain so during the current time interval before they jump to new levels at the beginning of the next time interval. The moisture content dependence of the coefficients would subsequently follow such step-wise pace with the moisture content.

The stress dependence of the coefficients is more difficult to deal with. In order to account for the stress dependence of the coefficients, stresses must be known. Stresses, however, can not be obtained for the current interval before the determination of the coefficient values. This indetermination results from the nonlinearity of the viscoelastic behavior where the coefficients (coefficients determine compliance) depend on the stress levels. The approach taken here to break the impasse is to use the stresses already found at the previous time interval as the basis for computation of the stress dependence of the coefficients for the current interval, and then obtain strain rates, strains, and stresses. It should be a good approximation since the time interval is very small and thus the step-wise stress increase from the previous time interval to the current one is not significant.

A better method however is by iteration of computation to reach convergence. Specifically, stress dependence of the coefficients for the current time interval is first calculated based on the stress values from the previous time interval, followed by the computation of the stress values using the obtained coefficient values. The computed stress value for this time interval is the first approximation. In the next iteration, stress dependence of the coefficients for the current interval are again computed, but this time on the basis of the first approximation of the stress values. The resulting new coefficient

values when used to compute the stress should result in new stress values called the second approximation which are different from those of the first approximation. This iteration computation could carry on until the difference of the stress values of the newest iteration from those of the previous iteration is relatively insignificant indicating that convergence has been achieved. Such technique should yield better results. However, it is not adopted here because the intensive interaction computation was expected to take too much computing time, slowing down the computing speed on a desktop PC. It should pose no such problem when the numerical LVP is implemented on mainframes. Such implementation of the computer program is not difficult.

Of the four coefficients (E_{ms}, E_{ks}, η_{md}, η_{kd}) which determine the relaxation moduli $[Y(t)]$, η_{md} defined as

$$\eta_{md}(t,MC,\sigma) = \frac{t^{1-m(MC,\sigma)}}{a(MC,\sigma)m(MC,\sigma)} \qquad 4.3.15$$

needs special attention since it is also dependent on time in addition to moisture content and stresses, as indicated in Chapter 3. Therefore, time into the warping process must somehow be factored into the value of this coefficient. As we only know of the variation of the coefficient with time under given constant stress and moisture content, certain treatment must be adopted to approximate its variation under changing moisture content and stress during the warping process.

If it is assumed that the stress σ and the moisture content MC are to increase step-wise along the discretized time scale shown in Figure 46, the flow component of the creep compliance due to $\Delta\sigma_1$ and MC_1 in the first time interval is by Eq. 3.3.24

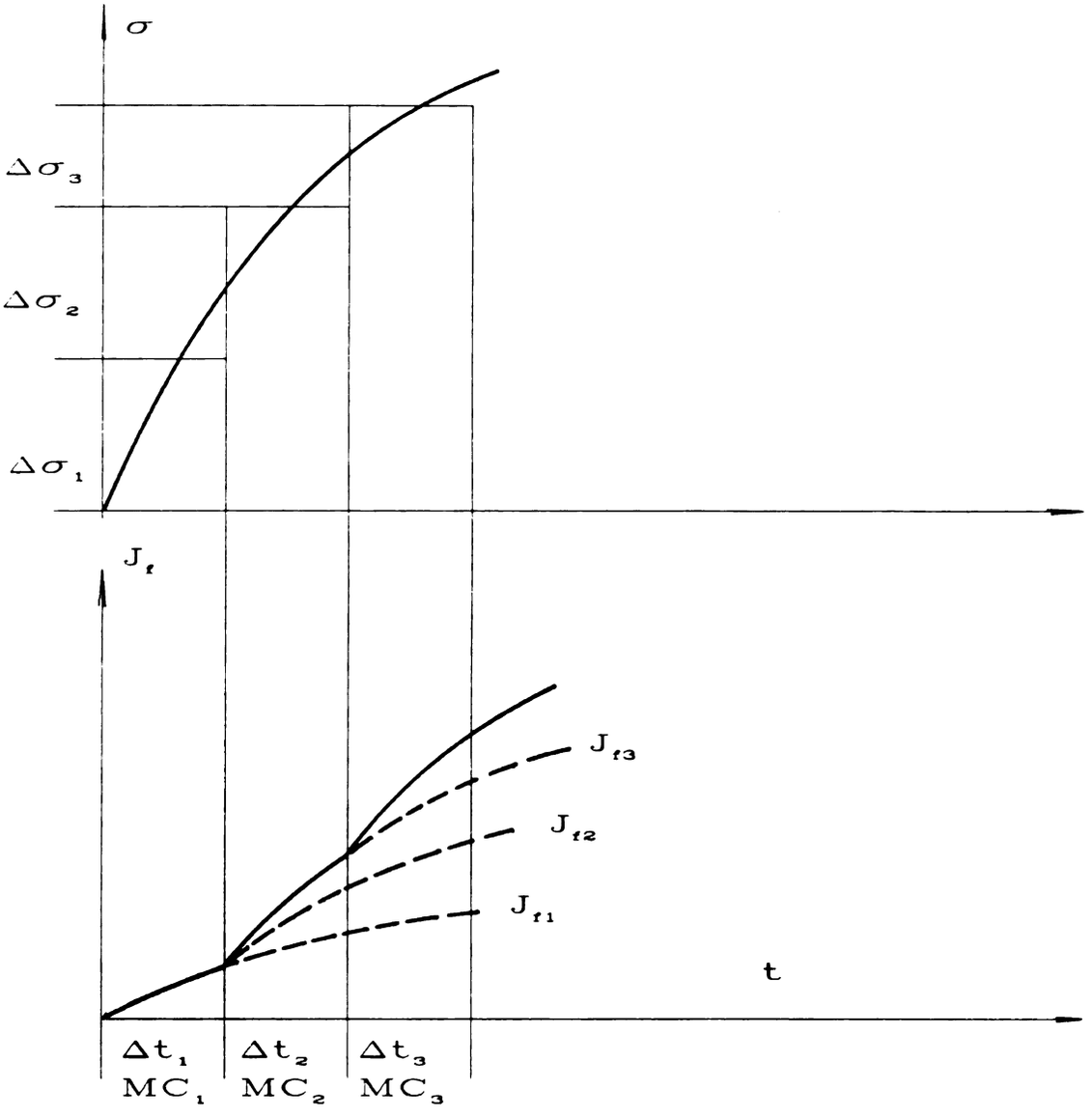

Figure 46. Superposition scheme for flow compliance.

$$J_f(MC_1, \Delta\sigma_1, t)|_{\Delta t_1} = a(MC_1, \Delta\sigma_1)t^{m(MC_1, \Delta\sigma_1)} \qquad 4.3.16$$

Therefore, the reciprocal of the coefficient $1/\eta_{md}$ which is assumed constant in the small time interval Δt_1 takes the following value at the midpoint $\Delta t_1/2$, which is the differentiation of 4.3.16 at $\Delta t_1/2$

$$\frac{1}{\eta_{md}}|_{\Delta t_1} = \frac{1}{\eta_{md}(\frac{\Delta t_1}{2}, MC_1, \Delta\sigma_1)} = a(MC_1, \Delta\sigma_1)m(MC_1, \Delta\sigma_1)(\frac{\Delta t_1}{2})^{m(MC_1, \Delta\sigma_1)-1} \qquad 4.3.17$$

In the next interval where moisture content is elevated to MC_2 and stress incremented by another amount of $\Delta\sigma_2$ on top of $\Delta\sigma_1$, the part of the flow compliance due to the stress $\Delta\sigma_1$ at the second interval (Δt_2) is not directly available since moisture content and stress have changed, but could be approximated by

$$J_f(\frac{MC_1 \times \Delta t_1 + MC_2 \times \Delta t_2}{\Delta t_1 + \Delta t_2}, \Delta\sigma_1, t)|_{\Delta t_2} \qquad 4.3.18$$

where the creep is supposedly to occur under the weighted average moisture content of the two intervals. Another part of the flow compliance is due to the $\Delta\sigma_2$ at the beginning of the second interval which contributes an amount of

$$J_f(MC_2, \Delta\sigma_2, t)|_{\Delta t_2} \qquad 4.3.19$$

Superimposing the two parts results in the flow compliance for the second interval. The reciprocal of the flow coefficient for the second interval is then the differentiation of the sum compliance at $(\Delta t_2/2)$

$$\frac{1}{\eta_{md}}\Big|_{\Delta t_2} - \frac{1}{\eta_{md}\left(\frac{MC1\times\Delta t_1 + MC2\times\Delta t_2}{\Delta t_1+\Delta t_2}, \Delta\sigma 1, \Delta t_1 + \frac{\Delta t_2}{2}\right)}\Big|_{\Delta t_2} + \frac{1}{\eta_{md}\left(MC2, \Delta\sigma 2, \frac{\Delta t_2}{2}\right)}\Big|_{\Delta t_2} \qquad 4.3.20$$

At the next or third time interval, there will be three parts of the coefficient summed up due to the presence of three stress jumps, $\Delta\sigma_1$, $\Delta\sigma_2$, and $\Delta\sigma_3$. By this superimposing scheme, the coefficient η_{md} for every discretized time interval along the time scale of the warping process may be approximately and numerically obtained.

The resulting relaxation moduli *[Y(t)]* as input for the application of the LVP theory therefore accounts for the changing of its four coefficients with moisture content, stress level, and time in the warping process.

4.3.2 Hygroscopic Strain Rates

The hygroscopic strain $\{\epsilon^{MC}(t)\}$ may be expressed as

$$\begin{Bmatrix} \varepsilon_{11}^{MC}(t) \\ \varepsilon_{22}^{MC}(t) \\ \varepsilon_{12}^{MC}(t) \end{Bmatrix} = \int_{MC(0)}^{MC(t)} \begin{Bmatrix} \alpha_{11}(t) \\ \alpha_{22}(t) \\ \alpha_{12}(t) \end{Bmatrix} dMC = \int_0^t \begin{Bmatrix} \alpha_{11}(t) \\ \alpha_{22}(t) \\ \alpha_{12}(t) \end{Bmatrix} MC(t)'\, dt \qquad 4.3.21$$

or

$$\{\varepsilon^{MC}(t)\} = \int_0^t \{\alpha(t)\}\, MC(t)'\, dt \qquad 4.3.22$$

where $\{\epsilon^{MC}(t)\}$ and $\{\alpha(t)\}$ are hygroscopic strains and hygroscopic expansion coefficients, respectively. $MC(t)'$ is the rate of moisture content variation. It follows that the strain

rates are

$$\begin{Bmatrix} \varepsilon_{11}^{MC}(t) \\ \varepsilon_{22}^{MC}(t) \\ \varepsilon_{12}^{MC}(t) \end{Bmatrix}' = \begin{Bmatrix} \alpha_{11}(t) \\ \alpha_{22}(t) \\ \alpha_{12}(t) \end{Bmatrix} MC(t)' \qquad 4.3.23$$

due to

$$(y)' = \left(\int_0^x f(x)\,dx \right)' = f(x) \qquad 4.3.24$$

For a small time increment Δt, hygroscopic strain rates could be approximated by

$$\begin{Bmatrix} \varepsilon_{11}^{MC}(t) \\ \varepsilon_{22}^{MC}(t) \\ \varepsilon_{12}^{MC}(t) \end{Bmatrix}' \approx \begin{Bmatrix} \alpha_{11}(t) \\ \alpha_{22}(t) \\ \alpha_{12}(t) \end{Bmatrix} \frac{\Delta MC}{\Delta t} \qquad 4.3.25$$

since

$$MC(t)' \approx \frac{\Delta MC}{\Delta t} \qquad 4.3.26$$

$\alpha_{11}(t)$ and $\alpha_{22}(t)$ are the expansion coefficients in the grain and across the grain direction, respectively, while $\alpha_{12}(t)$ would be zero. If the x-y coordinates are rotated clock-wise by an angel θ relative to the *1-2* coordinates as indicated in Figure 12, then the strain rates in x-y coordinates become

$$\begin{Bmatrix} \varepsilon_{xx}^{MC}(t) \\ \varepsilon_{yy}^{MC}(t) \\ \varepsilon_{xy}^{MC}(t) \end{Bmatrix}' \approx \begin{Bmatrix} \alpha_{xx}(t) \\ \alpha_{yy}(t) \\ \alpha_{xy}(t) \end{Bmatrix} \frac{\Delta MC}{\Delta t} \qquad 4.3.27$$

The $\{\alpha(t)\}_{x\text{-}y}$ (hygroscopic expansion coefficients in x-y coordinates), are related to $\{\alpha(t)\}_{1\text{-}2}$ (hygroscopic expansion coefficient in *1-2* material principle coordinates) through coordinate transformation *[T]*

$$\begin{Bmatrix} \alpha_{11} \\ \alpha_{22} \\ 0 \end{Bmatrix} = [T] \begin{Bmatrix} \alpha_{xx} \\ \alpha_{yy} \\ \frac{\alpha_{xy}}{2} \end{Bmatrix} \qquad 4.3.28$$

where

$$[T] = \begin{bmatrix} \cos^2\theta & \sin^2\theta & 2\cos\theta\sin\theta \\ \sin^2\theta & \cos^2\theta & -2\cos\theta\sin\theta \\ -\sin\theta\cos\theta & \sin\theta\cos\theta & \cos^2\theta - \sin^2\theta \end{bmatrix} \qquad 4.3.29$$

4.3.3 Computer Programming of the Numerical Form of the LVP Theory

The numerical form of the LVP was implemented in the Microsoft QuickBASIC language. The computation is automatically carried out on a 486DX50 IBM compatible desktop computer, given the necessary inputs. The detailed programming codes are presented in Appendix A. It is to be pointed out that the programming focus was on the main computing body. The preprocessing which handles the accepting of inputs and

postprocessing which handles the output function are merely functional and sufficient for the author, but by no means fancy and user friendly. However, these two parts can be refined to a user friendly and efficient level without much difficulty if necessary in the future.

4.3.4 Preparation of Inputs

Aside from the relaxation moduli and the hygroscopic expansion strain rates already formulated in previous sections, the remaining necessary inputs are the thickness and grain orientations of constituent layers. The yellow-poplar laminate in this study consisted of two cross laminated lamina of equal thickness, each assumed to be comprised of an equal number of imaginary thin layers.

4.4 Theoretical Predictions and Analysis

In Figure 41, theoretical predictions by the LVP on the vertical deflections are plotted against the measured values for the yellow-poplar laminate and beam (refer to Figure 18 for the coordinate positions and locations). Moisture content developments with respect to time are presented as a reference on the progress of the warping process. Also included for comparison are the elastic predictions which are achieved by replacing the viscoelastic relaxation moduli with the elastic moduli for inputs in the LVP, equivalent to using a mechanical model of only a spring.

The laminate and beam are seen to deflect very quickly in the early stages of the warping process where the moisture content gain is rather steep. Their vertical

deflections, however, level off at about 200 hours into warping process - 80 hours before moisture content equilibrium.

The overestimate by the elastic prediction is expected because the viscoelastic nature of the warping process is not accounted for in the elastic moduli. The leveling off of the elastic predictions occurs exactly where anticipated as the hygroscopic strains ceases to increase at moisture content equilibrium. The elastic prediction gave somewhat better estimates than the elastic beam theory [Suchsland, 1985]], possibly due to the incorporation of the effect of moisture content on elastic moduli during warping. The latter, however, is much simpler in that it only requires inputs of the total moisture content increase for the whole warping process, the average expansion coefficients, and the elastic moduli at the end condition. The small improvement by the former whose complexity results from accounting for the moisture content effect on the elastic moduli during the warping process only proves that the elastic beam theory yields a sufficiently precise and practical estimate. It further demonstrates that extra effort within the realm of elasticity is of very limited reward, and such effort should be directed towards the study of viscoelasticity. It is worth mentioning that the elastic beam theory has provided warping estimates that are sufficiently accurate at low and moderate moisture contents [Suchsland, 1985].

The viscoelastic predictions show quick deflection increase due to rapid moisture content increase, and reach a peak at about 130 hours of exposure when they start to relax to final values that are within 5% of the measured at 800 hours. The LVP theory reflects the early domination by the large hygroscopic expansion resulting from rapid

moisture content increase. Even though deformation creep and stress relaxation must be occurring simultaneously and picking up due to the rise in stresses, they are still overshadowed. However, as the moisture content increase slows down, deformation creep and stress relaxation increase their share. When the predicted vertical deflection peaks at 130 hours,deformation creep and stress relaxation start to dominate. As stresses are relaxed, less deformation creep and stress relaxation take place, which is seen as the decrease in the relaxation rate. When the moisture content is completely equalized at 300 hours, no further hygroscopic strains are introduced. The LVP responds with a inflection point in the theoretical predictions. From that point on, only deformation creep and stress relaxation take place. They slow themselves down due to the stress reduction till the leveling off point at 800 hours.

Though the LVP theory is clearly able to simulate the warping process and provide much improved predictions over its elastic counterpart, it deviates from the actual warping development, especially in the early stages. In the theoretical predictions, peaks are observed and it is well after moisture content equalization that predictions relax to stable levels, while actual vertical deflections have no such peaks and reach a stable levels at about 200 hours, well before the point of moisture content equalization (about 300 hours). It is evident that there exists in the warping process a mechanism responsible for the much earlier and faster relaxation than described in the LVP theory. This disparity could possibly be due to either the limitations of the LVP theory itself or the inaccurate description of the constituent's (yellow-poplar) viscoelastic response. The former can not be verified before the latter is investigated and corrected. Regarding the

latter, the effects of moisture content and stresses on wood and wood-based materials are not as simple as characterized in this study, where only the separate effects of stress and moisture content are considered. When moisture content is changed under stress, creep and relaxation are much larger and faster than if moisture content is changed prior to stressing as has been discussed in detail in the review section. Moisture content and stresses change simultaneously in a warping process, and assuming separate effects of moisture content and stress is obviously not realistic, very possibly resulting in the large variance between the theoretical predictions and the measured vertical deflections.

As the LVP theory requires the discretization of the panel into a number of layers, theoretical predictions are computed based on both a 10 layer and a 6 layer discretization. Slight differences resulted, as listed in Table 11. Theoretically, more layer elements generate better results, but require more computing time.

Table 11. Theoretical predictions vs. measured vertical deflections of the yellow-poplar laminate and beam.

	Vertical Deflection					
	Measured	Viscoelastic Prediction		Elastic Prediction		Elastic Beam Theory
	(in)	(in)		(in)		(in)
		6-layer	10-layer	6-layer	10-layer	
Laminate						
@ (±14.1, 0, 0)	-0.623	-0.625	-0.642	-2.699	-2.698	-3.050
@ (0, ±9.15, 0)	0.246	0.263	0.270	1.137	1.136	1.285
Beam						
@ (0, ±9.15, 0)	0.291	0.263	0.270	1.137	1.136	1.285

Since the agreement of theoretical predictions and the measured vertical deflections was checked for only discrete locations ***(±14.1, 0)*** and ***(0, ±9.15)*** of the laminate, it is not known yet how well the overall warped shape of the laminate is simulated by the LVP theory. One way to examine this is to check the vertical deflections at as many locations on the laminate as necessary. However, this can be achieved by a much simpler test.

The Kirchhoff Hypothesis (the displacement field) - the foundation of both the CLT and the LVP theory - assumes a quadratic surface for laminates as defined in Eq. 2.4.9. For the particular 2-ply cross laminated yellow-poplar laminate, the LVP theory predicts that curvatures κ_x and κ_y are of equal magnitude but of opposite sign, while the twist curvature rotation κ_{xy} is zero. The cross lamination of the two identical layers determines that the same degree of curvature but in opposite direction should develop in the x and y directions, respectively, and that no twist should occur in the laminate. Therefore, by Eq. 2.4.9, no vertical deflections should occur along the two 45° diagonal lines, if the warped shape of the laminate agrees with the quadratic surface. Placing a straight edge along the diagonal lines on the laminate showed little vertical deflections, thereby confirming that the actual deformation of the laminate does approximately follow a quadratic surface as the LVP theory assumes.

CHAPTER V

Summary and Suggestions on Future Investigations

This work is probably the first attempt ever to formulate a viscoelastic plate theory in solvable numerical form integrated with viscoelastic properties of constituent materials to theoretically approach the hygroscopic warping phenomenon - a nonlinear nonisothermal viscoelastic process.

The LVP theory was developed on the basis of CLT and linear viscoelasticity theory. The viscoelastic properties of yellow-poplar were characterized using a four element Burger body model with a non-Newtonian Maxwell dashpot to account for the non-Newtonian behavior of the flow component of the viscoelastic deformation. The numerical form of the LVP theory was achieved by applying linear finite approximation to the integral viscoelastic governing equation of the LVP theory (discretization of time domain). Numerical computations were implemented in QuickBASIC and conducted on a desktop PC computer. The treatment taken in applying this linear isothermal theory to nonlinear nonisothermal viscoelastic warping problem is that the viscoelastic coefficients determining the viscoelastic properties of the constituent materials were allowed to vary accordingly with moisture content, stresses, and time during warping. The validity of this theory and its superiority over elastic prediction in describing the viscoelastic warping process was demonstrated at least on a preliminary level in its

application to a two-ply cross laminated yellow-poplar laminate.

In characterizing the viscoelastic properties of yellow-poplar in the radial direction as inputs for the application, it is verified what many authors have found, namely that wood exhibits nonlinear viscoelasticity of its flow and recoverable components, while the instantaneous elastic component remains linearly elastic. The elastic component varies with moisture content according to the known moisture content effect on mechanical properties, while the other two components are shown to be dependent on both moisture content and stresses.

The development and computer implementation are somewhat involved. But once carried to completion as in this study, the application is reduced to running the program with required inputs on a desktop computer and retrieve the result files from the designated disk. The theory and its numerical form are material independent and could be applicable to a variety of panels of different materials and structures suffering from hygroscopic deformation, as long as the information regarding the structures and the viscoelastic properties of the composing materials are given.

The LVP theory loses its applicability when the actual displacement field gets more complicated than that of the Kirchhoff Hypothesis. It has been proven that beams and plates of small aspect ratios do not deform according to the Kirchhoff assumption because of the relative significance of transverse shear and normal components. Fortunately, most industrial wood and wood-based composite panels that are susceptible to hygroscopic warping have large aspect ratios which ensures convergence to the displacement field specified by the Kirchhoff Hypothesis, as supported by the simple

straight edge test.

The applicability of the described LVP theory very much depends on the availability and accuracy of the required inputs. Of the greatest importance is the formation of the two dimensional stress state relaxation moduli that characterize the viscoelastic properties of the involved materials. How accurately and completely the relaxation moduli account for the viscoelastic properties should greatly influence the quality of the theoretical predictions of the LVP theory. In this study only the separate effects of moisture content and stress were characterized into the relaxation moduli, which is why the theoretical predictions, though much better than the elastic approach, still deviate from the measured results. This shortcoming can be attributed in part to the exclusion of the mechano-sorptive behavior (coupling between stress and moisture content change). The mechano-sorptive effects are known to cause as much as many times more creep and faster relaxation than would occur when moisture content is changed prior to stressing. Such effect is very prevalent in a warping process where the moisture content changes during stress development, and therefore must be factored into the viscoelastic relaxation moduli for better results.

The moisture content gradient development and the hygroscopic expansion coefficients which are necessary for calculating the cause of hygroscopic deformation - hygroscopic strains - are also expected to influence theoretical predictions. As both the LVP theory and warping are process dependent, the in-process variation path of moisture content development and coefficients will definitely affect the final outcome.

How moisture content gradient development, expansion coefficients, material

viscoelastic properties, and laminate structures affect the hygroscopic warping have up to now been either qualitatively analyzed or experimentally determined. This could now be evaluated and analyzed relatively quickly on a computer by entering different variables into the LVP theory. The described method could serve as an efficient research tool in aiding further study and providing understanding of the hygroscopic warping process.

Several assumptions are essential in this study. Transverse normal and shear components were not considered as a result of the CLT structure of the LVP theory (the Kirchhoff Hypothesis). Their definite presence has been proven to exert minimum influences on the overall behavior of laminates of large aspect ratios (Chapter 2). Mechano-sorptive coupling of wood and wood-based materials (varying moisture content under creep load) is known to be heavily involved in the viscoelastic warping process, yet has not been well understood and mathematically defined. It was therefore not tested and characterized into the relaxation moduli input for the application of the LVP. Plane shear component was assumed to be zero in the yellow-poplar laminate due to the cross lamination structure. It was also assumed that there is no viscoelastic activity in the grain direction because of the relatively highly crystalline and elastic nature in the grain direction.

As to further improvements of the applicability of the LVP theory to the warping problem, the first to be suggested is a characterization approach that can integrate mechano-sorptive effects into the relaxation moduli. The mechano-sorptive effect in the warping process has been shown to be too significant to be ignored.

The applicability of the LVP theory was examined on a preliminary level in this

study. Further verification on a larger scale is necessary. In the meantime, it can offer some new insights into the warping process.

The programming of its numerical computation needs to be refined, especially the preprocessing and postprocessing portions that handle processing of inputs and outputs. Increased capability and versatility of the preprocessing portion would allow inputs in a variety of forms. Improved postprocessing would provide better illustration and interpretation of outputs.

APPENDIX

Computer Program of LVP in Mirosoft QuickBASIC

```
DECLARE SUB PRINTPARM (K!, P$, PARM!())
DECLARE SUB ERRLOCTN (LOC$)
DECLARE SUB MATRPRN1 (X(), S)
DECLARE SUB MATRPRN2 (X(), S)
DECLARE SUB MATRTRAN (X(), XT())
DECLARE SUB MATRINVS (A(), AI())
DECLARE SUB MATRMULT (A(), B(), AB())
DECLARE SUB INITSCRN ()
DECLARE SUB INPTSCRN (DLT, TT)
DECLARE SUB INMTMANU (M!, DLT!)
DECLARE SUB INPUTSEC (K, DLT, TT, CMIS, CTMP)
DECLARE SUB PLOTCMDF (K)
DECLARE SUB WRITECMD (NUM!, RANK!, NAME$())
DECLARE SUB SPLINQUD (X(), Y(), COF())
DECLARE SUB MOISTURE (K, DLT, M, CMIS)
DECLARE SUB MODELCOF (K, XFLAG$(), PARM())
DECLARE SUB EXPANSIN (K, DLT, M)
DECLARE SUB FILEINIT (K, DTL, CX, CY)
DECLARE SUB COEFFIN1 (I!, P!, K!, DLT!, M)
DECLARE SUB PARAMTR1 (X!(), Y!(), CEF!())
DECLARE SUB PARAMTR2 (M(), Y(), S(), CEF())
DECLARE SUB FUNCCOEF (X!(), Y!(), CEF!())
DECLARE SUB QTRAFORM (Q(), THETA, QXY())
DECLARE SUB STRAFORM (SXY(), THETA, S12())
DECLARE SUB STFHNMS1 (I!, P!, K!, DLT!)
DECLARE SUB MAINCOM1 (M!, P!, K!, DLT!)
DECLARE SUB SCRNPLOT (IL, NUM, A, B, C, D, E, F)
DECLARE FUNCTION INMTNUMR! (DLT!, TT)
DECLARE FUNCTION INMTAUTO! (I!)
DECLARE FUNCTION LEFTWORD$ (INT$)
DECLARE FUNCTION LEFTCHAR$ (INT$, N)
DECLARE FUNCTION TIMEVALU (TS$)
DECLARE FUNCTION TIMESTRG$ (TVL)
DECLARE FUNCTION RELXMODU (TYPE$, MS, RMV, KS, RKV, T)
COMMON K, DLT
COMMON SHARED INFNUM$, PREFIX$, INFILE$, STRESS$, STRAIN$, STRAMP$, DISMNT$, MOISTU$, PLTCMD$
COMMON SHARED DIRINP$, DIROUT$, TIMER$, LMOIST$, LSTRES$, CX, CY, SDL, SSL, SNL, SPL, MCL, TYPE$, SEQ$
DIM SHARED LSTRAIN$(1 TO 6), LSTRAMP$(1 TO 6)
COMMON LSTRAIN$(), LSTRAMP$()
COMMON SHARED SCRN$, DSPL$
KEY(1) ON
ON KEY(1) GOSUB KEYQ
KEY(2) ON
ON KEY(2) GOSUB DISPLAY
CALL INPTSCRN(DLT, TT)
CALL INITSCRN
IF TIMER$ = "Y" THEN
   TIMER ON
ELSE
   TIMER OFF
```

```
END IF
CTIM = 0
ON TIMER(1) GOSUB DISPLAY
OLD = TIMEVALU(TIME$)

OPEN DIRINP$ + INFILE$ FOR INPUT AS #1
  DO
    LINE INPUT #1, INT$
  LOOP UNTIL LEFTWORD$(INT$) = INFILE$
  DO
    LINE INPUT #1, INT$
  LOOP UNTIL LEFTWORD$(INT$) = "#" OR EOF(1)
  IF EOF(1) = -1 THEN CALL ERRLOCTN("2 IN MODULE")
  LINE INPUT #1, INT$
  K = VAL(INT$)
    M = INMTNUMR(DLT, TT)  'RETURN TOTAL # OF INCREMENTS
    DIM SHARED H(0 TO K)
    DIM SHARED ANGLE(1 TO K), MP(1 TO K)
    DIM SHARED MC$(1 TO 20), TM$(1 TO 20)
    DIM SHARED MC(M + 1, 1 TO K)
    DIM SHARED AVGMCW(M + 1, 1 TO K)
    DIM SHARED EXPCOF(1 TO K, 1 TO 2, 1 TO 4)
    DIM SHARED EXPVAL(0 TO M, 1 TO K, 1 TO 3, 1 TO 1)
    DIM SHARED ME12(1 TO K, 1 TO 3)
    DIM SHARED MEGM(1 TO K, 1 TO 3)
    DIM SHARED V12(1 TO K)
    DIM SHARED R(0 TO M + 1), RSUM(0 TO M + 1)
    DIM SHARED PARMA(1 TO K, 1 TO 3, 1 TO 6)
    DIM SHARED PARMB(1 TO K, 1 TO 3, 1 TO 3)
    DIM SHARED PARMC(1 TO K, 1 TO 3, 1 TO 10)
    DIM SHARED MSMC(M + 1, 1 TO K, 1 TO 3)
    DIM SHARED MSMCAVG(M + 1, 1 TO K, 1 TO 3)
    DIM SHARED KS(M, 1 TO K, 1 TO 3)
    DIM SHARED RMV(M, 1 TO K, 1 TO 3)
    DIM SHARED RKV(M, 1 TO K, 1 TO 3)
    DIM SHARED FLAG$(1 TO K, 1 TO 3)
    DIM SHARED YTR(1 TO K, 1 TO 3, 1 TO 3)
    DIM SHARED YEJ(1 TO K, 1 TO 3, 1 TO 1)
    DIM SHARED YKJ(1 TO K, 1 TO 3, 1 TO 1)
    DIM SHARED YHJ(1 TO K, 1 TO 3, 1 TO 1)
    DIM SHARED STRESS(M, 1 TO K, 1 TO 3)
    FOR J = 1 TO K
      FOR II = 1 TO 3
        STRESS(0, J, II) = 0
      NEXT II
    NEXT J
    DIM SHARED ABBD(1 TO 6, 1 TO 6)
    DIM SHARED HNBM(1 TO 6, 1 TO 1)
    DIM SHARED GRAND(1 TO 6, 1 TO 1)
    DIM SHARED EKPP(M, 1 TO 6)
    DIM SHARED EK(M + 1, 1 TO 6)
    FOR II = 1 TO 6
      EK(0, II) = 0
    NEXT II
    DIM SHARED PSX(1 TO 6), PSY(1 TO 6)
    DIM SHARED PDX(1 TO 6), PDY(1 TO 6)
    DIM SHARED PNX(1 TO 6), PNY(1 TO 6)
    DIM SHARED PPX(1 TO 6), PPY(1 TO 6)
    DIM SHARED PMX(1 TO 6), PMY(1 TO 6)
    FOR II = 1 TO 6
```

```
        PSX(II) = 0: PSY(II) = 0
        PDX(II) = 0: PDY(II) = 0
        PMX(II) = 0: PMY(II) = 0
        PPX(II) = 0: PPY(II) = 0
        PMX(II) = 0: PMY(II) = 0
      NEXT II
    CMIS = 0
    CTMP = 0
    CALL INPUTSEC(K, DLT, TT, CMIS, CTMP)
    CALL MMTMANU(DLT, TT)     'COMPUTE R() AND RSUM()
CLOSE #1

CALL PLOTCMDF(K)
CALL FILEINIT(K, DLT, CX, CY)
CALL MOISTURE(K, DLT, M, CMIS - 1)
CALL EXPANSION(K, DLT, M)

FOR N = 0 TO M
  FOR J = 1 TO K
    FOR II = 1 TO 3
      YEJ(J, II, 1) = 0
      YKJ(J, II, 1) = 0
      YHJ(J, II, 1) = 0
    NEXT II
  NEXT J
  FOR II = 1 TO 6
    GRAND(II, 1) = 0
  NEXT II
  IF N = 0 THEN
    CALL COEFFIN1(0, 0, K, DLT, M)
    FOR II = 1 TO 6
      FOR III = 1 TO 6
        ABBD(II, III) = 0
      NEXT III
      HMM(II, 1) = 0
    NEXT II
    CALL STFHMMS1(0, 0, K, DLT)
  ELSEIF N > 0 THEN
    FOR I = 1 TO N + 1
      CALL COEFFIN1(I, N, K, DLT, M)
      FOR II = 1 TO 6
        FOR III = 1 TO 6
          ABBD(II, III) = 0
        NEXT III
        HMM(II, 1) = 0
      NEXT II
      CALL STFHMMS1(I, N, K, DLT)
    NEXT I
  END IF
  CALL MAINCOM1(M, N, K, DLT)
NEXT N

LOCATE 24, 40 - LEN("Total computing time: ")
PRINT "Total computing time: ";
PRINT TIMESTRG$(TIMEVALU(TIME$) - OLD)

DO
  LOCATE 24, 40 - LEN("Save output [N]: ")
  INPUT "Save output [N]: ", CHOICE$
  IF CHOICE$ = "Y" THEN
```

```
      SHELL ("C:")
      SHELL ("CD\")
      SHELL ("CD\VPT\DF\OUTPUT")
      SHELL ("MD " + PREFIX$ + INFNUM$)
      SHELL ("CD\VPT\DF\OUTPUT\" + PREFIX$ + INFNUM$)
      SHELL ("DEL " + PREFIX$ + "*.*")
      SHELL ("COPY D:" + PREFIX$ + "*.*")
      SHELL ("DEL D:" + PREFIX$ + "*.*")
      SHELL ("DEL D:" + PREFIX$ + "*.PLT")
      SHELL ("CD\")
      SHELL ("CD\VPT\PF")
      EXIT DO
   ELSEIF CHOICE$ = "N" OR CHOICE$ = "" THEN
      EXIT DO
   END IF
   BEEP
   LOCATE 20, 1
   PRINT STRING$(79, " ")
LOOP

END


KEYQ:
   END
RETURN

DISPLAY:
   IF CTIM = 0 THEN
      LOCATE 25, 2
      PRINT "Time elapsed: ";
   END IF
   ROW = CSRLIN
   COL = POS(0)
   VIEW PRINT 13 TO 25
   LOCATE 25, 16
   PRINT TIMESTR$(TIMEVALU(TIME$) - OLD);
   VIEW PRINT 13 TO 24
   LOCATE ROW, COL
   CTIM = CTIM + 1
RETURN



SUB COEFFIN1 (I, P, K, DLT, M)

IF I = P + 1 THEN EXIT SUB

DIM SIG12(1 TO 3)

IF I = 0 AND P = 0 THEN
   LOCATE 17, 1
   PRINT STRING$(79, " ")
   LOCATE 17, 22
   PRINT "Adjusting visco-elastic coefficients!"
   FOR TM = 0 TO M + 1
      FOR J = 1 TO K
         FOR II = 1 TO 3
            MSMC(TM, J, II) = ME12(J, II) * (ME12(J, II) / MEGN(J, II)) ^ ((12 - MC(TM, J)) / (MP(J) - 12))
```

```
            MSMCAVG(TM, J, II) = ME12(J, II) * (ME12(J, II) / MEGN(J, II)) ^ ((12 - AVGMCW(TM, J)) / (MP(J) - 12))
        NEXT II
    NEXT J
NEXT TM
EXIT SUB
ELSE
  IF TYPE$ = "S" THEN
    EXIT SUB     'COMPLETE ELASTICITY
  ELSE           'VISCOELASTICITY
    IF I = 1 THEN 'ONLY THE 1ST CYCLE WITHIN THE INNER LOOP.
      FOR J = 1 TO K
        MC1 = (MC(P, J) + MC(P - 1, J)) / 2
        MC2 = MC1 * MC1
        FOR II = 1 TO 3
          IF FLAG$(J, II) = "V" THEN 'VISCOELASTIC LAYER
            S1 = ABS(STRESS(P - 1, J, II))
            AAA = PARMA(J, II, 1) + PARMA(J, II, 2) * MC1 + PARMA(J, II, 3) * MC2
            AAB = PARMA(J, II, 4) + PARMA(J, II, 5) * MC1 + PARMA(J, II, 6) * MC2
            AAC = PARMA(J, II, 7) * EXP(PARMA(J, II, 8) * MC1)
            KS(P, J, II) = MSMC(I, J, II) * (AAA * EXP(-AAB * S1) + AAC)
            BBB = PARMB(J, II, 1) * EXP(PARMB(J, II, 2) * MC1) + PARMB(J, II, 3)
            RKV(P, J, II) = BBB / KS(P, J, II)
          END IF
        NEXT II
      NEXT J
    END IF
    IF TYPE$ = "KS" OR I < > P THEN
      EXIT SUB
    ELSE
      IF 1 = 0 THEN
        FOR J = 1 TO K
          MC1 = MC(JJ, J)
          MC2 = MC1 * MC1
          FOR II = 1 TO 3
            IF FLAG$(J, II) = "V" THEN 'VISCOELASTIC LAYER
              CCA = PARMC(J, II, 1) * (1 - EXP(PARMC(J, II, 2) * (MC1 - PARMC(J, II, 3))))
              CCB = PARMC(J, II, 4) * (1 - EXP(PARMC(J, II, 5) * (MC1 - PARMC(J, II, 6)))) - PARMC(J, II, 7)
              CC = CCA * (1 - EXP(CCB * ABS(STRESS(P - 1, J, II))))
              DD = PARMC(J, II, 8) * EXP(PARMC(J, II, 9) * ABS(STRESS(P - 1, J, II))) + PARMC(J, II, 10)
              IF I = 1 THEN
                RMV(I, J, II) = 0   'ZERO MV() AT 1ST INNER CYCLE BEFORE SUMMATION.
              END IF
              RMV(I, J, II) = CC * DD * (P * DLT) ^ (DD - 1) / MSMC(JJ, J, II)
            END IF
          NEXT II
        NEXT J
      ELSEIF 1 = 1 THEN
        FOR J = 1 TO K
          FOR JJ = 1 TO I
            MC1 = AVGMCW(JJ, J)
            'MC1 = (MC(JJ, J) + MC(JJ - 1, J)) / 2
            MC2 = MC1 * MC1
            FOR II = 1 TO 3
              IF FLAG$(J, II) = "V" THEN 'VISCOELASTIC LAYER
                IF JJ = 1 THEN
                  SD = ABS(STRESS(0, J, II))
                  SIGN = 1
                ELSE
                  SD = STRESS(JJ - 1, J, II) - STRESS(JJ - 2, J, II)
                  SIGN = 1
```

```
                    IF STRESS(JJ - 1, J, II) <= 0 AND STRESS(JJ - 2, J, II) <= 0 THEN
                       IF SD < 0 THEN
                          SIGN = 1
                       ELSEIF SD > 0 THEN
                          SIGN = -1
                       END IF
                    ELSEIF STRESS(JJ - 1, J, II) <= 0 AND STRESS(JJ - 2, J, II) >= 0 THEN
                       SIGN = -1
                    ELSEIF STRESS(JJ - 1, J, II) >= 0 AND STRESS(JJ - 2, J, II) <= 0 THEN
                       SIGN = 1
                    ELSEIF STRESS(JJ - 1, J, II) >= 0 AND STRESS(JJ - 2, J, II) >= 0 THEN
                       IF SD < 0 THEN    'STRESS REDUCTION
                          SIGN = -1
                       END IF
                    END IF
                 END IF
                 CCA = PARMC(J, IL, 1) * (1 - EXP(PARMC(J, IL, 2) * (MC1 - PARMC(J, IL, 3))))
                 CCB = PARMC(J, IL, 4) * (1 - EXP(PARMC(J, IL, 5) * (MC1 - PARMC(J, IL, 6)))) - PARMC(J, IL, 7)
                 CC = CCA * (1 - EXP(CCB * ABS(SD)))
                 DD = PARMC(J, IL, 8) * EXP(PARMC(J, IL, 9) * ABS(STRESS(P - 1, J, II))) + PARMC(J, IL, 10)
                 'DD = PARMC(J, IL, 8) * EXP(PARMC(J, IL, 9) * ABS(SD)) + PARMC(J, IL, 10)
                 IF I = 1 THEN
                    RMV(I, J, II) = 0    'ZERO MV() AT 1ST INNER CYCLE BEFORE SUMMATION.
                    SUMD = RSUM(1)
                 ELSE
                    SUMD = RSUM(I) - RSUM(JJ - 1)
                 END IF
                 IF ABS(SD) < .01 THEN
                    RMVT = 0
                 ELSE
                    RMVT = CC * DD * (SUMD * DLT) ^ (DD - 1) / MSMCAVG(JJ, J, II)
                 END IF
                 IF RMV(I, J, II) = 0 AND SIGN * RMVT < 0 THEN
                    RMV(I, J, II) = RMVT
                 END IF
                 IF (RMV(I, J, II) + (SIGN * RMVT)) <= 0 THEN
                 ELSE
                    RMV(I, J, II) = RMV(I, J, II) + (SIGN * RMVT)
                 END IF
                 'PRINT I, J, IL, RMV(I, J, II)
                 'IF RMV(I, J, II) < 0 THEN STOP
              END IF
           NEXT II
        NEXT JJ
     NEXT J
  END IF
 END IF
END IF

EXIT SUB


END SUB


SUB ERRLOCTN (LOC$)

CLS
COLOR 7, 1
```

```
  LOCATE 15, 15
  PRINT "ERROR #"; LOC$; "!"
  LOCATE 16, 15
  PRINT "PROGRAM TERMINATED!"
  STOP

  END SUB

  SUB EXPANSN (K, DLT, M)

  DIM EXPC(1 TO 3, 1 TO 1), EXPP(1 TO 3, 1 TO 1)

  LOCATE 17, 1
  PRINT STRING$(79, " ")
  LOCATE 17, 23
  PRINT "Computing expansion coefficients!"

  FOR N = 0 TO M
    FOR J = 1 TO K
      MC1 = MC(N, J)
      MC2 = MC1 * MC1
      MC3 = MC2 * MC1
      EXPC(1, 1) = EXPCOF(J, 1, 1) * MC3 + EXPCOF(J, 1, 2) * MC2 + EXPCOF(J, 1, 3) * MC1 + EXPCOF(J, 1, 4)
      EXPC(2, 1) = EXPCOF(J, 2, 1) * MC3 + EXPCOF(J, 2, 2) * MC2 + EXPCOF(J, 2, 3) * MC1 + EXPCOF(J, 2, 4)
      EXPC(3, 1) = 0
      CALL QTRAFORM(EXPC(), ANGLE(J), EXPP())
      FOR MM = 1 TO 3
        EXPVAL(N, J, MM, 1) = EXPP(MM, 1)
      NEXT MM
    NEXT J
  NEXT N

  END SUB

  SUB FILEINT (K, DLT, CX, CY)

  LOCATE 17, 1
  PRINT STRING$(79, " ")
  LOCATE 17, 28
  PRINT "Initializing files!"

  OPEN DIROUT$ + STRAMP$ FOR OUTPUT AS #1
  CLOSE #1
  OPEN DIROUT$ + STRAMP$ FOR APPEND AS #1
    PRINT #1, TAB(1); STRAMP$
    PRINT #1, "UNIT = (0.001/hr)"
    PRINT #1, TAB(1); "HOUR";
    PRINT #1, TAB(9); CHR$(238) + "x'";
    PRINT #1, TAB(21); CHR$(238) + "y'";
    PRINT #1, TAB(33); CHR$(238) + "xy'";
    PRINT #1, TAB(45); "Kx'";
    PRINT #1, TAB(57); "Ky'";
    PRINT #1, TAB(69); "Kxy'"
  CLOSE #1

  FOR N = 1 TO 6
    SELECT CASE N
      CASE 1
        SYM$ = CHR$(238) + "x'"
      CASE 2
```

```
        SYM$ = CHR$(238) + "y'"
      CASE 3
        SYM$ = CHR$(238) + "xy'"
      CASE 4
        SYM$ = "Kx'"
      CASE 5
        SYM$ = "Ky'"
      CASE 6
        SYM$ = "Kxy'"
    END SELECT

    OPEN DIROUT$ + LSTRAINP$(II) FOR OUTPUT AS #1
    CLOSE #1
    OPEN DIROUT$ + LSTRAINP$(II) FOR APPEND AS #1
      PRINT #1, TAB(1); LSTRAINP$(II)
      PRINT #1, "UNIT = (0.001/hr)"
      PRINT #1, TAB(1); "HOUR";
      PRINT #1, TAB(9); SYM$
    CLOSE #1
  NEXT II

  OPEN DIROUT$ + STRAIN$ FOR OUTPUT AS #1
  CLOSE #1
  OPEN DIROUT$ + STRAIN$ FOR APPEND AS #1
    PRINT #1, STRAIN$
    PRINT #1, "UNIT = (0.001)"
    PRINT #1, TAB(1); "HOUR";
    PRINT #1, TAB(9); CHR$(238) + "x";
    PRINT #1, TAB(21); CHR$(238) + "y";
    PRINT #1, TAB(33); CHR$(238) + "xy";
    PRINT #1, TAB(45); "Kx";
    PRINT #1, TAB(57); "Ky";
    PRINT #1, TAB(69); "Kxy"

    PRINT #1, TAB(1); USING "####.##"; 0;
    FOR II = 1 TO 5
      PRINT #1, TAB(9 + (II - 1) * 12); USING "#.####^^^^"; 0;
    NEXT II
    PRINT #1, TAB(69); USING "#.####^^^^"; 0
  CLOSE #1

  FOR II = 1 TO 6
    SELECT CASE II
      CASE 1
        SYM$ = CHR$(238) + "x"
      CASE 2
        SYM$ = CHR$(238) + "y"
      CASE 3
        SYM$ = CHR$(238) + "xy"
      CASE 4
        SYM$ = "Kx"
      CASE 5
        SYM$ = "Ky"
      CASE 6
        SYM$ = "Kxy"
    END SELECT

    OPEN DIROUT$ + LSTRAIN$(II) FOR OUTPUT AS #1
    CLOSE #1
    OPEN DIROUT$ + LSTRAIN$(II) FOR APPEND AS #1
```

```
      PRINT #1, TAB(1); LSTRAIN$(II)
      PRINT #1, "UNIT = (0.001)"
      PRINT #1, TAB(1); "HOUR";
      PRINT #1, TAB(9); SYM$

      PRINT #1, TAB(1); USING "####.##"; 0;
      PRINT #1, TAB(9); USING "#.####^^^^"; 0
   CLOSE #1
NEXT II


OPEN DIROUT$ + STRESS$ FOR OUTPUT AS #1
CLOSE #1
OPEN DIROUT$ + STRESS$ FOR APPEND AS #1
   PRINT #1, STRESS$
   PRINT #1, "UNIT = (1000*psi)"
   PRINT #1, TAB(1); "HOUR";
   PRINT #1, TAB(9); "LAYER";
   PRINT #1, TAB(16); CHR$(229) + "xx";
   PRINT #1, TAB(28); CHR$(229) + "yy";
   PRINT #1, TAB(40); CHR$(231) + "xy"

   PRINT #1, TAB(1); USING "####.##"; 0;
   FOR II = 1 TO K
      PRINT #1, TAB(9); USING "###"; II;
      FOR III = 1 TO 2
         PRINT #1, TAB(16 + (III - 1) * 12); USING "#.####^^^^"; 0;
      NEXT III
      PRINT #1, TAB(40); USING "#.####^^^^"; 0
   NEXT II
CLOSE #1

FOR J = 1 TO K
   OPEN DIROUT$ + LSTRES$ + LTRIM$(STR$(J)) + ".PRN" FOR OUTPUT AS #1
   CLOSE #1
   OPEN DIROUT$ + LSTRES$ + LTRIM$(STR$(J)) + ".PRN" FOR APPEND AS #1
      PRINT #1, LSTRES$ + LTRIM$(STR$(J)) + ".PRN"
      PRINT #1, "UNIT = (1000*psi)"
      PRINT #1, "LAYER" + LTRIM$(STR$(J)); TAB(9); "TOP SURFACE"; TAB(44); "BOTTOM SURFACE"
      PRINT #1, "HOUR"; TAB(9); CHR$(229) + "xx"; TAB(20); CHR$(229) + "yy"; TAB(31); CHR$(231) + "xy";
      PRINT #1, TAB(44); CHR$(229) + "xx"; TAB(55); CHR$(229) + "yy"; TAB(67); CHR$(231) + "xy"
      PRINT #1, USING "####.##"; P * DLT;
      FOR II = 1 TO 3
         PRINT #1, TAB(9 + (II - 1) * 11); USING "#.####^^^^"; 0;
      NEXT II
      FOR II = 1 TO 3
         PRINT #1, TAB(11 + (II + 3 - 1) * 11); USING "#.####^^^^"; 0;
      NEXT II
      PRINT #1,
   CLOSE #1
NEXT J


FOR II = 1 TO 6
   SELECT CASE II
      CASE 1
         SYMB$ = "T1"
         DIR$ = "xx"
      CASE 2
         SYMB$ = "T2"
```

```
        DIR$ = "yy"
      CASE 3
        SYMB$ = "T3"
        DIR$ = "xy"
      CASE 4
        SYMB$ = "B1"
        DIR$ = "xx"
      CASE 5
        SYMB$ = "B2"
        DIR$ = "yy"
      CASE 6
        SYMB$ = "B3"
        DIR$ = "xy"
    END SELECT

    OPEN DIROUT$ + LSTRES$ + SYMB$ + ".PRN" FOR OUTPUT AS #1
    CLOSE #1
    OPEN DIROUT$ + LSTRES$ + SYMB$ + ".PRN" FOR APPEND AS #1
      PRINT #1, LSTRES$ + SYMB$ + ".PRN"
      PRINT #1, "UNIT = (1000*psi)"
      PRINT #1, "HOUR"; TAB(9); CHR$(229) + DIR$
      PRINT #1, USING "####.##"; P * DLT;
      PRINT #1, TAB(9); USING "#.####^^^^"; 0
    CLOSE #1
NEXT II

FOR II = 1 TO 2
    OPEN DIROUT$ + DISMNT$ + LTRIM$(STR$(II)) + ".PRN" FOR OUTPUT AS #1
    CLOSE #1
    OPEN DIROUT$ + DISMNT$ + LTRIM$(STR$(II)) + ".PRN" FOR APPEND AS #1
      PRINT #1, DISMNT$ + LTRIM$(STR$(II)) + ".PRN"
      PRINT #1, TAB(1); "HOUR";
      PRINT #1, TAB(9); "DISPLACEMENT (INCH)"
      IF II = 1 THEN
        X = CX: Y = CY
      ELSE
        X = -CX
      END IF
      PRINT #1, TAB(9); "(";
      PRINT #1, USING "###"; X;
      PRINT #1, ", ";
      PRINT #1, USING "###"; Y;
      PRINT #1, ")"

      PRINT #1, TAB(1); 0;
      PRINT #1, TAB(9); USING "#.####^^^^"; 0
    CLOSE #1
NEXT II

END SUB

SUB FUNCCOEF (X(), Y(), CEF())

X12 = X(1) / X(2)
X23 = X(2) / X(3)
M = (X(1) - X(2)) / (X(2) - X(3))
Y12 = Y(1, 1) / Y(2, 1)
Y23 = Y(2, 1) / Y(3, 1)

CEF(2, 1) = LOG(Y12 / (Y23 ^ M)) / LOG(X12 / (X23 ^ M))
```

```
CEF(3, 1) = LOG(Y12 / (X12 ^ CEF(2, 1))) / (X(1) - X(2))
CEF(1, 1) = Y(1, 1) / (X(1) ^ CEF(2, 1) * EXP(CEF(3, 1) * X(1)))

END SUB

SUB INITSCRN

SHARED OLD

SCREEN 1
SCREEN 9
CLS

COLOR 7, 1
LOCATE 5, 4
PRINT "Program running! ";
LOCATE 7, 4
PRINT "F1 = End      F2 = Time"
LOCATE 9, 4
PRINT "Pause = Pause  Enter = Continue"

IF TIMER$ = "Y" THEN
   LOCATE 25, 2
   PRINT "Time elapsed: ";
END IF

VIEW PRINT 13 TO 24
VIEW (280, 1)-(630, 145), 1, 2
WINDOW (-40, -110)-(520, 110)
LINE (0, 0)-(500, 0), 7
LINE (0, -100)-(0, 100), 7

FOR N = 1 TO 10
   LINE (N * 50, 0)-(N * 50, 3), 7
NEXT N

FOR N = 1 TO 4
   LINE (0, 25 * N)-(5, 25 * N), 7
   LINE (0, -25 * N)-(5, -25 * N), 7
NEXT N

END SUB

FUNCTION INMTAUTO (I)

'EQUATION TO AUTOMEATICALLY DETERMINE THE TIME INCREMENT YET TO BE DIFINED.
'TO ACTIVATE OR ENGAGE AUTOMATIC DETERMINATION, THE MANUAL DETERMINATION
'SUBROUTINE CALL IN INPTSCRN SUBROUTINE MUST BE TURNED OFF.

END FUNCTION

SUB INMTMANU (DLT, TT)

DIM TK(1 TO 15), TD(1 TO 15)

N = 0: SUM = 0
RPL$ = SEQ$
DO: N = N + 1
   TK(N) = VAL(LEFTWORD$(RPL$))
   TD(N) = VAL(LEFTWORD$(RPL$))
```

```
    SUM = SUM + TD(II)
  LOOP UNTIL TD(II) = 0
  TD(II) = (TT - SUM)
  R(0) = 0
  BEG = 0
  FOR I = 1 TO II
    NUM = (TD(I) / TK(I)) / DLT
    FOR III = 1 TO NUM
      R(III + BEG) = TK(I)
    NEXT III
    BEG = BEG + NUM
  NEXT I
  R(BEG + 1) = 1

  RSUM(0) = 0
  RSUM(M + 1) = 0
  FOR I = 1 TO BEG
    RSUM(I) = RSUM(I - 1) + R(I)
  NEXT I

  END SUB

  FUNCTION INMTNUMR (DLT, TT)

  SUM = 0
  BEG = 0
  RPL$ = SEQ$
  DO
    TI = VAL(LEFTWORD$(RPL$))
    TD = VAL(LEFTWORD$(RPL$))
    SUM = SUM + TD
    IF TD = 0 THEN EXIT DO
    BEG = BEG + TD / TI / DLT
  LOOP
  TD = TT - SUM
  BEG = BEG + TD / (TI * DLT)

  INMTNUMR = BEG

  END FUNCTION

  SUB INPTSCRN (DLT, TT)

  500  COLOR 7, 1
    CLS

  ROW = 4

  DO
    LOCATE ROW, 40 - LEN("Input data file (IN * .PRN): ")
    INPUT "Input data file (IN * .PRN): ", INFNUM$
    IF INFNUM$ < > "" THEN
      INFILE$ = "IN" + INFNUM$ + ".PRN"
      EXIT DO
    END IF
    BEEP
    LOCATE ROW, 1
    PRINT STRING$(79, " ")
  LOOP
```

```
LOCATE ROW + 1, 40 - LEN("Input directory (C:\VPT\DF\INPUT\): ")
INPUT "Input directory (C:\VPT\DF\INPUT\): ", DIRINP$
IF DIRINP$ = "" THEN
   DIRINP$ = "C:\VPT\DF\INPUT\"
   LOCATE ROW + 1, 40
   PRINT DIRINP$
END IF

LOCATE ROW + 2, 40 - LEN("Output directory (D:): ")
INPUT "Output directory (D:): ", DIROUT$
IF DIROUT$ = "" THEN
   DIROUT$ = "D:"
   LOCATE ROW + 2, 40
   PRINT DIROUT$
END IF

LOCATE ROW + 3, 40 - LEN("Prefix for output filenames: ")
INPUT "Prefix for output filenames: ", PREFIX$

STRAIN$ = PREFIX$ + "N" + INFNUM$ + ".PRN"
STRAMP$ = PREFIX$ + "P" + INFNUM$ + ".PRN"
FOR II = 1 TO 6
   LSTRAIN$(II) = PREFIX$ + "N" + INFNUM$ + LTRIM$(STR$(II)) + ".PRN"
   LSTRAMP$(II) = PREFIX$ + "P" + INFNUM$ + LTRIM$(STR$(II)) + ".PRN"
NEXT II
STRESS$ = PREFIX$ + "S" + INFNUM$ + ".PRN"
MOISTU$ = PREFIX$ + "M" + INFNUM$ + ".PRN"
LSTRES$ = PREFIX$ + "S" + INFNUM$
LMOIST$ = PREFIX$ + "M" + INFNUM$
DISMNT$ = PREFIX$ + "D" + INFNUM$
PLTCMD$ = PREFIX$ + INFNUM$ + ".PLT"

LOCATE ROW + 5, 40 - LEN("DELTA (1 hour): ")
INPUT "Delta (1 hour): ", DLT
IF DLT = 0 THEN
   DLT = 1
   LOCATE ROW + 5, 40
   PRINT DLT
END IF

DO
   LOCATE ROW + 6, 40 - LEN("Endding time (800 hours): ")
   INPUT "Endding time (800 hours): ", TT
   IF TT = 0 THEN
      TT = 800
      LOCATE ROW + 6, 40
      PRINT TT
      EXIT DO
   ELSEIF TT > DLT THEN
      EXIT DO
   END IF
   BEEP
   LOCATE ROW + 6, 1
   PRINT STRING$(79, " ")
LOOP

LOCATE ROW + 7, 40 - LEN("Time increment sequence: ")
INPUT "Time increment sequence: ", SEQ$
IF SEQ$ = "" THEN
   SEQ$ = "1 10 2 20 4 20 5 100 10 150 25 100 50"
```

```
    LOCATE ROW + 7, 40
    PRINT SEQ$
  END IF

  DO
    LOCATE ROW + 8, 40 - LEN("Panel size [20*1 in*in]: ")
    INPUT "Panel size [20*1 in*in]: ", TEMP$
    IF TEMP$ = "" THEN
      TEMP$ = "20*1"
      LOCATE ROW + 8, 40
      PRINT TEMP$
    END IF
    N = INSTR(TEMP$, "*")
    IF N < > 0 THEN
      CX = VAL(LEFT$(TEMP$, N - 1)) / 2
      CY = VAL(RIGHT$(TEMP$, LEN(TEMP$) - N)) / 2
      EXIT DO
    END IF
  LOOP

  DO
    LOCATE ROW + 9, 40 - LEN("Maximum moisture content [25%]: ")
    INPUT "Maximum moisture content [25%]: ", MCL
    IF MCL = 0 THEN
      MCL = 25
      LOCATE ROW + 9, 40
      PRINT MCL
      EXIT DO
    ELSEIF MCL < = 30 THEN
      EXIT DO
    END IF
    BEEP
    LOCATE ROW + 9, 1
    PRINT STRING$(79, " ")
  LOOP

  DO
    LOCATE ROW + 10, 40 - LEN("Maximum strain rate [0.0001/hr]: ")
    INPUT "Maximum strain rate [0.0001/hr]: ", SPL
    IF SPL = 0 THEN
      SPL = .0001
      LOCATE ROW + 10, 40
      PRINT SPL
      EXIT DO
    ELSEIF SPL < = .0015 THEN
      EXIT DO
    END IF
    BEEP
    LOCATE ROW + 10, 1
    PRINT STRING$(79, " ")
  LOOP

  DO
    LOCATE ROW + 11, 40 - LEN("Maximum strain [0.007]: ")
    INPUT "Maximum strain [0.007]: ", SNL
    IF SNL = 0 THEN
      SNL = .007
      LOCATE ROW + 11, 40
      PRINT SNL
      EXIT DO
```

```
    ELSEIF SNL < .01 THEN
        EXIT DO
    END IF
    BEEP
    LOCATE ROW + 11, 1
    PRINT STRING$(79, " ")
LOOP

DO
    LOCATE ROW + 12, 40 - LEN("Maximum warp (in) [2]: ")
    INPUT "Maximum warp (in) [2]: ", SDL
    IF SDL = 0 THEN
        SDL = 2
        LOCATE ROW + 12, 40
        PRINT SDL
        EXIT DO
    ELSEIF SDL < 5 THEN
        EXIT DO
    END IF
    BEEP
    LOCATE ROW + 12, 1
    PRINT STRING$(79, " ")
LOOP

DO
    LOCATE ROW + 13, 40 - LEN("Maximum stress (psi): ")
    INPUT "Maximum stress (psi): ", SSL
    IF SSL > 0 AND SSL < 10000 THEN EXIT DO
    BEEP
    LOCATE ROW + 13, 1
    PRINT STRING$(79, " ")
LOOP

DO
    LOCATE ROW + 14, 40 - LEN("Element type (S, M, KS, or KM): ")
    INPUT "Element type (S, M, KS, or KM): ", TYPE$
    IF TYPE$ = "M" OR TYPE$ = "KS" OR TYPE$ = "KM" OR TYPE$ = "S" THEN
        EXIT DO
    END IF
    BEEP
    LOCATE ROW + 14, 1
    PRINT STRING$(79, " ")
LOOP


DO
    LOCATE ROW + 15, 40 - LEN("Timer [N]: ")
    INPUT "Timer [N]: ", TIMER$
    IF TIMER$ = "" THEN
        TIMER$ = "N"
        LOCATE ROW + 15, 40
        PRINT TIMER$
    END IF
    IF TIMER$ = "Y" OR TIMER$ = "N" THEN
        EXIT DO
    END IF
    BEEP
    LOCATE ROW + 15, 1
    PRINT STRING$(79, " ")
LOOP
```

```
DO
   LOCATE ROW + 16, 40 - LEN("Edit comment [N]: ")
   INPUT "Edit comment [N]: ", CMT$
   IF CMT$ = "" THEN
      CMT$ = "N"
      LOCATE ROW + 16, 40
      PRINT CMT$
   END IF
   IF CMT$ = "Y" OR CMT$ = "N" THEN
      EXIT DO
   END IF
   BEEP
   LOCATE ROW + 16, 1
   PRINT STRING$(79, " ")
LOOP

DO
   LOCATE ROW + 17, 40 - LEN("Print on [Y]: ")
   INPUT "Print on [Y]: ", SCRN$
   IF SCRN$ = "" THEN
      SCRN$ = "Y"
      LOCATE ROW + 17, 40
      PRINT SCRN$
   END IF
   IF SCRN$ = "Y" OR SCRN$ = "N" THEN
      EXIT DO
   END IF
   BEEP
   LOCATE ROW + 17, 1
   PRINT STRING$(79, " ")
LOOP

DO
   LOCATE ROW + 18, 40 - LEN("Display on [Y]: ")
   INPUT "Display on [Y]: ", DSPL$
   IF DSPL$ = "" THEN
      DSPL$ = "Y"
      LOCATE ROW + 18, 40
      PRINT DSPL$
   END IF
   IF DSPL$ = "Y" OR DSPL$ = "N" THEN
      EXIT DO
   END IF
   BEEP
   LOCATE ROW + 18, 1
   PRINT STRING$(79, " ")
LOOP

DO
   LOCATE ROW + 19, 40 - LEN("Correct [Y]: ")
   INPUT "Correct [Y]: ", YorN$
   IF YorN$ = "Y" OR YorN$ = "y" OR YorN$ = "" THEN
      IF CMT$ = "Y" THEN
         SHELL (DIROUT$)
         SHELL ("PE2 " + PREFIX$ + INFNUM$ + ".CMT")
      END IF
      EXIT DO
   ELSEIF YorN$ = "N" OR YorN$ = "n" THEN
      GOTO 500
```

```
    ELSE
      BEEP
      LOCATE ROW + 19, 39
      PRINT " ";
    END IF
LOOP

END SUB

SUB INPUTSEC (K, DLT, TT, CMIS, CTMP)

DIM THK(1 TO K)

LOCATE 17, 1
PRINT STRING$(79, " ")
LOCATE 17, 23
PRINT "Reading and preprocessing inputs!"

LINE INPUT #1, INT$
LINE INPUT #1, INT$
FOR II = 1 TO K
   ANGLE(II) = VAL(LEFTWORD$(INT$))
NEXT II

LINE INPUT #1, INT$
LINE INPUT #1, INT$
FOR II = 1 TO K
   THK(II) = VAL(LEFTWORD$(INT$))
NEXT II
TTHK = 0
FOR II = 1 TO K
   TTHK = TTHK + THK(II)
NEXT II
H(0) = -TTHK / 2
FOR II = 1 TO K
   H(II) = H(II - 1) + THK(II)
NEXT II

LINE INPUT #1, INT$
LINE INPUT #1, INT$
FOR II = 1 TO K
   MP(II) = VAL(LEFTWORD$(INT$))
NEXT II

LINE INPUT #1, INT$
LINE INPUT #1, INT$
FOR J = 1 TO K
   LINE INPUT #1, INT$
   LW1$ = LEFTWORD$(INT$)
   IF VAL(LW1$) = J THEN
      LW2$ = LEFTWORD$(INT$)
      IF LW2$ = "SAME" THEN
         FOR II = 1 TO 7
            IF II <= 3 THEN
               ME12(J, II) = ME12(J - 1, II)
            ELSEIF II >= 4 AND II <= 6 THEN
               MEGN(J, II - 3) = MEGN(J - 1, II - 3)
            ELSEIF II = 7 THEN
               V12(J) = V12(J - 1)
            END IF
```

```
        NEXT II
      ELSE
        INT$ = LW2$ + " " + INT$
        FOR II = 1 TO 7
          IF II <= 3 THEN
            ME12(J, II) = VAL(LEFTWORD$(INT$))
          ELSEIF II <= 6 AND II >= 4 THEN
            MEGN(J, II - 3) = VAL(LEFTWORD$(INT$))
          ELSEIF II = 7 THEN
            V12(J) = VAL(LEFTWORD$(INT$))
          END IF
        NEXT II
      END IF
    ELSE
      FOR JJ = J TO K
        FOR II = 1 TO 7
          IF II <= 3 THEN
            ME12(JJ, II) = ME12(J - 1, II)
          ELSEIF II >= 4 AND II <= 6 THEN
            MEGN(JJ, II - 3) = MEGN(J - 1, II - 3)
          ELSEIF II = 7 THEN
            V12(JJ) = V12(J - 1)
          END IF
        NEXT II
      NEXT JJ
      EXIT FOR
    END IF
  NEXT J

  LINE INPUT #1, INT$
  LINE INPUT #1, INT$
  FOR J = 1 TO K
    LINE INPUT #1, INT$
    LW1$ = LEFTWORD$(INT$)
    IF VAL(LW1$) = J THEN
      LW2$ = LEFTWORD$(INT$)
      IF LW2$ = "SAME" THEN
        FOR II = 1 TO 2
          FOR III = 1 TO 4
            EXPCOF(J, II, III) = EXPCOF(J - 1, II, III)
          NEXT III
        NEXT II
      ELSE
        INT$ = LW2$ + " " + INT$
        FOR II = 1 TO 2
          FOR III = 1 TO 4
            EXPCOF(J, II, III) = VAL(LEFTWORD$(INT$)) / 100
          NEXT III
        NEXT II
      END IF
    ELSE
      FOR JJ = J TO K
        FOR II = 1 TO 2
          FOR III = 1 TO 4
            EXPCOF(JJ, II, III) = EXPCOF(J - 1, II, III)
          NEXT III
        NEXT II
      NEXT JJ
      EXIT FOR
    END IF
```

```
NEXT J

LINE INPUT #1, INT$
CALL MODELCOF(K, FLAG$(), PARMC())
LINE INPUT #1, INT$
CALL MODELCOF(K, FLAG$(), PARMA())
LINE INPUT #1, INT$
CALL MODELCOF(K, FLAG$(), PARMB())

LINE INPUT #1, INT$
LINE INPUT #1, INT$
LINE INPUT #1, INT$
FOR III = 1 TO 6
   EK(0, III) = VAL(LEFTWORD$(INT$))
NEXT III

LINE INPUT #1, INT$
LINE INPUT #1, INT$
LINE INPUT #1, INT$
CMIS = 0
DO
   LINE INPUT #1, INT$
   COPY$ = INT$
   IF LEFTWORD$(COPY$) = "END" THEN EXIT DO
   CMIS = CMIS + 1
   MC$(CMIS) = INT$
LOOP


DO
   LOCATE 17, 1
   PRINT STRING$(79, " ")
   LOCATE 17, 40 - LEN("Print inputs [N]: ")
   INPUT "Print inputs [N]: ", IN$
   IF IN$ = "" THEN
      IN$ = "N"
      LOCATE 17, 40
      PRINT IN$
   END IF
   IF IN$ = "Y" OR IN$ = "N" THEN
      IF IN$ = "N" THEN
         NUM = 1
      ELSE
         NUM = 2
      END IF
      LOCATE 17, 1
      PRINT STRING$(79, " ")
      EXIT DO
   END IF
LOOP
FOR I = 1 TO NUM
   IF NUM = 2 THEN
      OPEN "LPT1:" FOR OUTPUT AS #2
   ELSEIF NUM = 1 THEN
      OPEN DIROUT$ + PREFIX$ + INFNUM$ + ".INP" FOR OUTPUT AS #2
   END IF
      LOCATE 17, 1
      PRINT #2, TAB(5); "INPUT FILE"; TAB(18); INFILE$
      PRINT #2, TAB(5); "INPUT DIR"; TAB(18); DIRINP$
      PRINT #2, TAB(5); "OUTPUT DIR"; TAB(18); DIROUT$
```

```
PRINT #2, TAB(5); "FILE PREFIX"; TAB(18); PREFIX$
PRINT #2, TAB(5); "TYPE"; TAB(18); TYPE$
PRINT #2, STRING$(79, " ")
PRINT #2, TAB(5); "K"; TAB(18); K
PRINT #2, TAB(5); "DLT"; TAB(18); DLT; TAB(30); "(hour)"
PRINT #2, TAB(5); "ENDING"; TAB(18); TT; TAB(30); "(hour)"
PRINT #2, TAB(5); "INCREMENT SEQUENCE"
PRINT #2, TAB(18); SEQ$
PRINT #2, TAB(5); "PANEL SIZE"; TAB(18); CX * 2; "by"; CY * 2; TAB(30); "(in*in)"
PRINT #2, TAB(5); "ANGLE (degree)"
FOR N = 1 TO K
   PRINT #2, TAB(18 + 8 * (N - 1)); USING "###.##"; ANGLE(N);
NEXT N
PRINT #2,

PRINT #2, TAB(5); "THK (in)";
FOR N = 1 TO K
   PRINT #2, TAB(18 + 8 * (N - 1)); USING "#.####"; THK(N);
NEXT N
PRINT #2,

PRINT #2, TAB(5); "H (in)";
FOR N = 0 TO K
   PRINT #2, TAB(18 + 8 * (N)); USING "#.####"; H(N);
NEXT N
PRINT #2,

PRINT #2, TAB(5); "MCp (%)";
FOR N = 1 TO K
   PRINT #2, TAB(18 + 8 * (N - 1)); USING "##.##"; MP(N);
NEXT N
PRINT #2,
PRINT #2,

PRINT #2, TAB(5); "MOE (million psi)"
PRINT #2, TAB(10); "LAYER"; TAB(18); "E11"; TAB(30); "E22"; TAB(42); "E12"; TAB(54); "V12"
PRINT #2, TAB(5); "12%";
FOR J = 1 TO K
   PRINT #2, TAB(10); J;
   FOR N = 1 TO 3
      PRINT #2, TAB(18 + 12 * (N - 1)); USING "#.####^^^^"; ME12(J, N);
   NEXT N
   PRINT #2, TAB(54); USING "#.#####"; V12(J)
NEXT J

PRINT #2, TAB(5); "GRN";
FOR J = 1 TO K
   PRINT #2, TAB(10); J;
   FOR N = 1 TO 3
      PRINT #2, TAB(18 + 12 * (N - 1)); USING "#.####^^^^"; MEGN(J, N);
   NEXT N
   PRINT #2, TAB(54); USING "#.#####"; V12(J)
NEXT J
PRINT #2,

PRINT #2, TAB(5); "EXPANSION COEFFICIENT PARAMETERS"
PRINT #2, TAB(18); "AA1"; TAB(30); "AA2"; TAB(42); "AA3"; TAB(54); "AA4"
PRINT #2, TAB(5); "EXP";
FOR J = 1 TO K
   PRINT #2, TAB(10); J;
```

```
        FOR II = 1 TO 2
          IF II = 1 THEN : PRINT #2, TAB(14); "|/";
          IF II = 2 THEN : PRINT #2, TAB(14); "/_ ";
          FOR III = 1 TO 4
            PRINT #2, TAB(18 + 12 * (III - 1)); USING "#.######"; EXPCOF(J, II, III);
          NEXT III
          PRINT #2,
        NEXT II
      NEXT J
      PRINT #2,

      CALL PRNTPARM(K, "C", PARMC())
      CALL PRNTPARM(K, "A", PARMA())
      CALL PRNTPARM(K, "B", PARMB())

      PRINT #2, TAB(5); "INITAL TOTAL STRAINS"
      PRINT #2, TAB(10); "Ex"; TAB(18); "Ey"; TAB(26); "Exy"; TAB(34); "Kx"; TAB(42); "Ky"; TAB(50); "Kxy"
      FOR II = 1 TO 6
        PRINT #2, TAB(10 + (II - 1) * 8); EK(0, II);
      NEXT II
      PRINT #2,

      PRINT #2, TAB(5); "MC"; TAB(20); "HOUR"; TAB(30); "LAYER";
      FOR II = 1 TO K
        PRINT #2, TAB(37 + (II - 1) * 7); II;
      NEXT II
      PRINT #2,
      FOR II = 1 TO CMIS
        PRINT #2, TAB(18); MC$(II)
      NEXT II
      PRINT #2, TAB(5); "TIMP";
      FOR II = 1 TO CTIMP
        PRINT #2, TAB(18); TM$(II)
      NEXT II
    CLOSE
NEXT I

END SUB



FUNCTION LEFTCHAR$ (INT$, N)

DO WHILE LEFT$(INT$, 1) = " "
  INT$ = RIGHT$(INT$, LEN(INT$) - 1)
LOOP

TEMP$ = LEFT$(INT$, N)
LT$ = TEMP$

END FUNCTION

FUNCTION LEFTWORD$ (INT$)

'DO WHILE LEFT$(INT$, 1) = " "
'  INT$ = RIGHT$(INT$, LEN(INT$) - 1)
'LOOP
INT$ = LTRIM$(INT$)

IF INSTR(INT$, " ") > 1 THEN
```

```
    TEMP$ = LEFT$(INT$, INSTR(INT$, " ") - 1)
    INT$ = RIGHT$(INT$, LEN(INT$) - LEN(TEMP$))
    LEFTWORD$ = TEMP$
    DO WHILE LEFT$(INT$, 1) = " "
       INT$ = RIGHT$(INT$, LEN(INT$) - 1)
    LOOP
 ELSEIF INT$ < > "" THEN
    LEFTWORD$ = INT$
    INT$ = ""
 ELSE
    LEFTWORD$ = INT$
 END IF

 END FUNCTION

 SUB MAINCOM1 (M, P, K, DLT)

 DIM ABBDINV(1 TO 6, 1 TO 6), EKPINT(1 TO 6, 1 TO 1)
 DIM YINT(1 TO 3, 1 TO 3), EP(1 TO 3, 1 TO 1), KP(1 TO 3, 1 TO 1)
 DIM EXPP(1 TO 3, 1 TO 1)
 DIM YE(1 TO 3, 1 TO 1), YK(1 TO 3, 1 TO 1), YH(1 TO 3, 1 TO 1)
 DIM TEMP(1 TO 3), SIG12(1 TO 3), WARP(1 TO 2)

 IF P = 0 THEN
    LOCATE 17, 1
    PRINT STRING$(79, " ")
 END IF

 CALL MATRINVS(ABBD(), ABBDINV())
 CALL MATRMULT(ABBDINV(), GRAND(), EKPINT())

 FOR II = 1 TO 6
    EKPP(P, II) = EKPINT(II, 1)
 NEXT II

 OPEN DIROUT$ + STRAINP$ FOR APPEND AS #1     'COMBINED
    PRINT #1, TAB(1); USING "####.##"; RSUM(P) * DLT;
    FOR II = 1 TO 6
       PRINT #1, TAB(9 + (II - 1) * 12); USING "#.####^^^^"; EKPINT(II, 1) * 1000;
    NEXT II
    PRINT #1,
 CLOSE #1
 FOR II = 1 TO 6                    'EACH LAYER
    OPEN DIROUT$ + LSTRAINP$(II) FOR APPEND AS #1
       PRINT #1, TAB(1); USING "####.##"; RSUM(P) * DLT;
       PRINT #1, TAB(9); USING "#.####^^^^"; EKPINT(II, 1) * 1000
    CLOSE #1
 NEXT II

 IF P = M THEN
    INCT = DLT              'STRAIN RATES
    INCTSUM = (RSUM(P) + 1)     'STRAIN
    DLTT = (RSUM(P) + 1) * DLT   'WARPAGE
 ELSE
    INCT = R(P + 1) * DLT       'STRAIN RATES
    INCTSUM = RSUM(P + 1)       'STRAIN
    DLTT = RSUM(P + 1) * DLT    'WARPAGE
 END IF

 FOR II = 1 TO 6
```

```
    EK(P + 1, II) = EK(P, II) + EKPINT(II, 1) * INCT
  NEXT II

  OPEN DIROUT$ + STRAIN$ FOR APPEND AS #1     'COMBINED
    PRINT #1, TAB(1); USING "####.##"; INCTSUM * DLT;
    FOR II = 1 TO 6
      PRINT #1, TAB(9 + (II - 1) * 12); USING "#.####^^^^"; EK(P + 1, II) * 1000;
    NEXT II
    PRINT #1,
  CLOSE #1
  FOR II = 1 TO 6                    'EACH LAYER
    OPEN DIROUT$ + LSTRAIN$(II) FOR APPEND AS #1
      PRINT #1, TAB(1); USING "####.##"; INCTSUM * DLT;
      PRINT #1, TAB(9); USING "#.####^^^^"; EK(P + 1, II) * 1000
    CLOSE #1
  NEXT II

  OPEN DIROUT$ + STRESS$ FOR APPEND AS #1        'AGGREGATED
    PRINT #1, TAB(1); USING "####.##"; RSUM(P) * DLT;
    FOR J = 1 TO K
      PRINT #1, TAB(9); USING "###"; J;
      DMC = (MC(P + 1, J) - MC(P, J)) / (R(P + 1) * DLT)
      FOR II = 1 TO 3
        FOR III = 1 TO 3
          YINT(II, III) = YTR(J, II, III)
        NEXT III
      NEXT II
      IF P > 0 THEN      'EP(), KP() AND EXPP() ARE STRAIN RATES.
        FOR II = 1 TO 3
          EP(II, 1) = EKPINT(II, 1)
          KP(II, 1) = EKPINT(II + 3, 1)
          EXPP(II, 1) = EXPVAL(P, J, II, 1) * DMC
        NEXT II
      ELSEIF P = 0 THEN  'THE ABOVE QUANTITIES ARE STRAINS AT P=0
        FOR II = 1 TO 3
          EP(II, 1) = EK(0, II)
          KP(II, 1) = EK(0, II + 3)
          EXPP(II, 1) = 0
        NEXT II
      END IF
      CALL MATRMULT(YINT(), EP(), YE())
      CALL MATRMULT(YINT(), KP(), YK())
      CALL MATRMULT(YINT(), EXPP(), YH())
      IF P = 0 THEN
        RPLC = 1      'STRESSES AT P=0
      ELSE
        RPLC = .5 * R(P) * DLT
      END IF
      FOR II = 1 TO 3
        YEJ(J, II, 1) = YEJ(J, II, 1) + RPLC * YE(II, 1)
        YKJ(J, II, 1) = YKJ(J, II, 1) + RPLC * YK(II, 1)
        YHJ(J, II, 1) = YHJ(J, II, 1) + RPLC * YH(II, 1)
      NEXT II
      FOR II = 1 TO 3    'AT THE CENTER OF EACH LAYER
        TEMP(II) = (YEJ(J, II, 1) + YKJ(J, II, 1) * .5 * (H(J) + H(J - 1)) - YHJ(J, II, 1)) * 1000
        PRINT #1, TAB(16 + (II - 1) * 12); USING "#.####^^^^"; TEMP(II);
      NEXT II
      CALL STRAFORM(TEMP(), ANGLE(J), SIG12())
      FOR II = 1 TO 3
        STRESS(P, J, II) = SIG12(II)
```

```
    NEXT II
    PRINT #1,
  NEXT J
CLOSE #1

FOR J = 1 TO K          'AT THE SURFACE OF EACH LAYER
  OPEN DIROUT$ + LSTRES$ + LTRIM$(STR$(J)) + ".PRN" FOR APPEND AS #1
    PRINT #1, USING "####.##"; RSUM(P) * DLT;
    HH = H(J - 1) + (H(J) - H(J - 1)) / 2   '** FOR STRESS AT THE MIDPOINT OF EACH LAYER
    FOR II = 1 TO 3
      TMP = (YEJ(J, II, 1) + YKJ(J, II, 1) * HH - YHJ(J, II, 1)) * 1000
      PRINT #1, TAB(9 + (II - 1) * 11); USING "#.####^^^^"; TMP / 1000;
    NEXT II
    FOR II = 1 TO 3
      TMP = (YEJ(J, II, 1) + YKJ(J, II, 1) * H(J) - YHJ(J, II, 1)) * 1000
      PRINT #1, TAB(11 + (II + 3 - 1) * 11); USING "#.####^^^^"; TMP / 1000;
    NEXT II
    PRINT #1,
  CLOSE #1
NEXT J
FOR II = 1 TO 6                 'TOP AND BOTTOM SURFACES
  SELECT CASE II
    CASE 1
      SYMB$ = "T1"
    CASE 2
      SYMB$ = "T2"
    CASE 3
      SYMB$ = "T3"
    CASE 4
      SYMB$ = "B1"
    CASE 5
      SYMB$ = "B2"
    CASE 6
      SYMB$ = "B3"
  END SELECT
  OPEN DIROUT$ + LSTRES$ + SYMB$ + ".PRN" FOR APPEND AS #1
    PRINT #1, USING "####.##"; RSUM(P) * DLT;
    IF II < 4 THEN     'TOP LAYER
      TMP = (YEJ(1, II, 1) + YKJ(1, II, 1) * H(0) - YHJ(1, II, 1)) * 1000
      PRINT #1, TAB(9); USING "#.####^^^^"; TMP / 1000
    ELSEIF II > 3 THEN  'BOTTOM LAYER
      TMP = (YEJ(K, II - 3, 1) + YKJ(K, II - 3, 1) * H(K) - YHJ(K, II - 3, 1)) * 1000
      PRINT #1, TAB(9); USING "#.####^^^^"; TMP / 1000
    END IF
  CLOSE #1
NEXT II

FOR II = 1 TO 2
  OPEN DIROUT$ + DISMNT$ + LTRIM$(STR$(II)) + ".PRN" FOR APPEND AS #1
    PRINT #1, TAB(1); USING "###.##"; DLTT;
      IF II = 1 THEN
        X = 14.1: Y = 0
      ELSE II = 2
        X = 0: Y = 9.15
      END IF
      WARP(II) = -(-.5) * (EK(P + 1, 4) * X * X + EK(P + 1, 5) * Y * Y + EK(P + 1, 6) * X * Y)
      PRINT #1, TAB(9); USING "#.####^^^^"; WARP(II);
    PRINT #1,
  CLOSE #1
NEXT II
```

```
IF SCRN$ = "Y" OR (SCRN$ = "N" AND P = M) THEN
   PRINT " SP"; TAB(6); USING "###.##"; RSUM(P) * DLT;
   FOR H = 1 TO 6
      PRINT TAB(15 + (H - 1) * 11); USING "#.###^^^^"; EKPINT(H, 1);
   NEXT H
   PRINT

   PRINT " SN"; TAB(6); USING "###.##"; INCTSUM * DLT;
   FOR H = 1 TO 6
      PRINT TAB(15 + (H - 1) * 11); USING "#.###^^^^"; EK(P + 1, H);
   NEXT H
   PRINT

   PRINT " SS"; TAB(6); USING "###.##"; RSUM(P) * DLT;
   FOR H = 1 TO 3
      TMP = (YEJ(1, H, 1) + YKJ(1, H, 1) * H(0) - YHJ(1, H, 1)) * 1000
      PRINT TAB(15 + (H - 1) * 11); USING "#.###^^^^"; TMP;
   NEXT H
   FOR H = 1 TO 3
      TMP = (YEJ(K, H, 1) + YKJ(K, H, 1) * H(K) - YHJ(K, H, 1)) * 1000
      PRINT TAB(15 + (H + 3 - 1) * 11); USING "#.###^^^^"; TMP;
   NEXT H
   PRINT

   PRINT " DS"; TAB(6); USING "###.##"; DLTT;
   FOR H = 1 TO 2
      PRINT TAB(15 + (H - 1) * 11); USING "#.###^^^^"; WARP(H);
   NEXT H
   PRINT
   PRINT STRING$(79, " ")
END IF


IF DSPL$ = "Y" THEN
   FOR H = 1 TO 3
      CALL SCRNPLOT(1, 14, RSUM(M), RSUM(P), MCL - 10, MC(P, H) - 10, PMX(H), PMY(H))
   NEXT H

   FOR H = 1 TO 4 STEP 3
      IF H = 1 THEN
         RPLSPL = SPL
      ELSEIF H = 4 THEN
         RPLSPL = SPL * 8
      END IF
      CALL SCRNPLOT(1, 15, RSUM(M), RSUM(P), RPLSPL, EKPINT(H, 1), PPX(H), PPY(H))
   NEXT H

   FOR H = 1 TO 4 STEP 3
      IF H = 1 THEN
         RPLSNL = SNL
      ELSEIF H = 4 THEN
         RPLSNL = SNL * 10
      END IF
      CALL SCRNPLOT(1, 7, RSUM(M), RSUM(P), RPLSNL, EK(P + 1, H), PNX(H), PNY(H))
   NEXT H

   FOR H = 1 TO 2
      IF H < 4 THEN
```

```
        TB = 0
      ELSEIF II > 3 THEN
        TB = K
      END IF
      TMP = (YEJ(1, II, 1) + YKJ(1, II, 1) * H(TB) - YHJ(1, II, 1)) * 1000
      CALL SCRNPLOT(1, 2, RSUM(M), RSUM(P), SSL, TMP, PSX(II), PSY(II))
    NEXT II

    FOR II = 1 TO 1
      CALL SCRNPLOT(1, 14, RSUM(M), RSUM(P), SDL, WARP(II), PDX(II), PDY(II))
    NEXT II
  END IF

  END SUB

  SUB MATRINVS (A(), AI())
  ' Matrix inversion subroutine by Gauss-Jordan elimination
  ' matrix [A] is input, matrix [B] is output
  ' dim [A]=L%*L%  temporary dim [B]=L%*2L%
  ' First create matrix with [A] on the left and [I] on the right

  L% = UBOUND(A, 1)
  DIM B(1 TO L%, 1 TO 2 * L%)

  FOR I% = 1 TO L%
    FOR J% = 1 TO L%
      B(I%, J% + L%) = 0
      B(I%, J%) = A(I%, J%)
    NEXT J%
    B(I%, I% + L%) = 1
  NEXT I%

  ' Perform row oriented operations to convert the left hand
  ' side of [B] to the identity matrix.  The inverse of [A] will
  ' then be on the right.

      FOR KK% = 1 TO L%
        IF KK% = L% THEN GOTO 42424
          M% = KK%

          ' Find the maximum element
          FOR I% = KK% + 1 TO L%
            IF ABS(B(I%, KK%)) > ABS(B(M%, KK%)) THEN M% = I%
          NEXT I%

        IF M% = KK% THEN GOTO 42424
          FOR J% = KK% TO 2 * L%
            B = B(KK%, J%)
            B(KK%, J%) = B(M%, J%)
            B(M%, J%) = B
          NEXT J%

          ' divide row K
42424 :     FOR J% = KK% + 1 TO 2 * L%
            B(KK%, J%) = B(KK%, J%) / B(KK%, KK%)
          NEXT J%

        IF KK% = 1 THEN GOTO 42434
          FOR I% = 1 TO KK% - 1
            FOR J% = KK% + 1 TO 2 * L%
```

```
            B(I%, J%) = B(I%, J%) - B(I%, KK%) * B(KK%, J%)
          NEXT J%
        NEXT I%

      IF KK% = L% THEN GOTO 42439
42434 :     FOR I% = KK% + 1 TO L%
            FOR J% = KK% + 1 TO 2 * L%
              B(I%, J%) = B(I%, J%) - B(I%, KK%) * B(KK%, J%)
            NEXT J%
          NEXT I%
42439 :   NEXT KK%

' retrieve inverse from the right side of [B]
FOR I% = 1 TO L%
  FOR J% = 1 TO L%
    A(I%, J%) = B(I%, J% + L%)
  NEXT J%
NEXT I%


END SUB

SUB MATRMULT (A!(), B!(), AB!())

'AB=A*B  A is L%*M%  B is M%*N%  AB is L%*N%
'COMPUTE THE PRODUCT MATRIX
'MATRIX AB() DOES NOT NEED TO BE INITIALIZED.

L% = UBOUND(A, 1)
M% = UBOUND(A, 2)
N% = UBOUND(B, 2)

DIM C(1 TO L%, 1 TO N%)

FOR I = 1 TO L%
  FOR J = 1 TO N%
    FOR K = 1 TO M%
      C(I, J) = C(I, J) + A(I, K) * B(K, J)
      AB(I, J) = C(I, J)
    NEXT K
  NEXT J
NEXT I

END SUB

SUB MATRPRN1 (X(), S)

L = UBOUND(X, 1)

IF S = 0 THEN
  FOR I = 1 TO L
    PRINT TAB(1); USING "#.###^^^^"; X(I)
  NEXT I
  PRINT
ELSE
  CLOSE
  OPEN "LPT1:" FOR OUTPUT AS #1
    FOR I = 1 TO L
      PRINT #1, TAB(1); USING "#.###^^^^"; X(I)
    NEXT I
```

```
        PRINT #1,
        PRINT #1,
      CLOSE #1
  END IF

  PRINT

  END SUB

  SUB MATRPRN2 (X(), S)

  L = UBOUND(X, 1)
  M = UBOUND(X, 2)

  IF S = 0 THEN
     FOR I = 1 TO L
        FOR J = 1 TO M
           PRINT TAB(1 + (J - 1) * 10); USING "#.###^^^^"; X(I, J);
        NEXT J
        PRINT
     NEXT I
     PRINT
  ELSE
     CLOSE
     OPEN "LPT1:" FOR OUTPUT AS #1
        FOR I = 1 TO L
           FOR J = 1 TO M
              PRINT #1, TAB(1 + (J - 1) * 10); USING "#.###^^^^"; X(I, J);
           NEXT J
           PRINT #1,
        NEXT I
        PRINT #1,
        PRINT #1,
     CLOSE #1
  END IF

  END SUB

  SUB MATRTRAN (X(), XT())

  D = UBOUND(X, 1)
  IF UBOUND(X, 2) < > D OR UBOUND(XT, 1) < > D OR UBOUND(XT, 2) < > D THEN CALL ERRLOCTN("1 IN MATRTRAN")

  FOR I = 1 TO D
     FOR J = 1 TO D
        XT(I, J) = X(J, I)
     NEXT J
  NEXT I

  END SUB

  SUB MODELCOF (K, XFLAG$(), PARM())

  NUM = UBOUND(PARM, 3)

  LINE INPUT #1, INT$
  LINE INPUT #1, INT$

  FOR J = 1 TO K
     LINE INPUT #1, INT$
```

```
LW1$ = LEFTWORD$(INT$)
IF VAL(LW1$) = J THEN
   LW2$ = LEFTWORD$(INT$)
   IF LW2$ = "SAME" THEN
      FOR I = 1 TO 3
         IF NUM > 9 THEN
            XFLAG$(J, I) = XFLAG$(J - 1, I)
         END IF
         FOR II = 1 TO NUM
            PARM(J, I, II) = PARM(J - 1, I, II)
         NEXT II
      NEXT I
   ELSE
      FOR I = 1 TO 3
         LW3$ = LEFTWORD$(INT$)
         IF LW3$ = "E" THEN
            IF NUM > 9 THEN    'ONLY ON READING PARAMETER C
               XFLAG$(J, I) = LW3$
            END IF
         ELSEIF LW3$ = "N" THEN
            IF NUM > 9 THEN    'ONLY ON READING PARAMETER C
               XFLAG$(J, I) = LW3$
            END IF
         ELSE
            IF NUM > 9 THEN    'ONLY ON READING PARAMETER C
               XFLAG$(J, I) = "V"
            END IF
            INT$ = LW3$ + " " + INT$
            FOR II = 1 TO NUM
               PARM(J, I, II) = VAL(LEFTWORD$(INT$))
            NEXT II
         END IF
         IF I < 3 THEN
            LINE INPUT #1, INT$
            LW2$ = LEFTWORD$(INT$)
         END IF
      NEXT I
   END IF
ELSE
   FOR JJ = J TO K
      FOR I = 1 TO 3
         IF NUM > 9 THEN
            XFLAG$(JJ, I) = XFLAG$(J - 1, I)
         END IF
         FOR II = 1 TO NUM
            PARM(JJ, I, II) = PARM(J - 1, I, II)
         NEXT II
      NEXT I
   NEXT JJ
   EXIT FOR
END IF
NEXT J

END SUB

SUB MOISTURE (K, DLT, M, PTS)

DIM MCCOF(1 TO K, 1 TO (PTS - 1), 1 TO 3)
DIM Y(1 TO PTS), YY(1 TO K, 5)
DIM RCOF(1 TO (PTS - 1) * 3, 1)
```

```
DIM TIME(1 TO PTS)
DIM B(1 TO PTS, 1 TO 3)

LOCATE 17, 1
PRINT STRING$(79, " ")
LOCATE 17, 23
PRINT "Computing moisture development!"

FOR I = 1 TO PTS
   TIME(I) = VAL(LEFTWORD$(MC$(I)))
   FOR II = 1 TO 3
      B(I, II) = VAL(LEFTWORD$(MC$(I)))
   NEXT II
NEXT I

FOR J = 1 TO K
   DEPTH = ABS(H(J - 1) - H(0)) + (H(J) - H(J - 1)) / 2
   FOR N = 1 TO PTS
      Y(N) = B(N, 1) + B(N, 2) * DEPTH + B(N, 3) * DEPTH * DEPTH
   NEXT N
   CALL SPLINQUD(TIME(), Y(), RCOF())
   FOR I = 1 TO (PTS - 1)
      FOR N = 1 TO 3
         MCCOF(J, I, N) = RCOF((I - 1) * 3 + N, 1)
      NEXT N
   NEXT I
NEXT J

FOR J = 1 TO K
   FOR I = 0 TO M + 1
      IF I = M + 1 THEN
         DLT1 = (RSUM(I - 1) + 1) * DLT
      ELSE
         DLT1 = RSUM(I) * DLT
      END IF
      DLT2 = DLT1 * DLT1
      IF DLT1 <= TIME(PTS) THEN
         C = 1
         DO
            IF DLT1 <= TIME(C + 1) THEN
               MC(I, J) = MCCOF(J, C, 1) * DLT2 + MCCOF(J, C, 2) * DLT1 + MCCOF(J, C, 3)
               EXIT DO
            ELSE
               C = C + 1
            END IF
         LOOP
      ELSE
         MC(I, J) = MC(I - 1, J)
      END IF
   NEXT I
NEXT J


FOR J = 1 TO K
   IF TYPE$ = "KM" OR TYPE$ = "M" THEN
      FOR N = 1 TO M
         AVGMC = (MC(N, J) + MC(N - 1, J)) / 2
         DRSUM = (RSUM(N) - RSUM(N - 1)) * DLT
         AVGMCW(N, J) = AVGMCW(N - 1, J) * RSUM(N - 1) * DLT + AVGMC * DRSUM
         AVGMCW(N, J) = AVGMCW(N, J) / (RSUM(N) * DLT)
```

```
      NEXT II
   END IF
   OPEN DIROUT$ + LMOIST$ + LTRIM$(STR$(J)) + ".PRN" FOR OUTPUT AS #1
   CLOSE #1
   OPEN DIROUT$ + LMOIST$ + LTRIM$(STR$(J)) + ".PRN" FOR OUTPUT AS #1
      PRINT #1, LMOIST$ + LTRIM$(STR$(J)) + ".PRN"
      PRINT #1, "MOISTURE CONTENT (%)"
      PRINT #1, "HOUR"; TAB(10); "LAYER" + STR$(J)
      FOR II = 0 TO M + 1
         IF II = M + 1 THEN
            TIME = RSUM(II - 1) + 1
         ELSE
            TIME = RSUM(II)
         END IF
         PRINT #1, USING "###.##"; TIME * DLT;
         PRINT #1, TAB(10); USING "###.###"; MC(II, J)
      NEXT II
   CLOSE #1
NEXT J

END SUB

SUB PARAMTR1 (M(), Y(), CEF())

D = UBOUND(M, 1)
IF D < > UBOUND(Y, 1) THEN CALL ERRLOCTN("1 IN PARAMTR1")
IF D < > UBOUND(CEF, 1) THEN CALL ERRLOCTN("2 IN PARAMTR1")

DIM MCT(1 TO D, 1 TO D)
DIM MCTK(1 TO D, 1 TO D)

FOR L = 1 TO D
   FOR M = 1 TO D
      MCT(L, M) = M(L) ^ (D - M)
   NEXT M
NEXT L

CALL MATRINVS(MCT(), MCTK())
CALL MATRMULT(MCTK(), Y(), CEF())

END SUB

SUB PARAMTR2 (M(), Y(), S(), CEF())

D = UBOUND(M, 1)
IF D < > UBOUND(Y, 1) THEN CALL ERRLOCTN("1 IN PARAMTR2")

DIM MCT(1 TO D, 1 TO D)
DIM MCTK(1 TO D, 1 TO D)
DIM STS(1 TO D, 1 TO D)
DIM STSK(1 TO D, 1 TO D)
DIM STSIT(1 TO D, 1 TO D)
DIM XY(1 TO D, 1 TO D)

FOR L = 1 TO D
   FOR M = 1 TO D
      MCT(L, M) = M(L) ^ (D - M)
      STS(L, M) = S(L) ^ (D - M)
   NEXT M
NEXT L
```

```
  CALL WRITECMD(2, 0, FID$())      '1 WARP CURVE
  CALL WRITECMD(3, K + 8, FID$())  '3 NORMAL STRAIN CURVES
  CALL WRITECMD(3, K + 2, FID$())  '3 NORMAL STRAIN RATE
  CALL WRITECMD(3, K + 5, FID$())  '3 CURVATURE STRAIN RATE
  CALL WRITECMD(3, K + 11, FID$()) '3 CURVATURE STRAIN
  CALL WRITECMD(6, 2 * K + 14, FID$())  '3 TOP SURFACE STRESS CURVES
                                        '3 BOTTOM SURFACE STRESS CURVES

  SPF$ = SUBDIR$ + PREFIX$ + INFNUM$ + ".SPF"
  PRINT #1, "M"          'COMMENT
  PRINT #1, "RESET 1,7"
  PRINT #1, SPF$
  PRINT #1, "W"
  PRINT #1, "E"

  PRINT #1, "C"          'EOP
  PRINT #1, "SAVE"       'SAVE *.SPF
  PRINT #1, SPF$
  PRINT #1, "PLOTIT,1,"  'CREATE *.PIC
  PRINT #1, SUBDIR$ + PREFIX$ + INFNUM$ + ".PIC"
  PRINT #1, SPF$
  PRINT #1, "PLOT"
  PRINT #1, SPF$
  PRINT #1, "%"
CLOSE #1

END SUB

SUB PRNTPARM (K, P$, PARM())

PRINT #2, P$ + " PARAMETERS:"
PRINT #2, "LAYER DIR";
FOR N = 1 TO UBOUND(PARM, 3)
   PRINT #2, TAB(14 + (N - 1) * 5); N;
NEXT N
PRINT #2,

FOR J = 1 TO K
   PRINT #2, J;
   FOR I = 1 TO 3
      DIR = 11 * I: IF I = 3 THEN DIR = 12
      PRINT #2, TAB(6); DIR;
      FOR N = 1 TO UBOUND(PARM, 3) STEP 2
         PRINT #2, TAB(11 + (N - 1) * 5); USING "#.##^^^^"; PARM(J, I, N);
      NEXT N
      PRINT #2,
      FOR N = 2 TO UBOUND(PARM, 3) STEP 2
         PRINT #2, TAB(16 + (N - 2) * 5); USING "#.##^^^^"; PARM(J, I, N);
      NEXT N
      PRINT #2,
   NEXT I
NEXT J

END SUB


SUB QTRAFORM (Q(), ANGLE, QXY())

FDIM = UBOUND(Q, 1)
SDIM = UBOUND(Q, 2)
```

```
IF FDIM < > UBOUND(QXY, 1) THEN CALL ERRLOCTN("1 IN TRANSFORM")
IF SDIM < > UBOUND(QXY, 2) THEN CALL ERRLOCTN("2 IN TRANSFORM")

THETA = ANGLE / 180 * 3.1415926544#
C = COS(THETA)
S = SIN(THETA)
CS = C * S
C2 = C * C
S2 = S * S

IF SDIM = 3 THEN
   C3 = C2 * C
   C4 = C3 * C
   S3 = S2 * S
   S4 = S3 * S
   C2S2 = C2 * S2
   TC2S2 = 2 * C2S2
   FC2S2 = 4 * C2S2
   C3S = C3 * S
   CS3 = C * S3

   QXY(1, 1) = Q(1, 1) * C4 + Q(2, 2) * S4 + Q(1, 2) * TC2S2 + Q(3, 3) * FC2S2
   QXY(2, 2) = Q(1, 1) * S4 + Q(2, 2) * C4 + Q(1, 2) * TC2S2 + Q(3, 3) * FC2S2
   QXY(1, 2) = Q(1, 1) * C2S2 + Q(2, 2) * C2S2 + Q(1, 2) * (C4 + S4) + Q(3, 3) * -FC2S2
   QXY(3, 3) = Q(1, 1) * C2S2 + Q(2, 2) * C2S2 + Q(1, 2) * -2 * C2S2 + Q(3, 3) * (C2 - S2) * (C2 - S2)
   QXY(1, 3) = Q(1, 1) * C3S + Q(2, 2) * -CS3 + Q(1, 2) * (CS3 - C3S) + Q(3, 3) * 2 * (CS3 - C3S)
   QXY(2, 3) = Q(1, 1) * CS3 + Q(2, 2) * -C3S + Q(1, 2) * (C3S - CS3) + Q(3, 3) * 2 * (C3S - CS3)
   QXY(2, 1) = QXY(1, 2)
   QXY(3, 1) = QXY(1, 3)
   QXY(3, 2) = QXY(2, 3)

ELSEIF SDIM = 1 THEN
   DIM T(1 TO 3, 1 TO 3), TK(1 TO 3, 1 TO 3)

   T(1, 1) = C2
   T(2, 2) = C2
   T(1, 2) = S2
   T(2, 1) = S2
   T(3, 1) = -CS
   T(3, 2) = CS
   T(1, 3) = 2 * CS
   T(2, 3) = -2 * CS
   T(3, 3) = C2 - S2

   CALL MATRINVS(T(), TK())
   CALL MATRMULT(TK(), Q(), QXY())
   QXY(3, 1) = QXY(3, 1) * 2
ELSE
   CALL ERRLOCTN("3 IN Tranform")
END IF

END SUB

FUNCTION RELXMODU (TYPE$, MS, RMV, KS, RKV, T)

'IF RMV = 0 THEN FREE OF MAXWELL DASHPOT
'IF RKV = 0 THEN FREE OF KELVIN ELEMENT

SELECT CASE TYPE$
   CASE "KM"
```

```
      UK = KS * RKV
      UM = MS * RMV
      BI = UK + MS * RKV + UM
      CI = UK * UM
      PI1 = .5 * (BI + (BI ^ 2 - 4 * CI) ^ .5)
      PI2 = .5 * (BI - (BI ^ 2 - 4 * CI) ^ .5)
      IF PI1 = PI2 AND PI1 = 0 THEN
         RELXMODU = 1
      ELSEIF PI1 = PI2 THEN
         RELXMODU = EXP(-PI1 * T)
      ELSE
         A = (PI1 - UK) / (PI1 - PI2)
         B = (UK - PI2) / (PI1 - PI2)
         RELXMODU = A * EXP(-PI1 * T) + B * EXP(-PI2 * T)
      END IF
   CASE "M"
      UM = MS * RMV
      RELXMODU = EXP(-UM * T)
   CASE "KS"
      A = KS / (MS + KS)
      B = MS / (MS + KS)
      C = (MS + KS) * RKV * T
      RELXMODU = A + B * EXP(-C)
   CASE ELSE
      CALL ERRLOCTN("1 IN RELXMODU")
END SELECT

END FUNCTION

SUB SCRNPLOT (N, NUM, A, B, C, D, E, F)

CSX = 500 / A * B
CSY = 100 / C * D
SELECT CASE N
   CASE 1
      STYLE = &HFFFF
   CASE 2
      STYLE = &HCCCC
   CASE 3
      STYLE = &H8888
END SELECT
LINE (E, F)-(CSX, CSY), NUM, , STYLE
E = CSX
F = CSY

END SUB

SUB SPLINCUB (X(), Y(), COF())

D = UBOUND(X, 1)
IF D < > UBOUND(Y, 1) OR (D / 3) * 4 < > UBOUND(COF, 1) OR UBOUND(COF, 2) < > 1 THEN
   CALL ERRLOCTN("1 IN SPLINCUB")
END IF
DIM XX(1 TO (D / 3) * 4, 1 TO (D / 3) * 4)
DIM XXI(1 TO (D / 3) * 4, 1 TO (D / 3) * 4)
DIM YY(1 TO (D / 3) * 4, 1 TO 1)

FOR I = 1 TO (D / 3)
   XX(1 + 4 * (I - 1), 1 + 4 * (I - 1)) = X(I) * X(I) * X(I)
   XX(1 + 4 * (I - 1), 2 + 4 * (I - 1)) = X(I) * X(I)
```

```
    XX(1 + 4 * (I - 1), 3 + 4 * (I - 1)) = X(I)
    XX(1 + 4 * (I - 1), 4 + 4 * (I - 1)) = 1
    XX(2 + 4 * (I - 1), 1 + 4 * (I - 1)) = X(I + 1) * X(I + 1) * X(I + 1)
    XX(2 + 4 * (I - 1), 2 + 4 * (I - 1)) = X(I + 1) * X(I + 1)
    XX(2 + 4 * (I - 1), 3 + 4 * (I - 1)) = X(I + 1)
    XX(2 + 4 * (I - 1), 4 + 4 * (I - 1)) = 1
    XX(3 + 4 * (I - 1), 1 + 4 * (I - 1)) = X(I + 2) * X(I + 2) * X(I + 2)
    XX(3 + 4 * (I - 1), 2 + 4 * (I - 1)) = X(I + 2) * X(I + 2)
    XX(3 + 4 * (I - 1), 3 + 4 * (I - 1)) = X(I + 2)
    XX(3 + 4 * (I - 1), 4 + 4 * (I - 1)) = 1
    XX(4 + 4 * (I - 1), 1 + 4 * (I - 1)) = 3 * X(I + 2) * X(I + 2)
    XX(4 + 4 * (I - 1), 2 + 4 * (I - 1)) = 2 * X(I + 2)
    XX(4 + 4 * (I - 1), 3 + 4 * (I - 1)) = 1
    IF I < D - 1 THEN
       XX(4 + 4 * (I - 1), 5 + 3 * (I - 1)) = -3 * X(I + 2) * X(I + 2)
       XX(4 + 4 * (I - 1), 6 + 3 * (I - 1)) = -2 * X(I + 2)
       XX(4 + 4 * (I - 1), 7 + 3 * (I - 1)) = -1
    END IF
    YY(1 + 4 * (I - 1), 1) = Y(1 + (I - 1))
    YY(2 + 4 * (I - 1), 1) = Y(2 + (I - 1))
    YY(3 + 4 * (I - 1), 1) = Y(3 + (I - 1))
    YY(4 + 4 * (I - 1), 1) = 0
 NEXT I

 CALL MATRINVS(XX(), XXI())
 CALL MATRMULT(XXI(), YY(), COF())

 END SUB

 SUB SPLINQUD (X(), Y(), COF())

 D = UBOUND(X, 1)
 IF D < > UBOUND(Y, 1) OR (D - 1) * 3 < > UBOUND(COF, 1) OR UBOUND(COF, 2) < > 1 THEN
    CALL ERRLOCTN("1 IN SPLINQUD")
 END IF
 DIM XX(1 TO (D - 1) * 3, 1 TO (D - 1) * 3)
 DIM XXI(1 TO (D - 1) * 3, 1 TO (D - 1) * 3)
 DIM YY(1 TO (D - 1) * 3, 1 TO 1)

 FOR I = 1 TO D - 1
    XX(1 + 3 * (I - 1), 1 + 3 * (I - 1)) = X(I) * X(I)
    XX(1 + 3 * (I - 1), 2 + 3 * (I - 1)) = X(I)
    XX(1 + 3 * (I - 1), 3 + 3 * (I - 1)) = 1
    XX(2 + 3 * (I - 1), 1 + 3 * (I - 1)) = X(I + 1) * X(I + 1)
    XX(2 + 3 * (I - 1), 2 + 3 * (I - 1)) = X(I + 1)
    XX(2 + 3 * (I - 1), 3 + 3 * (I - 1)) = 1
    XX(3 + 3 * (I - 1), 1 + 3 * (I - 1)) = 2 * X(I + 1)
    XX(3 + 3 * (I - 1), 2 + 3 * (I - 1)) = 1
    IF I < D - 1 THEN
       XX(3 + 3 * (I - 1), 4 + 3 * (I - 1)) = -2 * X(I + 1)
       XX(3 + 3 * (I - 1), 5 + 3 * (I - 1)) = -1
    END IF
    YY(1 + 3 * (I - 1), 1) = Y(1 + (I - 1))
    YY(2 + 3 * (I - 1), 1) = Y(2 + (I - 1))
    YY(3 + 3 * (I - 1), 1) = 0   '1ST DIFFERENTIATION AT LAST POINT IS ZERO.
 NEXT I

 CALL MATRINVS(XX(), XXI())
 CALL MATRMULT(XXI(), YY(), COF())
```

```
END SUB

SUB STFHNMS1 (I, P, K, DLT)

DIM RR(1 TO 3)
DIM Y(1 TO 3, 1 TO 3), YINT(1 TO 3, 1 TO 3)
DIM EXPINT(1 TO 3, 1 TO 1), YEXP(1 TO 3, 1 TO 1)
DIM EP(1 TO 3, 1 TO 1), KP(1 TO 3, 1 TO 1)
DIM YE(1 TO 3, 1 TO 1), YK(1 TO 3, 1 TO 1), YH(1 TO 3, 1 TO 1)
DIM ABBDEKP(1 TO 6, 1 TO 1), EKP(1 TO 6, 1 TO 1)

IF P > 0 AND I < = P THEN
   FOR II = 1 TO 6
      EKP(II, 1) = EKPP(I - 1, II) 'PREVIOUS STRAIN RATES
   NEXT II
   FOR II = 1 TO 3
      EP(II, 1) = EKP(II, 1)
      KP(II, 1) = EKP(II + 3, 1)
   NEXT II
END IF

IF P = 0 AND I = 0 THEN
   RPLT = 0
   RPLEXP = 0
   RPLMC = 1
ELSE
   RPLT = (RSUMM(P) - RSUMM(I - 1)) * DLT
   RPLEXP = I - 1
   RPLMC = I
END IF

FOR J = 1 TO K
   FOR II = 1 TO 3
      IF RPLT < > 0 THEN
         IF TYPE$ < > "S" THEN    'VISCOELASTIC
            IF FLAG$(J, II) = "E" THEN
               RR(II) = 1
            ELSEIF FLAG$(J, II) = "N" THEN
               RR(II) = 1    'SHEAR RELAXATION MODULUS YET TO BE DEFINED.
            ELSEIF FLAG$(J, II) = "V" THEN
               RR(II) = RELXMODU(TYPE$, MSMC(P, J, II), RMV(I, J, II), KS(P, J, II), RKV(P, J, II), RPLT)
            END IF
         ELSE              'COMPLETE ELASTIC
            RR(II) = 1
         END IF
      ELSEIF RPLT = 0 THEN  'AT T=0 RELAXATION MODULUS DEGENERATES TO MOE.
         RR(II) = 1
      END IF
   NEXT II
   V21 = (RR(2) * MSMC(I, J, 2)) / (RR(1) * MSMC(I, J, 1)) * V12(J)
   V121 = 1 / (1 - V12(J) * V21)
   Y(1, 1) = MSMC(I, J, 1) * RR(1) / V121
   Y(1, 2) = Y(1, 1) * (-V21)
   Y(1, 3) = 0
   Y(2, 2) = MSMC(I, J, 2) * RR(2) / V121
   Y(2, 1) = Y(2, 2) * (-V12(J))
   Y(2, 3) = 0
   Y(3, 1) = 0
   Y(3, 2) = 0
   Y(3, 3) = MSMC(I, J, 3) * RR(3)
```

```
    CALL QTRAFORM(Y(), ANGLE(J), YINT())
    FOR II = 1 TO 3
      FOR III = 1 TO 3
        YTR(J, II, III) = YINT(II, III)
      NEXT III
      EXPINT(II, 1) = EXPVAL(RPLEXP, J, II, 1)
    NEXT II
    CALL MATRMULT(YINT(), EXPINT(), YEXP())
    DMC = (MC(RPLMC, J) - MC(RPLMC - 1, J)) / (R(RPLMC) * DLT)
    FOR II = 1 TO 3
      YH(II, 1) = YEXP(II, 1) * DMC
    NEXT II
    IF I <= P AND P > 0 THEN 'EXCLUDE 1ST RUN OF STFHNMS1 AT P=0
                  'EXCLUDE FINAL ITERATION WHICH IS I=P+1
                  'THE FINAL SUM WILL BE TAKEN IN MAINCOM1 SUBROUTINE.
      CALL MATRMULT(YINT(), EP(), YE())
      CALL MATRMULT(YINT(), KP(), YK())
      DR = .5 * (R(I - 1) + R(I)) * DLT
      FOR II = 1 TO 3
        YEJ(J, II, 1) = YEJ(J, II, 1) + DR * YE(II, 1)
        YKJ(J, II, 1) = YKJ(J, II, 1) + DR * YK(II, 1)
        YHJ(J, II, 1) = YHJ(J, II, 1) + DR * YH(II, 1)
      NEXT II
    END IF
    HJ1 = H(J): HJ2 = HJ1 * HJ1: HJ3 = HJ2 * HJ1
    H1 = H(J - 1): H2 = H1 * H1: H3 = H2 * H1
    FOR II = 1 TO 3
      FOR III = 1 TO 3
        ABBD(II, III) = ABBD(II, III) + YTR(J, II, III) * (HJ1 - H1)
        ABBD(II, III + 3) = ABBD(II, III + 3) + YTR(J, II, III) * .5 * (HJ2 - H2)
        ABBD(II + 3, III) = ABBD(II, III + 3)
        ABBD(II + 3, III + 3) = ABBD(II + 3, III + 3) + YTR(J, II, III) * (1 / 3) * (HJ3 - H3)
      NEXT III
      HNBM(II, 1) = HNBM(II, 1) + (YH(II, 1) * (HJ1 - H1))
      HNBM(II + 3, 1) = HNBM(II + 3, 1) + YH(II, 1) * .5 * (HJ2 - H2)
    NEXT II
  NEXT J

  IF P > 0 THEN        'EXCLUDE 1ST RUN OF STFHNMS1 AT P=0
    IF I <= P THEN     'EXCEPT FINAL ITERATION
      CALL MATRMULT(ABBD(), EKP(), ABBDEKP())
      RPLR = (R(I - 1) + R(I)) / R(P)
      FOR II = 1 TO 6
        GRAND(II, 1) = GRAND(II, 1) + RPLR * (HNBM(II, 1) - ABBDEKP(II, 1))
      NEXT II
    ELSE           'BUT FINAL ITERATION
      FOR II = 1 TO 6
        GRAND(II, 1) = GRAND(II, 1) + HNBM(II, 1)
      NEXT II
    END IF
  ELSE
    FOR II = 1 TO 6
      GRAND(II, 1) = HNBM(II, 1)
    NEXT II
  END IF

  END SUB

  SUB STRAFORM (SXY(), ANGLE, S12())
```

```
THETA = ANGLE / 180 * 3.1415926554#
C = COS(THETA)
S = SIN(THETA)
CS = C * S
C2 = C * C
S2 = S * S

S12(1) = C2 * SXY(1) + S2 * SXY(2) + 2 * CS * SXY(3)
S12(2) = S2 * SXY(1) + C2 * SXY(2) - 2 * CS * SXY(3)
S12(3) = -CS * SXY(1) + CS * SXY(2) + (C2 - S2) * SXY(3)

END SUB

FUNCTION TIMESTRG$ (TVL)

H1$ = "0"
H2$ = "0"
M1$ = "0"
M2$ = "0"
S1$ = "0"
S2$ = "0"

IF TVL >= 36000 THEN
   H1$ = LEFTWORD$(STR$((TVL \ 36000)))
   TVL = TVL MOD 36000
END IF
IF TVL >= 3600 THEN
   H2$ = LEFTWORD$(STR$(TVL \ 3600))
   TVL = TVL MOD 3600
END IF
IF TVL >= 600 THEN
   M1$ = LEFTWORD$(STR$(TVL \ 600))
   TVL = TVL MOD 600
END IF
IF TVL >= 60 THEN
   M2$ = LEFTWORD$(STR$(TVL \ 60))
   TVL = TVL MOD 60
END IF
IF TVL >= 10 THEN
   S1$ = LEFTWORD$(STR$(TVL \ 10))
   TVL = TVL MOD 10
END IF

S2$ = LEFTWORD$(STR$(TVL))

TIMESTRG$ = (H1$ + H2$ + ":" + M1$ + M2$ + ":" + S1$ + S2$)

END FUNCTION

FUNCTION TIMEVALU (TS$)

H1$ = LEFT$(TS$, 1): TS$ = RIGHT$(TS$, LEN(TS$) - 1)
H2$ = LEFT$(TS$, 1): TS$ = RIGHT$(TS$, LEN(TS$) - 2)
M1$ = LEFT$(TS$, 1): TS$ = RIGHT$(TS$, LEN(TS$) - 1)
M2$ = LEFT$(TS$, 1): TS$ = RIGHT$(TS$, LEN(TS$) - 2)
S1$ = LEFT$(TS$, 1): S2$ = RIGHT$(TS$, 1)

TIMEVALU = VAL(H1$) * 10 * 60 * 60 + VAL(H2$) * 60 * 60 + VAL(M1$) * 10 * 60 + VAL(M2$) * 60 + VAL(S1$) * 10 + VAL(S2$)

END FUNCTION
```

```
SUB WRITECMD (NUM, RANK, NAME$())

IF RANK = 0 THEN
   X = 1
ELSE
   X = 2
END IF

FOR II = 1 TO X
   PRINT #1, "C"
NEXT II
PRINT #1, "M"
FOR II = 1 TO NUM
   PRINT #1, "RESET " + STR$(II) + ",14"          'NUM CURVES
   PRINT #1, "C:\VPT\DF\OUTPUT\" + PREFIX$ + INFNUM$ + "\" + NAME$(RANK + II) + ".SDF"
NEXT II
PRINT #1, "W"
PRINT #1, "E"

END SUB
```

REFERENCES

REFERENCES

Alfrey, Jr., T.. 1948. The Mechanical Behavior of High Polymers. Interscience, New York.

Alexopoulos, J.. 1989. Effect of Resin Content on Creep and Other Properties of Waferboard. M.S. Thesis, Department of Forestry, University of Toronto, Toronto, Canada.

Arima, T.. 1967. The Influence of High Temperature on Compressive Creep of Wood. Journal of Japan Wood Research Society, 13(2):36-40.

Armstrong, L. D. and R. S. T. Kingston. 1960. Effect of Moisture Changes on Creep in Wood. Nature, 185(4716):862-863.

Armstrong, L. D. and G. N. Christensen. 1961. Influence of Moisture Changes on Deformation of Wood Under Stress. Nature, 191(4791):869-870.

Bach, L. and R. E. Pentoney. 1968. Nonlinear Mechanical Behavior of Wood. Forest Products Journal, 18(3):60-68.

Bodig, J. and B. A. Jane. 1982. Mechanics of Wood and Wood Composites. Van Nostrand Reinjold Co., New York.

Christensen, G. N.. 1962. The Use of Small Specimens for Studying Effects of Moisture Content Changes on the Deformation of Wood Under Load. Australian Journal of Applied Science, 13(4):242.

Christensen, R. M.. 1982. Theory of Viscoelasticity. Academic Press. New York.

Clouser, W. S.. 1959. Creep of Small Wood Beams Under Constant Bending Loads. Forest Products Laboratory, Madison, Report No. 2150.

Davidson, W. R.. 1962. The Influence of Temperature on Creep of Wood. Forest Products Journal, 12(8):377-381.

Ethington, R. L. and R. L. Youngs. 1965. Das rheologische Verhalten von Roteiche (Quercus rubra L.) bei Beanspruchung quer zur Faserrichtung. Holz als Roh- und Werkstoff, 23(5):196-201.

Feng, Y. and O. Suchsland. 1993. Improved Technique for Measuring Moisture Content Gradients in Wood. Forest Products Journal, 43(3):56-58.

Flugge, W.. 1967. Viscoelasticity. Blaisdell Publishing Co., Waltham, Massachusetts.

Forest Products Laboratory. 1987. Wood Handbook (Agriculture Handbook 72). Forest Service, U.S. Agriculture Department, Washington D.C..

Gibson, E. J.. 1965. Role of Water and Effects of a Changing Moisture Content. Nature, 206(4980):213-215.

Gross, B.. 1953. Mathematical Structures of the Theories of Viscoelasticity. Herman. Paris, France.

Grossman, P. U. A.. 1976. Requirements for a Model that Exhibits Mechano-Sorptive Behavior. Wood Science and Technology, 10(3):163-168.

Heramon, R. F. S. and M. M. Paton. 1964. Moisture Content Changes and Creep of Wood. Forest Products Journal, 14(8):357-379.

Ismar, H. and M. Paulitsch. 1973. Effect of Climate on the Residual Stress and Deformation of Multi-layered Particleboard. Holz als Roh- und Werkstoff, 31(22):469-474.

Jones, R. M.. 1975. Mechanics of Composite Materials. Scripta Book Co., Washington.

King, E. G. Jr.. 1961. Time Dependent Behavior of Wood in Tension Parallel to the Grain. Forest Products Journal, 11(3):156-165.

Kingston, R. S. T. and L. N. Clarke. 1961. Some Aspects of the Rheological Behavior of Wood. I, II. Australian Journal of Applied Science, 12(2):211-226, 227-240.

Kitahara, K. and N. Okabe. 1959. The Influence of Temperature on Creep of Wood by Bending Test. Journal of Japan Wood Research Society, 5(1):12-18.

Kitahara, K. and K. Yukawa. 1964. The Influence of the Change of Temperature on Creep in Bending. Journal of Japan Wood Research Society, 10(5):169-175.

Koch, P.. 1971. Process for Straightening and Drying Southern Pine 2 by 4's in 24 Hours. Forest Products Journal, 21(5):17.

Kühne, H.. 1961. Beitrag zur Theorie des mechanischen Formänderungsverhaltens von Holz. Holz als Roh- und Werkstoff, 19(3):81-82.

Kunesh, R. H.. 1961. The Inelastic Behavior of Wood. A New Concept for Improved Panel Forming Processes. Forest Products Journal, 11(9):395-406.

Lawniczak, M.. 1958. Investigations on Creep Deformation and Stress Relaxation in Steamed Beech Wood. CSIRO, Australia, Translation No. 4395, from Instytut Technologii Drewna. Prace 5(1):61-81.

Leaderman, H.. 1958. Viscoelastic Phenomena in Amorphous High Polymeric Systems. Rheology: Theory and Applications. Edited by F. R. Eirich. Chapter1, vol. 2. Academic Press, New York.

Liu, D.. 1987. Unpublished. Class Notes for Nonmetallic Composite Materials (MMM4-44). MMM Department, Michigan State University.

Lo, K. H., R. M. Christensen, and E. M. Wu. 1977. A Higher-Order Theory of Plate Deformation, Part2: Laminated Plates. Journal of Applied Mechanics, 44(4):669-676.

Mindlin, R. D.. 1951. Influence of Rotary Inertia and Shear on Flexural Motions of Isotropic, Elastic Plates. Journal of Applied Mechanics, 18(1):31-38.

Nemeth, L. L. J.. 1964. The Influence of Moisture on Creep in Wood. M.S. Thesis, University of California at Berkeley.

Nielsen, A.. 1972. Rheology of Building Materials. Document D6:1972. National Swedish Institute Bldg. Res.:213.

Norimoto, M. and T. Yamada. 1965. The Effect of Temperature on the Stress Relaxation of Hinoki. Wood Research Bulletin, Wood Research Institute, Kyoto University, 35:44-50.

Norimoto, M., H. Hiyano and T. Yamada. 1965. On the Torsional Creep of Hinoki Wood. Bulletin of Wood Research Institute, Keyoto University, 34:37-44.

Norris, C. B.. 1942. Technique of Plywood. I. F. Laucks, Inc., Seattle, Washington.

Ota, M. and Y. Tsubota. 1966. Several Investigations on the Static Viscoelasticity of Wood Subjected to Bending Test. Journal of Japan Wood Research Society, 12(1):26-29.

Pagano, N. J.. 1970. Exact Solution for Rectangular Bidirectional Composites and Sandwich Plates. Journal of Composite Materials, 4(January):20-34.

Pagano, N. J.. 1970. Influence of Shear Coupling in Cylindrical Bending of Anisotropic Laminates. Journal of Composite Materials, 4(July):330-343.

Pagano, N. J.. 1969. Exact Solutions for Composite Laminates in Cylindrical Bending. Journal of Composite Materials, 3(July):398-411.

Pagano, N. J. and A. S. D. Wang. 1971. Further Study of Composite Laminates Under Cylindrical Bending. Journal of Composite Materials, 5(October):521-528.

Pagano, N. J. and S. R. Soni. 1983. Global-local Variational Model. International Journal of Solids & Structure, 19(3):207-228.

Pagano, N. J.. 1972. Elastic Behavior of Multilayered Bidirectional Composites. AIAA Journal, 10(7):931-933.

Perkitny, T. and R. S. T. Kingston. 1972. Wood Science and Technology, 6(3):215.

Pentoney, R. E. and R. W. Davidson. 1962. Rheology and the Study of Wood. Forest Products Journal, 12(5):243-248.

Reddy, J. N.. 1984. A Simple Higher-Order Theory for Laminated Composite Plates. Journal of Applied Mechanics, 51(4):745-752.

Rehfield, L. W. and R. R. Valesetty. 1983. A Comprehensive Theory for Planar Bending of Composite Laminates. Computer Structures, 16(1-4):441-447.

Rose, G.. 1965. Das mechanische Verhalten des Kiefernholzes bei dynamischer Dauerbeanspruchung in Abhängigkeit von Belastungsart, Belastungsgröße, Feuchtigkeit und Temperatur. Holz als Roh- und Werkstoff, 23(7):271-284.

Schapery, R. A.. 1967. Stress Analysis of Viscoelastic Composite Materials. Journal of Composite Materials, 1(3):228-267.

Schniewind, A.. 1968. Recent Progress in the Study of the Rheology of Wood. Wood Science and Technology, 2(3):188-206.

Schwarzl, F. and A. J. Staverman. 1953. Higher Approximation Methods for the Relaxation Spectrum from Static and Dynamic Measurements of Viscoelastic Materials. Applied Science Research, A4(2):127.

Sims, D.. 1972. Viscoelastic Creep and Relaxation Behavior of Laminated Composite Plates. Ph.D. Dissertation. Southern Methodist University.

Suchsland, O.. 1970. Optical Determination of Linear Expansion and Shrinkage of Wood. Forest Products Journal, 20(6):26-29.

Suchsland, O. and J. D. McNatt. 1985. On the Warping of Laminated Wood Panels. Report on Cooperative Study Between the Forest Products Laboratory; the Forestry Department and the Agricultural Experiment Station of Michigan State University.

Takemura, T. and Y. Ikeda. 1963. The Stress Relaxation in Relation to the Non-equilibrium State in the Wood-water System. Bulletin of Shimane Agricultural College, Matsue, 11A:105-133.

Takemura, T.. 1967. Plastic Properties of Wood in Relation to Non-equilibrium States of Moisture Contents. Journal of Japan Wood Research Society, 13(3):77-81.

Takemura, T.. 1966. Plastic Properties of Wood in Relation to Non-equilibrium States of Moisture Contents. Memoirs of the College of Agriculture, Keyoto University, 88:31-48.

Tong, Y. H. and O. Suchsland. 1992. Application of Finite Element Method to Panel Warping. Holz als Roh- und Werkstoff, 51(1993) 55-57.

Ugolev, B. N.. 1964. Determination of Rheological Properties of Wood. CSIRO, Australian Translation 7161.

Ugolev, B. N.. 1963. Determination of the Rheological Properties of Wood. Derev. Prom. 12(2):17-19. (CSIRO, Australia, Translation 7161).

Ugolev, B. N. and W. I. Pimenowa. 1963. Investigation of the Effect of Temperature and Moisture Content on the Rheological Behavior of Beech Wood. Derev. Prom., 12(6):10-12.

Whitney, J. M. and C. T. Sun. 1973. A Higher Order Theory for Extensional Motion of Laminated Composites. Journal of Sound and Vibration, 30(1):85-97.

Whitney, J. M. and N. J. Pagano. 1970. Shear Deformation in Heterogeneous Anisotropic Plates. Journal of Applied Mechanics, 37(4):1031-1036.

Yamada, T., T. Takemura and S. Kadita. 1961. On the Rheology of Wood III. The Creep and Relaxation of Buna. Journal of Japan Wood Research Society, 7(2):63-67.

Ylinen, A.. 1957. Zur Theorie der Dauerstandfestigkeit des Holzes. Holz als Roh- und Werkstoff, 15(5):213-215.

Youngs, R. L.. 1957. The Perpendicular-to-Grain Mechanical Properties of Red Oak as Related to Temperatures, Moisture Content, and Time. U. S. Forest Products Laboratory, Madison, Wisconsin, Report 2079.

Youngs, R. L. and H. C. Hilbrand. 1963. Time Related Flexural Behavior of Small Douglas-fir Beams Under Prolonged Loading. Forest Products Journal, 13(6):227-232.

Xu, H and Otto Suchsland. 1991. The Expansion Potential: A New Evaluator of the Expansion Behavior of Wood Composites. Forest Products Journal, 41(6):39-42.